Steam Generator Tube Integrity Program/Steam Generator Group Project

Final Project Summary Report

Prepared by R. J. Kurtz, R. A. Clark, E. R. Bradley, W. M. Bowen,
P. G. Doctor, R. H. Ferris, F. A. Simonen

Steam Generator Tube Integrity Program/Steam Generator Group Project

Final Project Summary Report

Prepared by
R. J. Kurtz, R. A. Clark, E. R. Bradley, W. M. Bowen,
P. G. Doctor, R. H. Ferris, F. A. Simonen

Pacific Northwest Laboratory
Richland, WA 99352

ABSTRACT

The Steam Generator Tube Integrity Program/Steam Generator Group Project was a three-phase program conducted for the U.S. Nuclear Regulatory Commission (NRC) by Pacific Northwest Laboratory.[a] The main goal of the program was to provide the NRC with validated information on the reliability of nondestructive examination techniques to detect and size flaws in steam generator tubing and to determine the remaining integrity of service-degraded tubing. The information was used to determine the effectiveness of NRC Regulatory Guides 1.83, Rev. 1, and 1.121 to 1) define the frequency, extent and procedure for conducting nondestructive inservice inspections of steam generator tubing, and 2) define plugging limits of service-degraded tubing under normal operating and accident loading conditions. The program was performed in three phases. The first phase involved burst and collapse tests and single-frequency eddy-current (EC) examinations of typical steam generator tubing with precision machined flaws. The goal of Phase I was to develop empirical models of remaining tube integrity as a function of flaw type and size, and to determine the capability of EC inspection methods to detect and size tube degradation. In Phase II, a smaller number of specimens with the same flaw types were investigated, but tube specimens were degraded by chemical means rather than machining methods. This approach was used to better simulate the irregular geometry of service-induced degradation. In the final phase of the program, the retired-from-service Surry 2A Steam Generator was used as a test bed to investigate the reliability of inservice EC inspection equipment, personnel, and procedures, and as a source of service-degraded tubes for further validating the empirical equations of remaining tube integrity. In addition, the generator was also used to study the effects of primary-side chemical decontamination, the effectiveness of secondary-side visual examinations, characterization of tubesheet crevice corrosion products and sludge pile composition, and demonstrations of tube unplugging and repair techniques. This portion of the program also included participation by three foreign countries.

This report summarizes the findings of more than eleven years of research activity on steam generator tube integrity and inspection issues. The results of the Phase I pressure tests on mechanically-flawed steam generator tubing are presented. In addition, the laboratory EC sizing results on those tubes are summarized. A discussion of Phase II pressure test results on chemically-degraded tubes is given, along with a brief overview of leak-rate data for tubes with laboratory-produced axial or circumferential stress-corrosion cracks (SCC). Comparisons with a simple analytical leak rate model are discussed. Laboratory EC estimates of flaw size in Phase II specimens are described. To supplement the laboratory EC data and obtain an estimate of EC reliability to detect and size SCC, results of a mini-round robin involving several firms that routinely perform field inservice inspections are presented.

A major portion of the report is devoted to summarizing and integrating the results from the more than six years of research on the Surry 2A Steam Generator. A brief description of the acquisition, transportation and placement of the steam generator into a specially built examination facility is given. Prior to performing extensive nondestructive examination (NDE) of the generator tubing, dilute chemical decontamination of the channel head and removal of plugs placed during service was performed. To determine a post-service baseline condition of the generator, two nearly 100% multifrequency EC inspections were performed along with visual inspections from the secondary side. From these inspections, a subset of 320 tubes was selected for round robin inspection and development of the data base on EC inspection reliability. A description of the four round robins conducted is provided. A summary of the methods used to remove more than 550 tube segments to validate the round robin inspection data is given. Results from the metallurgical and visual examinations of these specimens are discussed. Burst tests of removed-from-generator specimens with pitting/wastage-type degradation are presented and correlated with the empirical models of remaining tube integrity. Statistical analyses of the combined metallurgical and EC data to determine probability of detection and sizing accuracy are reported along with a discussion of the factors which influenced the results. Analyses and Monte Carlo simulations used to evaluate and compare various sampling plans for inservice inspection are described. Finally, recommendations for improved inservice inspection and maintenance of steam generator tube integrity are given.

SUMMARY

In 1976, the U.S. Nuclear Regulatory Commission (NRC) initiated the Steam Generator Tube Integrity Program (SGTIP) in response to an Atomic Safety and Licensing Board inquiry regarding the existence of NRC data on the integrity of service-degraded steam generator tubes. At that time the available data were limited in quantity and had been generated solely by industry. The NRC authorized the Pacific Northwest Laboratory (PNL) to perform a research program to develop validated information on the reliability and effectiveness of inservice inspection techniques to detect and size tube degradation and the margin-to-failure of service degraded tubes under normal operating and accident loading conditions.

The program was conducted in three phases. The first phase involved burst and collapse tests, and single-frequency EC examinations of typical steam generator tubing with machined flaws. Three flaw types were utilized: uniform wall thinning, elliptical wastage and an axial crack-type flaw that was simulated by an electrodischarge-machined (EDM) slot. These flaw geometries were selected because they simulated the known or expected flaws in pressurized water reactor (PWR) steam generators. Burst and collapse tests were conducted in simulated PWR steam generator chemical and thermal environments in a high-pressure autoclave assembly.

Due to the high burst pressure of unflawed steam generator tubing, even tubing with fairly large flaws had burst pressures higher than could occur during the worst credible burst mode accident. Typically, tubes with flaws less than 80% through-wall had burst pressures higher than would be experienced during such accident conditions. All of the collapse pressures of the flawed tubing specimens were higher than would occur during the worst credible collapse mode accident.

The laboratory EC test results showed that single-frequency EC techniques did not accurately size many of the machined flaw geometries. However, it was also shown that the current plugging practices are conservative from the viewpoint of margins-to-failure for the machined flaws studied.

Phase II of the program continued the tube integrity and EC examination work of Phase I, but tube specimens were flawed by chemical means rather than machining methods. This approach was chosen to better simulate service-induced flaw geometries and thereby validate the equations developed in Phase I. Uniform-thinning and elliptical-wastage specimens were produced by electroetching techniques, and stress-corrosion-crack-type degradation was created by autoclaving mill-annealed tubing in a water environment with impurity additions.

The Phase II burst and collapse tests were also performed in a simulated PWR steam generator environment. Phase II failure pressures showed the same general trends as the Phase I results with similar data scatter. Burst pressures of SCC-flawed tubes were about 10% higher, on the average, than those measured from the EDM slot flaw simulations. On the other hand, burst pressures of uniform-thinning and elliptical-wastage flaws were less than 10%

lower, on the average, than those predicted from the Phase I empirical relationships. Thus, additional conservatism for evaluation of uniform-thinning and elliptical-wastage type flaws from the Phase I relationships may be justified.

A review of the available leak-rate data for SCC-flawed steam generator tubes subjected to normal operating and accident pressure differentials indicated that the measured leak rates were highly variable when compared to analytical predictions. Predicted leak rates were, in some cases, ten times greater than measured. Nevertheless, most (but not all) of the tubes leaked at detectable rates for normal operating conditions and none of the tubes burst at main-steam-line-break accident loadings. The data suggest that a substantial level of conservatism should be applied to predictions of leakage that are used for leak-before-break evaluations, and that such conservatism would also appear appropriate for establishing leak detection limits for detection systems.

Laboratory EC measurements of SCC depths indicated that this type of flaw was, on the average, undersized, with the data displaying a great deal of scatter. Elliptical-wastage and uniform-thinning flaws were more accurately sized than SCC, with less scatter observed. Flaw sizing conservatism increased as the amount of material removed by the degradation mechanism increased. Thus, uniform-thinning specimens were the most conservatively sized flaw geometry.

The Phase I and II single-frequency EC results discussed above should be considered only as a rough indicator of EC capability, since 1) the tests were conducted under non-blind laboratory conditions and 2) the test specimens all had idealized flaws and no complicating factors to simulate real-world conditions, such as copper deposits, denting, support plates, and antivibration bars. In addition, the tests were performed so that inspectors were aware of the type of degradation being examined. The Phase III Surry investigation provided a unique opportunity to gather NDE reliability information on tubes with service-induced degradation and extraneous effects under simulated field conditions using multifrequency EC equipment. Thus, the information developed more closely represents the reliability of actual inservice EC inspections rather than a measure of the capability of the equipment to detect and size degradation under ideal conditions.

Phase III of the SGTIP because of its ambitious scope was organized as the Steam Generator Group Project (SGGP). In this phase the retired-from-service Surry 2A Steam Generator was used to 1) provide additional validation of the tube integrity equations through burst testing of service-degraded specimens, and 2) provide an extensive data base on the reliability of conventional and near-term field practice EC inspection techniques to detect, characterize and size degradation in an actual steam generator under simulated field conditions. The SGGP was performed for the NRC with additional participation by the Electric Power Research Institute (EPRI) and consortia from France, Italy and Japan that included both industry and government organizations.

The Surry 2A steam generator was transported by barge to the Hanford Reservation near Richland, Washington. It was stored while the Steam

Generator Examination Facility (SGEF) was completed. The SGEF was specifically designed and constructed to house a removed-from-service steam generator in its normal operating position. After completion of the SGEF, the generator was placed into the facility by lowering it through a removable roof panel. Radiological mapping of the generator and facility was then conducted. A visual examination of the secondary side through shell penetrations originally made at the Surry site and additional penetrations made at Hanford then followed. These examinations confirmed that the generator condition had not significantly changed during shipment to Hanford. The secondary-side examinations proved useful for qualitatively identifying conditions that could lead to loss of steam generator integrity such as sludge accumulation at the top of tube sheet or corrosion in the tube-to-tube support-plate crevice. However, these observations did not provide quantitative information on remaining tube integrity, except in cases of gross tube damage.

Following generator installation in the SGEF, the generator was prepared for extensive nondestructive characterization from the primary side. First, the channel head was decontaminated, using a different dilute chemical technique on each side (hot-leg and cold-leg). This resulted in an approximately 10-fold decrease in the radiation field in the channel head, with no significant corrosive effects observed from the decontamination solutions on the channel-head materials. Personnel dosimetry monitoring of channel-head workers indicated that exposure to the eyes was the limiting exposure. After this, 969 explosively placed tube plugs, used to remove tubes from service that were degraded or possibly subject to degradation, were machined out. This was performed to permit access to these tubes for nondestructive inspection.

To characterize the number, type and distribution of tubing defects, 100% of the accessible tubes were examined using multifrequency EC techniques. Two separate examinations were performed using field-experienced teams, one using Zetec personnel and MIZ-12 equipment and the other Intercontrole personnel and IC3FA equipment. The intent of these examinations was to determine as best possible the overall condition of the steam generator, and allow selection of a subset of tubes for more detailed round robin studies.

Following completion of the base-line inspections, a subset of 320 tubes was selected for additional NDE inspection and analysis. Four separate but related round robin exercises were conducted. The initial round robin involved data acquisition and analysis by five teams utilizing the Zetec MIZ-12 system and DDA-4 analyzer. This was followed by a nine team data analysis round robin, with all teams analyzing an identical set of Zetec MIZ-12 eddy-current signals. An equivalent round robin was also held in Europe, with teams from Italy and France analyzing signals acquired with Intercontrole IC3FA equipment. An advanced/alternate techniques round robin consisting of NDE inspections with equipment or analysis procedures significantly different from those used in either the base-line or other round robin inspections was also performed. The data from the various examinations were analyzed to establish the variability in defect detection and sizing. This information was used to determine locations for removal of specimens for destructive metallographic validation.

To validate the NDE round robin results and determine the condition of the Inconel 600 [a] tubing, more than 550 tube segments were selected and removed from the generator for metallurgical examinations and burst testing. Emphasis was given to selecting specimens where EC indications had been reported. However, specimens without EC defect indications were also removed to verify the lack of defects or to establish the condition of the tubing at specific locations. Specimens from all regions of the generator were removed and examined, although the majority of the defect indications were reported near the top of the tube sheet on the hot-leg side of the generator.

Pitting and wastage were the predominant tube defects found in the specimens examined. This type of tube degradation was identified in the sludge pile region above the top of the tube sheet (TTS), within the tube-to-tube support-plate (TSP) crevice, and to a lesser extent at antivibration bar (AVB) contact areas. The most severe pitting/wastage degradation was located in the region 0 to 2 in. above the hot-leg TTS where wall-losses ranged up to 87%. Wide variations in the distribution and depth of local degraded areas were observed both axially and circumferentially within the corroded region of the hot-leg TTS specimens. These variations in defect distributions appear to be a major factor in the variability of the EC depth estimates. In general, wall-loss from pitting/wastage type degradation in specimens from other regions of the generator was less than 20%.

Intergranular stress corrosion cracking was also identified by visual and metallurgical examinations at specific locations within the generator. Cracking was observed at the apex of Row 1 and Row 2 U-bends which was attributed to stresses produced by inward movement of the U-bend legs from corrosion of the seventh (uppermost) TSP. Denting at the TSP intersections also produced cracking in tubes removed from the hot-leg side of the generator. Axial cracks initiated on the inner surface were found in specimens with calculated strains as low as 10%. Calculated strains greater than 60% were required to produce cracking from the outer surface.

Burst testing showed that pitting/wastage type defects did not appreciably degrade tube strength. Comparison of the data with the empirical relationships of tube integrity developed in Phase I indicates these relationships adequately predict tube margin-to-failure. Defect length was found to be an important consideration in proper defect evaluation. The EC estimates of pitting/wastage depths were used to estimate remaining tube integrity. Since the EC inspection teams did not report defect length, the reported defect depths in combination with a defect length greater than or equal to one tube diameter was assumed. By assuming a long axial length, a conservative estimate of remaining tube integrity was obtained even when EC significantly undersized the defect depth.

The probability of detection (POD) depends on the location and severity of the defects. The POD for pitting/wastage type defects at the TTS increased with wall-loss and approached 0.9 for defects with greater than 40% through-

---

(a) Inconel is a registered trademark of INCO Alloys International (Huntington Alloys), Huntington, West Virginia.

wall penetrations. Conversely, signals due to denting at the TSP intersections interfered with the EC signals from cracks and the POD was near zero for these locations. Insufficient numbers of other defect types and locations where EC inspections were made precluded additional POD evaluations.

Wide variations in the reported EC depth estimates were observed between specimens with similar wall-loss and also within the same specimen for data from different inspection teams. The team-to-team variations for a given specimen appear to result from differences in analysis procedures or the analyst's interpretation of the complex EC patterns. Defect morphology and distribution within the corroded region was considered the major cause for the variations between specimens with similar wall-loss. However, dents and surface deposits near the defects also contributed to the sizing variations. In general, EC tended to undersize the pitting/wastage type defects, especially for the severely-degraded specimens. Improved sizing accuracy was noted for one team that employed special frequency mixes to enhance the signal-to-noise ratio by suppression of signals due to denting, copper deposits and support plates. Also, ultrasonic and rotating EC probes were successfully used to augment conventional EC/bobbin-coil data to obtain improved sizing of pitting/wastage.

Results from a mini-round robin performed with laboratory SCC-flawed tubes showed that sizing depth and length were highly variable. Assessments of remaining tube integrity based on EC estimated flaw dimensions and burst test results were conservative, except for a few cases in which the level of conservatism was somewhat less than the factor of safety of three currently specified for the normal operating condition. Further, the best average probability of detecting SCC for all inspection techniques was 0.63, indicating that crack detection was difficult.

Analysis of various candidate inservice inspection sampling plans indicated that even with 100% inspection most teams that inspected the steam generator would, on the average, detect and plug about 65% of the defective tubes (taken as $\geq$75% through-wall degradation). In contrast, the best performing team could be expected to identify about 95% of the defective tubes. Analytical studies and Monte Carlo simulations demonstrated that a 40% systematic sequential sampling plan was almost as effective as 100% inspection, assuming some clustering of degraded tubes. The simulation work also showed that all systematic sequential sampling schemes examined (20%, 40%, and 100%) were equally effective when the defective tubes are surrounded by large numbers of degraded and defective tubes.

ACKNOWLEDGMENTS

Ansaldo Componenti S.p.A.

R. De Santis
T. Badino
R. Gammino

Ansaldo S.p.A

F. Magris
M. Barberis

Energia Nuclear Ed Energie Alternativa

M. Cavaggioni
M. Brocco
F. Imperiali

Ente Nazionale Per L'Energia Elettrica

V. Regis
R. Pascali
G. Maciga
F. Bregani

Nuclear Power Engineering Test Center

M. Oishi
K. Ohno
H. Nakata

University of Tokyo

Y. Togo
H. Madarame

Mitsubishi Heavy Industries

O. Takaba

VEPCO

H. S. McKay

CONTENTS

FIGURES

TABLES

1.0 PHASE I SUMMARY

The objective of the Steam Generator Tube Integrity Program (SGTIP) was to experimentally determine the margin-to-failure and inspection reliability of degraded steam generator tubes. The program was initiated in 1976 by the NRC in response to an inquiry regarding the existence of NRC data on the integrity of service-degraded steam generator tubes. The initial program plan called for a three phase effort. The first phase involved burst and collapse testing and eddy current examination of typical steam generator tubing with machined flaws. The second phase of the SGTIP continued the integrity testing and NDE work of Phase I, but tubes were degraded by chemical means rather than machining methods. The third phase of the SGTIP was to validate the results from Phases I and II by testing tubes with service-induced flaws.

This section summarizes results of Phase I of the SGTIP. A detailed presentation of the experimental data and interpretation may be found in the Phase I Report by Alzheimer et al. (1979). During Phase I, segments of Inconel 600 steam generator tubing manufactured in accordance with 1977 practice were artificially degraded, then burst and collapse tested to determine the remaining margin-to-failure as a function of degradation type and size. The four common types of steam generator tube sizes used in the United States were tested. All specimens were tested under simulated steam generator operating conditions. In addition, single-frequency eddy-current (EC) examinations were performed on each degraded tube segment to assess the capability of EC techniques to detect and size machined wall-loss degradation.

1.1 TUBE INTEGRITY TESTS

Three forms of machined degradation were employed in the Phase I work. These included uniform-thinning, elliptical-wastage (localized wall thinning) and an electrodischarge-machined (EDM) slot representation of crack-like degradation. Figure 1.1 gives a schematic of each degradation type and Table 1.1 lists the range of dimensions used for each degradation type.

After machining each degradation type in each specimen, the dimensions of the degraded zone were determined by plastic replication. Specimens were tested at Pressurized Water Reactor (PWR) steam generator operating temperatures under controlled loading conditions. In all, over 500 specimens were tested.

Burst-test results on 0.875-in. diameter x 0.050-in. wall-thickness tubing with each type of degradation are given in Figures 1.2 to 1.6. These data typify the results for all tube geometries tested. The burst data were nondimensionalized by dividing the burst pressure of a degraded tube by the burst pressure of a nondegraded tube to minimize the effect of material property variations. Figures 1.2 and 1.3 show the effect of increasing degradation length on normalized burst pressure for different depths of EDM-slot and uniform thinning, respectively. The effect of variable elliptical-wastage length was not examined in this study, so no plot is presented. The normalized burst pressure was observed to decrease rapidly as

TABLE 1.1. Range of Degradation Dimensions

Flaw Type	Depth, %	Length, in.	End Radius, in.	Wrap Angle, °
EDM Slots	25-30	0.25	0.01-0.02	NA
	55-60	0.5		
	80-90	1.5		
Elliptical Wastage	25-30	≈1.5	NA	0
	55-60			45
	80-90			135
Uniform Thinning	25-30	0.188	0.063	NA
	55-60	0.375		
	70-80	0.75		
		1.5		

NA = Not Applicable.

degradation length increased. This effect tended to saturate for degradation
lengths greater than or equal to about one tube diameter. Figures 1.4 to 1.6
give plots of normalized burst pressure as a function of degradation depth
for different degradation lengths. It is evident from these plots that the
burst pressure decreased with increasing depth of degradation for fixed
degradation length. The elliptical-wastage data presented in Figure 1.6 was
partitioned with respect to wrap angle (i.e., circumferential extent of the
degraded zone) to determine if this variable had an affect on the resulting
burst pressure. No significant effect was observed for the range of wrap
angles investigated.

Empirical equations were developed from the test data by least squares
curve-fitting techniques. The curve fit equations developed were:

For EDM Slots

$$\Delta P/\Delta P_0 = 1 - (h/t) + (h/t)\exp\{-0.373\ L/\sqrt{Rt}\} \tag{1.1}$$

For Uniform Thinning

$$\Delta P/\Delta P_0 = (1 - h/t)^{1 - \exp\{-0.13\ L/\sqrt{R(t-h)}\}} \tag{1.2}$$

For Elliptical Wastage

$$\Delta P/\Delta P_0 = (1 - h/t)^{0.604} \tag{1.3}$$

(a) EDM SLOT

(b) ELLIPTICAL WASTAGE
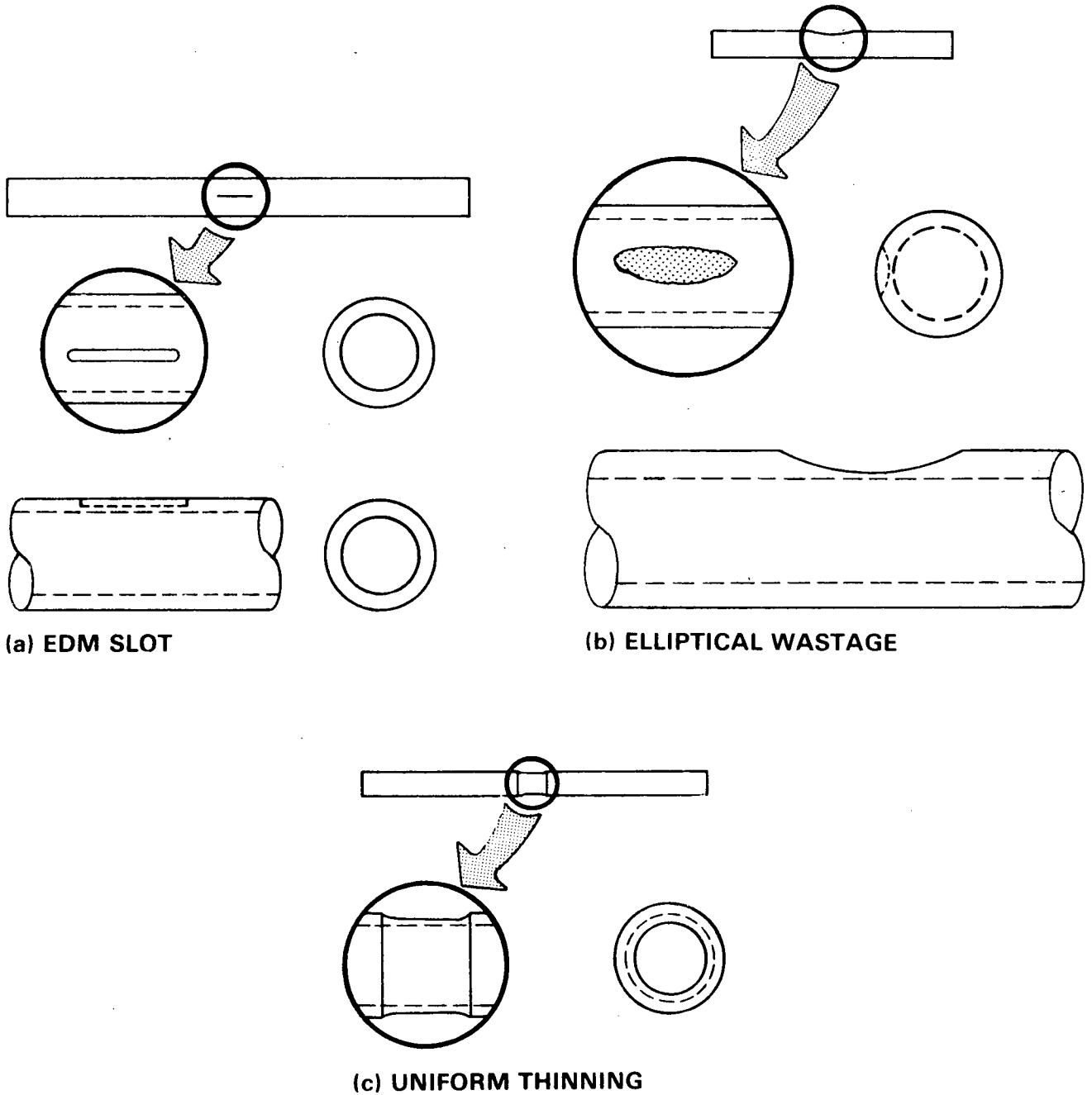
(c) UNIFORM THINNING

FIGURE 1.1. EDM-Slots, Elliptical-Wastage, and Uniform-Thinning Wastage Flaw Specimens
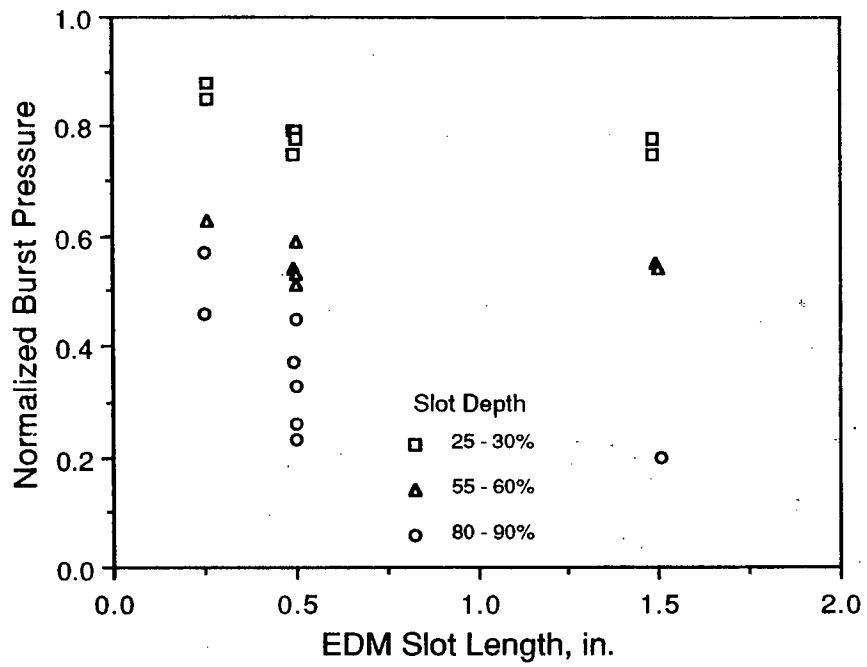
FIGURE 1.2. Normalized Burst Pressure vs
EDM Slot Length for 0.875-in.
x 0.050-in. Tubes
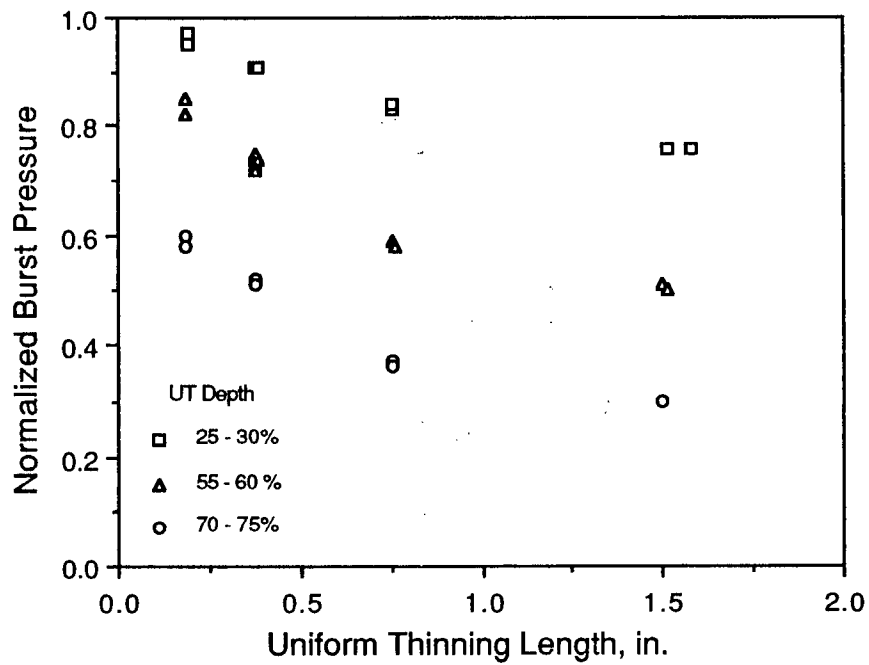
FIGURE 1.3. Normalized Burst Pressure vs
Uniform-Thinning Length for
0.875-in. x 0.050-in. Tubes

1.4
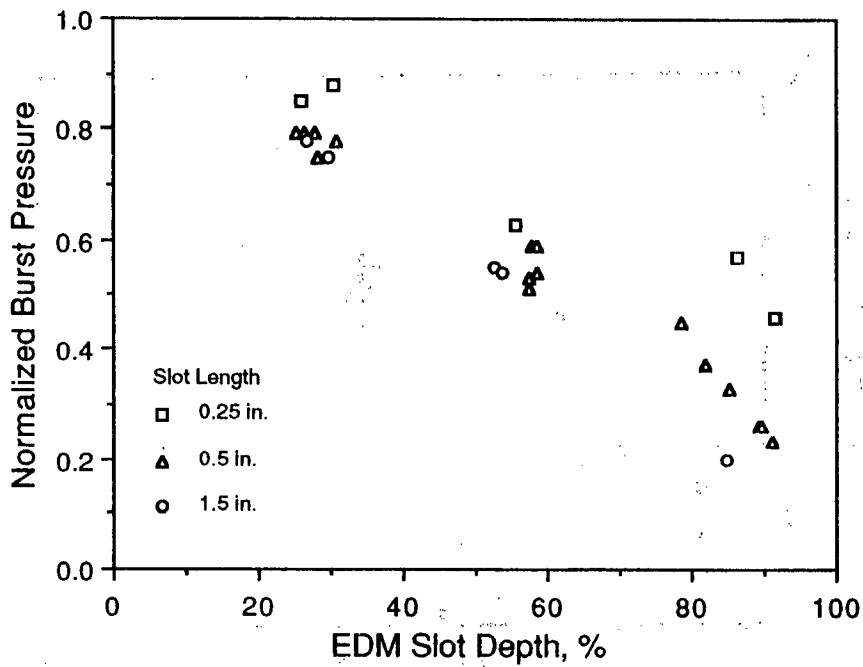
FIGURE 1.4. Normalized Burst Pressure vs
EDM-Slot Depth for
0.875-in. x 0.50-in. Tubes
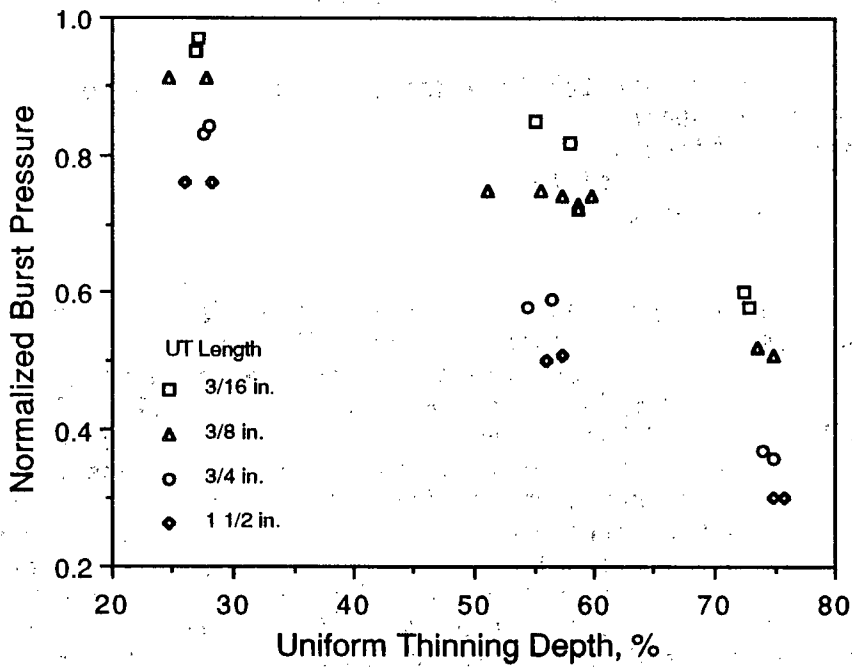
FIGURE 1.5. Normalized Burst Pressure vs
Uniform-Thinning Depth for
0.875-in. x 0.050-in. Tubes

1.5
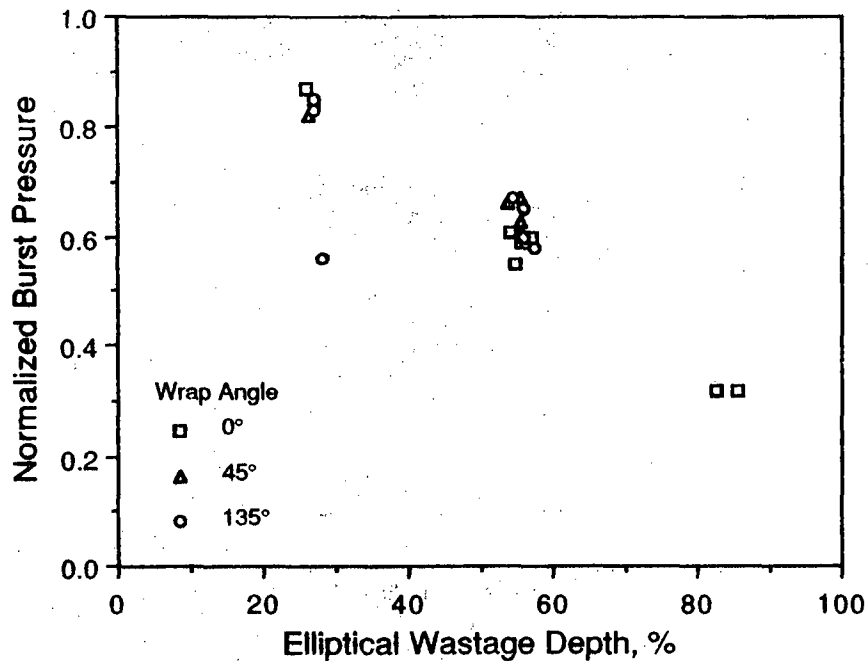
FIGURE 1.6. Normalized Burst Pressure vs
            Elliptical-Wastage Depth
            for 0.875-in. x 0.050-in. Tubes

where $\Delta P/\Delta P_0$ = Ratio of defected to undefected burst pressures
        h = Defect depth
        t = Wall thickness
        R = Inner radius of tube
        L = Defect length

    These equations are applicable to all of the different sizes of steam
generator tubing tested. In addition, three different strength levels of a
single tubing size were tested and the equations are valid for tubing with
yield strengths ranging from 40 ksi to 48 ksi. Figures 1.7 to 1.9 give plots
of the predicted normalized burst pressure versus the measured normalized burst
pressure for the 0.875-in. diameter x 0.050-in. wall-thickness tubing degraded
with EDM slots, uniform thinning and elliptical wastage, respectively. The
diagonal line in the plots corresponds to the line of perfect agreement
between predicted and measured values. Note the predicted burst pressures
for uniform-thinning and elliptical-wastage degradation agreed quite closely
with measured values. In contrast, the EDM slot data displayed more scatter.
This was due to greater variation in the uniformity of the EDM slot
degradation. Some of the EDM slot specimens had fairly straight walls and
flat bottoms; whereas, other specimens had slot widths and depths that were not
uniform along the length.
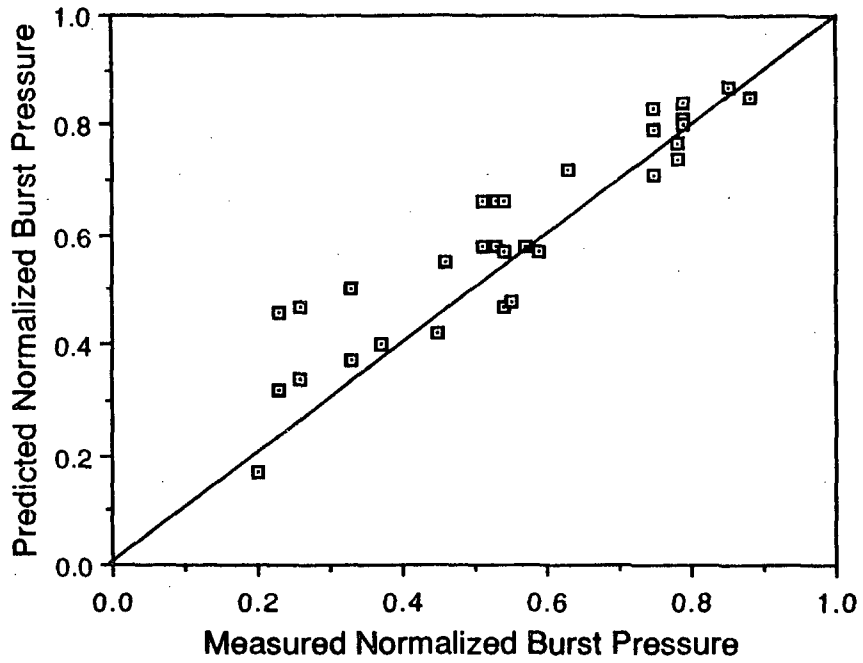
FIGURE 1.7. Predicted Normalized Burst Pressure (EDM-Slot
Eqn.) vs Measured Normalized Burst Pressure for
0.875-in. x 0.050-in. Tubes
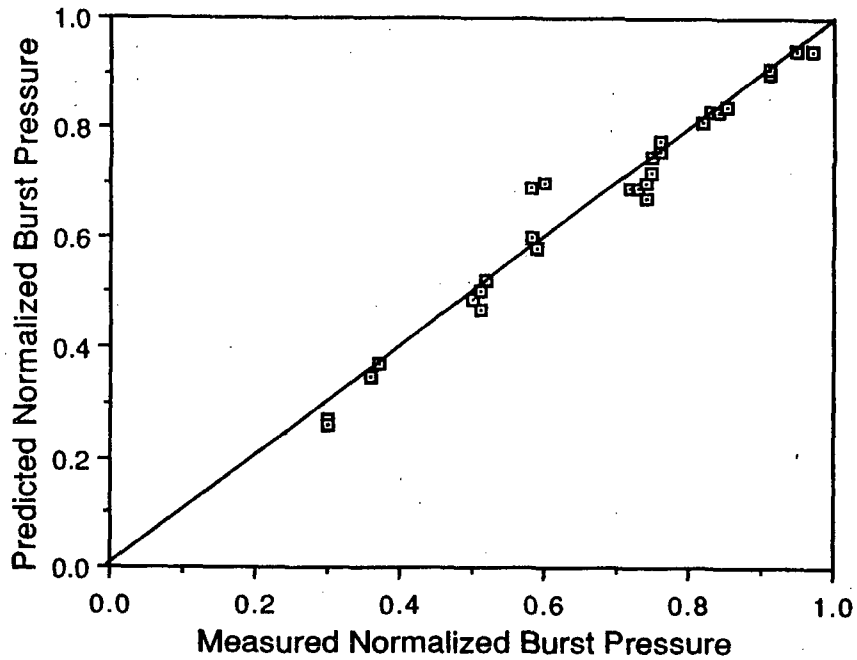
FIGURE 1.8. Predicted Normalized Burst Pressure (Uniform-
Thinning Eqn.) vs Measured Normalized Burst
Pressure for 0.875-in. x 0.050-in. Tubes
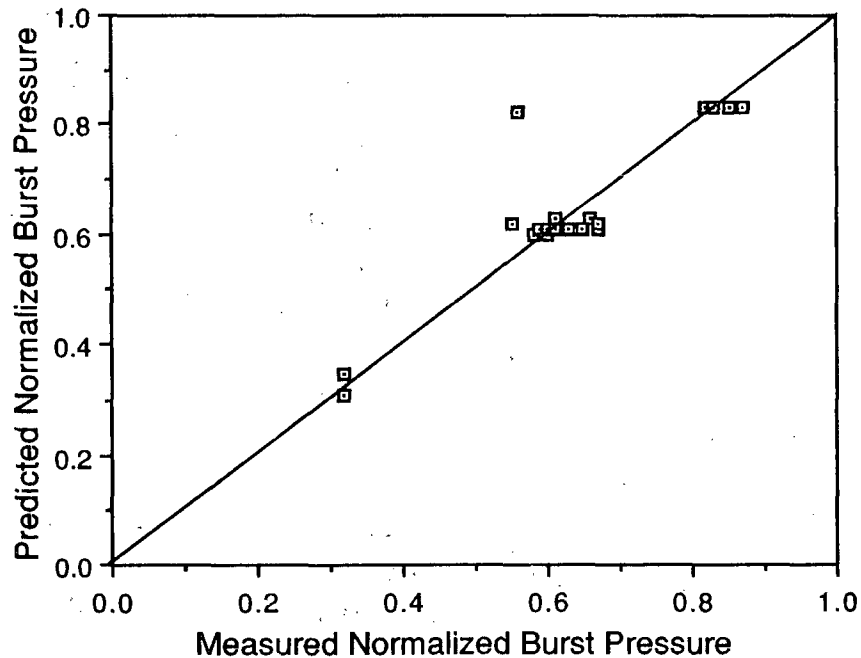
Predicted Normalized Burst Pressure (Elliptical-
Wastage Eqn.) vs Measured Normalized Burst
Pressure for 0.875-in. x 0.050-in. Tubes

It is instructive to compare the burst pressure equations for the above
flaw types versus flaw length for three through-wall depths, as shown in
Figure 1.10. Note the similarity of the EDM slot and uniform-thinning
equations over the full range of defect dimensions. Conversely, the
relationship for elliptical-wastage flaws consistently gives higher indicated
burst pressures for the same length and depth of flaw compared to an EDM slot
or a uniformly-thinned specimen.

A plot of the measured normalized burst strengths for all three flaw types
versus values predicted from the tables presented in Section XI, Subsection
IWB-3640 of the American Society of Mechanical Engineers (ASME) Code (1986)
is shown in Figure 1.11. The replicated flaw depths and lengths were
substituted into the ASME equation to compute the predicted burst strengths.
It is evident from the results that the ASME equation gives conservative
results in most cases, especially when the actual normalized burst pressure
is below 0.5. The ASME equation was developed for analysis of axial flaws in
degraded stainless steel piping. Hydraulic failure of stainless steel piping
is controlled by net section yielding of the unflawed ligament. Thus, it
seems reasonable to postulate that Inconel 600 steam generator tubes fail by
the same mechanism.
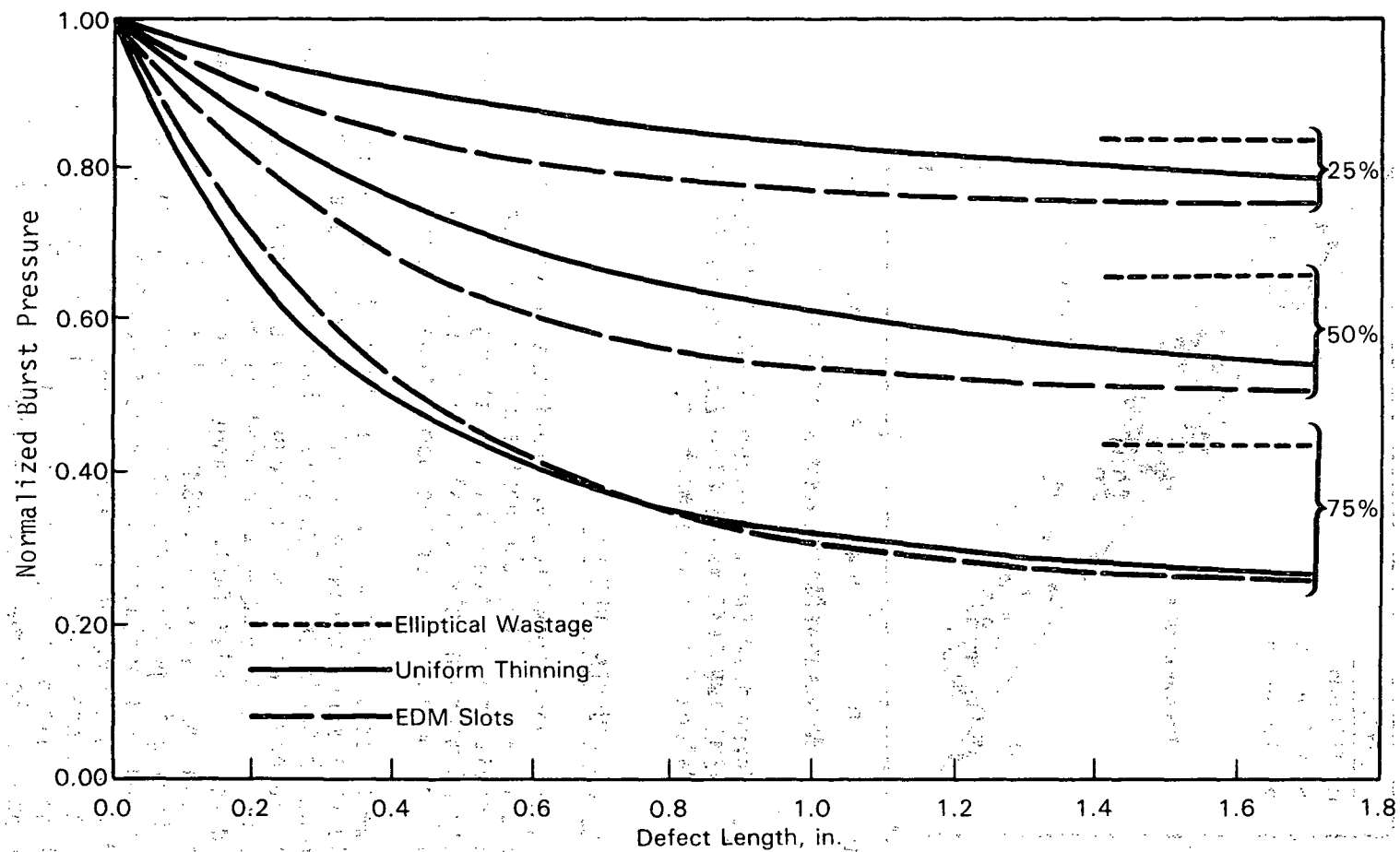
FIGURE 1.10. Comparison of Burst Pressure Equations for Elliptical Wastage, Uniform Thinning, and EDM Slots
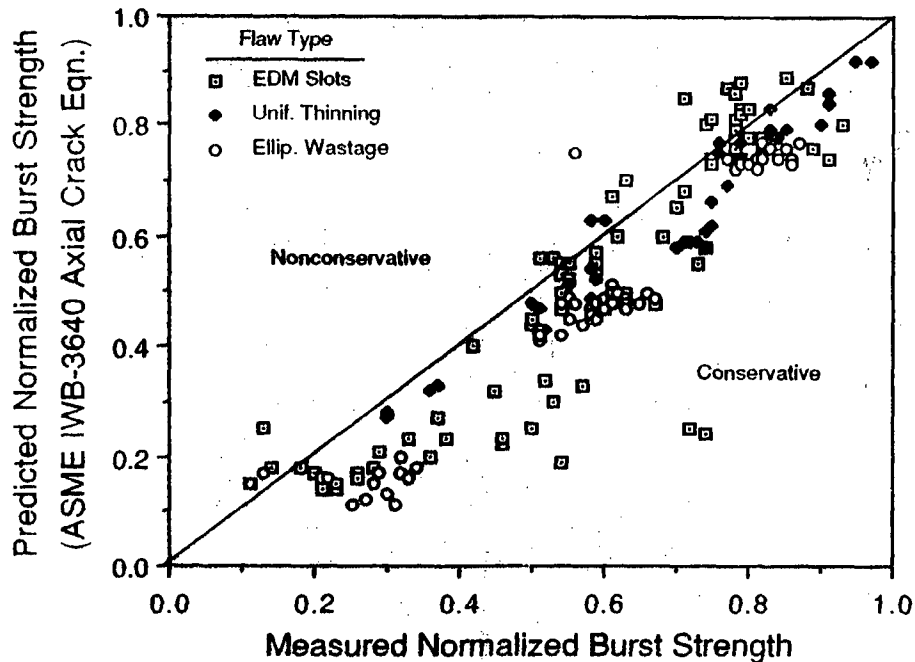
FIGURE 1.11. Normalized Burst Pressure Predicted from the ASME IWB-3640 Axial Flaw Equation vs Actual Values for Phase I Machined Flaws

1.2 SINGLE-FREQUENCY EDDY-CURRENT RESULTS

After developing the above constitutive equations between defect size/geometry and remaining tube strength, the next step was to relate eddy-current inservice inspection results to the tube failure strength. It is desirable to know how accurately EC measures the actual flaw size. Knowledge of EC error would result in appropriate use of the above tube integrity equations.

The Phase I nondestructive testing and evaluation effort focused on single-frequency (400 kHz) eddy-current examination of each defect type. An EM-3300 test instrument, a Gould Brush 220 strip-chart recorder and a Hewlett-Packard magnetic tape recorder were used to acquire the EC inspection data. Several differential bobbin-coil probes were used for the inspections, depending on tubing diameter. Fill factors ranged from 0.78 to 0.87. Each probe was calibrated using an appropriate ASME flat-bottom hole standard for each tube diameter. During inspection the specimens were positioned horizontally and examined by translating the probe through the tube until a scan of the degraded zone was completed. A recording of the instrument response was made as the probe was pulled back through the tube at a constant rate. Nonsymmetrical degradation (i.e., degradation not uniformly distributed around the circumference of the tube such as elliptical wastage and EDM slots) was examined in three orientations. The specimen was initially placed with the degraded area oriented at 0° (zenith); then the tube was successively rotated and tested with the degraded zone in the 90° (horizontal) and 180° (downward)

positions, respectively. The results from the three test records were averaged to minimize the effect of probe-to-degradation spacing and variations caused by probe wobble and misalignment.

The EC estimates of EDM-slot, elliptical-wastage and uniform-thinning depth for all tubing geometries versus actual degradation depth are plotted in Figures 1.12 to 1.14. It is evident from these figures that the accuracy of degradation depth sizing depended on the volume of metal removed by the degradation mechanism (i.e., degradation volume). For small-volume degradation such as EDM slots, and elliptical wastage, EC overestimated the depth when the degradation was shallow. As the actual depth increased, the EC results reverted from an overestimate of depth to an underestimate. The degree of undersizing continued to increase with increasing degradation depth. For large volume degradation, such as uniform thinning, EC consistently overestimated flaw depth.

To quantify these trends, a linear regression, $Y = A(X) + B$, was curve fit to the data, where Y is the EC estimated degradation depth and X is the actual depth. Table 1.2 gives the results from these calculations. The column denoted "Number" in the table refers to the number of data points in the curve fit, and the column denoted "R" gives the correlation coefficient. It is evident from these results that the smallest volume degradation type, EDM slots, yielded the highest intercept and lowest slope. The intermediate volume degradation, elliptical wastage, gave the smallest intercept and an intermediate slope. The large volume degradation type, uniform thinning, produced an intermediate intercept and the highest slope. A plot of these equations shows that oversizing was greatest for the EDM-slot flaw for degradation less than 20% through-wall, with the elliptical-wastage flaw oversized the least for flaws in this range. Uniform thinning was on the average oversized at all depths, with the magnitude decreasing from 16% at shallow flaw depths to about 6% for the deepest thinning. Undersizing of EDM slots and elliptical wastage began at about 60% through-wall penetration and increased with increasing flaw depth, with EDM slots being undersized more than elliptical wastage of equal depth. The EC results on machined flaw types clearly illustrate the difficulty of accurately measuring flaw depth for EDM slot and elliptical wastage flaw types. This is an important result since as flaw depth increased, the EC estimated depth was increasingly nonconservative.

TABLE 1.2. Phase I Single-Frequency EC Depth-Sizing Models

Type	Intercept	Slope	Number	R
EDM Depth	26.7	0.52	119	0.65
EW Depth	11.5	0.77	114	0.88
UT Depth	17.4	0.87	62	0.95
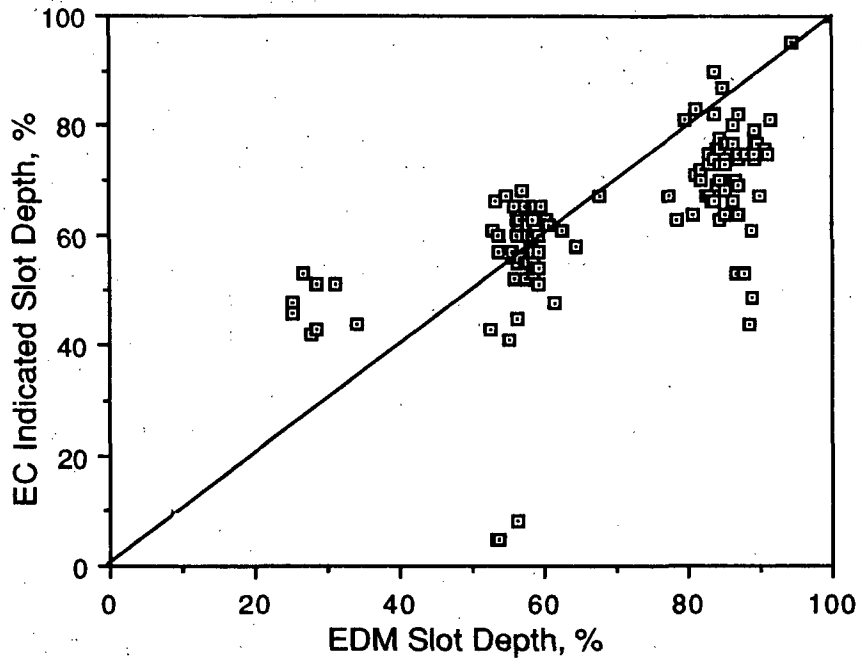
FIGURE 1.12.   EC-Indicated vs Actual
EDM-Slot Depth
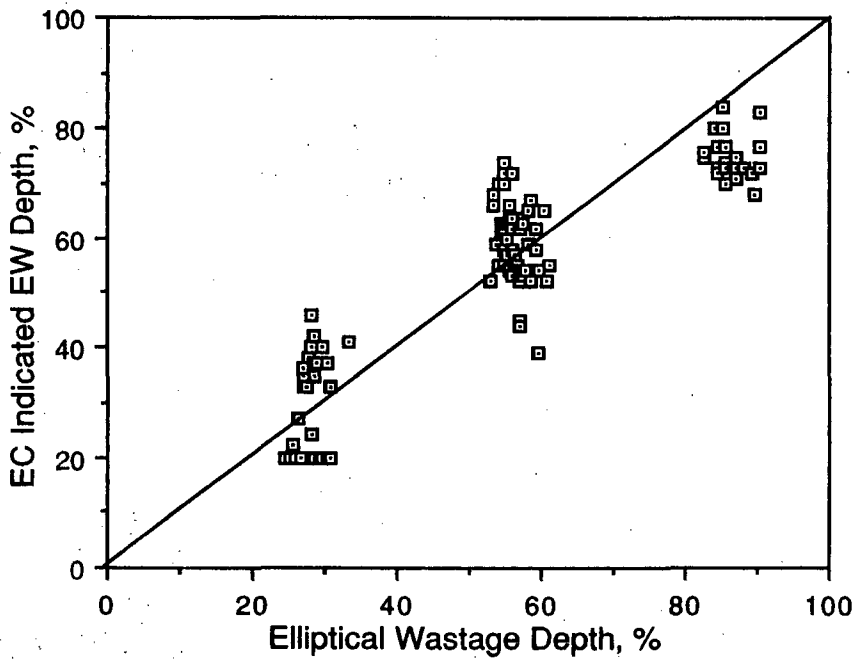
FIGURE 1.13.   EC-Indicated vs Actual
Elliptical-Wastage Depth

1.12
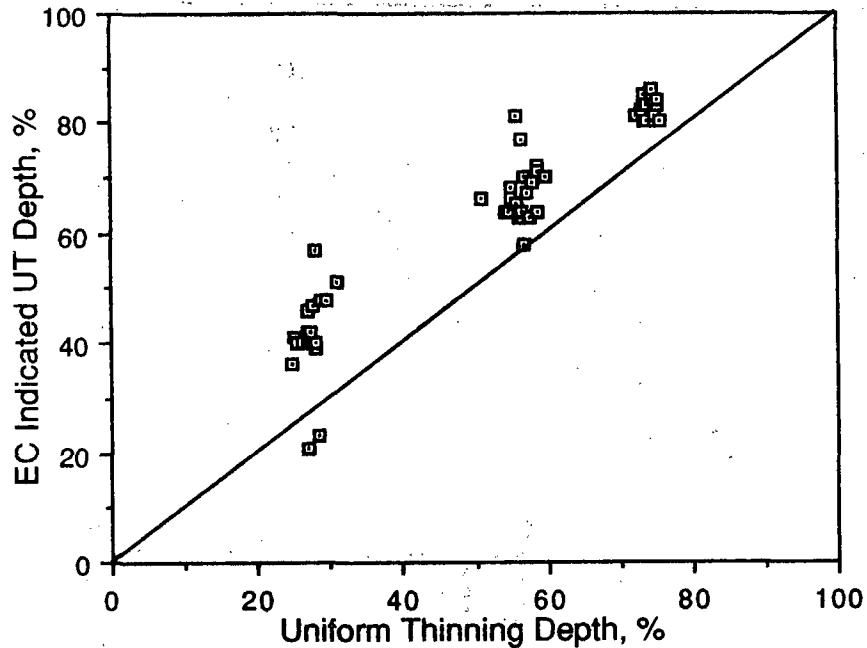
FIGURE 1.14. EC-Indicated vs Actual Uniform-Thinning Depth

The accuracy of degradation length sizing was also investigated from the Phase I EC data as shown in Figures 1.15 and 1.16 for EDM slots and uniform thinning, respectively. The results indicate the average EC estimated flaw length was quite close to the actual value. This is reflected in the linear regression results shown in Table 1.3. Note the equations for both flaw types have very similar intercept and slope numbers.

TABLE 1.3. Phase I Single-Frequency EC Length-Sizing Models

Type	Intercept	Slope	Number	R
EDM Length	-0.04	1.03	169	0.96
UT Length	-0.02	1.02	42	1.00

It was mentioned above that tube burst strength depended strongly on flaw length. Based on the above equations one would conclude that length sizing of both small and large volume defects is very accurate, since for degradation greater than 0.6-in. long the difference between calculated and actual values is less than ±3%. However, the EC data on EDM slots display considerably more scatter than for uniform-thinning degradation as depicted in Figure 1.15.

1.13
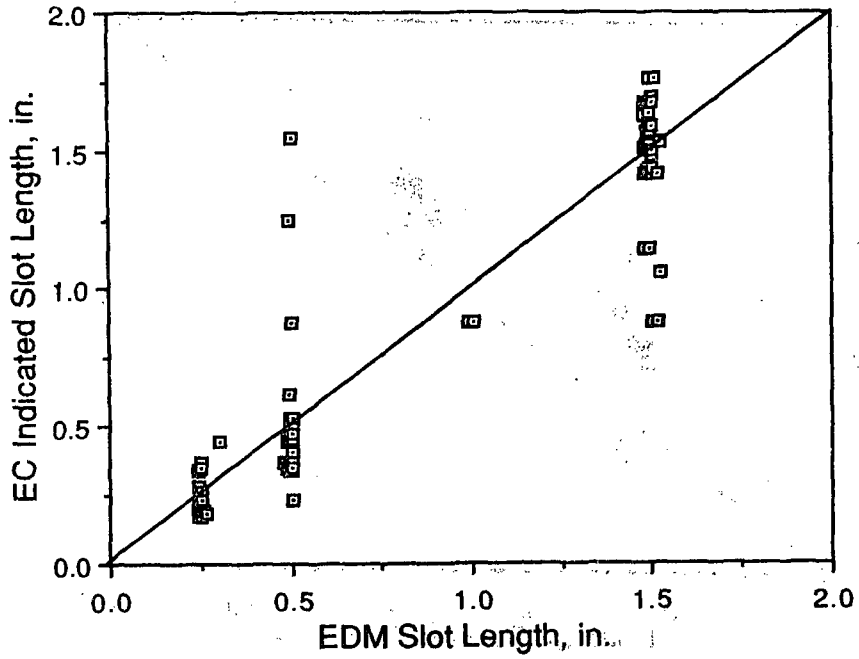
FIGURE 1.15.   EC-Indicated vs Actual
EDM-Slot Length
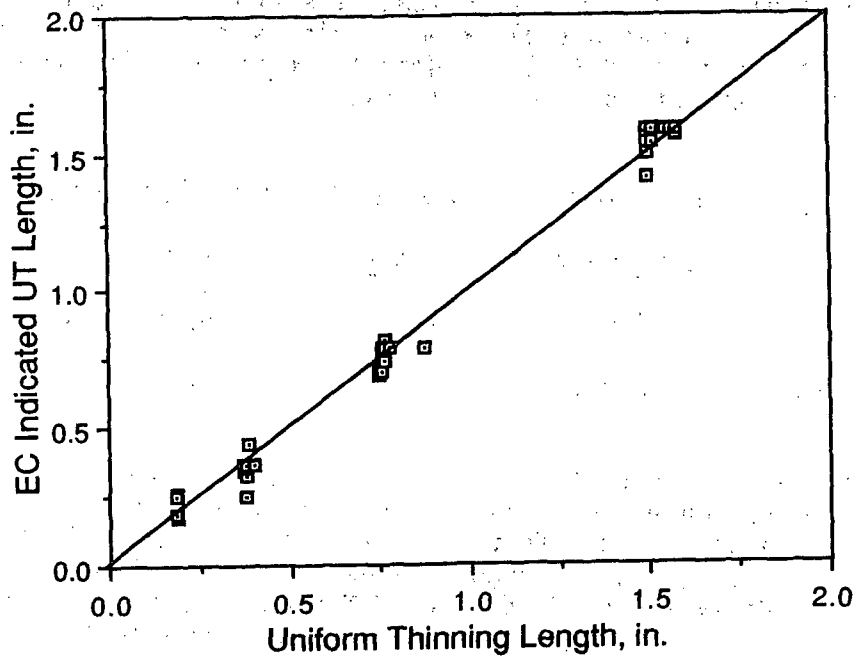
FIGURE 1.16.   EC-Indicated vs Actual
Uniform-Thinning Length

1.14

For example, slots 0.5-in. long had EC estimated lengths ranging from 0.228 in. to 1.545 in., and for 1.5-in. slots the range was between 0.880 in. and 1.760 in. Thus, it may be concluded that length sizing of small- and large-volume machined degradation was fairly accurate, but measurement precision was acceptable only for large volume degradation.

2.0 PHASE II SUMMARY

This section summarizes the results of Phase II of the SGTIP. The objectives of Phase II were to perform burst, collapse, leak-rate and EC testing of representative steam generator tubing with chemically-induced degradation to validate and refine the empirical relations developed during Phase I. It was considered necessary to test the Phase I constitutive equations against specimens containing flaws more closely simulating actual service-induced degradation. Of particular importance was the effect of the methods used to introduce the tube degradation on the reliability of EC to characterize those flaws. Phase II of the SGTIP utilized a considerably reduced number of specimens compared with Phase I. The flaw geometries and sizes represented a subset of the Phase I specimen matrix. This section summarizes the tube integrity, leak-rate and nondestructive evaluation results for this portion of the program. A more detailed discussion may be found in a report by Kurtz et al. (1988).

2.1 TUBE INTEGRITY TESTS

The tube integrity specimen matrix for Phase II consisted of 86 chemically-degraded tubes from material heats B, E and F. The tubing from these heats were all 0.875-in. diameter x 0.050-in. wall thickness. It was felt that flaws produced by chemical methods more closely approximate service-induced flaws with respect to variable shape, size, depth and orientation. Three flaw geometries were investigated: stress corrosion cracking (SCC), uniform thinning and elliptical wastage. The flaws were created by exposing segments of tubing to various aggressive environments. Flaw shape, location and orientation were controlled by masking the tubing with Teflon[R] (a) tape.

Results from burst testing of SCC and uniform-thinning degraded specimens are plotted in Figures 2.1 and 2.2, respectively. The measured normalized burst pressures are plotted against calculated values from the appropriate Phase I empirical relationship. These data are typical of Phase II results. As shown in Figure 2.1, the EDM slot constitutive equation, in almost all instances, yielded conservative estimates of remaining tube strength when bounding crack dimensions were used in the evaluation. Figure 2.2 gives burst-test results for uniform-thinning specimens flawed by two different procedures. No significant difference due to the defecting mechanism is evident from the burst-test results. Further, the Phase I uniform-thinning burst equation closely predicted the burst pressure of chemically-flawed tubes with a slight nonconservative trend. This result was typical for elliptical-wastage specimens as well.

The data from Phase II were used to update the Phase I equations. The functional form of the equations was not changed. Wherever appropriate, the constants in the predictive relationships were recalculated by least squares regression analysis using the Phase II data alone and in conjunction with the

---

(a) Teflon is a registered trademark of E. I. du Pont De Nemours and Co., Inc., Wilmington, Delaware.
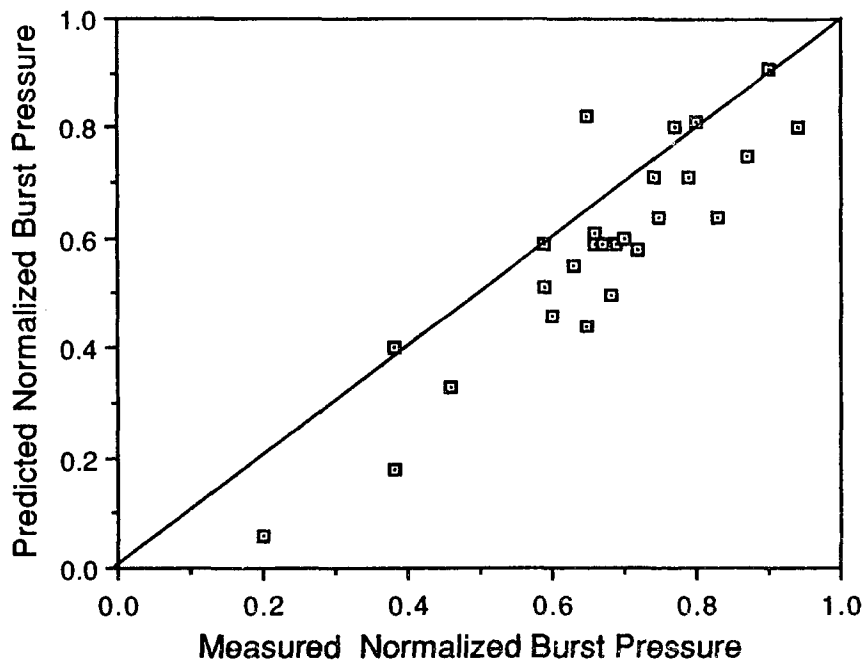
FIGURE 2.1. Predicted Normalized Burst Pressure
(Phase I EDM-Slot Eqn.) vs
Measured Normalized Burst Pressure
for IGSCC-Flawed Tubes
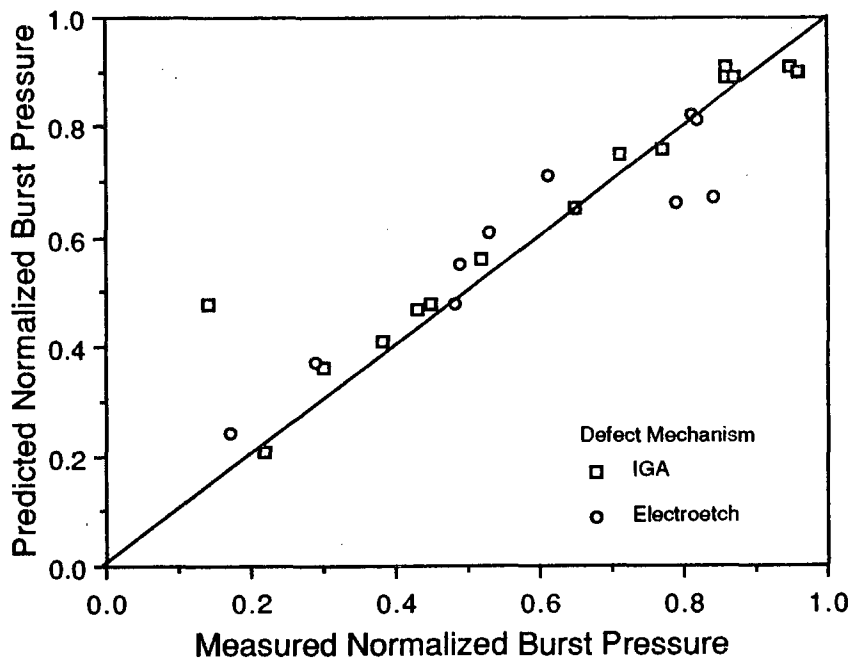
FIGURE 2.2. Predicted Normalized Burst Pressure
(Phase I Uniform-Thinning Eqn.) vs
Measured Normalized Burst Pressure for
Chemically-Produced Uniform Thinning

2.2

Phase I data. Since collapse data for the elliptical-wastage flaw type were very sparse and nonexistent for SCC specimens, the Phase I relationships were not changed. Table 2.1 lists the functional form of the six empirical relationships obtained along with the constant C.

TABLE 2.1. Predictive Failure Equations

| | Values of C | | |
EDM Slot - Burst	Phase I	Phase II	Phase I & II
$\Delta P / \Delta P_0 = 1 - h/t + h/t \exp\{CL/\sqrt{Rt}\}$	-0.373	---	---
Elliptical Wastage - Burst			
$\Delta P / \Delta P_0 = (1 - h/t)^C$	0.604	0.700	0.626
Uniform Thinning - Burst			
$\Delta P / \Delta P_0 = (1 - h/t)^{1 - \exp\{CL/\sqrt{R}(t-h)\}}$	-0.130	-0.200	-0.142
EDM Slot - Collapse			
$\Delta P / \Delta P_0 = 1 - \exp\{CL/\sqrt{Rt}\}$	-2.49	---	---
Elliptical Wastage - Collapse			
$\Delta P / \Delta P_0 = (1 - h/t)^C$	0.396	---	---
Uniform Thinning - Collapse			
$\Delta P / \Delta P_0 = 1 - h/t + h/t \exp\{CL/\sqrt{R}(t-h)\}$	-0.066	-0.118	-0.079

The definitions of the variables in the above equations is the same as given in Section 1.1.

2.2 LEAK-RATE TESTS

This section briefly describes a survey of data from leak-rate tests on tubes with laboratory-produced SCC. The objective of this work was to determine if a crack will leak at a rate that is consistent with the length of crack and the fluid pressure differential across the tube wall. The accuracy of leak-rate predictions is an important consideration in evaluation of leak-before-break analyses and in the determination of leak detection limits as they relate to allowable leak rates given in plant technical specifications.

Three sets of experimental data were utilized in the evaluation. Data from Powell and Hall (1987) and Berge (1987), and data from Battelle-Columbus Laboratories produced under subcontract to the SGTIP. A simple predictive

model was developed to aid in the interpretation and comparison of the data from the various laboratories. This model was adapted from one developed for leakage from axial cracks in reactor pressure vessels described by Simonen et al. (1986). The model used fracture mechanics concepts to predict the crack opening area as a function of crack length and pressure differential across the tube wall. Given this crack opening area, well-known equations from the fluid mechanics literature for flow through an elongated orifice were then used to predict leak rates.

Figure 2.3 shows a representative plot of the leak-rate data at normal reactor operating conditions as a function of axial crack length. Curves giving predicted leak rates are also plotted for comparison with the experimental data points. Powell and Hall (1987) reported crack lengths as bounding values; in Figure 2.3 these are indicated as a line. In examination of the Powell and Hall (1987) data, it was apparent that a large number of tests had a reported leak rate of exactly 0.1 gal/min. This was interpreted as an indication on the sensitivity of the flow rate measurements. It should be noted that for purposes of clarity in displaying the data in Figure 2.3, many of the data points were slightly offset from the 0.1 gal/min value to prevent superposition of data. In addition, Berge's (1987) data were not reported in a tabular format suitable for plotting, so the bounding correlation curves were plotted in Figure 2.3.

The data show a large degree of uncertainty in expected leak rates. This scatter may be substantially reduced by plotting the data as a function of the average crack length. Even with this refinement, some of the data points would still remain as much as a factor of ten from the expected trend line. Some of the reasons for the unpredictability of leak rates may be: 1) small crack openings that could be plugged by impurities in the water; 2) residual stresses from fabrication and precracking of the tube which could cause either crack opening or closure; 3) crack roughness, which can only be approximately estimated and is subject to considerable variation; and 4) the lengths were reported with a wide range of uncertainty, and no doubt differed from the ideal through-wall cracks used in the model.

A representative plot of leak-rate data obtained from experiments conducted at Battelle-Columbus Laboratories (BCL) is shown in Figure 2.4. The results of the BCL tests are presented in an alternate format, since complete traces of pressure, temperature and flow rates for a full range of pressure differentials could be compared with predictions. In Figure 2.4, the measured flow rate as a function of time is shown. The length of axial crack in the specimen was determined as between 0.5 in. and 1.0 in. The end-of-test flow rate reached a maximum level of about 1.6 gal/min, corresponding to a pressure in the range of 2200 psi (simulating a steam line break condition). For the lower bound crack length of 0.5 in., the predicted flow rates were somewhat less than those measured in the test. However, the differences between prediction and measurement were well within the variation expected on the basis of the uncertainty in crack length. For example, when the upper bound of 1.0 in. was used for the crack length, the model over predicted the flow rate by a factor of about 60. The measurement and prediction would be in very good agreement for an assumed crack length of 0.6 in.
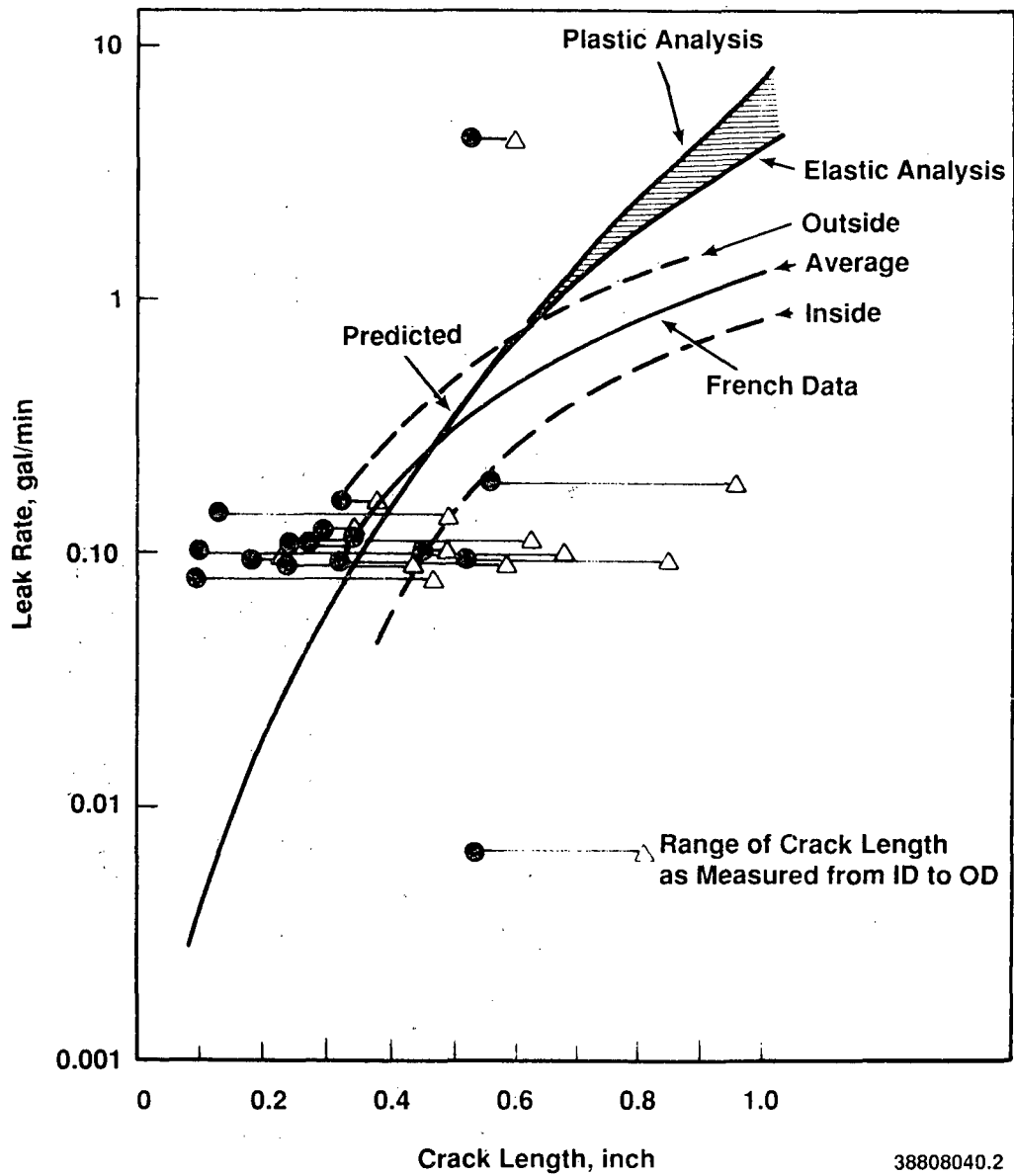
FIGURE 2.3. Comparison of Hall and Powell (1987) and Berge (1987) Leak-Test Data With Model Predictions, Normal Operating Condition
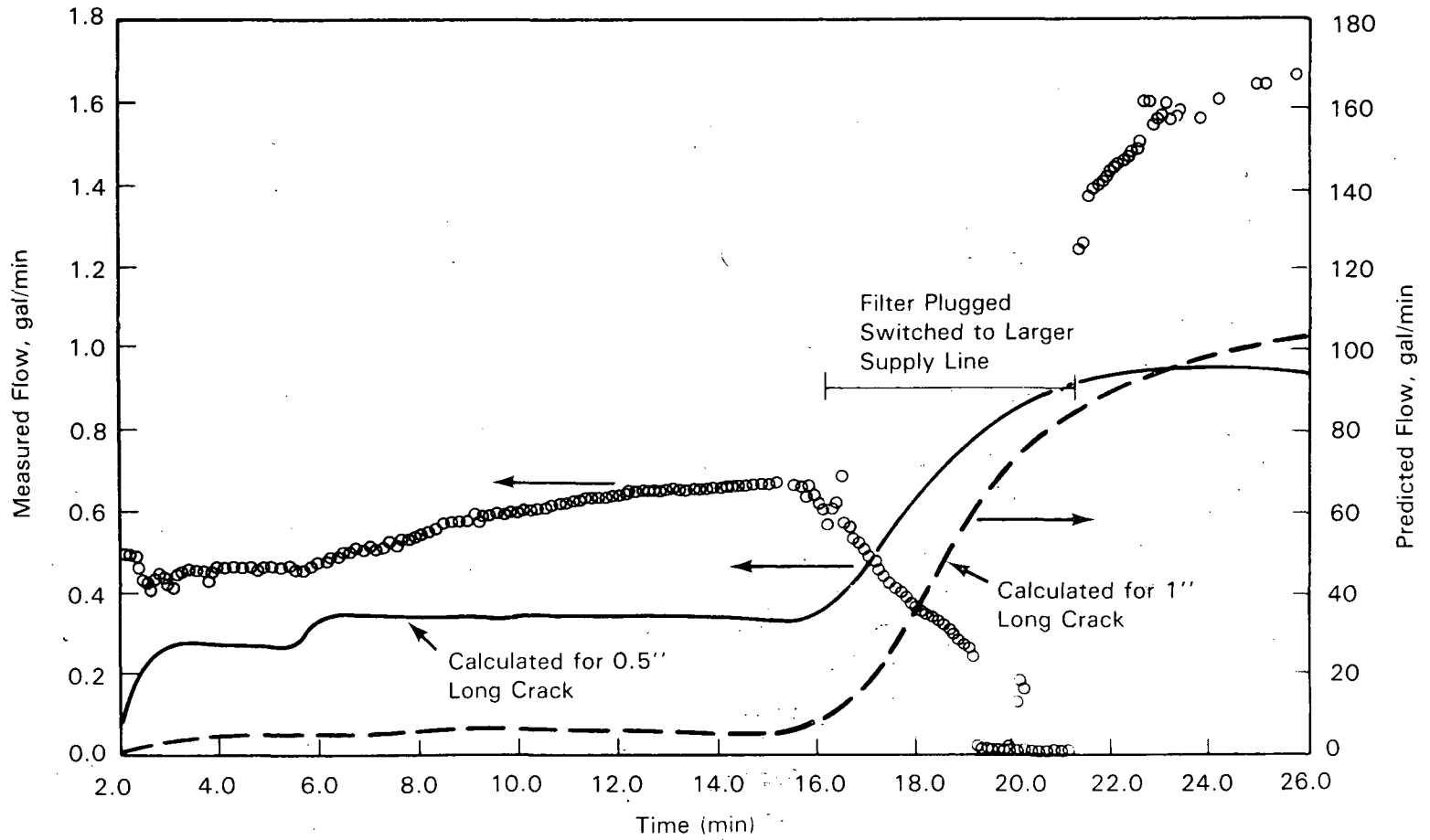
FIGURE 2.4.   Comparison of Battelle-Columbus Leak-Test Data
With Model Predictions, Test #10, Axial Crack

The main conclusion of this evaluation was that leak rates measured during tests can be highly variable. These leak rates can be strongly influenced by "random" variables that are not addressed in the predictive models that have formed the basis of leak-before-break evaluations. Measured leak rates are sometimes up to a factor of ten less than the predicted rates. This suggests that a substantial level of conservatism should be applied to the predictions of leakage that are used for evaluations of leak-before-break. Such conservatism would also appear appropriate for the calculations used to establish leak detection limits for detection systems.

2.3 SINGLE-FREQUENCY EDDY-CURRENT RESULTS

As in the Phase I work, an integral part of the Phase II effort involved single-frequency EC inspection and evaluation of the chemically-degraded tube specimens. This section discusses the EC inspection results obtained by PNL NDE specialists on the SCC- and wastage-degraded tubes. Section 3.7 discusses a mini-round robin conducted on a subset of the Phase II SCC-degraded tubes conducted during 1987 to supplement results from round robins performed on the Surry generator.

Single-frequency EC measurements were made with Zetec MIZ-7 single-frequency test equipment. The system consisted of an Automation Industries EM-3300 2-channel EC tester, a Gould Brush 220 2-channel strip-chart recorder, a Teac A-2300SX tape recorder and a 2-coil differential wound bobbin probe of 0.750-in. diameter. Results for these inspections are presented in Figures 2.5 to 2.7 for SCC, elliptical-wastage and uniform-thinning specimens, respectively. The results roughly correspond to the Phase I data, in that small-volume flaws were undersized while large-volume flaws were oversized. The trend seen in the Phase I data concerning oversizing of shallow, small-volume flaws and undersizing of deep, small-volume flaws was not observed in the Phase II results. In addition, the smallest volume flaws, SCC, were depth sized with the least precision.
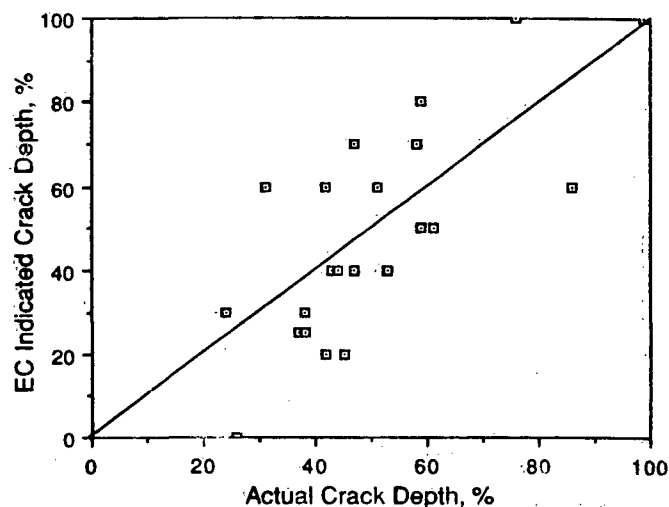
FIGURE 2.5. EC-Indicated vs Actual SCC Depth
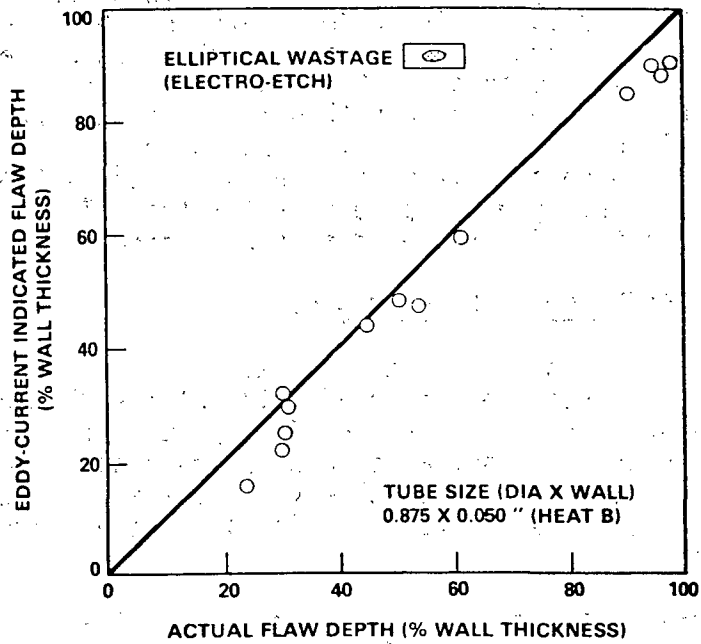
FIGURE 2.6. EC-Indicated vs Actual
Elliptical-Wastage Depth
(Electroetch)
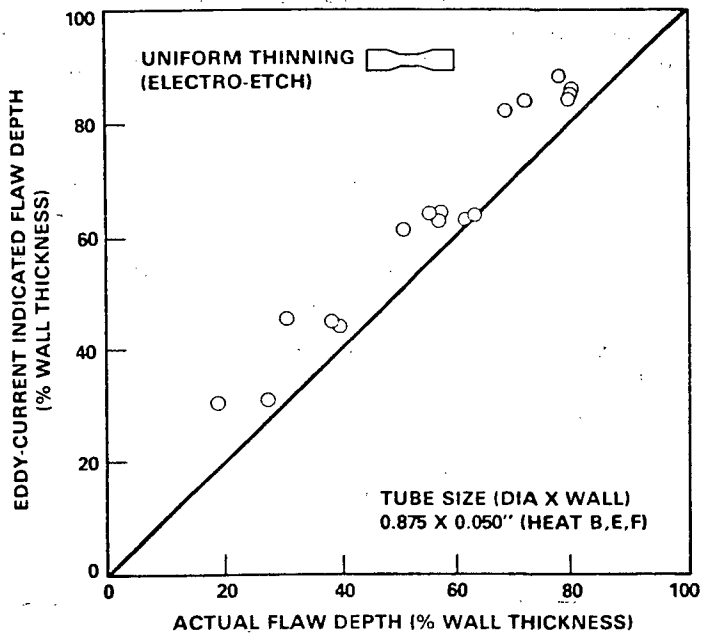
FIGURE 2.7. EC-Indicated vs Actual
Uniform-Thinning Depth
(Electroetch)

3.0 PHASE III SUMMARY

Phase III of the original SGTIP was to have been a verification of Phase I and II research results utilizing service-degraded tubing. The objectives were to validate the flaw geometry assumptions, the empirical models of remaining tube integrity and the EC test results developed during Phases I and II. The Phase III research effort as originally planned could not be conducted, however, since suitable samples of service-degraded tubing were generally unavailable. The small amount of removed-from-service tubing that could be located was in short sections and usually not flawed. Those specimens that were flawed often exhibited damage due to removal. Many others had been metallographically sectioned for degradation mechanism determinations.

Concurrent with the research in Phase II of the SGTIP, new forms of service degradation were gaining public attention, such as intergranular attack in the tube sheet crevice, and primary-side initiated cracking in roll transitions, in conjunction with denting and in the inner row U-bends. All of these flaws were proving difficult to detect and characterize with the NDE techniques in use at the time. Also, at this time steam generator degradation had progressed to the point at several units that the issue of replacement began to be addressed. The potential for an actual service-degraded unit to be used as a test bed was recognized by the NRC because of the unique opportunities represented by the generator and because of lower estimated cost compared to removal of tube samples from operational steam generators. As a result, the retired-from-service Surry 2A Steam Generator was acquired to conduct a research project to validate the tube integrity equations developed in Phases I and II, and to generate an extensive data base on the reliability of conventional and near-term field practice EC inspection techniques to detect and size tube degradation. Phase III was organized as the Steam Generator Group Project and included participation by the Electric Power Research Institute and consortia from France, Italy, and Japan. This section summarizes the results of the more than six years of research conducted under the Steam Generator Group Project (SGGP).

3.1 SGGP OBJECTIVES AND ORGANIZATION

The primary objectives of the SGGP were to utilize a service-degraded unit to 1) evaluate the types of degradation that had actually occurred, 2) establish the effect of this degradation on primary system integrity to validate the Phase I and Phase II empirical models, 3) determine the reliability of NDE inspection methods to detect and characterize the tube degradation, 4) evaluate the reliability of near-term advanced/alternate NDE technology, and 5) use the generator for demonstrating repair techniques.

In addition to the above objectives, the unique opportunity to study a retired steam generator led to development of additional objectives. They included 1) an evaluation of the usefulness of secondary-side visual inspection for characterizing tube and support structure condition, 2) an evaluation of sludge-pile chemistry and analysis of tube surface deposits, 3) a large-scale unplugging of tubes by plug drilling, 4) characterization of tube sheet crevice

corrosion products by removal and metallurgical evaluation of tube sheet sections, and 5) an evaluation of primary-side chemical decontamination techniques.

The program was divided into four major elements. The first element consisted of the activities essential to preparing the steam generator for the research program. These efforts included providing a facility, placing the generator into the facility and making the generator ready for research. The latter included radiological mapping and health physics activities aimed at keeping exposures as low as reasonably achievable (ALARA), decontamination of the channel head, removal of inservice placed plugs and providing access to the secondary side through the generator shell. The second element involved the data gathering phase. This included secondary-side characterization and the acquisition of NDE data. Following these activities, the third element consisted of a massive effort to remove segments of tubing from the generator for validation of the NDE data and to acquire specimens for mechanical integrity testing. The last program element consisted of visual and destructive metallographic analysis of the removed specimens and statistical evaluation of the data to derive improved methods for steam generator inservice inspection and maintenance of tube integrity.

Because examination of a retired-from-service steam generator represented a unique opportunity, the NRC sought participation by the domestic and foreign nuclear power industry and governments. The SGGP was formed with participation by the Electric Power Research Institute (EPRI), a French participation including Framatome, Electricite de France (EdF) and Commissariat a L'Energie Atomique (CEA), an Italian participation including Energia Nucleare Ed Engeria Alternativa (ENEA), Ente Nazionale per L'Energia Elettrica (ENEL), and the Breda Division of Ansaldo Componenti S.p.A., and participation of a Japanese consortium managed through the Nuclear Power Engineering Test Center (NUPEC), including Mitsubishi Heavy Industries and several Japanese utilities. The multi-sponsor nature of the program contributed to a broad technical review of program activities, opened the program to many technical and technology inputs and provided a forum for the discussion of steam generator issues on a world scale.

3.2 THE SURRY STEAM GENERATOR

3.2.1 Generator History

The Surry 2 steam generators had been in service only about 6 years at the time of their removal. However, they exhibited, or had potential for exhibiting, many of the defect types identified at the time the SGGP was being formulated. The Surry nuclear station is sited near the brackish James River near where it empties into Chesapeake Bay. The Surry Plant utilized 90:10 Cu:Ni alloy condensers that had a history of leakage during service. Water chemistry records at the plant indicated periods of significant chloride ingress into the secondary water. Oxygen ingress into the generator was also not well controlled. The generator started operation in March of 1973 under a phosphate secondary-side water chemistry. After about a year-and-a-half of operation, the secondary water chemistry was switched to an all volatile treatment (AVT). The unit was subject to sludge lancing several times, includ-

ing an effort during the shutdown at the time of water treatment switch-over. However, eddy-current sludge height data indicate this mainly succeeded in moving the sludge around as opposed to a significant removal. During the short period of phosphate water chemistry, wastage was found and tubes plugged in the nozzle-side central tube region of the hot-leg (commonly referred to as the 'banana zone').

Shortly after conversion to AVT water chemistry, the first indications of denting were discovered. Initially, these were listed as unspecified indications during the generator ISIs. The Surry generator has drilled hole carbon steel support plates. The generator is tubed with mill annealed Inconel 600. The acid conditions of the brackish water intrusions plus the presence of chlorides and oxygen resulted in a rapid deterioration of the Surry unit due to corrosion of the support plates. This corrosion led to extensive tube denting, "hourglassing" of the support-plate flow slots and fracturing of the support plates between tube ligaments. Additionally, the hourglassing of the uppermost support-plate flow slots caused inward deflection of the U-bend legs that resulted in high stress at the U-bend apex and initiated IGSCC which ultimately resulted in a large leak failure. Following this event, the inner two rows of U-bends were preventively plugged.

Another feature that was of potential interest was the tube sheet crevice, where the tubes have only been rolled into the bottom about 2-1/2 in. of the 21-in.-thick tube sheet. This extended crevice was the location of a "new" degradation mechanism, intergranular attack of the tubing, at the time the program was evaluating acquisition of a steam generator.

The Surry steam generator was judged suitable for the SGGP based on several considerations. The unit was of a type found in a large number of reactors; generators of this general design were licensed and produced in Japan and France. The Surry unit was also believed to have defects representative of those of concern at the time this program began. The Surry units were also the only generators of this type scheduled for removal in a time frame compatible to the desired program start-up. A detailed report describing the inservice history of the Surry steam generator was prepared by Doctor et al. (1983).

3.2.2 Generator Acquisition and Transport

Prior to acquiring the Surry generator, an examination was conducted at the Surry site to evaluate the generator from the secondary side. This examination was to determine the condition of the generator after storage in the vault at Surry. This examination, attended by representatives from NRC, EPRI, Combustion Engineering, Westinghouse, Babcock and Wilcox, and Kraftwerk Union, determined that the unit was in a condition typical of the service condition at end of life. Thus, it was felt that no noticeable continued deterioration had occurred during storage of the unit. A report by Wheeler (1984) documented the results of this investigation. At the time of this inspection, a small amount of water was visibly present in the generator secondary side at the low point while the generator was on its side; however, magnetite deposits had not changed to hematite. The examination at Surry also ascertained that the service degradation did not preclude a successful

3.3

shipment to Hanford. Along with the visual inspection and photographic documentation of the generator, internal dimensional measurements were made for post-shipment comparison. Repeat inspection of the unit after transport to Hanford and installation in the Steam Generator Examination Facility (SGEF) indicated that no damage occurred during the transport (Wheeler 1984).

The Surry unit was barged from the Virginia reactor site, through the Panama Canal, to the Hanford Reservation in Washington State. Licensing for the transport was pursued through the U.S. Department of Transportation. A draft Environmental Impact Statement (EIS) was prepared and accepted for barge transport of the generator as single item cargo. This report included data from radiologic inventory measurements as well as risk analysis of various accident scenarios. The generator shell was accepted as a low specific activity (LSA) package, based on the radioactivity being evenly distributed throughout the tubing, and retained in place in the oxide coating on the inner diameter of the tubes.

During shipment, precautions were taken to prevent ingress of oxygen and water into the unit as well as to monitor and limit accelerations. Once at Hanford, the unit was stored outdoors until the Steam Generator Examination Facility was completed. While stored, the unit was kept under an inert atmosphere by continuous feed and bleed of gas. The system was set up to bleed in sufficient gas to prevent the entry of atmosphere into the unit during normal daily thermal cycling. Shortly after storage, the unit was tapped through the shell at its lowest point and several liters of water were drained from the unit. This water had very low chloride content and apparently existed in the unit prior to transport. It probably had drained into the unit from the primary side of leaking tubes or was, in part, a result of condensation during the barge trip. Figure 3.1 shows the steam generator as it arrived by barge at Hanford.

3.2.3 Steam Generator Examination Facility

The Steam Generator Examination Facility, a cut-away drawing of which is shown in Figure 3.2, was especially designed and constructed to meet the anticipated programmatic needs of the SGGP. Initiation of SGEF construction was delayed until after successful transport to Hanford of the Surry steam generator. This sequential approach was necessary because of uncertainties concerning the ability to license shipment of the generator. The SGEF was more fully described by Clark and Lewis (1982). The main facility feature is a 5-story high bay or tower with removable roof, which allowed positioning of the generator in its normal vertical operating position. Vertical positioning was judged crucial to the ability to obtain representative nondestructive examinations of the generator. It was also beneficial to activities such as decontamination and some specimen removals. The tower portion of the SGEF was environmentally [High Efficiency Particle Arrestor (HEPA)] filtered to allow destructive sectioning operations on the generator. The remainder of the SGEF contained a laboratory with filtered hoods, a truck lock/remote operating area, change rooms and mechanical equipment to support the tower operation. The SGEF met the needs of the SGGP; however, the tower portion was somewhat cramped for optimum efficiency at positioning sectioning equipment.

FIGURE 3.1. Surry Steam Generator Upon Arrival at Hanford

3.5

STEAM GENERATOR EXAMINATION FACILITY

16 TON BRIDGE CRANE

1 TON JIB CRANE

4th LEVEL

3rd LEVEL

2nd LEVEL

STEAM GENERATOR

GROUND LEVEL

BASEMENT LEVEL
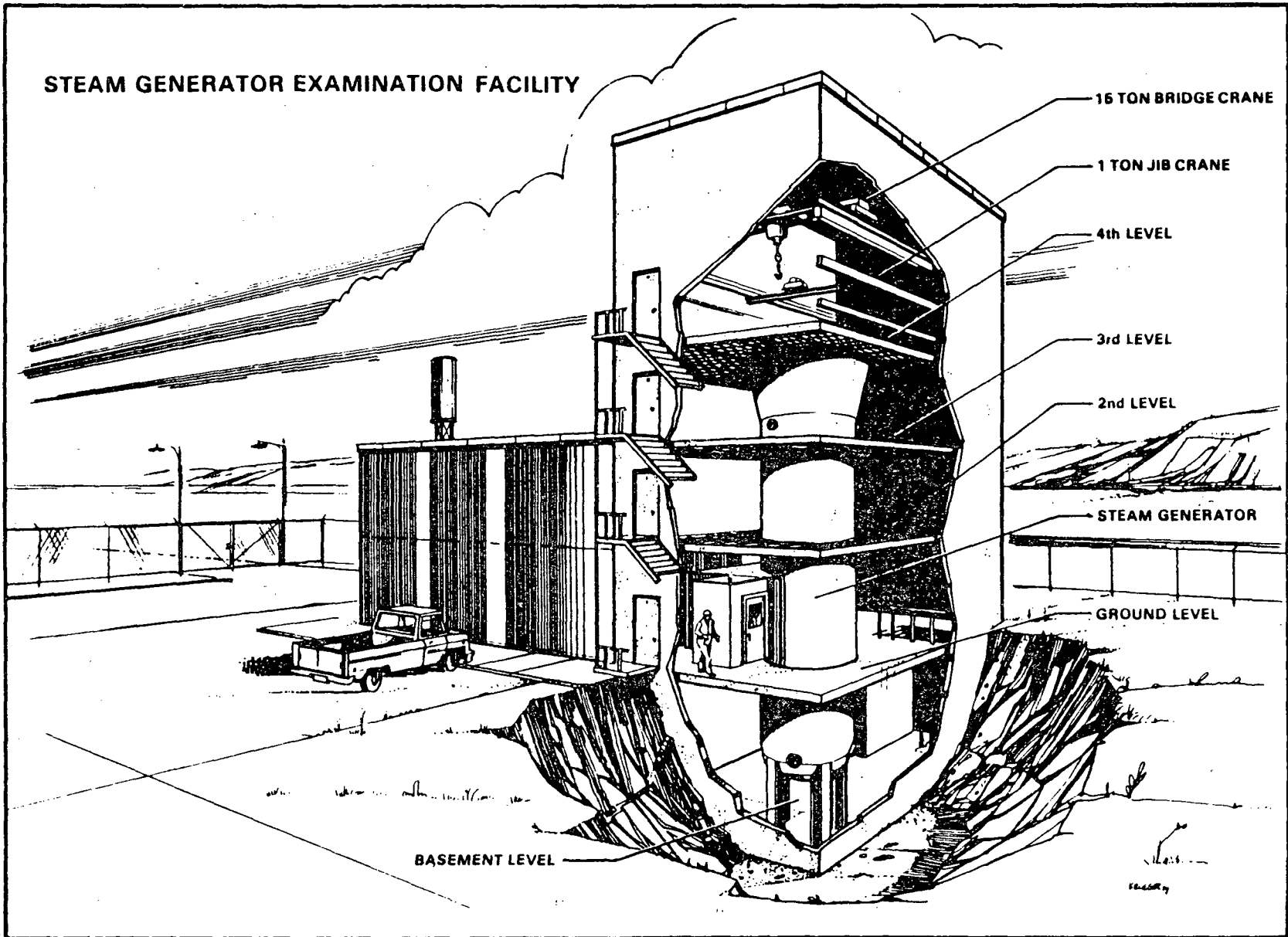
FIGURE 3.2. Cut-Away of SGEF Showing Position of Steam Generator

The facility could also have benefited from additional capacity to store radioactive samples.

3.3   PREPARATION OF THE GENERATOR FOR RESEARCH

This section provides details on those tasks which were not central to the primary objectives of the program, however were necessary precursors to obtaining the data vital to accomplishing the primary objectives. These activities included health physics, decontamination of the channel-head region, and removal of plugs from tubes which were isolated during the generator service life. While the tasks discussed in this section were subsidiary to the major program goals, they were by no means trivial accomplishments. Most of these activities often required first-of-a-kind solutions to engineering and operational problems.

3.3.1   Health Physics, ALARA Radiation Control

One of the earliest and continuing concerns throughout the SGGP was the potential for large amounts of staff radiation exposure. While there was continuing concern with minimizing staff exposure in general, there was the additional potential in this program of excessive exposure burden on the relatively few scientific staff possessing the expertise to accomplish program objectives. A separate Health Physics task was established to accomplish ALARA control of radiation exposures. This task was responsible for reviewing operating procedures from a radiation control/exposure standpoint, overseeing the accumulation of staff exposure information on a time as well as job basis, and assisting in experimental design for minimizing exposures, such as through the use of selective shielding. Beyond the immediate needs of the SGGP, the Health Physics staff sought information, in conjunction with another NRC program (Reece and Harty, 1983), to aid in accurately monitoring and reducing worker exposures in the nuclear industry.

Initial Health Physics activities included a scan at the Surry site to determine the radionuclide inventory. The inventory was estimated to be between 120 Ci and 180 Ci, composed almost exclusively of Co-60. These radiologic data were used during the shipment licensing activities, and as a design basis for transport shielding. A health physicist accompanied the barge shipment on the tow boat, in case there was a necessity to provide radiation monitoring upon putting into a port. This was indeed the case when entering the Panama Canal.

Once the generator was lowered into the SGEF, the first subsequent effort was establishing and mapping the radiation fields inside and around the SGEF. The inside maps, an example is provided in Figure 3.3, allowed the design of shielding, the training of personnel, and experimental activities/setups, to be conducted in a manner which minimized staff radiation exposure. The outside mapping was the beginning of an environmental monitoring program which lasted throughout the SGGP. This effort included location of dosimeters at 10 points surrounding the facility perimeter. Periodic monitoring of these environmental dosimeters exhibited a close correlation to activities inside the SGEF, such as decontamination, and removal and storage of artifacts in different portions of the facility. Based on environmental monitoring,

LEVEL - 1st FLOOR

<25
50-25
100-50
>100
SG
VESSEL
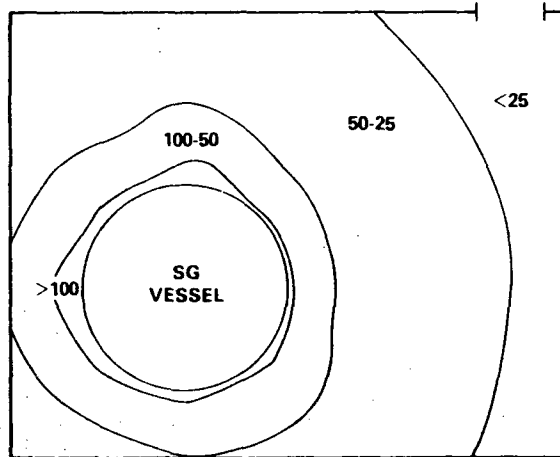
*DOSE RATES ARE IN mR/hr

LEVEL - 2nd FLOOR

<25
50-25
100-50
>100
SG
VESSEL
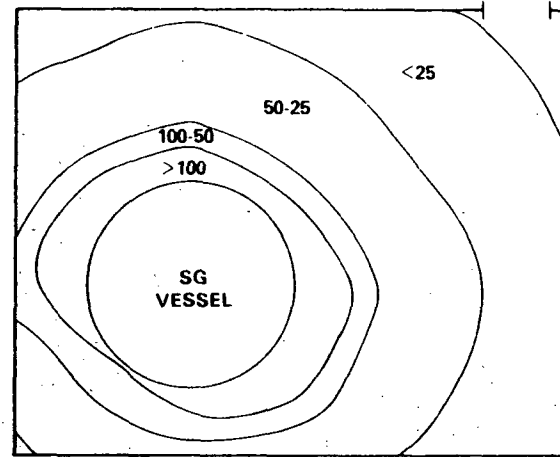
*DOSE RATES ARE IN mR/hr

LEVEL - 3rd FLOOR

<25
50-25
100-50
>100
SG
VESSEL
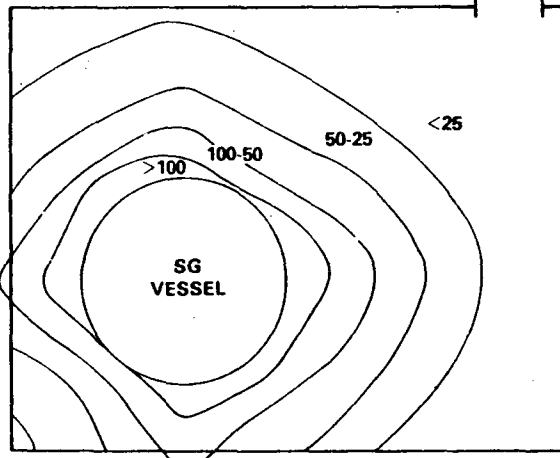
*DOSE RATES ARE IN mR/hr

LEVEL - 4th FLOOR

<10
15-10
50-15
SG
VESSEL
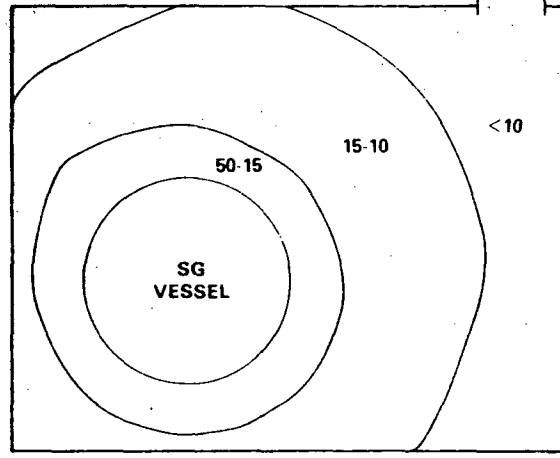
*DOSE RATES ARE IN mR/hr

FIGURE 3.3. Radiological Maps - Floors 1-4 SGEF

additional concrete shielding was placed outside the SGEF when needed to maintain perimeter exposure levels well below legal limits.

The Health Physics task was also charged with developing an on-line dosimetry system to keep close track of personnel exposures. Each entry into the radiation zone was monitored by individual pencil dosimeter, and logged into a computer data base by a radiation protection technician assigned to the facility. All personnel using the SGEF were subject to radiation training, building-specific training, and task-specific training. This resulted in an extremely low accident rate and personnel contamination incidence during the program.

In addition to mapping around the generator, the radiation fields throughout the inside of the generator were also mapped, both using thermoluminescent detectors (TLDs) through shell penetrations and utilizing a special probe through the inside of the generator tubes. Maximum dose rates in excess of 11 R/h were recorded near the generator center. The through-tube measurements were conducted using a specially constructed single crystal 0.5-in. diameter CdTe probe. The detector was pushed through 48 selected tubes using a NDE probe pusher-puller. Figures 3.4 and 3.5 show typical hot-leg and cold-leg detector scan results. Note that the support-plate locations are discernible. The relative radiation level increases from the inlet of the tube to the U-bend, and remains at the maximum value throughout the cold-leg side. This is typical of all of the tubes that were scanned. It is probably a result of increasing deposition of Co-60 along a tube as primary water temperature decreases (decreasing solubility of iron and cobalt). The radiation levels were consistently higher in the manway quadrant than the nozzle (inlet) quadrant of the hot-leg. Again, this is interpreted as resulting from decreasing solubility, owing to lower temperatures and, perhaps, less turbulence. On the cold-leg side, the levels were equal on the manway and nozzle (outlet) quadrants.

The internal radiation scan was an unsuccessful attempt at seeing if such measurements could be used to detect defects in the generator tubes or support structure. Eight tubes with eddy-current indications of 50%-100% through-wall defects were scanned. The negative finding was due to the fact that the contribution to the radiation field of the tube being inspected is small compared to the surrounding tubes. The radiological scans do appear to allow a good thermal map (i.e., relative operating temperature) of the generator to be developed (Clark and Lewis 1985).

Another activity under the health physics task, and in conjunction with another NRC program (Reece and Harty 1983), assessed the multiple dosimetry of channel-head workers (how many dosimeters are needed and where they should be located on an individual in order to ensure adequate dosimetry). The results of this study (Wheeler et al. 1984; Clark and Lewis 1985) was that exposure to the eye was the limiting exposure. The recommendation was that channel-head workers were adequately monitored with two dosimeters, one located on the forehead and the other on the chest.
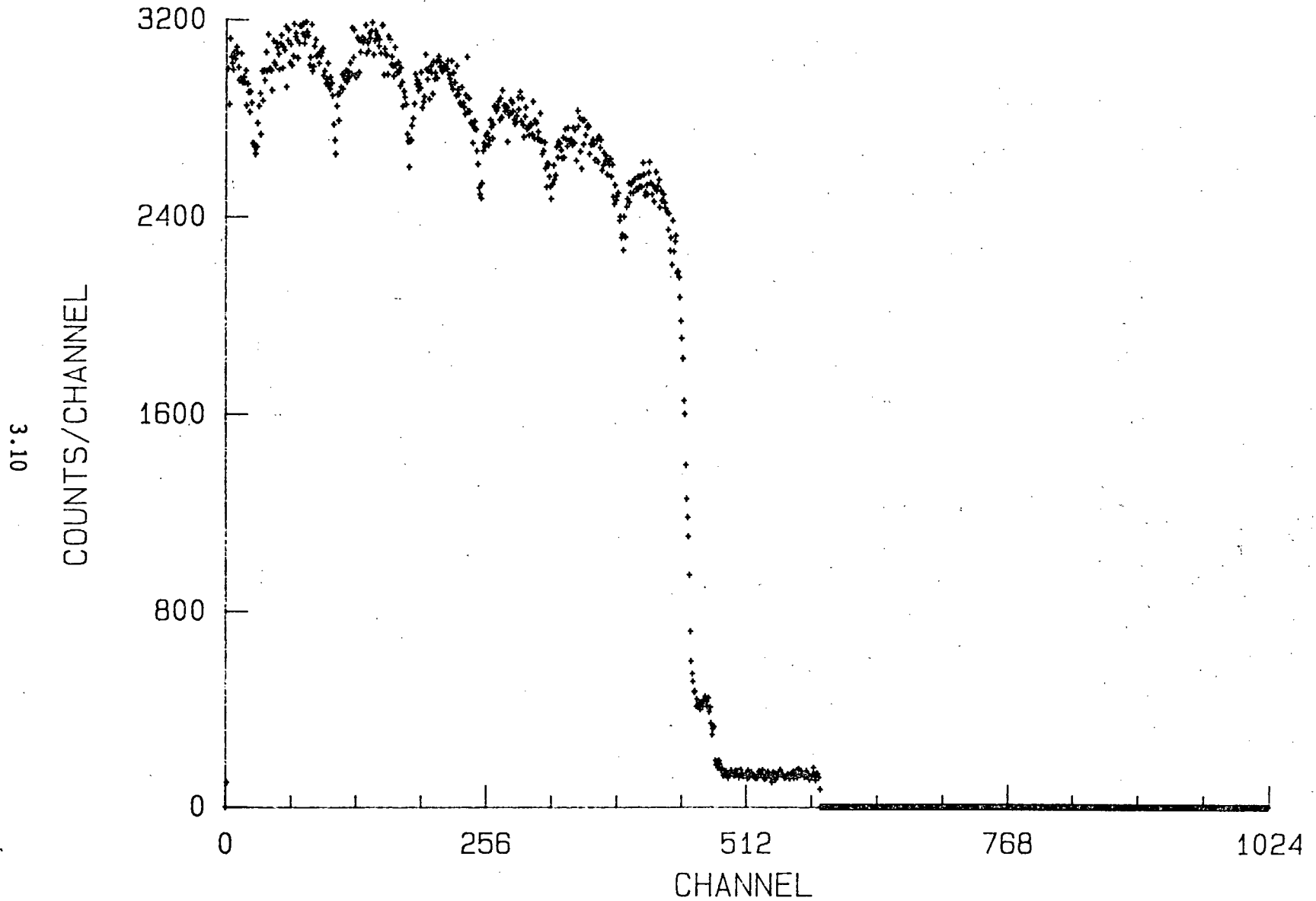
FIGURE 3.4. Relative Radiation Level Along a Typical Hot Leg Tube - R22C47
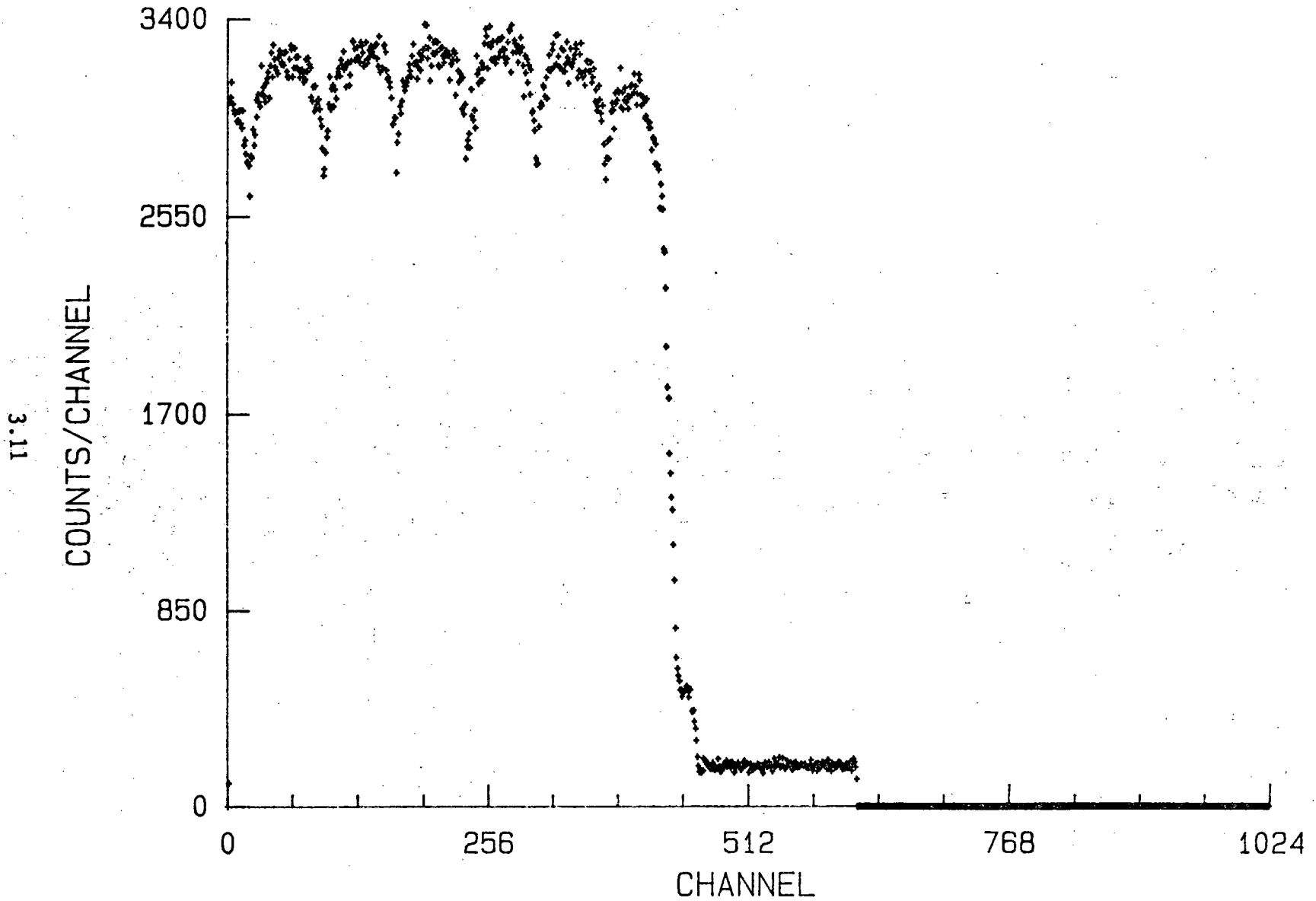
FIGURE 3.5. Relative Radiation Level Along a Typical Cold Leg Tube - R22C47

3.3.2 Channel-Head Decontamination

This task was included primarily to maintain staff radiation exposure on an ALARA basis. Access through the channel-head was needed for tube unplugging, primary-side nondestructive examinations, removal of specimens, and demonstration of generator repairs. The programmatic goal of the channel-head decontamination was to reduce the general area radiation level in the channel-head to below 1 R/h, without decontamination of the tubing.

The field practice technology for channel-head decontamination at the time of this activity was abrasive blasting using a robotic or semi-robotic manipulator system. The technique had several drawbacks such as: generation of substantial secondary waste, incomplete coverage with most manipulators, and staff exposure during installation of necessary equipment. The SGGP solicited for subcontractor bids to perform the channel-head decontamination. During the technical evaluation of the proposals received, it was decided to allow demonstration of two techniques, one on either side of the channel-head divider plate. The two techniques both utilized dilute reagent chemical decontamination; a CAN-DECON and a LOMI method were chosen. Both of these techniques had prior extensive laboratory data on decontamination effectiveness and potential corrosivity. Each technique had prior demonstrated success in boiling water reactor application. The contractors offering the techniques had previous radioactive field experience. Interest in the dilute chemical reagent decontamination techniques stemmed from their ability to cover all channel-head surfaces, to potentially avoid personnel exposure during setup and operation, and to provide reduced generation of secondary waste through the use of ion exchange water cleanup. Due to concerns regarding possible corrosivity, it was also felt these techniques required a full-scale demonstration before they could be used for the first time in the field.

A report by Allen et al. (1984), provides details on the execution and results of the decontamination efforts. This report contains information on the equipment and operations, corrosion tests conducted and radiologic measurements. In summary, both techniques achieved average surface decontamination factors (DF) up to a factor of 10, with higher decontamination on stainless steel surfaces and DFs of 4-6 for Inconel 600 surfaces. Both techniques were limited to decontaminating the channel-head bowl and bottom surface of the tube sheet. Decontamination into the tubes was prevented, to avoid any changes to the service-induced tube degradation conditions in the tube sheet region, and to avoid possible spillage of chemical decontamination solutions into the secondary side. Thus, after decontamination, considerable radiation field shine down the tubes remained. Fields in the channel-head, after the decontamination, averaged less than the program goal of 1 R/h.

Both decontaminations were continuously monitored with resistance type corrosion probes. In addition, numerous corrosion coupons, U-bend strain specimens, and metal couples were exposed to the solutions for post-process evaluation. The corrosion test results indicated essentially no detrimental effects for the period of exposure. It was also interesting to note that on-line process monitoring of radionuclide concentrations (see Figures 3.6 and 3.7) indicated that process times could probably be reduced, and provided detail on how the decontamination process proceeded.
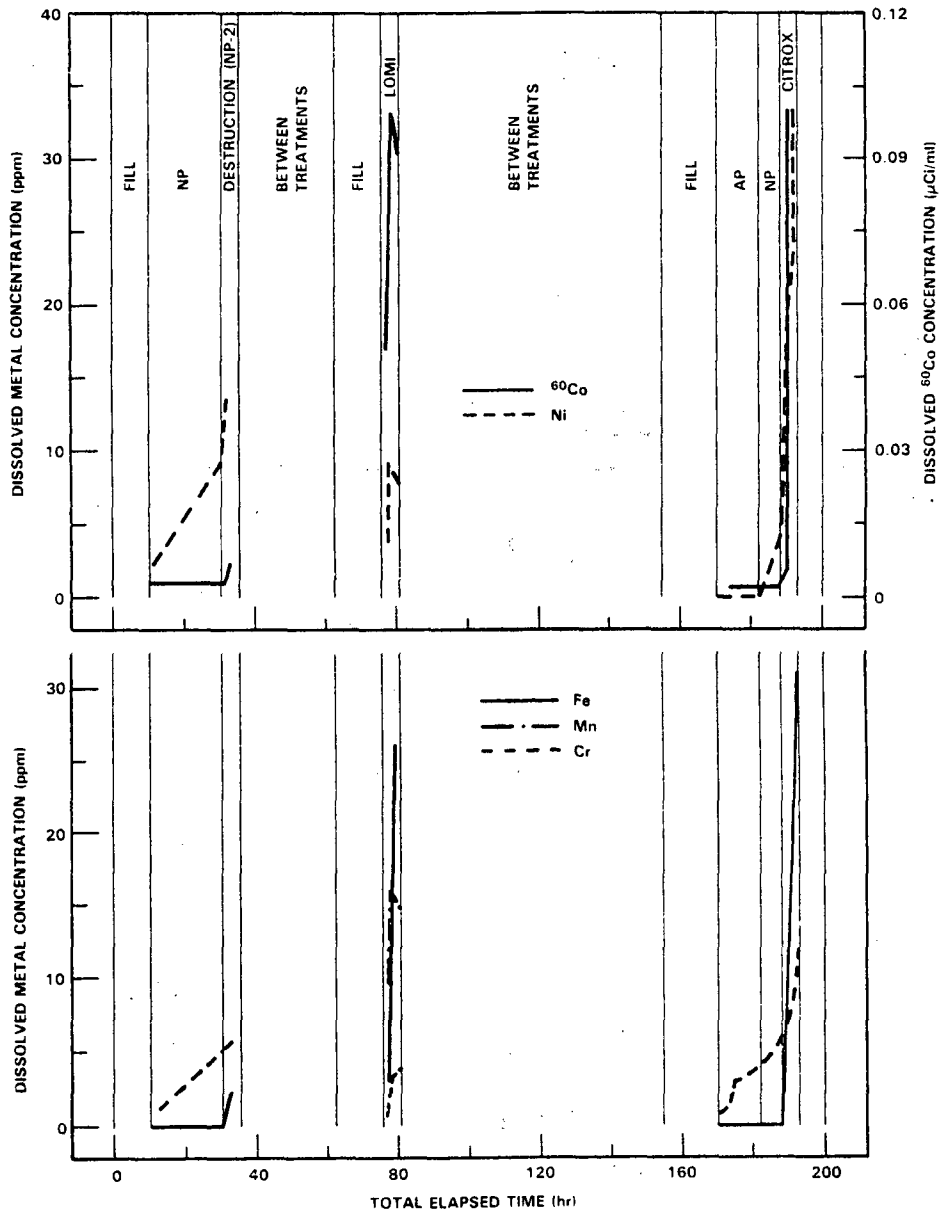
FIGURE 3.6. Fe, Cr, Ni, Mn, and Co-60 Concentrations in the Reagent During the Hot Leg Decontamination
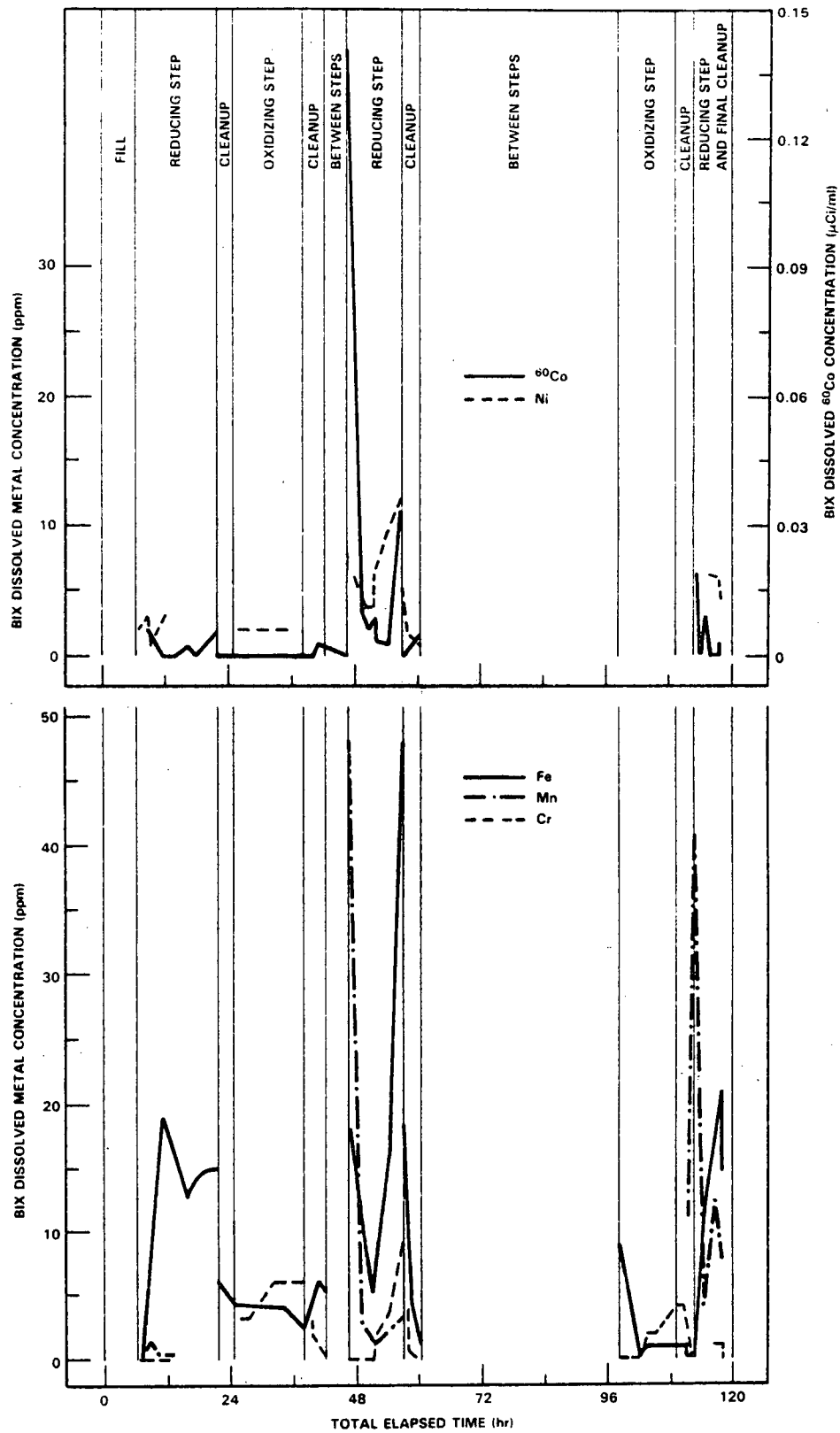
FIGURE 3.7. Fe, Cr, Ni, Mn, and Co-60 Concentrations in the Reagent Before Ion Exchange During the Cold Leg Decontamination

3.14

One of the processes demonstrated the ability to clean waste streams with ion exchange beds, providing for reduced volumes of secondary waste generation. One problem caused by the ion exchange was very high fields around the exchange columns, which necessitated additional personnel shielding and, in the case of the SGEF, additional facility shielding to maintain low radiation field values at the facility perimeter. The high concentration of radioactivity in a small portion of the ion exchange media, required some dilution to achieve fields of 3-5 R/h at surface contact on the radioactive waste disposal drums. The ion exchange media was buried at the disposal site at Hanford.

The main lessons demonstrated with this task were 1) dilute chemical decontamination as conducted in the Surry unit provided average field reductions approaching a factor of 10; 2) the processes used did not produce appreciable corrosion damage during implementation; 3) secondary radioactive waste generation could be minimized with use of ion exchange solution cleanup; and 4) operating personnel exposures were low, 1.6 R for the initial decontamination side, and 0.7 R for the second side of the channel head.

Other observations included: 1) Decontamination effectiveness was enhanced by proper design of the system to provide reasonable flowing circulation over all the surfaces to be decontaminated (this is a function of flow recirculation rate and in-channel-head solution distributor or nozzle design); 2) Post-decontamination high-pressure water spray removed residual loose deposits, though did not account for significant radioactivity reduction; and 3) A semi-remote electropolishing demonstration removed remaining corrosion films down to bare metal.

3.3.3 Tube Unplugging

During the approximately six years the Surry 2A generator was in service, 748 of the generator's 3388 tubes, just over 22%, were plugged. Plugging removes a generator tube from the pressurized primary water circuit. In a U-tube type steam generator, such as Surry, this involves closing the tube at the water entry and exit points, by obstructing it within the tube sheet region. The Surry tubes were plugged using an explosive plug, a cutaway section of which is shown in Figure 3.8. Tubes were plugged for a variety of reasons during the lifetime of the Surry unit. Reasons included: identified and unidentified types of tube wall degradation, preventive plugging based on engineering judgment to preclude tube failures from support-plate degradation, and preventive plugging of the inner two rows of U-bends after a U-bend burst failure. Figure 3.9 shows the end-of-service Surry 2A generator tube plugging map, provided by the Virginia Electric and Power Company.

The SGGP required access to a large number of the plugged tubes for nondestructive inspection. Tubes plugged due to wall-loss/degradation were of primary interest in the program efforts to validate NDE accuracy and reliability. Figure 3.9 indicates tube plugs to be removed, on both hot-leg and cold-leg sides. All tubes plugged for a wall degradation, a defect or leaker, were unplugged. In addition, half the preventively placed plugs, on one side of the tube sheet, were removed along with a selection from the opposing side to confirm symmetry of generator degradation.
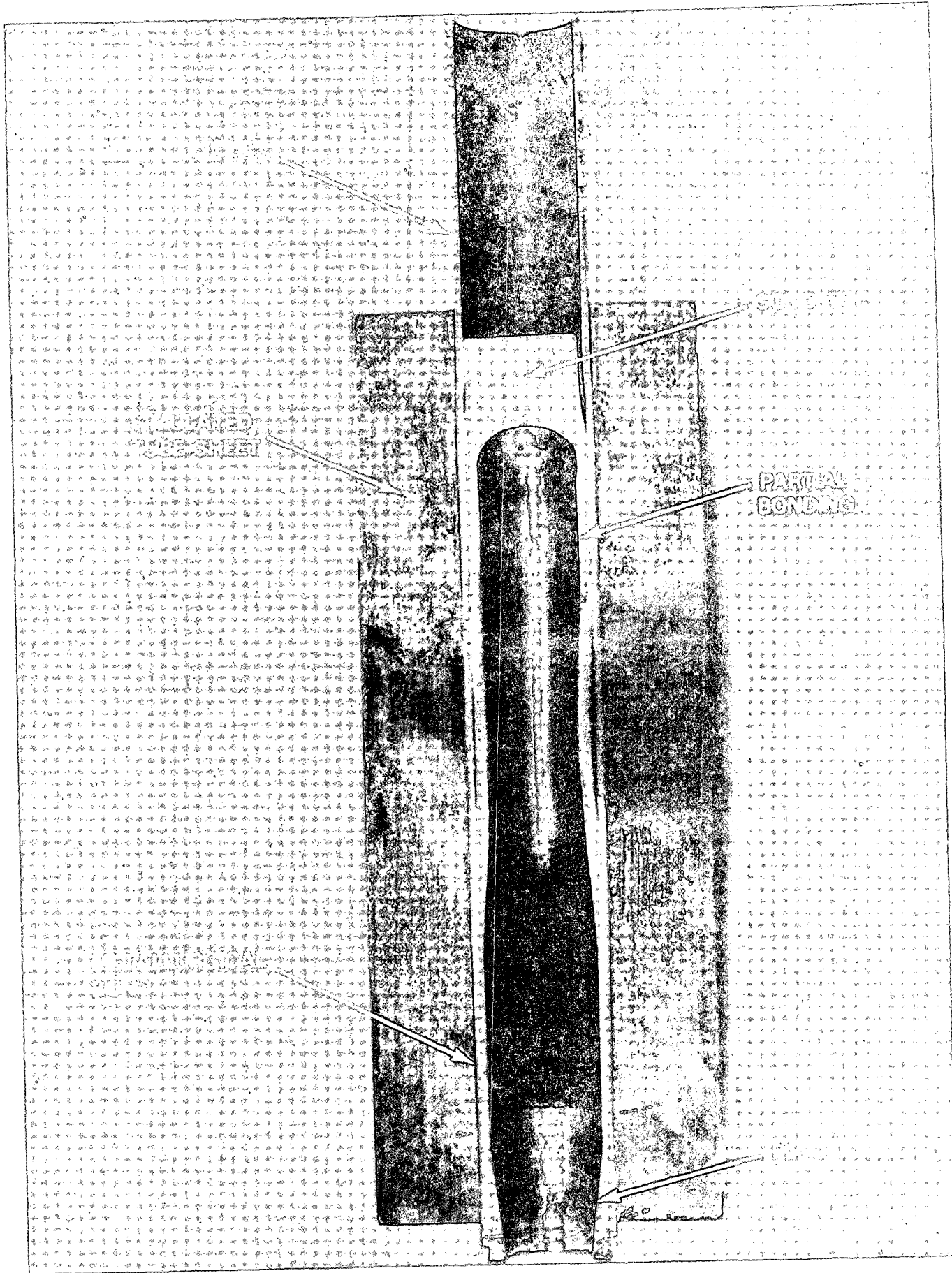
FIGURE 3.8. Sectioned Explosive Plug in Simulated Tube Sheet

3.16
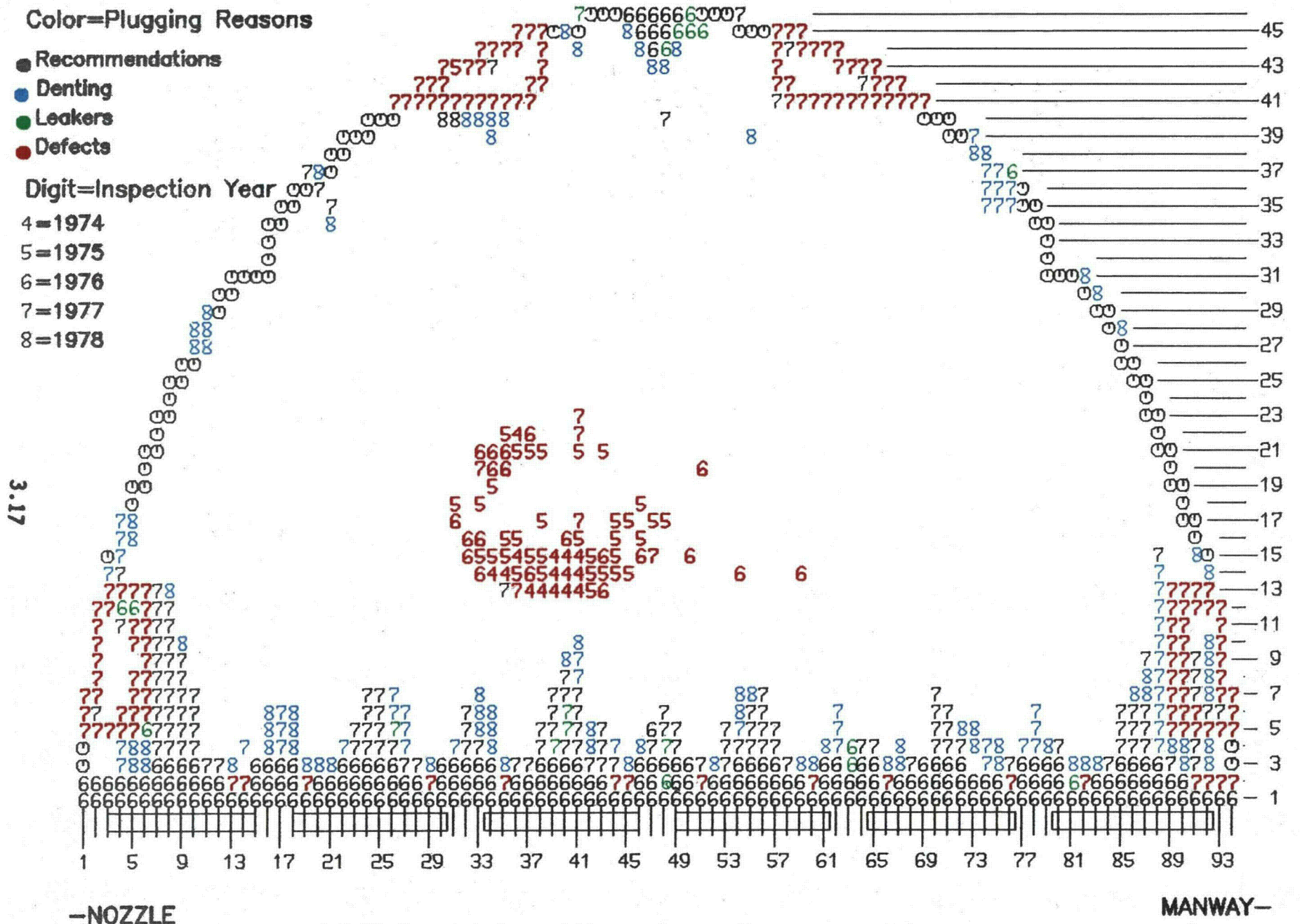
FIGURE 3.9. Surry 2A Steam Generator Tube-Plugging Map as of 8/8/78

The removal effort itself was a complex organizational activity. At the time, this was the largest plug removal operation undertaken in the U.S. Previous experience was limited to removals of one to a few plugs at a time. This project required the removal of close to a thousand plugs. Plug removal activities were documented in a report by Wheeler et al. (1984).

Removal of the plugs shown in Figure 3.8 involved a three step process. First, a small hole was drilled through the solid end of the plug. This hole released any trapped fluid above the plug and provided a gripping orifice for later stub removal. Next, the plug body was drilled out using a drill bit that matched the tubing inner diameter. Drilling proceeded until the solid top became free-moving. Finally, a special tool was inserted through the now loose plug end, and the end removed. The majority of removals utilized equipment diagrammed in Figure 3.10. The plug to be removed was indexed by a fixture attached to the tube sheet. To this fixture was attached a reversible air-powered drill motor with an electric feed. Channel-head workers, "jumpers," would attach the drilling equipment and change bits as needed. The trained drill operators used the equipment from a remote location with visual and audio inputs from the drilling operation. Using this technique along with two simultaneously operating drills, one on either side of the channel-head, plug removals in excess of 50 per day were routinely accomplished.

Containment of contamination and personnel exposure control were concerns during the unplugging operation. In addition to metal turnings from the drilling operation, a number of tubes contained water behind the plugs. Channel-head workers were required to wear two pairs of protective clothing, plus a water repellent suit, and leather gloves to prevent cuts from the metal turnings. Workers operated for 2-hour periods with a 2-hour break between periods. Pressurized breathing air was utilized, which also provided some cooling. In addition, the SGEF was air conditioned. The limiting channel-head worker radiation exposure was to the head/eyes. Exposure rates typically varied between approximately 25 mR/h and 115 mR/h. The exposure variation was a function of the number of channel-head entries made per work period and their duration. Duration was affected by any mechanical problems with the equipment, worker experience, and the difficulty of positioning the indexing device and tooling, which was a function of the plug location, especially for peripheral plugs. Total personnel exposure for the unplugging operation was 60.6 man-rem with channel-head workers accounting for 40.3 man-rem.

Several tubes which had been preventively plugged, and other tubes which were not leakers at the time of plugging, i.e., had no through-wall defect, were found to contain water and/or sludge deposits. Figure 3.11 shows the distribution of the water and sludge found while unplugging tubes. Water samples were obtained from 71 of the 102 plugs visually observed to leak during unplugging. Analysis of these samples indicated that most of them contained water typical of secondary-side chemistry, while a few indicated primary water. Water origin was identified mainly through high lithium and boron levels for primary water, and high copper, sodium and phosphorus for secondary water.

TUBE SHEET WITH
TUBING ARRAY

MOTOR & LEAD SCREW
LOCKING DEVICE

CAMLOCK PLATE

BASE PLATE
CAMLOCK

PLUGGED TUBE

DRILL

AIR DRIVEN
DRILL MOTOR

LEAD SCREW
ASSEMBLY

PLUGGED TUBE

HOLE GUIDE

SPACER PIN (3)

CAMLOCK (2)

CAMLOCK
PLATE
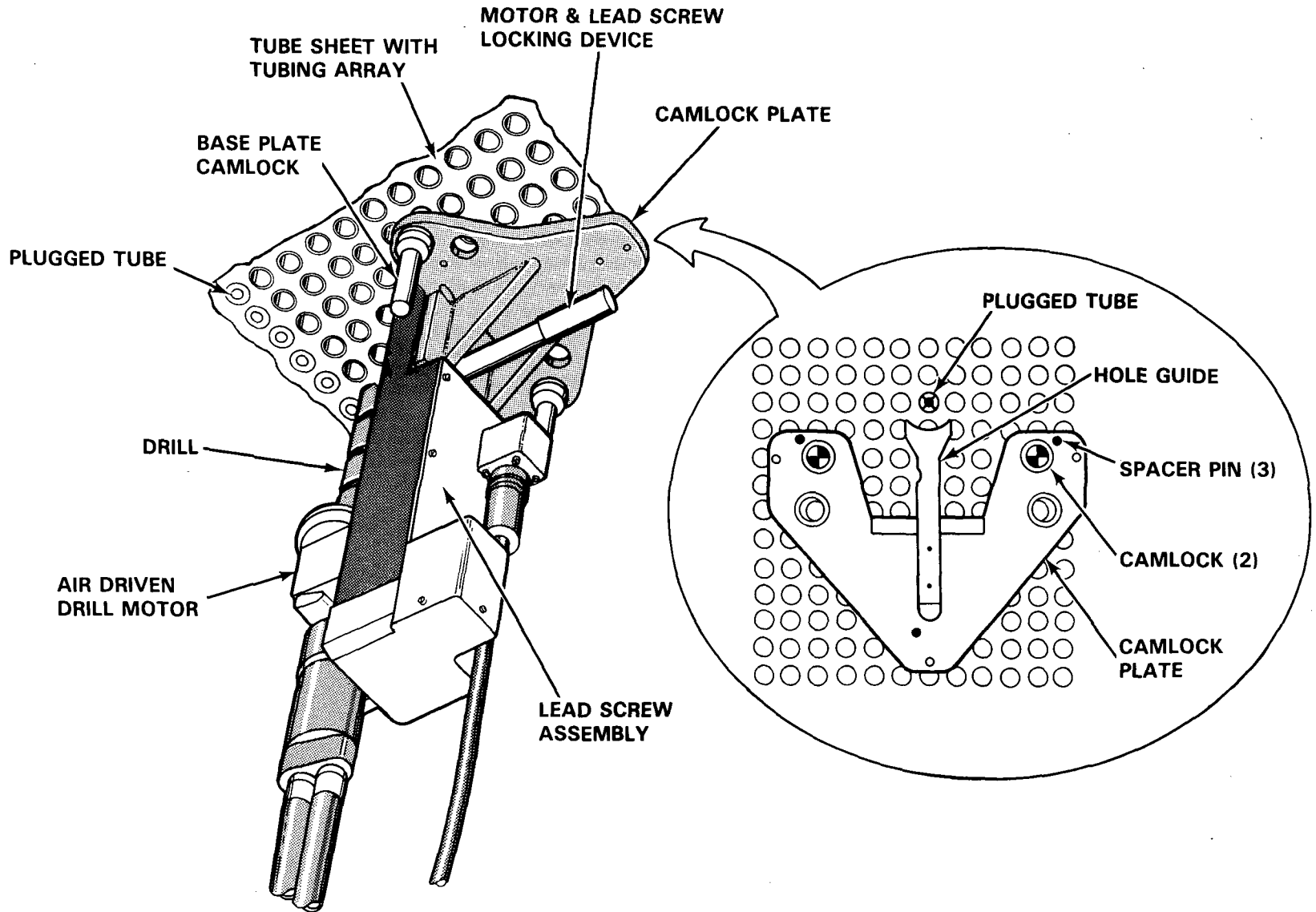
FIGURE 3.10. Schematic of Model D Plug Drilling Fixture
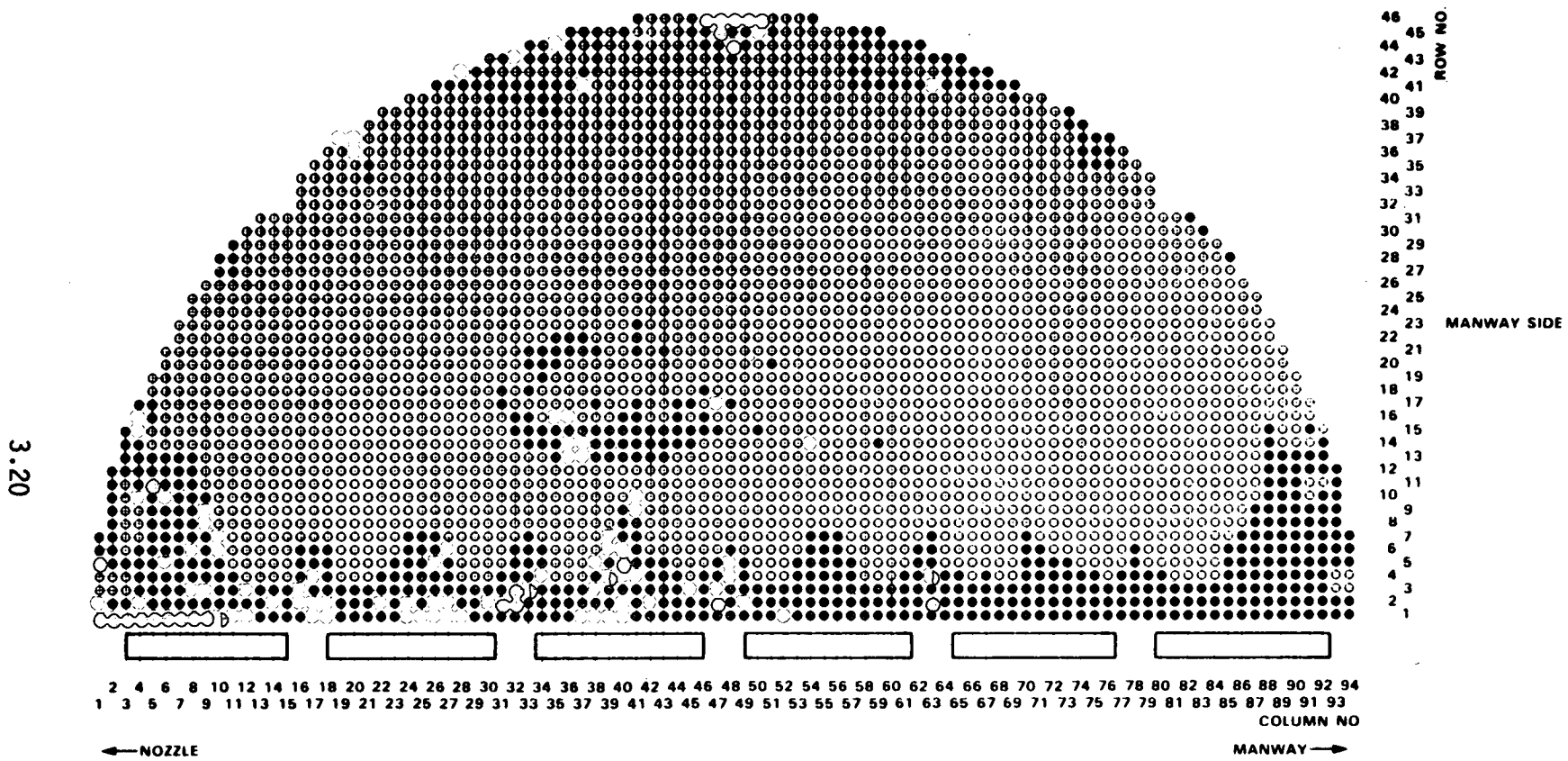
2A STEAM GENERATOR

(TUBE SHEET VIEWED FROM INSIDE PRIMARY PLENUM WITH OBSERVERS BACK TO DIVIDER PLATE)

Red = Water
Yellow = Sludge

NOTES

| 1 TOTAL NUMBER OF TUBES 3.388 |
| 2 "x" COORDINATE 1.281" |
| 3 "y" COORDINATE 1.281" |
| 4 TUBE O.D. 7.8" |
| 5 TUBE WALL 0.050" |

FIGURE 3.11. Location of Water and Sludge Samples

The drilling operation overall was very successful. A total of 969 plugs was removed during a 3-week period. Toward the end of the operation, productivity was affected due to equipment wear requiring increased maintenance. There was also a problem due to the drilling. After drilling, the tubes were mechanically gaged to determine that the drill hole was correctly sized. This gaging was mainly conducted so that "finger-walker" type eddy-current probe positioning equipment could later be used. The tube sheet holes had to be within a certain size tolerance for the finger-walker to maintain an adequate grip to prevent falling. However, the gaging operation was only to a depth affecting the finger-walker. What was missed were occasional ridges in the steam generator tubing left at the end of drill penetration, due to drilling at a slight angle (caused by misalignment of the indexing device) or when the drill was off center (caused by variation in the tube sheet hole spacing). These ridges later caused probe hang-up and damage during eddy-current inspection. Fortunately, the problem was limited to a few tubes.

3.4 NONDESTRUCTIVE INSPECTIONS

Following the preparatory tasks, the steam generator was examined visually and nondestructively to characterize the number, type and distribution of tubing defects. This section describes the results of visual inspection of the secondary side along with the two base-line EC inspections. Data developed from these inspections were used to select a subset of 320 tubes for the round robin activities which are described and summarized below.

3.4.1 Secondary-Side Examination

Examination of the Surry generator from the secondary side was conducted with several objectives in mind. These inspections provided information about the tube bundle support structure. They served as an alternate inspection of the generator tubing, providing comparison to the data derived through primary-side inspections. The secondary-side effort also provided sampling and assaying of materials and corrosion products and deposits. Another purpose was to see if anything could be determined concerning generator flow patterns, based on observing tubing films, coloration and sludge accumulation. Secondary-side inspections were also being discussed and under consideration by NRC for field application. The SGGP effort was partly aimed at determining if the inspections could be conducted, and what technology was available or needed to achieve useful data.

3.4.1.1 Inspection Techniques

Initial secondary-side characterization was conducted through the three relatively large 12-in. square penetrations torch-cut into the generator for the preshipment examination, along with the two 5-in. diameter handholes located between the top of tube sheet and the first support plate. Two of the preshipment penetrations, at the first and seventh (uppermost) support plates at the tube lane, provided reasonably spacious access for examination of the top of tube sheet and inner row U-bends, respectively. Characterization in these areas was conducted with a miniaturized 35-mm camera, modified for remote triggering, and with rigid boroscopes. Later, the outer row U-bends

were accessed through removal of the cover plate that closed the tube bundle portion of the steam generator. This region was also examined with the use of a periscope (Schwenk and Wheeler 1984).

None of the above techniques provided for viewing a significant distance into the tube bundle. The bundle consists of 3388, 0.875-in. diameter tubes in square array located on 1.28-in. centers, leaving a nominal 0.405-in. space between tubes. This space was usually further reduced due to corrosion-induced damage. Fiberscopes were employed to examine the inside of the tube bundle. While the fiberscopes did provide some useful secondary-side characterization information, they suffered from a number of shortcomings. Major problems resulted from the limited viewing area and great difficulty with remotely positioning the fiberscope. Knowing where an observation was being made (i.e., tube row and column) was quite difficult, as well as relocating a previous position.

To overcome the difficulties in performing these inspections within the often deformed tube bundle, the SGGP developed and used a series of miniature pinhole cameras. This technique was enormously successful in allowing photographic documentation virtually within any region of the tube bundle. A relatively large region could be photographed in a limited time, important for minimizing personnel radiation exposure. The minicameras also facilitated documenting the exact location of examination. The photographic techniques for secondary-side characterization are discussed in detail by Sinclair (1984). Figure 3.12 shows typical pinhole cameras. Figure 3.13 provides an example of the photographs obtained.

Access to the secondary side of the tube bundle was accomplished through multiple shell penetrations made using a 2-1/2-in. diameter rotabroach. Typically, penetration of the 2- to 3-in. thick generator shell could be made in approximately one hour, including tooling setup and drilling. Where necessary, overlapping penetrations were made, to provide larger access areas. Shell and bundle shroud penetration techniques had to be nondamaging to the tube bundle; this eliminated such thermal techniques as plasma arc or oxyacetylene torch. Electrodischarge machining was eliminated from consideration because of the need for large amounts of liquids that, during breakthrough, could enter the generator and possibly alter the character and disposition of sludge and other corrosion products.

3.4.1.2 Inspection Results

The majority of the secondary-side inspection work was conducted prior to completion of the primary-side nondestructive inspections. As such, the secondary-side inspections, and acquiring access for the inspections, had to be nondamaging to the tubing.

3.4.1.2.1 U-Bend Area

The inner two rows of U-bends were preventively plugged, following a sudden U-bend failure during service. Stress corrosion cracking of U-bends was affected by tube support-plate degradation and by fabrication-induced stresses. The secondary-side inspection revealed that as many as 20 Row 1
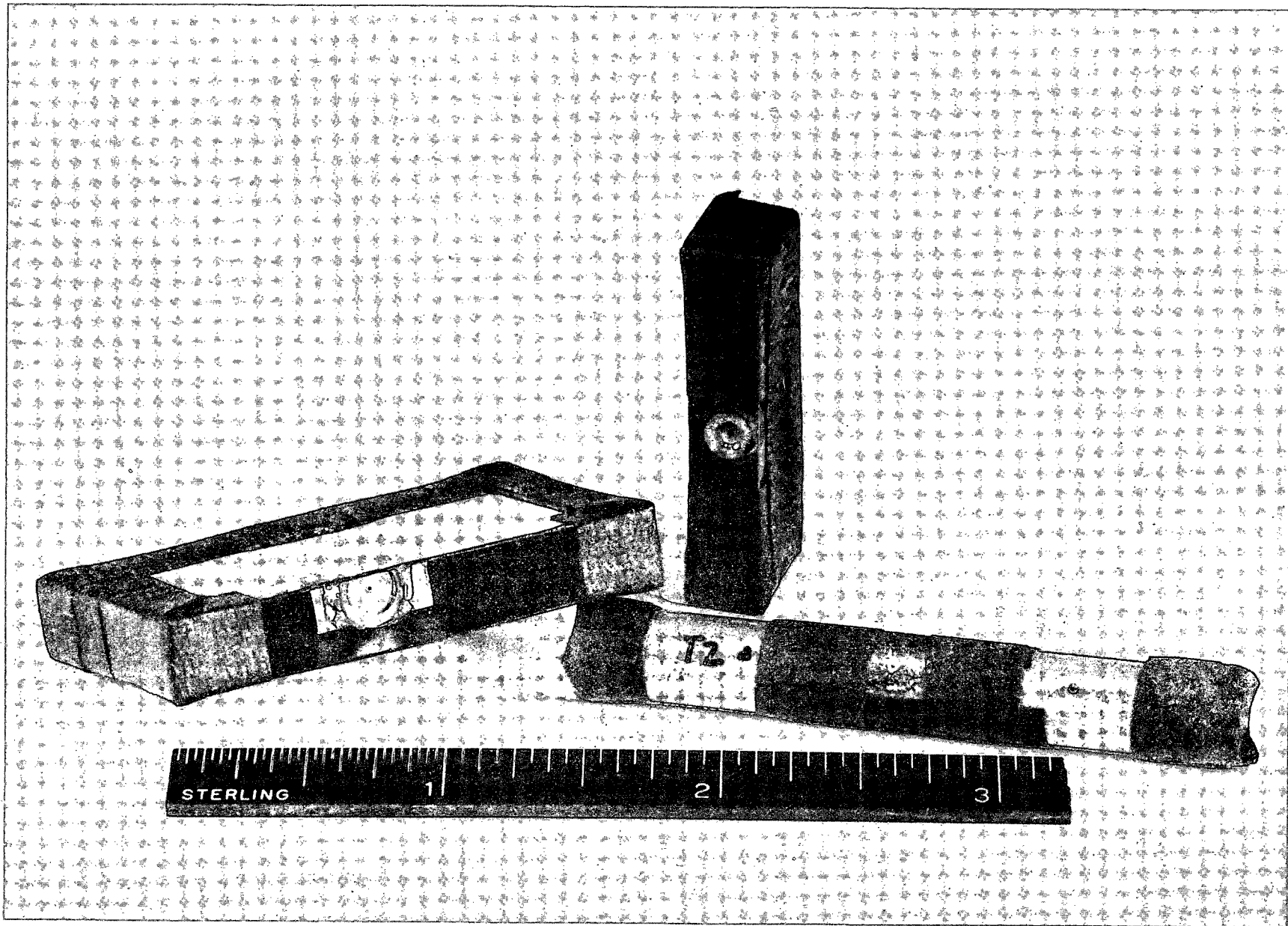
FIGURE 3.12. Cameras Fabricated for Use in Surry Generator

FIGURE 3.13.   Side Movement (Parallel to Lane) of Tubes Relative
                to the First Support Plate, Column 39-40

3.24

U-bends showed burst type cracks. In addition, 50 to 66 other Row 1 U-bends were probably cracked either on the extrados side of the U-bend or showed axial creases on the intrados side, probably indicative of primary-side initiated cracks that had penetrated part way through the wall. Figure 3.14 shows a creased tube.

FIGURE 3.14. Probable ID (Primary) Side Initiated Crack Which Appears as an Axial Crease in the Apex of Column 87

All inner row U-bend failures were located in tube columns which corresponded to support-plate flow slot "soft spots." Figure 3.15 reveals support-plate flow-slot hourglassing in the seventh support plate.

In general, visual and photographic inspection did not reveal cracks or shallow defects beneath the thin, brown-black outer scale found on most tubes. Instances of missing U-bend sections, such as shown in Figure 3.16c, were revealed. Since the inner two rows of U-bends were plugged after an initial U-bend failure, the numerous through-wall defects, and the missing tube sections, occurred after plugging. The cracking could, in part, be attributable to the increasing applied stresses as the support plates continued to corrode. No other U-bend damage was observed via the in situ secondary-side inspections.

Column 94

Column 46

Column 48

Column 1

8605834-4cn

FIGURE 3.15. Montage Photo of the Top of the Seventh Support
              Plate at the Tube Lane, Column 94 to Column 1
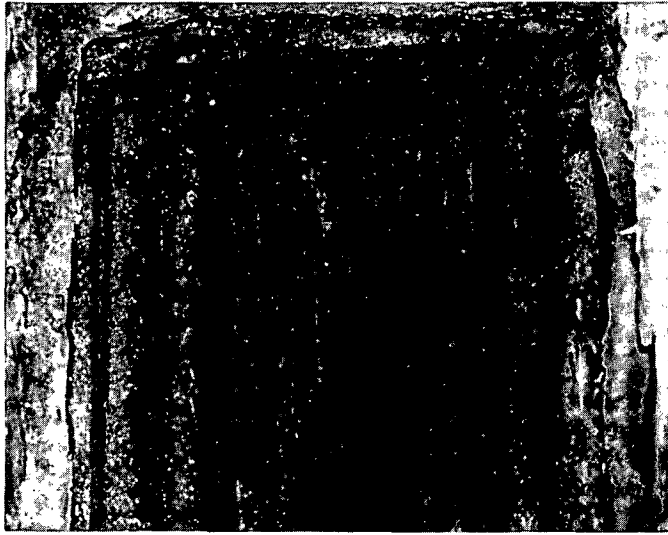
a)
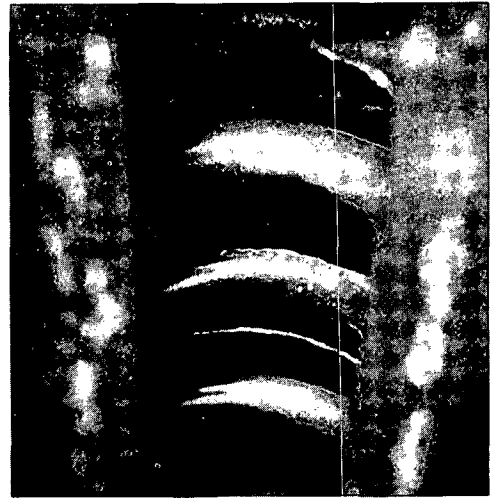
b)
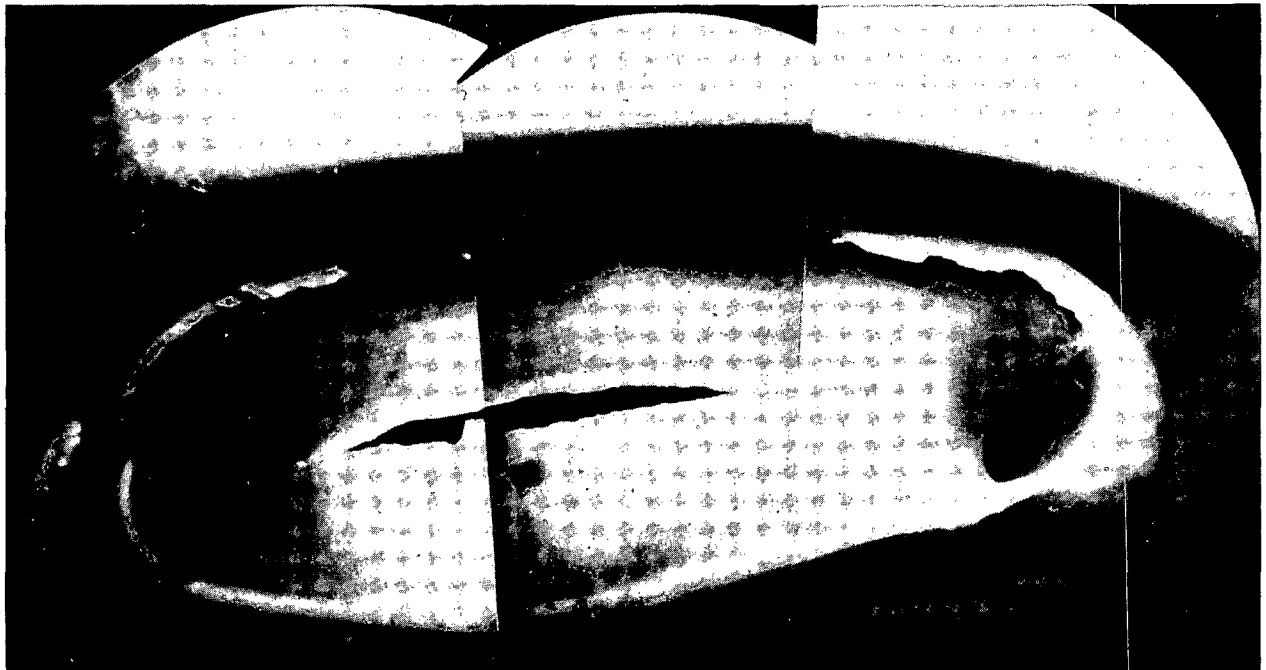
c)

FIGURE 3.16. Probable Burst-Type Fracture, U-Bend R1C85;
a) Penetration Below Seventh TSP, b) Looking Up
(Intrados Region), c) Looking Down (Extrados Region)

3.4.1.2.2 Tube Support Plates

Corrosion of the tube support plates leading to tube denting and support-plate damage (cracking and deformation) was the primary cause of tube plugging in the Surry generator, eventually leading to its early retirement from service. Secondary-side inspections documented support plate conditions throughout the generator and concentrated on an examination of the second support plate (Schwenk 1987). The second support plate was considered the most severely degraded based on eddy-current and profilometry testing.

Tube lane flow slots at each of the seven support plates were severely deformed. The traditional hourglassing of the flow slots was only seen on the uppermost support plate. At all other support-plate levels the hourglassing had progressed such that the flow slots were essentially closed due to deformation and collapse from the hot-leg side, such as shown in Figure 3.17. The detailed secondary-side examination of the second support plate was to determine how extensive damage was across the support plate and the potential effect on remaining structural integrity. A particular concern was how far back from the collapsed flow slots did significant tube damage occur. Figure 3.18 documents the support plate condition completely across the hot-leg side at one column. Several regions of the second tube support plate were documented in this manner (Schwenk 1987).

Flow hole compression/ovalization was documented near the expected support plate hard spots between flow slots and at block/wedge locations anchoring the support plates to the generator shell. Extensive flow-hole-to-tube-hole ligament cracking was noted, though this condition could not be fully photographically documented due to sludge/corrosion product accumulation on the support plates. Sections of support plate were found as loose parts within the generator.

After removal of the U-bends, full-length tube pulls from the top of the generator experienced little or no resistance on the hot-leg side, despite the expected compressive loadings anticipated from extensive corrosion and denting of the support plate structures into the tubing. The support plates on the hot-leg side readily broke up, indicating ligament failure across the entire hot-leg side. The cold-leg support-plates, especially those below the fourth support plate, did not readily break up during specimen removals (although they exhibited significant corrosion).

3.4.1.2.3 Top of Tube Sheet/Sludge Pile

The Surry generator experienced wastage damage during initial service, using a coordinated pH phosphate water chemistry control. Sludge lancing was conducted; however, eddy-current sludge height measurements indicated sludge was moved around on the top of tube sheet, but not effectively removed. The sludge pile was found to consist of two distinct regions, a granular black sludge (AVT origin) on top of a layer of phosphate sludge. The pile was located mainly in the center portion of the tube bundle; however, there was also sludge in the peripheral regions. The sludge in the peripheral regions was on the tubesheet and attached to the tubes. The phosphate sludge was hard and somewhat brittle. Sludge samples were acquired from tube sheet
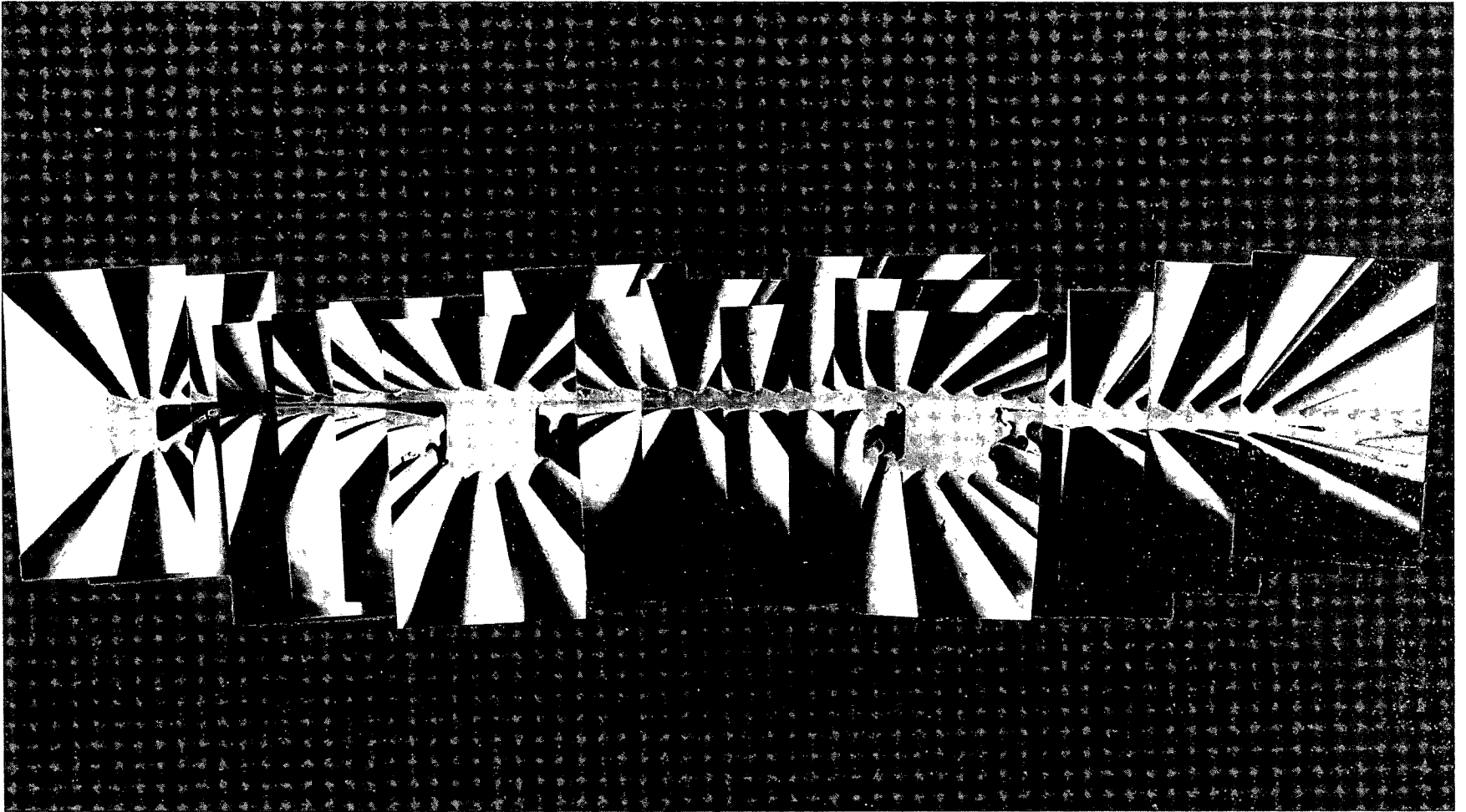
FIGURE 3.17. Bottom Side of First Support Plate, from 0° Handhole
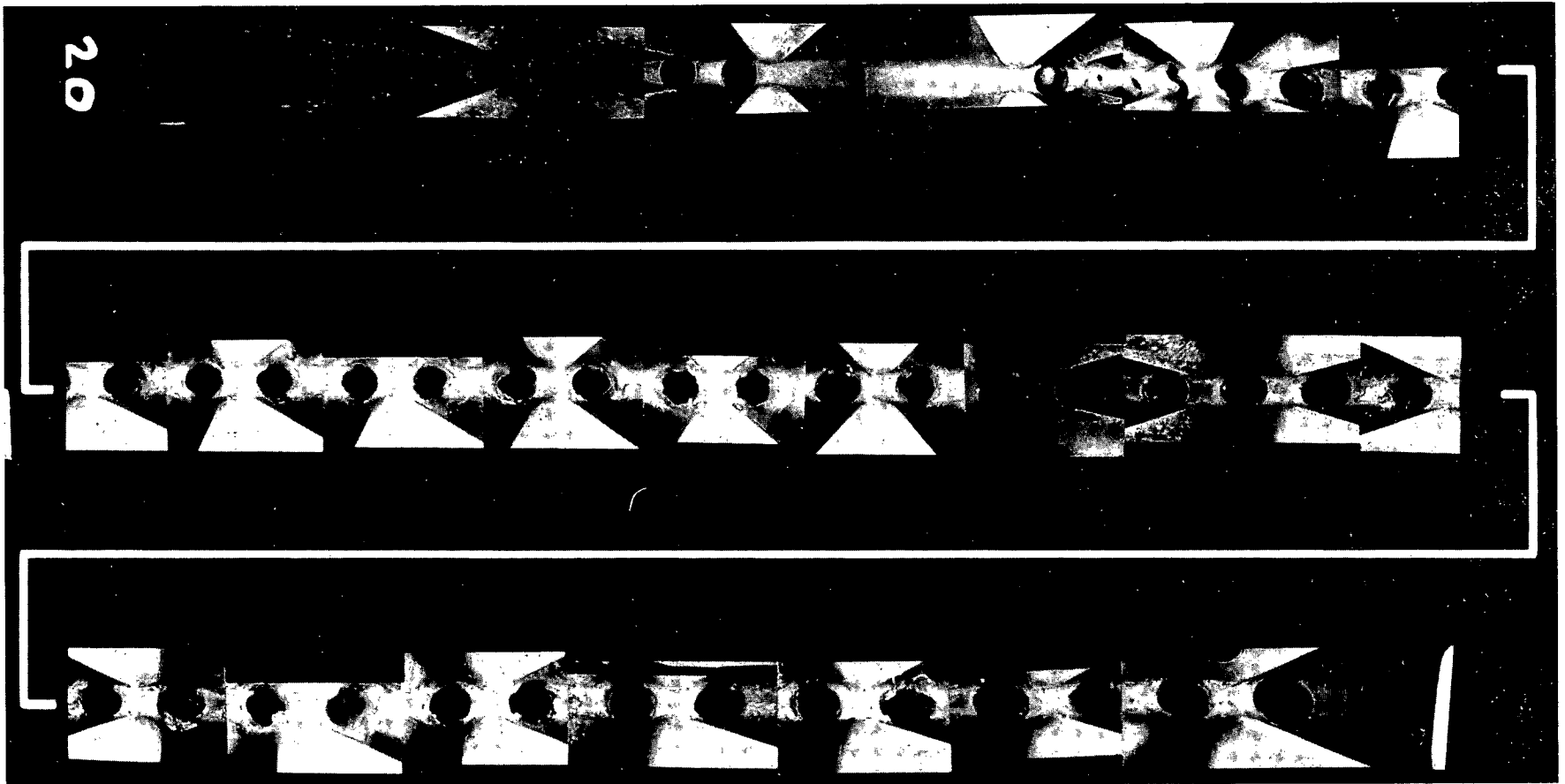
FIGURE 3.18. Montage Photo Looking Up at the Second Support Plate from Shell Wall (Hot Leg Side) to the Cold Leg Side at Column 62-63

section removals, as shown in Figures 3.19 and 3.20. Sludge composition varied considerably with height above the top of tube sheet (TTS) and from the hot-leg to the cold-leg side of the generator. There were also compositional variations from point to point in a local region. Tables 3.1 and 3.2 provide a summary of sludge analysis as a function of location above the TTS for hot-leg and cold-leg regions. Results from inductively-coupled plasma spectroscopy (ICP) are presented in Table 3.1. Iron, copper, and zinc were the primary elements found in the hot-leg sludge samples. The Cu and Zn concentrations increased with distance above the TTS with a sharp increase in copper observed in the AVT sludge. In addition to Fe, Cu, and Zn, high concentrations of Na and P were found in the cold-leg sludge samples from locations up to 1.5 in. above the TTS. A sharp increase in Cu and Zn and corresponding decrease in Na and P occurred when the sludge changed from phosphate to AVT origin.

X-ray diffraction (see Table 3.2) analysis indicated that AVT sludge was primarily composed of Fe_3O_4 and metallic Cu with a small amount of Fe_2O_3 in the cold-leg sample. The reddish phosphate sludge from the cold-leg sample was composed of Fe_2O_3, Fe_3O_4, and $NaFePO_4$ in decreasing order of relative concentration. Only a trace of Fe_3O_4 was detected in the X-ray diffraction patterns of the phosphate sludge samples taken from near the TTS of both the hot- and cold-leg sludge piles. A lack of diffraction peaks in these samples suggests either an amorphous or highly defected crystal structure with poor diffraction characteristics. Further information on sludge characterization may be found in reports by Kurtz et al. (1987) and Bradley et al. (1988).

3.4.1.2.4 General Secondary-Side Observations

The secondary side was characterized throughout the generator. In general, the tube-support structure appeared to be heavily corroded, cracked and deformed. This deformation often caused tube damage a considerable distance (~6-8 rows) back from boundaries between hard- and soft-spot tube support-plate regions. Several examples were documented of loose parts in the generator, consisting mainly of small sections of support plate. There was no positive association of tube damage with the loose parts. The loose part locations were used as inputs to the test matrix, to ascertain if the primary-side NDE would detect and define the resulting signal. Tube support-plate sections removed from the hot-leg invariably fell apart, indicating complete loss of structural integrity in the support plates.

Tube bursts in the inner row U-bends, as well as bulged tubes, were found. It did not prove feasible to attempt definition of fluid flow within the generator through assessing color changes on the outer film of the generator tubes. The main color differences noted were between plugged and nonplugged tubes, and these differences were mainly apparent within or near the sludge pile.

The most comprehensive summary of the secondary-side inspections is found in a report by Schwenk (1987). This effort did prove that the secondary side of a generator can be inspected. The resulting documentation is the most comprehensive ever published on the conditions which can derive from corrosion damage within a steam generator. The secondary-side characterization also
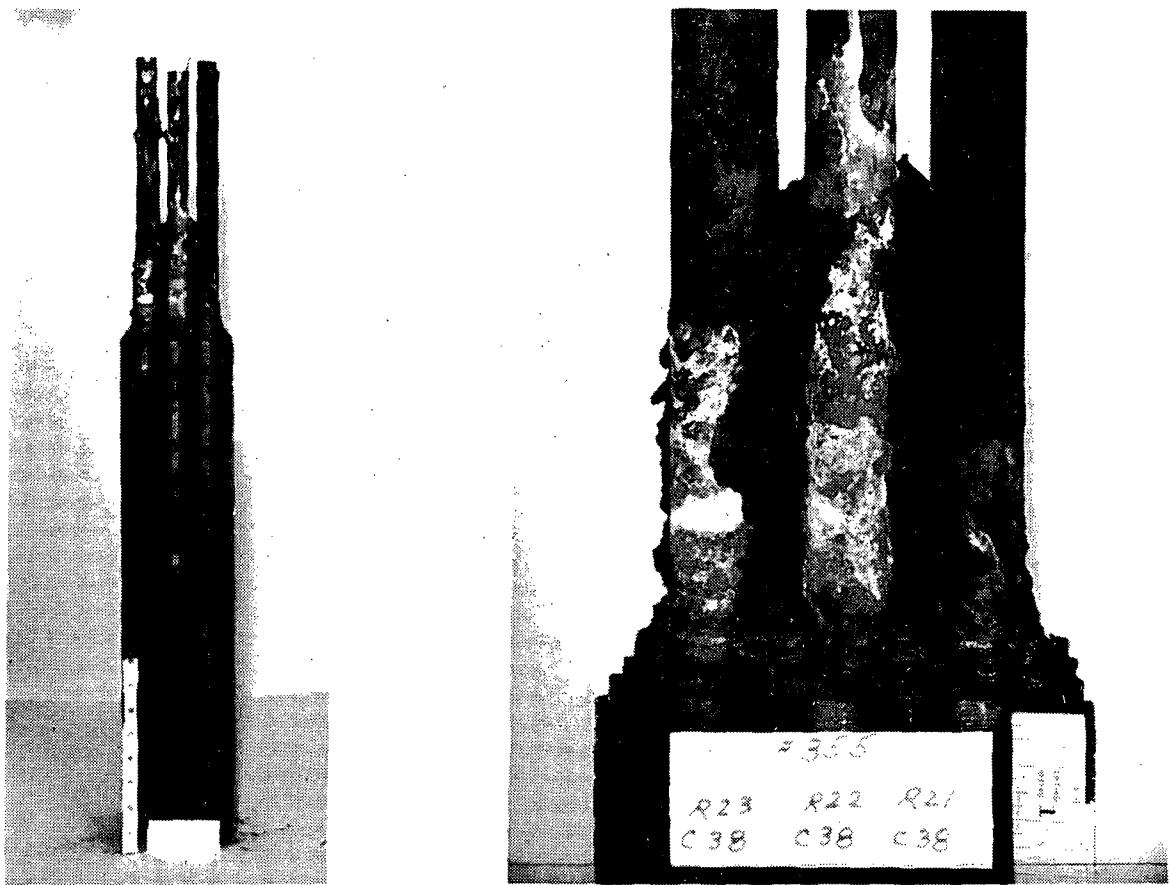
FIGURE 3.19. Overview and Sludge Pile Closeup of Hot Leg Tube
Sheet Section #355
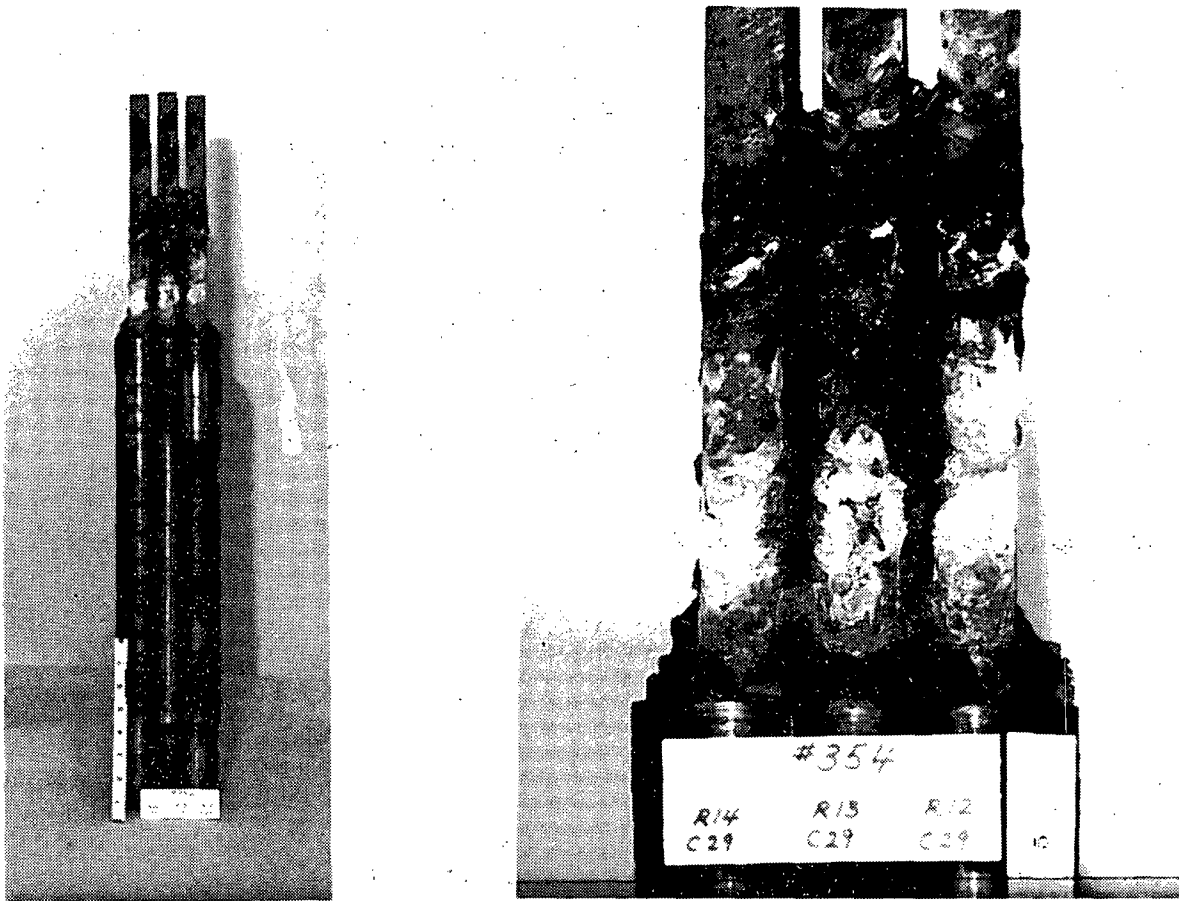
FIGURE 3.20. Overview and Sludge Pile Closeup of Cold Leg Tube
Sheet Section #354

TABLE 3.1. Results From ICP Analysis of Sludge Samples From
Tube Sheet Specimen #355 (HL) and #354 (CL)

Location Above Tube Sheet, mm

Element	0-10 HL	0-10 CL	10-20 HL	10-20 CL	25-35 HL	25-35 CL	50-70 HL	50-70 CL
Fe	67.00	35.05	55.41	34.69	42.53	36.28	40.17	44.51
Cu	0.81	1.44	3.76	3.20	18.07	4.57	21.90	14.46
Zn	0.28	0.27	1.05	0.39	2.24	0.57	6.94	11.27
Cr	0.26	0.29	0.25	0.13	0.27	0.26	0.14	0.20
Ni	0.62	0.49	0.89	0.33	1.19	1.07	0.12	0.81
Si	0.26	0.73	1.06	0.24	0.76	0.46	0.34	0.49
P	0.29	9.77	1.35	10.57	1.25	10.08	0.31	0.24
Na	0.15	12.90	0.13	13.35	0.17	8.70	0.80	0.96

Values reported as weight percent.

TABLE 3.2. Results From X-Ray Diffraction of Sludge Samples
From Tube Sheet Specimen #354 (HL) and #355 (CL)

Location Above Tube Sheet, mm.

Phase	0-10 HL	0-10 CL	10-20 HL	10-20 CL	25-35 HL	25-35 CL	50-70 HL	50-70 CL
Fe_3O_4	(a)	(a)	(a)	(a)	60%(b)	30%	60%	25%
Fe_2O_3	--	--	--	--	--	50%	--	15%
Cu	--	--	--	--	40%	--	40%	60%
$NaFePO_4$	--	--	--	--	--	20%	--	--

(a) Mostly amorphous with trace of Fe_3O_4.
(b) Relative phase concentrations were estimated from peak intensities.

provided valuable inputs into the selection of specimens for primary-side nondestructive inspection and for subsequent specimen removal to validate NDE and assess generator damage.

3.4.2 Base-Line Eddy-Current Inspection

The goal of this task was to characterize the generator throughout to establish the total defect conditions observable with eddy-current examination. The results of this characterization would then be amenable to statistical interpretation. This allowed a representative subset of specimens which were characteristic of conditions found in the steam generator to be chosen for the round robin examinations.

Prior to the post-service base-line examinations, an eddy-current profilometry examination (using a Zetec MIZ 15) had been conducted of 96 tubes selected to represent all regions of the generator. This examination was used to specify the probe sizes required for the base-line study, and had shown that the generator could be reasonably inspected with large-diameter (0.700-in.) probes over most regions. It also indicated that the location of maximum denting was at the hot-leg second support plate (Clark and Lewis 1984). The extent of denting and the effect on inspectability was a major preliminary concern since the Surry 2A tube plugging was largely denting related.

Two post-service base-line eddy-current examinations were conducted. One examination used the Zetec MIZ-12 multifrequency eddy-current data acquisition system with a Zetec DDA-4 data analyzer, which was the current field practice standard in the U.S. The other examination utilized an Intercontrole IC3FA multifrequency data acquisition system and an Intercontrole IC4AN data analyzer. It was felt that these two systems and their close derivatives account for the vast majority of current field inspections of nuclear steam generators. Two examination teams were chosen to conduct the post-service base-line examinations. Each team consisted of experienced ISI practitioners and were expert with their respective system. Both examination teams were requested to conduct the best possible examination, meeting as a minimum the requirements set forth in the ASME Boiler and Pressure Vessel Code, Sections V and XI. In addition, all wall-loss indications, including those less than 20% through wall, were requested to be reported. Both teams were aware of the research nature of the project, and each team included senior analysts from the respective vendors.

The base-line eddy-current examination of the steam generator often involved repeated scans with progressively smaller probes, to obtain access through dented support-plate regions. Probe diameters down to 0.610 in. were used by Zetec and down to 0.669 in. by Intercontrole.

Comparing the results of the two post-service base-line eddy-current examinations produced a spread in results greater than anticipated by the project staff. There was disagreement on defect sizing, on classification of eddy-current indications as a defect or as an artifact and, in a few cases, on the existence of an eddy-current signal. Many of these disagreements remained even after both teams were informed of specific differences and allowed an opportunity to modify their respective results. In a few cases,

the teams admitted an omission or reinterpreted their results. Both teams reported that the effects of denting and conductive deposits on eddy-current signals could not be eliminated by mixing the responses of various test frequencies. The differences in inspection results appear to be due to differences in the analysts' interpretations of complex eddy-current signals. As a result of the data review, the teams' analysts agreed to disagree in their interpretation of the data. Since the project could not determine a priori if one or the other base-line inspection team was correct, the selection of a subset of tubing specimens representative of the generator condition became more complex.

The results of the base-line inspections, summarized in Table 3.3, show that the majority of reported defects (wall-loss indications) were at the top of the hot-leg tube sheet in the sludge pile. There was a relative paucity of defects in other regions of the generator, except for some indications in the U-bend area not generally associated with AVB contacts. The base-line inspections did not indicate degradation in the tube sheet crevice, though some denting was present at the TTS. The base-line inspections also indicated the presence of tube bulging in previously plugged tubes. The only common detections between the two base-line inspection teams were at the top of tube sheet on hot- and cold-legs, the first support plate on the cold-leg and the seventh support plate on the hot-leg.

TABLE 3.3. Locations of Wall-Loss Indications
From the Base-Line Inspections

| | Number of Indications | | | |
| | Hot-Leg | | Cold-Leg | |
Reference Location	Team X	Team Y	Team X	Team Y
Tube End	1			
Tube Sheet Gap		1		
Unspecified Tube Sheet		2		4
Top of Tube Sheet	713	731	22	113
Support Plate 1	3	5	1	6
Support Plate 2		3		2
Support Plate 3	2	3	2	1
Support Plate 4		1	2	3
Support Plate 5	1	9		1
Support Plate 6		20	1	9
Support Plate 7	11	115	20	10
U-bend		22		

Further details on the base-line eddy-current inspections and analysis of results can be found in a report by Doctor et al. (1988a).

3.36

3.4.3 Round Robin Tube Selection

A major goal of the SGGP was to establish the reliability of eddy-current inspection of PWR steam generator tubing. The two base-line inspections of the Surry 2A generator were planned as a means to locate indications for selecting a subset of tubes for NDE round robin testing and to supplement the ISI reliability data base. The criteria for selecting an appropriate subset of tubes from the Surry generator were based on all available information on the generator, historical and derived by the SGGP. The first consideration was to ensure that sufficient numbers of defects were included in the sample to allow a statistically valid estimate of the ability of eddy-current procedures to detect and size defects.

There was information on the presence and locations of possible defects from two basic sources: 1) the inservice history of the generator (leakers, plugging reasons) and secondary-side and other observations made during the SGGP (defects, sludge-filled tubes at unplugging), and 2) the SGGP base-line eddy-current inspections. The historical data did not provide much information on possible wall-loss defects except in the crescent zone region near the center of the hot-leg top of tube sheet. The eddy-current inspections conducted in the two years prior to decommissioning were used only to determine the extent of denting. Some through-wall defects were reported because of observed leakage. Therefore, the majority of information on tubes containing possible defects was taken from the post-service base-line inspections.

A statistical sampling rationale was derived as explained by Doctor et al. (1988b). The sampling rationale involved a stratification of the base-line inspection results into wall-loss indication size catagories, <20%, 20%-40%, >40% of wall, and into three agreement catagories:

- Both teams reported an indication at the same location and agreed on the depth within 10%.

- Both teams reported an indication at the same location and differed in reported depth by >10%.

- Mismatch on detection - either the teams differed on the source (reportable indication versus artifact) of the signal they both detected, or one team did not detect a signal found by the other.

Each agreement category (strata) was sampled equally and the size strata were sampled such that the final defect set contained 45%, 35% and 20%, respectively, for wall-loss indications of >40%, 20%-40%, and <20%. Sampling within the strata was done on a random basis. Eighty percent of the tubes, ~240, were chosen because defects were reported by the base-line inspection teams. The remaining 20% of tubes selected for the round robin sample were chosen for several reasons. They included tubes in which 1) a defect was expected, but none was reported by the base-line inspections (i.e., surrounding tubes all showed indications), 2) tubes in which no defects were expected and none were reported, and 3) tubes in which non-wall-loss conditions were reported (bulging, permeability variations, conductive deposits and loose parts).

3.37

Table 3.4 shows the number of tubes selected for the round robin subset in each category. Figure 3.21 illustrates the location of the round robin tubes across the generator bundle.

TABLE 3.4. Numbers of Tubes in the Round Robin Sample
Listed by Size and Agreement Substrata

Indication Depth	Matched Detection Size Diff <10%	Matched Detection Size Diff >10%	Unmatched Detection
>40%	35	36	32
20%-40%	30	30	29
<20%	16	16	16

Miscellaneous Tubes Added to Matrix - 80
Total Round Robin Tubes - 320

3.4.4 Round Robin Inspections

A series of round robin nondestructive examinations were conducted on the generator. These examinations were divided into:

• Data Acquisition and Analysis Round Robin (DAARR) using Zetec multi-frequency EC inspection equipment

• Advanced/Alternate Techniques Round Robin (AATRR) consisting of NDE inspections with equipment or analysis procedures significantly different from those used in the base-line or other round robin inspections

• Analysis Round Robin I using EC data tapes produced by the base-line inspection conducted with Zetec multifrequency equipment

• Analysis Round Robin II using EC data tapes produced by the base-line inspection conducted with Intercontrole multifrequency equipment.

The DAARR and the two Analysis Round Robin experiments were designed to provide data for estimating the variability in inspection results. The DAARR showed the variability related to personnel differences for the overall inspection (data acquisition and analysis) process using the same instrumentation. Conversely, data from the two Analysis Round Robins provided an estimate of the variability associated with only the analysis and interpretation of recorded EC signals. The AATRR was designed to provide NDE equipment developers with the opportunity to test equipment and/or analysis procedures on service-degraded tubes in exchange for providing inspection results. The intent of this round robin was not to compare the various techniques, since some of the techniques were designed to detect specific defect conditions, but to determine the improvement in defect detection and

SERIES 51

NOZZLE ◄—   MANWAY —►
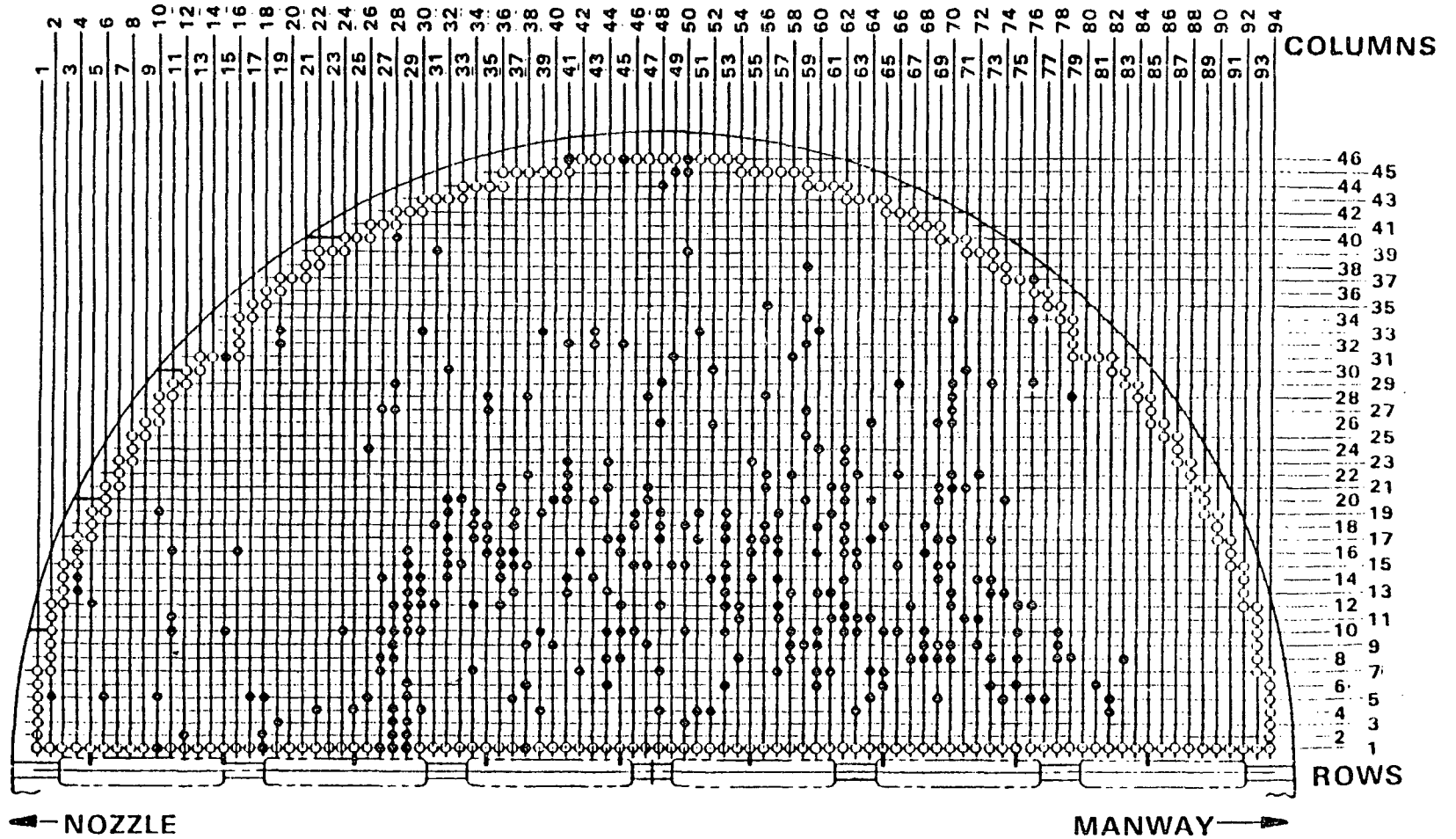
FIGURE 3.21.   Subset of Tubes Selected for Round Robin Inspections

3.39

sizing to be expected from emerging NDE technologies. Results of the round robin exercises were described in a report by Doctor et al. (1988b).

3.4.4.1 Data Acquisition and Analysis Round Robin (DAARR)

The DAARR comprised five teams investigating the round robin subset of steam generator tubes using the Zetec MIZ-12 multifrequency eddy-current data acquisition system and a Zetec DDA-4 data analyzer. Four of the teams were selected from proposals received in response to a request for proposal, and one team was provided by a SGGP sponsor. All teams were provided by commercial vendors that perform eddy-current NDE services. A minimum of four teams was determined to be necessary to provide a statistically valid measure of NDE reliability. Each team was provided with information on the operational history of the steam generator, along with a work statement describing test objectives, applicable codes and personnel qualification requirements. In addition, several test parameters were standardized to eliminate extraneous variables from the inspections. This included a protocol to control testing procedures and reporting of results. Three of the examination frequencies were specified: 400 kHz using the differential mode and 100 kHz using the differential and absolute modes. A fourth optional frequency was selected by each team at its own discretion. While the teams were required to take data on the three designated frequencies, they were encouraged to analyze the signals by their standard field practice procedures. Each team had five working days to acquire and analyze the data from 320 tubes. Most teams completed the task in less time.

A Zetec Type SFM EC probe was specified. The SFM type, typical of those used for U.S. steam generator examinations, contains a permanent magnet which is designed to saturate ferromagnetic elements in the tube (permeability variations), canceling their affect on the EC signal. The teams were instructed to use specific probe sizes in specific tubes. This was done to ensure the maximum extent of inspection of each tube by using probes with the largest fill factor that would pass through the tube. The probe sizes were either 0.700 in. or 0.720 in. in diameter. All teams used the same probe positioning equipment and probe pusher-puller, supplied by PNL.

Table 3.5 provides a summary of the origin and types of wall-loss indications reported by each of the teams participating in the DAARR. Strictly speaking, "indication" can mean the presence of an EC signal; however, EC inspections of this generator produced many signals, some of them caused by denting and conductive deposits, which are not directly related to tube failures. Henceforth, "indication" and "wall-loss indication" are used synonymously, both referring to a tube wall degradation. The first line of each table shows the total number of indications reported by each team.

The second line of the table shows the number of indications after multiple indications were removed. During the base-line examination, there were numerous instances of multiple indications reported at the top of the tube sheet. This noticeably complicated the task of comparing the two inspections, since it was often difficult to ascertain which indications from the two

TABLE 3.5. Numbers and Types of Indications Reported by
Acquisition and Analysis Round Robin Teams

| | Numbers of Indications | | | | |
| | Team | | | | |
	A	B	C	D	E
Total Indications	287	207	292	267	270
Total Indications (Multiples Removed)	255	205	226	265	223
OD Indications	234	195	226	261	212
ID Indications	16	3		1	
Unidentified Origin	5	7		3	11
Wastage*	2				
Cracking*	1				
Possible IGA*			20		
Unidentified Indication Type	252	205	206	265	223

*Reporting of type of indication not required.

inspections matched. Therefore, the instructions for the round robin teams explicitly stated that the location of the deepest part of an indication should be reported; however, the decision of where one indication ended and another began was a subjective judgment of the data analyst. For the round robins, the propensity for reporting adjacent multiple indications varied among the teams. To avoid misrepresenting the numbers of common detections caused by multiple indications, multiple OD calls within 3 in. on the same tube were considered to reference different parts of the same large defect and were combined. The resulting OD indication was given the size and location of the largest (in terms of percent through-wall) of the original multiple indications. Comparing the numbers in the first two lines of Table 3.5 shows the effect of the removal of multiple indications.

The three lines of the tables show the number of indications in each origin category, outer diameter (OD), inner diameter (ID), or unidentified origin. Unidentified indication origins refer to reported indications where no origin data was provided or the data provided was ambiguous. In most cases, this data omission was probably inadvertent, although some teams seemed more prone to leaving out information than others.

The last four lines of the table show the numbers of each type of indication reported. The teams were not required to provide this information, and some teams were somewhat more disposed to doing so than others. If no indication type was provided, this was included in the unidentified type category.

The data presented in Table 3.5 shows that the total number of wall-loss indications ranged from 207 to 292. The removal of multiple indications reduced the range of the number of indications reported from 205 to 265. The number of OD indications reported varied from 195 to 261. The number of ID

3.41

indications varied from 0 to 16. Most teams elected not to report indication types, although Team C did report 20 tubes contained intergranular attack (IGA). In all but two cases, these were associated with reported OD wastage at the top of the tube sheet.

For comparison purposes, note that the number of indications reported from the base-line inspections of the round robin tubes is 242 for Team X and 292 for Team Y.

The reference locations of the indications reported by each DAARR team are given in Table 3.6. The teams were instructed to reference indications to the tube sheet or nearest support plate. When this did not occur, the indication locations were established during statistical analysis. In the case where the nearest reference point was the seventh support plate, this instruction apparently caused confusion. Some teams referenced indications up to 14 feet into the U-bend to the seventh support plate. Other teams referenced U-bend indications as simply "U-bend," thereby providing no means to unambiguously locate the indication. The reference locations of indications at the seventh support plate and U-bends have been left the way the teams reported them. Some of the indications referenced to the seventh support plate were, therefore, actually in the U-bend region. There were also cases where no location was provided, an incomplete location was provided (for example, "HL"), or the location reference was illegible. These were tabulated in the "Unidentified Location" category.

Similar to what was observed for the base-line inspections (see Table 3.3), a few wall-loss indications are scattered among the support plates, with the majority of indications located at the top of the tube sheet on the hot-leg side of the generator. The next highest number of indications reported is usually at the cold-leg top of tube sheet. Again, it is important to remember that similar numbers of reported indications by two or more teams does not imply the teams are referring to the same defects. However, it is interesting to compare the total numbers of indications reported by the teams at given locations. Table 3.6 shows that the number of indications at the hot-leg top of tube sheet was relatively constant throughout the five Acquisition and Analysis Round Robin inspections, ranging from 192 to 223. An area of significant disagreement in numbers of reported indications was the cold-leg top of tube sheet.

3.4.4.2 Advanced/Alternate Techniques Round Robin (AATRR)

As previously indicated, this round robin consisted of nondestructive inspection with equipment or analysis procedures different from those used in the base-line or other round robin inspections discussed in the preceding paragraphs. While it was encouraged for these examinations to be conducted using the round robin subset of generator tubes, it was not required. In fact, most of the advanced technique examinations utilized special equipment which was designed to characterize a specific defect type or inspect a specific region of the generator. Also, several of the techniques utilized in this category were experimental or developmental in nature. While this inhibited direct correlation of results with previous work, this effort was

TABLE 3.6. Location of Indications Reported by
Acquisition and Analysis Round Robin Teams

Reference	Numbers of Indications Location Team				
	A	B	C	D	E
Hot Leg					
Tube End	8				
Tube Sheet Roll	2				
Tube Sheet Crevice					
Top of Tube Sheet	216	192	212	223	218
Support Plate 1					
Support Plate 2	3	1			
Support Plate 3					
Support Plate 4	1			1	
Support Plate 5	1				
Support Plate 6					
Support Plate 7	6	4	2	4	4
Cold Leg					
Tube End	10	1			
Tube Sheet Roll		5			
Tube Sheet Crevice					
Top of Tube Sheet	6	1	8	36	1
Support Plate 1	2	1		1	
Support Plate 2			1		
Support Plate 3			1		
Support Plate 4					
Support Plate 5					
Support Plate 6					
Support Plate 7			1		
U-bend					
Unidentified Location			1		

intended to provide a validation opportunity for potentially improved
inspection techniques.

Examinations under this task, with the exception of the profilometry, were
conducted at participant expense. Eddy-current NDE, utilizing special eddy-
current probes, included tube sheet crevice examinations with an 8x1 pancake
probe and with a French rotating eddy-current probe. A special three
frequency double mix, using a MIZ-12 was unsuccessfully attempted by another
team to define tube damage under support plates. A developmental multi-
frequency/multiparameter eddy-current system was applied to the generator.
This examination experienced difficulties due to failure of special eddy-
current probes with surface-riding pancake coils. The ridges left during
plug removal caused particular problems for this system. In addition, the
system analysis software required modification to allow a greater range of

signal inputs without saturation. A Japanese examination concentrated on characterization of inner row U-bends for stress corrosion cracking, with a special flexible probe, and at studying the tube-sheet crevice area for primary-side stress corrosion cracking at the roll transition. A surface-riding four-coil focused probe was used. One team utilized computer-aided data interpretation. This involved an in-line computer system for signal gating, mixing and data analysis (Doctor et al. 1988b).

Two teams applied ultrasonic (UT) inspection procedures. One team utilized a rotating UT probe, the other an electronically sequenced probe with eight sections. Both probes were utilized to inspect the tube sheet region for intergranular attack (IGA) and stress corrosion cracking (SCC). One team utilized UT to characterize defects found near the top of tube sheet with eddy-currents. The UT sizing results were used to modify the eddy-current reported results throughout the generator.

Table 3.7 shows the number of wall-loss indications reported during the advanced/alternate techniques round robin. It is not appropriate to compare all teams with each other (or with the other round robin teams) based on the number and type of indications, since one team inspected only a subset of the round robin tubes. The advanced/alternate techniques were often designed specifically to detect certain types of defects that a conventional bobbin-coil inspection would not detect.

TABLE 3.7. Numbers and Types of Indications Reported by Advanced/Alternate Technique Teams

| | Numbers of Indications | | | |
| | Team | | | |
	U*	V	UU	VV
Total Indications	151	279	119	130
Total Indications (Multiples Removed)	145	279	118	126
OD Indications	145	257		
ID Indications		22		
Unidentified Origin			118	126
Wastage**	48	256		
Wastage/Cracking**	2			
IGA*	95			
Unidentified Indication Type		22	118	126

*Team U inspected a subset of round robin tubes.
**Reporting of type of indication not required.

3.44

The locations of advanced/alternate techniques wall-loss indications are given in Table 3.8. As the advanced/alternate techniques inspected different numbers of tubes (Team U inspected a subset of the round robin tubes) and the other teams inspected different locations within the tubes, it is not appropriate to compare the teams based on numbers of reported indications given at any location other than the hot-leg top of the tube sheet.

TABLE 3.8. Location of Indications Reported by Advanced/Alternate Technique Teams

| Location Reference | Numbers of Indications Team | | | |
	U*	V	UU	VV
Hot Leg				
Tube End				
Tube Sheet Roll				
Tube Sheet Crevice				
Top of Tube Sheet	56	239	95	104
Support Plate 1	.6	3		
Support Plate 2	2	2		
Support Plate 3	1			
Support Plate 4		7		
Support Plate 5		2		
Support Plate 6	2			
Support Plate 7	10	1		2
Cold Leg				
Tube End				
Tube Sheet Roll				
Tube Sheet Crevice				
Top of Tube Sheet	47	17	16	19
Support Plate 1	1		7	
Support Plate 2	4			
Support Plate 3	2	1		
Support Plate 4		1(1)		
Support Plate 5		2		
Support Plate 6	3			
Support Plate 7	10			
U-bend		3		
Unidentified Location	1			1

*Team U inspected a subset of round robin tubes.
()Denotes indications referenced between support plate and next higher support plate.

Under subcontract, Babcock and Wilcox performed a profilometry examination using the PROFILE-360 system. The primary purpose was to provide a measure of deformation from which strain levels in dented tubes are computed, for comparison to metallographic analyses. The presence or absence of IGSCC as a function of denting-induced strain is an issue in developing/evaluating a strain-based tube-plugging criteria. Profilometry examinations were made in 100 tubes, including some round robin tubes, and a distribution of tubes through various regions of the generator. Results of this examination are detailed in a report by Doctor et al. (1988b) and summarized in Table 3.9.

TABLE 3.9. Statistical Summary of Profilometry Data

Number of Tubes Examined: 101

TSP	NUMBER	MAX DIA	SIGMA	MIN DIA	SIGMA	MAX STRAIN	SIGMA
7	91	781.	18.	731.	40.	8.3	13.5
6	91	781.	12.	736.	20.	6.7	5.1
5	91	783.	12.	733.	19.	6.9	3.6
4	92	785.	17.	728.	29.	7.7	6.0
3	95	786.	17.	727.	39.	8.4	10.3
2	99	791.	24.	723.	36.	8.9	8.3
1	101	789.	21.	726.	32.	9.1	10.2
0	101	771.	10.	755.	4.	2.6	1.1
SUM	761	783.	18.	732.	31.	7.3	8.4

Distribution Summary

	DIAMETER REDUCTION (MIL)				STRAIN (%)		
TSP	> 20	> 50.	> 100.		> 10.0	> 15.0	> 25.0
7	39	12	4		8	2	4
6	51	10	1		7	2	2
5	55	14	1		11	1	1
4	61	12	5		7	3	2
3	58	12	5		8	4	3
2	58	16	9		11	6	5
1	52	15	8		13	5	8
0	0	1	0		1	0	0
SUM	374	92	33		66	23	25

3.4.4.3 Analysis Round Robin I

The eddy-current data tapes from the base-line examination conducted with Zetec multifrequency equipment were copied for 424 tube scans. These data were from scans of the 320 round robin tubes as conducted in the DAARR, plus additional scans, including multiple scans of a tube with different probe sizes. Each inspection was assigned a random identification number which was recorded on the tape and used in place of the tube row and column numbers. Six teams (analysts) were selected through a competitive procurement. In

addition, 3 teams participated through Project sponsors. The teams were not required to perform their data analysis at PNL and were given substantially more time to perform the analysis than the DAARR teams had been given. They were allowed to use any data analysis system; however, all teams chose to use the Zetec DDA-4. Detailed reporting instructions were provided to each team including a visit by a PNL eddy-current NDE analyst. The participants were provided with historical information on the Surry steam generator similar to that provided the DAARR teams. The 424 tube scans were codified so that data on tube location was not available.

Table 3.10 contains data from Analysis Round Robin I (Doctor et al. 1988b). This round robin produced the largest variation in number of reported indications of any of the round robins. The smallest number of indications reported was 186 while the largest was 630. Removal of multiple indications did not reduce the range significantly: 179 to 600. Discounting Team K's indications, which had missing information on the origin of the indications, the number of OD indications ranged from 163 to 588. The number of ID indications ranged from 0 to 156. While the acquisition and Analysis Round Robin teams elected not to report the types of indications, four of the nine analysis round robin teams (FF, J, I, and M) reported a substantial number. Of the four, three (FF, J, and I) reported mostly wastage, while the fourth team (M) reported mostly cracking.

TABLE 3.10. Numbers and Types of Indications Reported
by Analysis Round Robin I Teams

	Numbers of Indications Team								
	F	FF	G	H	I	J	K	L	M
Total Indications	227	196	401	359	243	630	186	190	334
Total Indications (Multiples Removed)	222	196	377	358	227	600	182	179	313
OD Indications	221	196	221	262	219	588	17	163	301
ID Indications	1		156	96	6	11			12
Unidentified Origin					2	1	165	16	
Wastage*		196			156	573			67
Cracking*					69	21	2		234
Possible IGA*						3			
Unidentified Indication Type	222		377	358	2	3	175	179	12

*Reporting of type of indication not required.

Table 3.11 shows the locations of wall-loss indications reported by Analysis Round Robin I teams. The numbers of indications reported at the hot-leg top of tube sheet differs by a maximum of 71 indications. This is notable, in that the difference between the smallest and largest total number of indications reported is 421. The areas of greatest disagreement in terms of absolute numbers of indications were the hot-leg second support plate and the cold-leg top of tube sheet.

TABLE 3.11. Location of Indications Reported
by Analysis Round Robin I Teams

Location Reference	Numbers of Indications Location Team								
	F	FF	G	H	I	J	K	L	M
Hot Leg									
Tube End									1
Tube Sheet Roll									4
Tube Sheet Crevice									
Top of Tube Sheet	208	159	206	137(8)	192	208	163	169	147
Support Plate 1			3	1(10)	2	5			6
Support Plate 2	2		3	5(3)		99	1		5
Support Plate 3			1	5(8)		61			6
Support Plate 4			3	2(12)1*		10			1
Support Plate 5			7	0(3)		15			7
Support Plate 6			1	2(5)		14			5
Support Plate 7	1		10	1	1	112	1	1	79
Cold Leg									
Tube End									
Tube Sheet Roll									3
Tube Sheet Crevice									
Top of Tube Sheet	10	37	107	109(1)1*	28	37	14	9	32
Support Plate 1	1		7	0(6)		2			1
Support Plate 2			3	1(2)		3			1
Support Plate 3			3	0(6)		6			3
Support Plate 4			4	3(4)		2			1
Support Plate 5			1	1(3)1*		3			
Support Plate 6			2	3(2)		9			1
Support Plate 7			14	2	4	11			9
U-bend				9		1			
Unidentified Location			2	1		2	3		1

() Denotes indications referenced between support plate and next higher support plate.
* Denotes indications referenced between support plate and 2nd next higher support plate.

3.48

3.4.4.4 Analysis Round Robin II

This round robin was similar to the Analysis Round Robin I, only utilizing data copied from the base-line eddy-current tapes produced with Intercontrole multifrequency equipment (Doctor et al. 1988b). Six European teams who routinely use this type equipment (an Intercontrole IC4AN analyzer) participated under the direction of the French SGGP sponsor. Slight differences to the other analysis round robin existed. Some of the tube signals examined were different and the data tapes included actual row and column information.

Table 3.12 shows the numbers of reported wall-loss indications from Analysis Round Robin II. The variation in numbers reported was much less in this round robin than for Analysis Round Robin I. The smallest number of indications reported was 254 while the largest number reported was 376. The range with the multiple indications removed was 227 to 291. The ranges of numbers of ID and OD indications were also relatively small, despite the substantial amount of origin information omitted by Teams O and Q.

TABLE 3.12. Numbers and Types of Indications Reported by Analysis Round Robin II Teams

	Numbers of Indications Team					
	N	O	P	Q	R	S
Total Indications	254	316	337	284	340	376
Total Indications (Multiples Removed)	227	283	270	272	258	291
OD Indications	212	235	265	200	252	266
ID Indications	8	6	4	6	5	7
Unidentified Origin	7	42	1	66	1	18
Wastage*			102			
Cracking*			11			
Pitting			1			
Shock*			1			
Unidentified Indication Type	227	283	155	272	258	291

*Reporting of type of indication not required.

For Analysis Round Robin II teams, the largest between-team difference in number of indications was reported at hot-leg top of tube sheet (Table 3.13). The second area of least agreement in terms of numbers of reported indications was consistent with the other two round robins, the cold-leg top of tube sheet.

Location Reference	Numbers of Indications Team					
	N	O	P	Q	R	S
Hot Leg						
Tube End						
Tube Sheet Roll						
Tube Sheet Crevice				1		
Top of Tube Sheet	211	246	225	211	224	243
Support Plate 1			(1)			1
Support Plate 2	4	1	4	4	2(1)	
Support Plate 3		1	3		2(1)	2
Support Plate 4					(1)	1
Support Plate 5		3			1(2)	2
Support Plate 6			1		3	
Support Plate 7	5	1	1	2	2	7
Cold Leg						
Tube End						
Tube Sheet Roll						
Tube Sheet Crevice						
Top of Tube Sheet		18	26	47	15	21
Support Plate 1	1	1	1	1	1	
Support Plate 2					1	1
Support Plate 3	1		1		1(1)	1
Support Plate 4	1					
Support Plate 5	1					1
Support Plate 6						1
Support Plate 7	1	3	2	1		3
U-bend		8	3	3		1
Unidentified Location	2		3	2		6

()Denotes indications referenced between support plate and
next higher support plate.

3.5 SPECIMEN REMOVALS AND NDE VALIDATION

A prime purpose in utilizing a removed-from-service steam generator was
to accurately characterize service-induced degradation, mainly to provide
correlation with the results of the nondestructive inspections. Thus, the
removal of specimens from the generator, without altering their
characteristics, was of prime importance. This was also a formidable task,
considering both the physical magnitude of the operation and the fact that
the work involved sectioning radioactive material.

To validate the NDE round robin results and determine the condition of the tubing, tube segments were selected and removed from the generator for visual and metallurgical examination. This section describes the logic used for selecting specimens from the hundreds of tubes inspected during the various round robins, the methods used for removal of these specimens, the results of the visual and metallurgical examinations, and results of burst tests performed on selected specimens. A more detailed description has been presented by Bradley et al. (1988).

3.5.1 Specimen Selection

The purpose of the specimen removal plan was to select tube sections for removal, and visual and metallographic examination to ensure that a technically valid estimate of the reliability of the NDE of steam generator tubes could be made. A detailed description of the specimen removal logic, methods and validation results is presented in the Task 13 report (Bradley et al. 1988). The following criteria had to be met:

- Sufficient numbers of specimens with defects were needed to estimate the probability of detection (POD) of the inspection methods as a function of defect size.

- A representative cross section and a sufficient number of defects were required to estimate the POD for different types of defects in the generator.

- A representative selection and number of specimens without reported defects were needed to estimate the "false negative" (i.e., no defect reported when one exists) error rate.

The selection of the tube specimens for the NDE validation was governed by the following considerations:

- The total number of tube sections that could be removed based on the cost of post-removal examination and analysis was 500 to 600.

- With a few exceptions, the selected tube section had to have been inspected by all of the DAARR teams to ensure that the maximum information was obtained for NDE reliability.

Since the purpose of the validation was to establish the reliability of NDE, there was a need to have a large number of specimens with defects from which to estimate the POD. Three major strata (categories) of potential specimens were defined to reflect the lack of direct knowledge of the physical condition of the tube sections and to ensure that proper emphasis was given to the selection of a large number of specimens with defects. The three strata were as follows:

- tube sections with a possible defect based on evidence of a reported defect indication by at least one inspection team

3.51

- tube sections with a potential defect based on past history but with no indication reported

- tube sections in which a defect was not expected and for which no indication was reported.

The number of specimens to be allocated to each stratum was based on the goal that 80% of the specimens should contain defects. It was felt that slightly more weight should be placed on the specimens with reported indications; thus, Stratum 1 was to contain about 50% of the specimens; Stratum 2, 30%; and Stratum 3, 20%.

Each stratum was then subdivided into finer substrata to ensure proper representation of the various locations within the generator.

Table 3.14 summarizes the numbers of specimens in each of the strata by the major regions of the generator (tube sheet, support plate, U-bend). The first line for each stratum lists the total number of specimens. The subsequent lines give the number of specimens in the substrata. Of the 556 specimens removed from the generator, 48% were from Stratum 1, 30% from Stratum 2, and 22% from Stratum 3. This demonstrates that the specimen removal plan was satisfied. The division of specimens into regions of the generator

TABLE 3.14. Numbers of Specimens per Strata and Major Location Within the Generator

	No. of Specimens in Region		
Stratum	Tube Sheet	Support Plate	U-Bend
1. Reported indications	191	54	24
Defects	159	27	21
Advanced technique defects	32	27	3
2. Defects expected	65	71	29
Sludge pile	34		
Crevice	19		
Roll transition	12		
Strain		29	
Hard/soft spots		42	
Inner row U-bends			29
3. Defects not expected	16	78	28
Conditions	16	39	1
Straight sections		39	
Outer row U-bends			27

is as follows: 49% in the tube sheet, 37% in the support plates, and 14% in the U-bend region. Although the tube sheet was the location of most of the reported indications, it accounted for only half of the specimens; the support-plate and U-bend regions of the generator were adequately represented.

3.5.2 Specimen Removal

Removal of specimen tubes from the steam generator was a critical step in the NDE validation effort. Proper specimen identification and removal with minimal damage to the tube sections was essential for comparing postremoval inspection results with data from in situ NDE. The large number of specimens and widespread distribution within the generator required the development of complex methods and procedures for identifying and removing specimens from each region of the generator. The procedures and methods used for removing tubes from the U-bend, tube support-plate, and tube sheet regions are discussed in the following sections (for more detail see Bradley et al. 1988).

3.5.2.1 U-Bend Region

About 2600 U-bends were removed from the generator during the U-bend removal operation. U-bend specimen tubes were identified by inserting a probe in an adjacent cut tube from the channel head, where identification of tube locations could be made. The specimen was then marked with a dry paint marker on a pole.

A pair of abrasive cut-off saws were the main tools used to remove U-bend specimens. A picture of one of the cut-off saws is shown in Figure 3.22. The two saws were located opposite each other and at 90° to the tube lane. Shell penetrations just above the seventh TSP permitted cut-off wheel access to the tube bundle. These tools were operated semiremotely as shown in Figure 3.23. U-bends were cut flush with the top of the seventh TSP from both the hot- and cold-leg sides. The U-bends were subsequently lifted out through the top of the generator. To permit handling within the confines of the SGEF, the larger outer row U-bends were cut in half with a hydraulically assisted shear, prior to removal.

3.5.2.2 Tube Support-Plate Region

One of two methods was used to remove specimens from the support-plate region of the steam generator, depending on specimen location. Specimens that included the seventh TSP intersection or that contained defect indications <1 in. above the seventh TSP were removed as individual specimens concurrently with the U-Bend specimens. The remaining specimens from the support-plate region were removed by full-length tube pulls following the U-bend removals.

Specimens that included the seventh TSP were removed concurrently with or immediately after removal of the U-bends. The specimen and adjacent tubes were cut about 6 inches above the seventh TSP with the abrasive saw, and the U-bend portion of the tube was removed. The sample tube was then positively identified by inserting a probe from the channel head. As the probe emerged from the cut tube, the specimen was marked with a dry paint marker. Cutting the specimen off below the seventh TSP required an access hole in front of
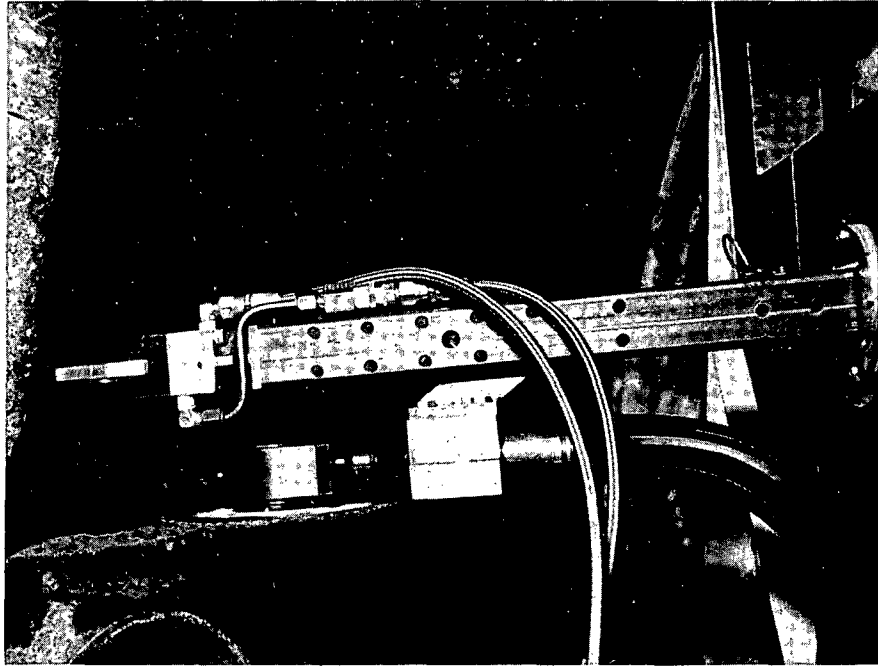
FIGURE 3.22. Abrasive Cut-Off Wheel
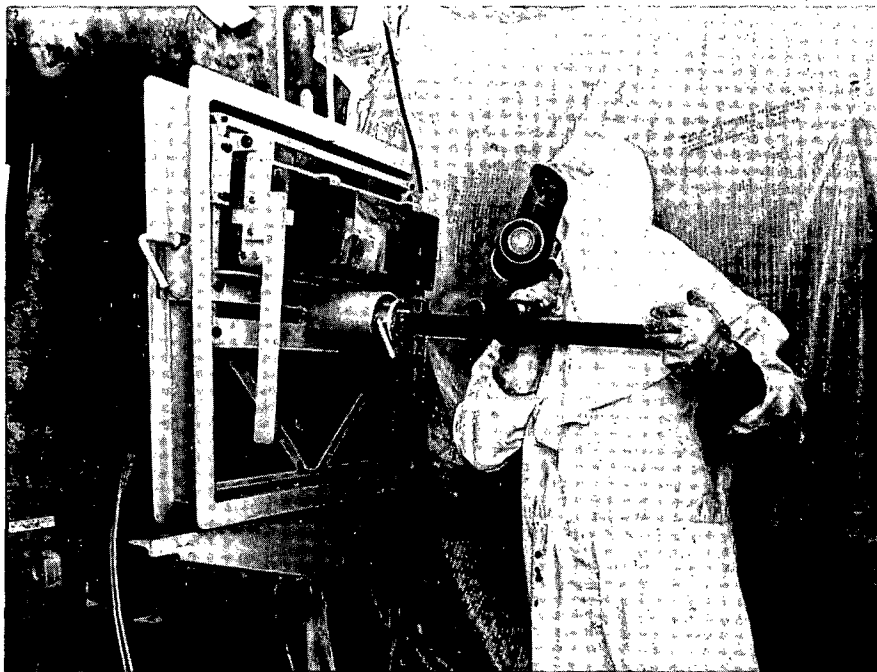
FIGURE 3.23. Semi-Remote Abrasive Wheel Cutting at Top of Seventh TSP

the specimen for a plasma arc torch. Thus, several adjacent tubes were cut from above with an internal tube cutter and a hole was broken in the seventh TSP. The specimen was then cut off below the seventh TSP with a plasma arc torch and removed from the generator.

Removing specimens from below the seventh TSP was an especially difficult problem, and several approaches were considered. An early plan to penetrate the shell at many locations and to tunnel in from the side to retrieve specimens was discarded because of the following serious disadvantages: 1) the diverse location of the specimens within the tube bundle would have required a large number of shell penetrations; 2) unsupported portions of tube bundle might collapse or otherwise require support; and 3) the potential for incorrectly identified specimens was deemed unacceptably high. Consequently, specimen removal by pulling tubes from the top of the tube bundle was considered the most practical approach because it eliminated or minimized these difficulties.

A major advantage in pulling tubes from the top of the bundle was the ability to positively identify specimen tubes at the seventh TSP. A Zetec template plug was tagged with the row, column, and hot-leg/cold-leg information and inserted into the probed tube. After all specimen tubes had been tagged, photographs were taken to provide permanent records of the tube identifications.

Full-length tubes were pulled by first cutting the tube with an internal tube cutter at a point above the TTS. Once cut, the tube was then gripped at an appropriate point and pulled out with the SGEF bridge crane as shown in Figure 3.24. Tubes removed by this method were minimally damaged because the TSPs broke apart during the pulling operation. On the hot-leg side of the generator, all seven TSPs were so heavily corroded that they broke easily. Damage of the specimen tube was kept to a minimum by first pulling several adjacent non-specimen tubes, which broke the surrounding TSPs and freed the tube of interest. Generally, TSPs 1 through 4 on the cold-leg side would not break. Therefore, cold-leg specimens with defect indications above the fourth TSP were pulled after pulling neighboring tubes, until the specimen tube could be gripped below the defect zone. Cold-leg specimens with defects below the fourth TSP were also pulled after surrounding tubes had been removed to reduce the force necessary to pull the specimen tube. In no case was the applied force great enough to break the tube, but several were plastically deformed during the process.

3.5.2.3 Tube Sheet Region

Most specimens removed from the tube sheet and sludge pile region of the generator were retrieved by jacking the tubes out of the tube sheet into the channel head. A multi-step process was used: 1) internally cutting the tube above the sludge pile, 2) inspecting the cut tube using a video probe, 3) removing the tube-to-tube-sheet fillet weld, 4) heating the roll-expanded region to free the tube, 5) inserting the pulling mandrel, and 6) attaching the hydraulic jack and pulling the tube. Each tube specimen to be removed was cut above the sludge pile from the inside with a rotary hand cutter. A completely cut tube was essential for reducing the pulling forces and
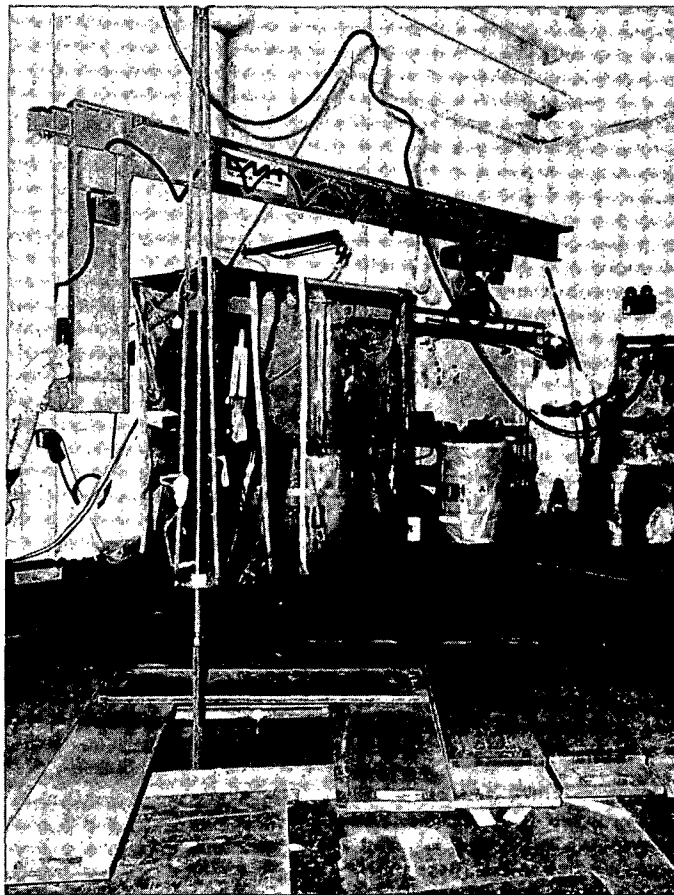
FIGURE 3.24. Full-Length Tube Being Pulled Up by SGEF Bridge Crane

minimizing tube damage, so the cut tube was inspected with a video probe
before removal. Next, the tube-to-tube-sheet fillet weld was milled off. A
fixture was used to hold the air motor and cutting tool in proper alignment
against the tube sheet. The fillet weld was then removed by raising the motor
and single-blade cutting tool using the lever device of the holding fixture.
After the fillet weld had been removed, the roll-expanded region was heated
with an oxyacetylene torch, which reduced the force required to pull the tube
from the tube sheet. A threaded mandrel was then inserted into the tube end.
A 2-ton hydraulic jack was positioned over the mandrel and the specimen was
pulled out as the jack operated on the mandrel. A photograph of a tube being
removed from the tube sheet is presented in Figure 4.25. The mandrel was
removed from the tube by grinding an axial slit along the lower three inches
of the tube end.

FIGURE 3.25. Tube Pulling Through Tube Sheet;
Hydraulic Jack in Operation

Some specimens that had been plugged during service, in which the plugs
had subsequently been removed by drilling (Wheeler et al. 1984), fractured
during the tube-pulling operation. The fractures usually occurred in the roll-
expanded region, although some failures occurred above the roll transition
but within the region drilled out to remove the plugs. The fractures were
caused by weakening of the tube due to the presence of IGSCC. The IGSCC
probably formed because of incomplete bonding, leading to a crevice
environment and high residual stresses due to plug installation. These
specimen tubes were removed by repetitive insertion and jacking of mandrels
with various diameters and lengths until the complete specimen was removed.

In addition to the specimens removed by tube pulling, two hot-leg and one
cold-leg sections of tube sheet, each containing nine tubes in a 3x3 array,
were removed from the generator. The tube sheet sections were successfully
removed by an overbore drilling technique after initial attempts using metal
disintegration machining were unsuccessful. The process was developed by

3.57
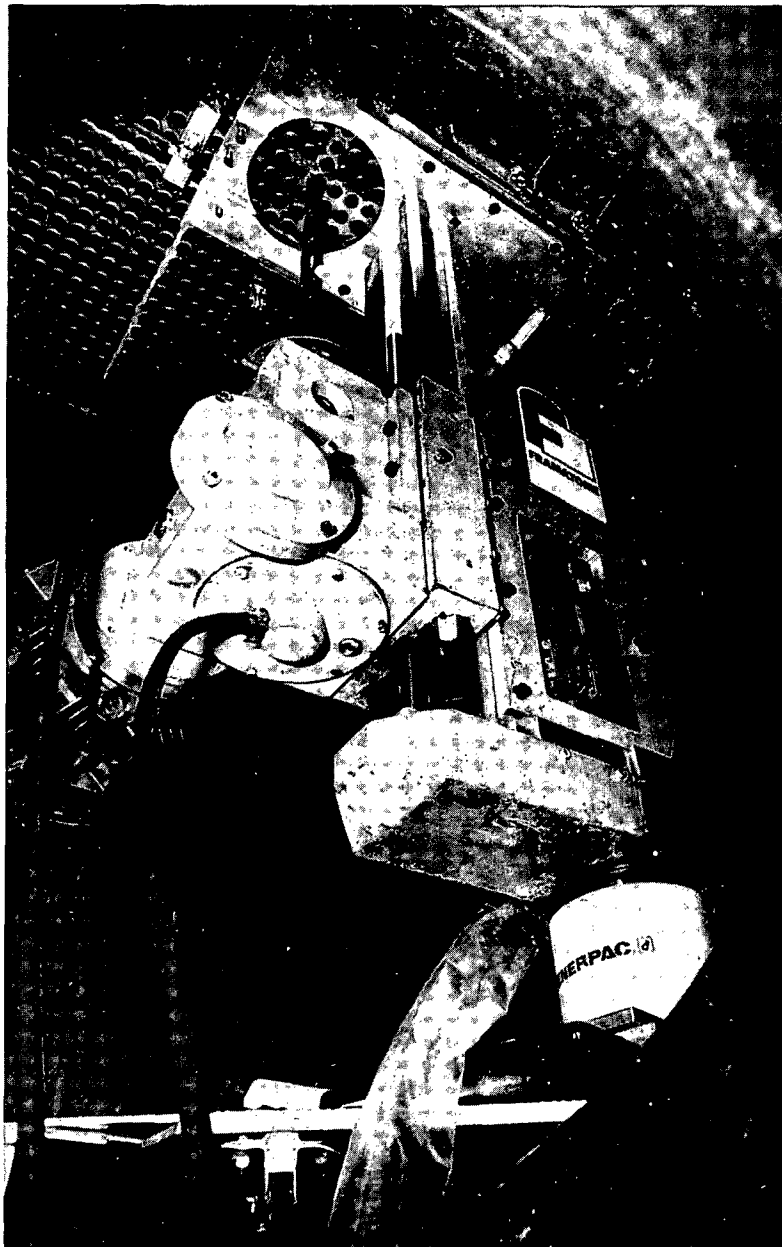
FIGURE 3.26. Tube Sheet Section Drilling Equipment in Place in Channel Head

Framatome, Inc., of France; the removal technique and equipment are illustrated in Figure 3.26. The process consisted of over-boring the tube holes surrounding the desired section so that the holes overlapped slightly. The apparatus was essentially a modified lathe operating in a vertical

position. Two oil holes running the full-length of each drill bit provided lubrication to the cutting edges. Approximately one inch before breakthrough, oil flow was stopped to prevent contamination of the crevices. After all the surrounding holes were drilled, the tubes in the section were internally cut above the sludge pile to free the section for removal. Sixteen tubes were overbored to release one 3x3 tube sheet section.

3.5.3 Validation of NDE Round Robins

The purpose of the NDE validation studies was to determine the reliability of NDE, primarily bobbin-coil eddy-current, to detect and size defects in steam generator tubing. A secondary purpose was to establish the condition of the tubing throughout the generator and identify degradation mechanisms in regions normally inaccessible to direct visual or destructive examinations. Tube segments removed from the generator were prepared for validation by 1) reducing the length to minimize radiation exposure to personnel and facilitate handling, 2) permanently identifying each specimen by inscribing a unique identification number on the tube surface, 3) deburring the cut ends for safety, and 4) chemically removing the deposits to enable visual inspection of the tube surfaces. Post-removal eddy-current inspections were conducted on specimens both before and after the deposit removal. These inspections aided the validation by establishing the effect of the deposits on EC signal characteristics.

Detailed visual examinations were a major facet to the specimen validation effort. The outside surfaces of all specimens and the inside surfaces of selected specimens were examined in detail using a stereo microscope at magnifications ranging from 10X to 70X. The type and location of tube degradation observed was recorded and a visual estimate of wall-loss for surface defects such as pitting and wastage was made. In general, it was not possible to estimate the depth of cracking or intergranular attack (IGA) by visual means. Three ranges of wall-loss were used in making the visual estimates: light (<20%), medium (20 to 40%), and heavy (>40%). These estimates provided a qualitative ranking of specimen degradation and were used in selecting specimens for destructive metallographic examinations and burst testing.

In selecting specimens for destructive metallographic examination, emphasis was given to validating defect indications reported by NDE, which were primarily located at the hot-leg TTS. Selections were made to obtain a range of defect distributions and depths within the metallographic data in order to establish the accuracy of NDE in detecting and sizing tube defects. Metallographic sections were also prepared for a limited number of specimens without significant visible degradation to ensure that unidentified defects were not present or to evaluate the nature of the OD deposits. The type of degradation observed and the maximum wall-loss were recorded for each specimen.

The visual and metallographic data were assembled in a computer data file that could be combined with the EC inspection results from the base-line and round robin experiments. Statistical evaluation and analysis of the combined data provided estimates of NDE reliability in detecting and accuracy of sizing

steam generator tube defects. A detailed report of the NDE validation studies has been prepared by Bradley et al. (1988).

3.5.3.1 Metallurgical Validation Results

Metallurgical examinations of the validation specimens included detailed visual inspection of all specimens and metallographic examination of selected specimens. The visual examinations identified the type and location of tube degradation and provided a qualitative estimate of wall-loss for surface type defects, such as wastage, pitting, etc., while a more precise estimate of wall-loss and defect characterization was obtained from the metallography. The following types of defects and conditions were found during the metallurgical examinations:

- U-Bend Region

  - anti-vibration bar (AVB) contact wear with corrosion
  - stress corrosion cracking (SCC) in Row 1 and 2 U-bends
  - grinder marks
  - Cu-rich surface deposits

- Support-Plate Region

  - within TSP intersections
    • denting
    • pitting, wastage, and IGA
    • SCC
    • Cu-rich surface deposits

  - between TSP intersections
    • pitting and wastage
    • hole

- Tube Sheet Region

  - sludge pile above TTS
    • pitting
    • wastage
    • SCC

  - roll expansion
    • SCC in plugged tubes

A brief description of these defects is given below.

3.5.3.1.1 U-Bend Region. Shallow wear and corrosion at AVB contact areas, SCC at the apex of Row 1 and 2 U-bends, and two grinder marks produced during an inservice repair operation were the only defects found in specimens from the U-bend region of the generator. Evidence of wear and/or corrosion was found on 13 of the 70 AVB contact areas examined, see Figure 3.27. Metallographic sections through seven of the most severely-degraded areas showed a maximum wall-loss of 25% for one specimen. The wall-loss for the

3.60

50 μm
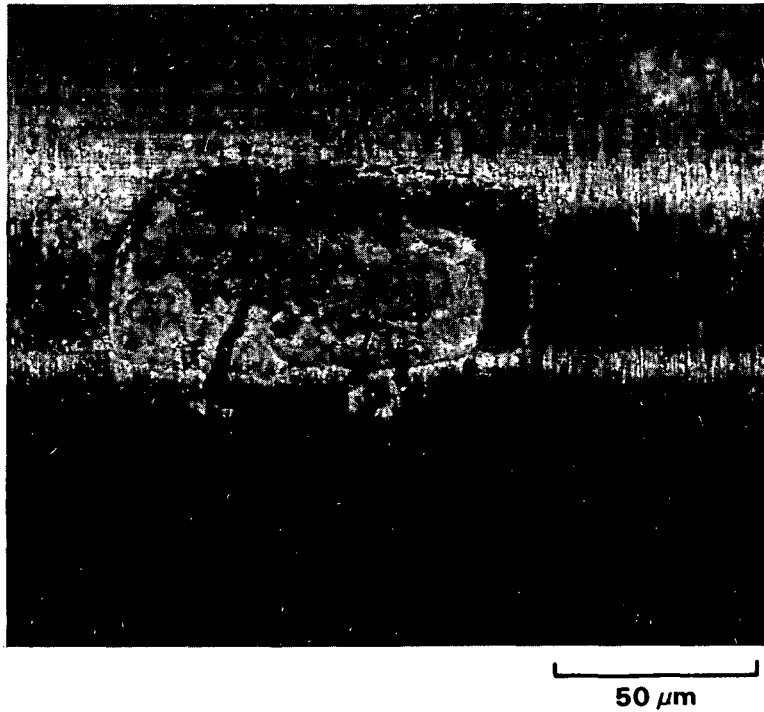
FIGURE 3.27. Wear and Corrosion at AVB Contact Areas on
U-Bend Specimens 416A and 416B (R31 C58)

remaining specimens was less than 12%. The SCC was found only at the apex of
Row 1 and 2 U-bends. Both OD and ID initiated cracks were observed in Row 1
U-bends, while only OD initiated cracks were found in Row 2 specimens.
Figure 3.28 provides an example of the cracking observed in a Row 2 U-bend.
The IGSC cracking was attributed to high stresses produced from the inward
movement of the seventh TSP into the flow slots due to denting. SCC was not
observed at the apex of Row 3 U-bends or at the bend transition region of any
specimen examined.

For the defects found during validation, the two grinder marks were the
only U-bend defects detected by the EC inspection teams. However, Row 1 and
2 U-bends were not inspected because of severe denting at support plates and
tube ovalization at the U-bend apex. The lack of detection of the AVB contact
wear is likely associated with the shallow nature of the defects and possible
interference from the AVB and copper-containing deposits on the OD surface
surrounding the AVB wear location.
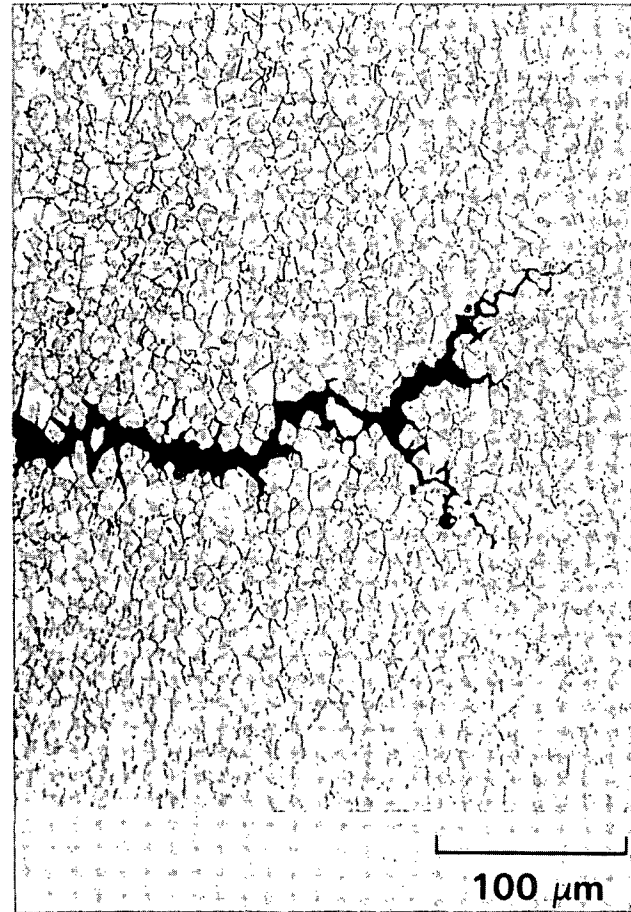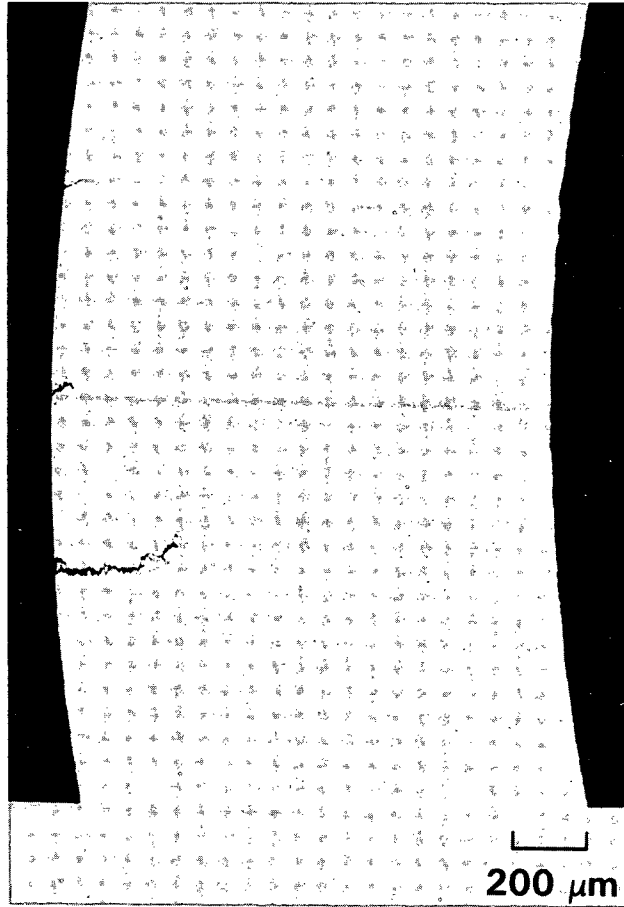
FIGURE 3.28. Optical Micrographs Showing Axial IGSCC at the Apex of U-Bend Specimen 1049 (R2 C27)

Tubes removed from the U-bend and support-plate regions of the generator were covered with a dark granular deposit. The outer layer could be easily removed by washing in water with a soft-bristled brush, leaving a tenacious copper-colored deposit. This deposit generally covered the tube surface except for small spots or axial strips where the Inconel was visible. A photograph showing two spots and an axial strip where the metal is visible is presented in Figure 3.29. Axial strips without the copper-colored deposits were often found intermittently along the entire tube surface.

Metallographic examination showed that the thickness of the deposits varied around the circumference of the tube. Deposit thicknesses ranged up to 10 mils for the tubes examined. The deposits had a layered microstructure with metallic Cu particles observed throughout. As described below, these Cu-rich surface deposits were found to be the primary cause of false calls made by the various inspection teams. Post-removal EC inspection indicated that interruptions in the Cu-rich deposit gave rise to indications similar to defects. Chemical cleaning of specimens to remove the Cu-rich deposit followed by reinspection revealed that EC indications had disappeared.
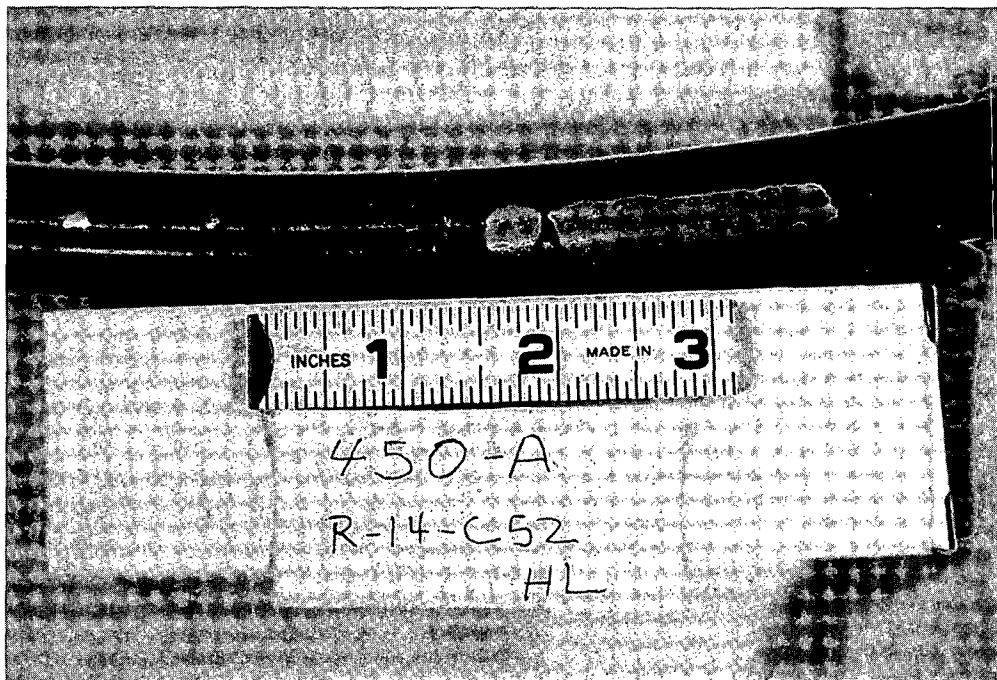
FIGURE 3.29. U-Bend Specimen 450A (R14 C52 HL) Showing Discontinuities in the Copper-Rich OD Surface Deposit

3.63

3.5.3.1.2 Support-Plate Region. Almost all of the tube degradation observed in specimens from the support-plate region of the generator was associated with the dented TSP intersections. Corrosion in the form of shallow pitting, wastage, and IGA occurred in the crevice region between the tube and support plate in most of the 117 TSP intersections examined. Figure 3.30 shows a photograph of a typical TSP intersection. The severity of the OD corrosion attack appeared greater in the more heavily dented tubes although the visual estimate of wall-loss was generally less than 20% for all specimens. Metallographic examination of 10 specimens with calculated strain values ranging up to 39% confirmed the shallow nature of the OD corrosion as evidenced by the data in Table 3.15. Various combinations of pitting (P), wastage (W), and IGA were observed in the metallographic cross sections with the maximum wall-loss ranging from 2 to 12%. Axial cracks were also visually observed on the OD surface at regions of high tensile hoop stress in specimens with calculated strains greater than 60%.

Intergranular stress corrosion cracking that initiated at the inside surface was also found in the more heavily dented specimens. The internal surfaces of 27 hot-leg and 11 cold-leg specimens were examined, and axial SCC was observed in 10 of the hot-leg specimens. An example of typical ID cracking observed is shown in Figure 3.31. Maximum crack depth for the 10 specimens ranged from 27% to 88% through-wall penetration. Calculated strain values were available for 17 of the hot-leg specimens and provided a means for evaluating the effect of tube deformation on the propensity for ID cracking. Table 3.16 summarizes the results of visual and metallographic examination of these specimens. The results may be divided into three strain regions: 0% to 10%, 10% to 20%, and greater than 20%. No ID cracking was observed below 10% strain, while approximately one-third of the specimens with 10% to 20% exhibited ID cracks. Above 20% strain, all of the specimens contained cracks. Thus, strain-based plugging criteria between 17%-25% may not be low enough to ensure a low probability for crack initiation. A definite relationship between crack depth and calculated strain was not observed, which is consistent with the complex stress distributions produced by the nonuniform nature of the denting and temperature variations within the hot-leg region of the generator.

Tube defects observed between TSPs consisted of a through-wall hole produced during an inservice repair operation and pitting/wastage type defects immediately above the TSP in two specimens. Most of the EC inspection teams identified the hole as a defect but, with few exceptions, did not locate the two pitting/wastage type defects or any of the defects within the TSP intersections. Apparently denting interfered with the EC signal and prevented the defects from being detected. Only three of the specimens with ID cracking were inspected by EC and no defects were reported from these inspections.

3.64

5 mm
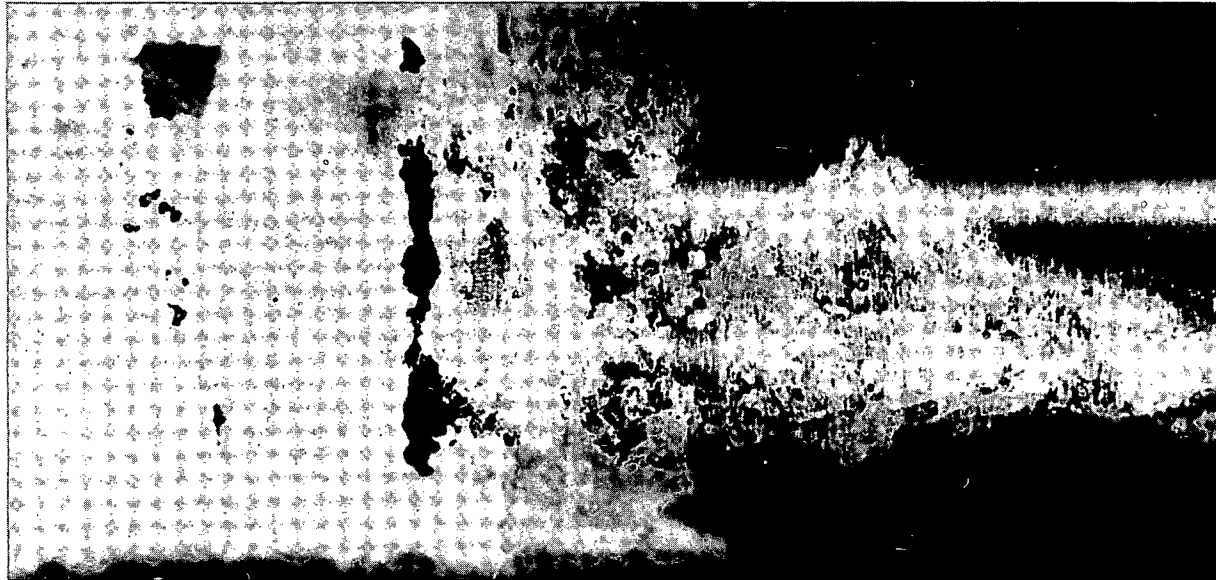
FIGURE 3.30. Typical TSP Intersection; Specimen 665 (R7 C57 HL)

TABLE 3.15. Summary of Metallography Results Regarding
OD Corrosion of Dented TSP Intersections

Specimen No.	Tube No.	Defect Type	Maximum Wall-Loss, %	Calculated Strain, %
851	R5 C26 HL1	P/W	4	---
856	R5 C77 HL1	W/IGA	<2	---
1041	R4 C51 HL1	P/W/IGA	12	26.9
921	R42 C47 HL4	W	<2	11.1
909	R10 C39 HL5	IGA	6	11.9
925	R4 C51 HL5	P/W/IGA	5	27
935	R42 C52 HL5	P/W/IGA	10	17
926	R4 C51 HL6	P/W/IGA	6	39.1
947	R45 C55 HL6	W/IGA	5	16.5
455	R9 C47 HL7	P/W	8	7

P   = Pitting
W   = Wastage
IGA = Intergranular Attack

5 mm
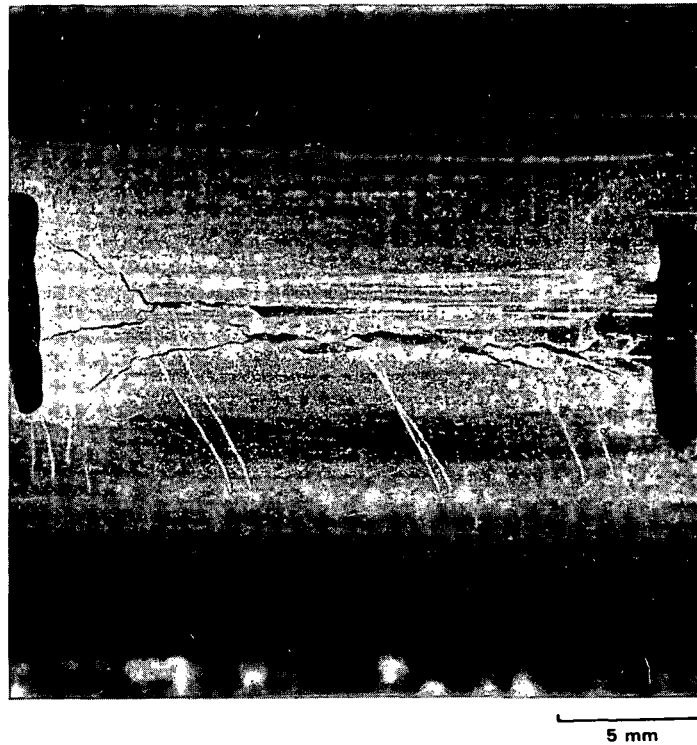
FIGURE 3.31. First TSP Specimen 1041 (R4 C51 HL) Showing ID Cracking
(26.9% strain)

TABLE 3.16.   Summary of ID Cracking at Dented TSP
              Intersections With Various Strain Levels

ID No.	Row	Col	TSP Location	Strain, %(a)	ID(b) Cracking	Crack(c) Depth, %
553	9	70	HL7	4.2	No	
567	21	71	HL7	4.9	No	
525	12	36	HL7	5.4	No	
455	9	47	HL7	7.0	No	0
922	4	20	HL5	9.9	No	
929	12	36	HL5	10.1	No	
921	42	47	HL4	11.1	Yes	44
909	10	39	HL5	11.9	Yes	70
927	5	37	HL5	12.5	No	
923	4	36	HL5	13.4	No	
924	4	36	HL4	14.1	No	
947	45	55	HL6	16.5	No	0
935	45	52	HL5	17.1	Yes	64
908	10	39	HL4	17.9	No	
1041	4	51	HL1	26.9	Yes	88
925	4	51	HL5	27	Yes	67
926	4	51	HL6	39.1	Yes	57

(a) Based on profilometry data.
(b) Based on visual examination.
(c) Metallography results.

3.5.3.1.3 Tube Sheet Region. Several types of tube defects were found
in the sludge pile region immediately above the TTS. These defect types
include pitting, wastage, localized circumferential corrosion (LCC), shallow
IGA, and OD initiated SCC. Pitting and wastage were the predominant defects
as can be seen in Table 3.17, which summarizes the visual inspection results.
Only 14 of the 241 specimens examined showed no evidence of corrosion in the
sludge pile region. Areas with wastage were observed on all the remaining
specimens, while additional areas with pitting and other forms of nonuniform
corrosion were found on 138 specimens. Cracking was found within the corroded
region of two hot-leg specimens. The severity of the degradation was much
greater on the hot-leg side of the generator, as evidenced by the differences
in the visual estimates of wall-loss.

Tube degradation within the cold-leg sludge pile consisted mostly of
wastage. Typically, tubes exhibited a slightly roughened surface and light
wall-loss, with small pits or pit clusters in the wasted region of some
specimens. Metallographic examination of 11 cold-leg specimens showed the
maximum wall-loss to range from 2% to 24%, with the average maximum wall-loss
being 10.7%.

TABLE 3.17. Summary of OD Visual Examinations of TTS Specimens From the Sludge Pile Region of the Generator

Degradation Type	Hot-Leg Specimens				Cold-Leg Specimens			
	Number of Specimens	Estimated Wall Loss, %			Number of Specimens	Estimated Wall Loss, %		
		<20	20-40	>40		<20	20-40	>40
None	7				7			
Pitting/ Wastage	105	10	46	49	23	22	1	
Wastage	15	10	5	0	74	73	1	
Other(a)	9	3	3	3	1	1		

(a) Includes various combinations of wastage, pitting, localized circumferential corrosion and cracking.

The hot-leg TTS specimens also showed regions with wastage in the sludge pile region for all of the degraded specimens. Wall-loss by wastage was normally quite shallow with the estimated depth being less than 20%. However, a few hot-leg specimens exhibited more severe wastage in the form of a ring or groove that encircled the tube at various shallow angles. The axial extent of this form of wastage was less than one-half inch, with a gradual taper in wall thickness from both axial directions. Maximum wall-loss from this ring-type wastage measured from metallographic sections ranged from 20% to 52%. An example of this type of degradation is given in Figure 3.32.

Although wastage was found in all degraded hot-leg TTS specimens, the primary mode of degradation in most of the severely-degraded tubes was from pitting and/or other localized corrosion processes. The pits were distributed intermittently but not uniformly within the degraded region of the tube. The axial extent of the degraded region varied from one specimen to another but was typically less than 2 inches above the TTS. There was also a tendency for clustering, which resulted in localized areas with a wide range of wall-loss within the overall degraded region. The appearance of these more severely-degraded areas is best described as clusters of overlapping pits, although the mechanism by which they form may have included wastage or other forms of corrosion.

Large variations in the number, severity, and distribution of degraded areas (defect clusters) were observed in the hot-leg TTS specimens. A few specimens exhibited a single pit or cluster of pits along with shallow wastage in the corroded region. However, the majority of the hot-leg specimens exhibited multiple-degraded areas that were often connected by shallow wastage. The degraded areas were distributed both axially and circumferentially within

2 mm
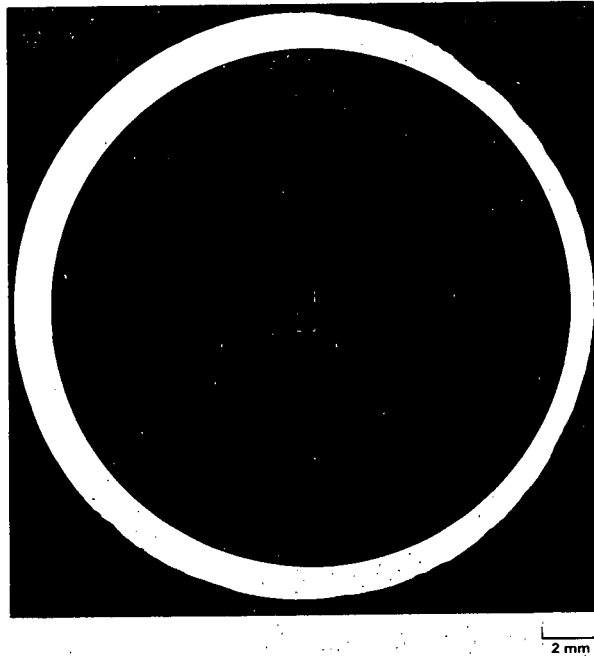
FIGURE 3.32. Optical Micrograph Showing Ring Type Wastage on
              Hot-Leg TTS Specimen 632 (R13 C37 HL)

the corroded region of the tube surface. Figures 3.33 and 3.34 show examples
of the variation in degradation observed around the tube circumference in
specimens with combined pitting and wastage. A few degraded areas were seen
in some sections, Figure 3.33, while others showed extensive local areas of
degradation around most of the tube circumference, Figure 3.34. Maximum wall-
loss in specimens with pitting/wastage type degradation ranged up to 87%.

     Most of the reported EC defect indications were located at the TTS and the
best agreement between inspection teams occurred at the hot-leg TTS. The
severely-degraded specimens above the hot-leg TTS were generally reported by
most of the inspection teams, while detection was quite low for the lightly
degraded specimens from both the hot-leg and cold-leg regions of the generator.
Both hot-leg specimens having SCC within the corroded region of the specimen
were reported as defective by most of the inspection teams, see Figure 3.35.
However, it was not possible to determine if detection was based on the
presence of the cracks or the pitting/wastage type degradation.

3.5.3.2 Evaluation of NDE Reliability

     The reliability of the inservice inspection of steam generators depends
on the ability of the NDE technique to detect and size defects in the tubing.
To evaluate the probability of detection (POD) and sizing accuracy of EC
inspections, the results of the metallurgical validation data were combined
with the EC results from twelve inspection teams, two Base-Line inspections,
five Data Acquisition and Analysis Round Robin (DAARR) inspections, and five

3.69
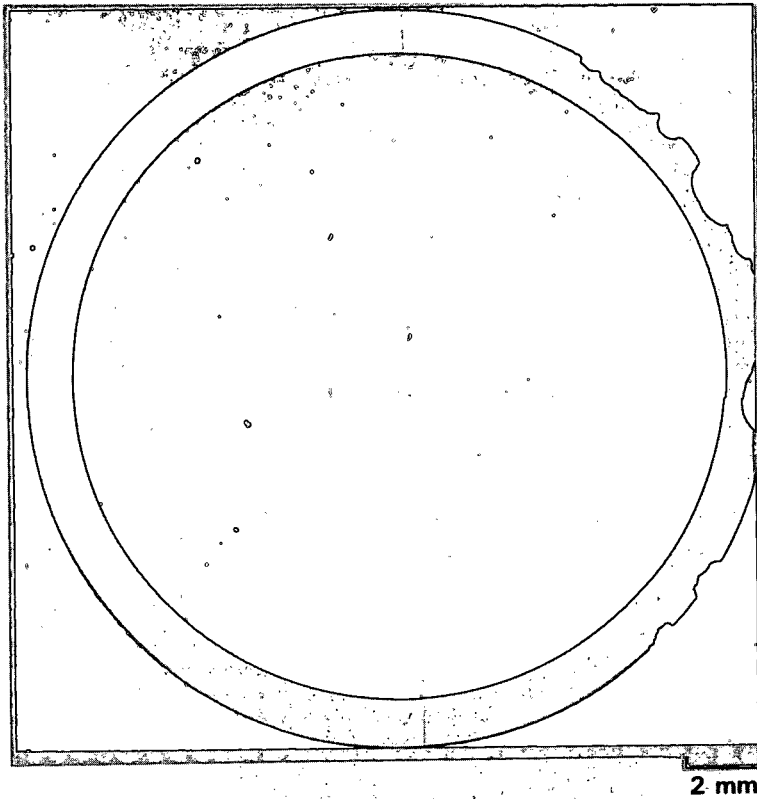
FIGURE 3.33. Pitting/Wastage Type Degradation of a Hot Leg TTS Specimen
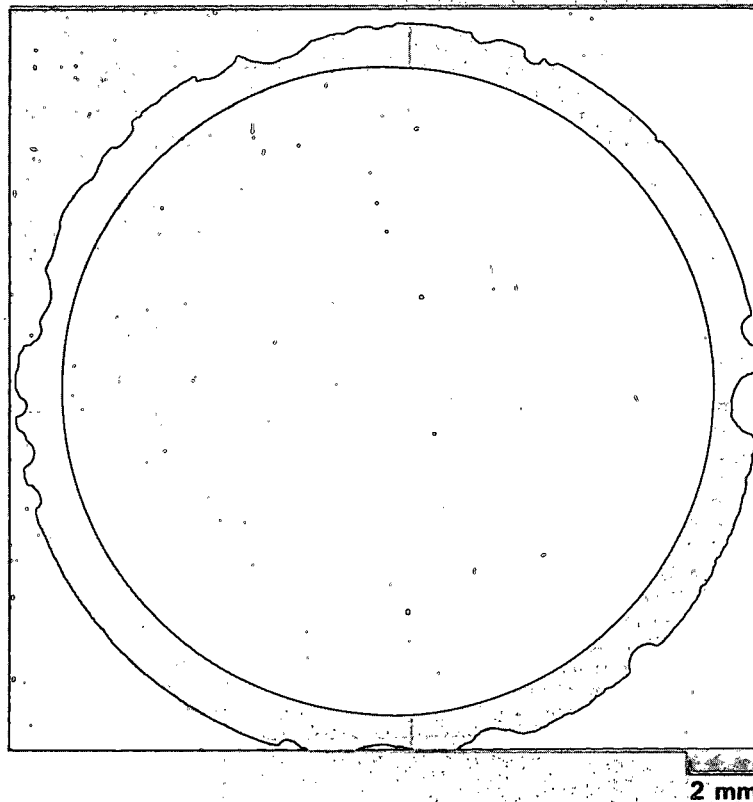
FIGURE 3.34. Pitting/Wastage Type Degradation of a Hot Leg TTS Specimen
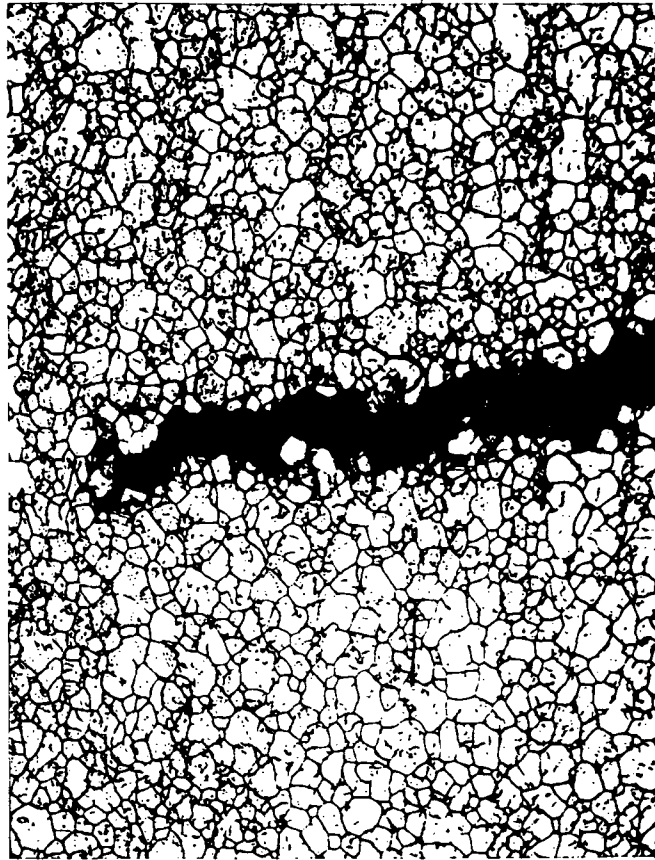
100 μm
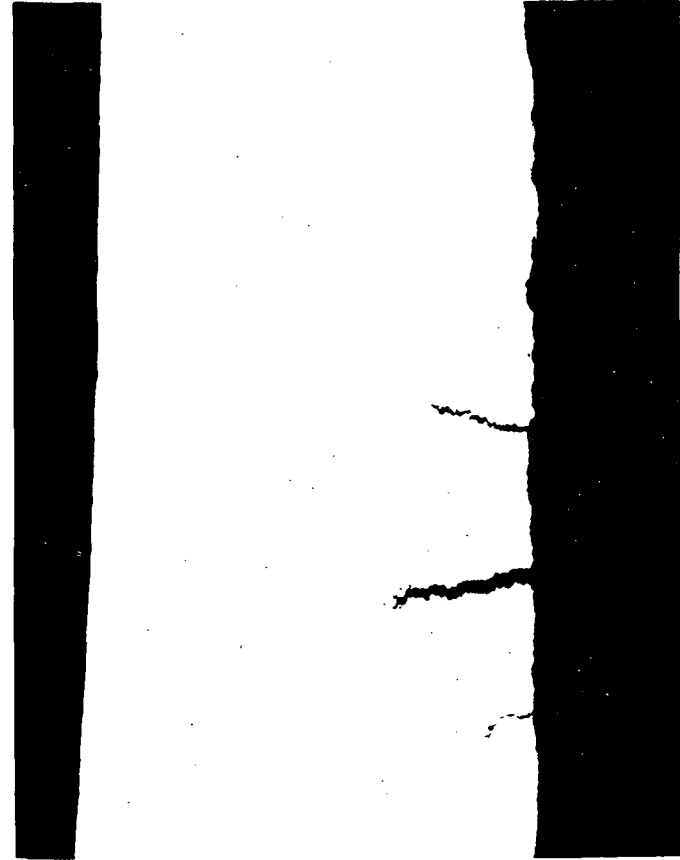
200 μm

FIGURE 3.35. Optical Micrographs from a Longitudinal Section Showing OD Circumferential
Cracking of TTS Specimen 633C (R13 C44 HL at TTS + 0.2 in.)

Advanced/Alternate Techniques Round Robin (AATRR) inspections. The Base-Line and DAARR teams inspected most of the validation specimens using bobbin-coil technology, and their results are directly comparable. Except for one AATRR team, limited inspection data were available from these teams, and comparisons are therefore uncertain.

Table 3.18 gives a summary of the numbers of detections, false calls, and nondetections from the visual examination data for each of the five DAARR teams (A through E), the two base-line inspection teams (X,Y), and the five AATRR teams (U, UU, V, VV, W). These calls are listed separately for the three regions of the generator (TTS, TSP, U-bend). The detections and nondetections for the OD defects are listed by the amount of wall-loss based on a visual examination (L = light, M = medium, and H = heavy). Since the depth cracks cannot be determined visually, the ID cracks are listed separately as K. However, the two OD cracks that were found are included in the heavy category because they were associated with pitting and wastage.

For the base-line and DAARR teams, the number of specimens inspected and evaluated ranged between 481 and 497. The number of specimens inspected by the AATRR teams ranged from 22 for Team W to 392 for Team V. For the DAARR and the base-line teams, the numbers of wall-loss defects ranged from 312 to 324. The range was from 20 to 245 for the AATRR teams. Because of the small number of specimens examined by the AATRR (with the exception of Team V), a direct comparison with the base-line and DAARR teams is not appropriate.

For the TSP and U-bend regions, there may be more than one number reported for a team, with the second number in parentheses. For the TSP region, the first number is the number of reported and/or actual defects at the support-plate intersection, which is the primary location for wall-loss defects to occur. For the U-bend region, the first number is the number of reported and/or actual defects at the AVB contact points. The number in parentheses for both regions is the number of reported and/or actual defects at other locations within a specimen.

Several patterns emerge from a study of Table 3.18. There is remarkable consistency among the two base-line inspection and five DAARR (multifrequency EC/bobbin-coil equipment) teams for the three areas of the generator. At the TTS, where most of the defects occurred, the largest number of detections occurred in the heavy size category and the largest number of nondetections were in the light category. There was only one false call reported by one team. There were 13 heavy wall-loss defects that were missed by at least one of the teams. Seven of these were single team misses; five specimens were missed by two teams, and one was missed by four teams.

In the support-plate region there were numerous nondetections of light pitting and wastage at the support-plate intersections. The NDE inspections were not able to pick them up because of the signal distortion caused by the dented tube at these intersections. The one nondetection of a heavy wall-loss defect was an OD pit that was not at the support-plate intersection, but was missed by all DAARR and base-line teams. In addition, there were several cracks in dented tubes at support-plate intersections that were missed by all teams that inspected that section of tube.

TABLE 3.18. Summary Classification of Individual Team NDE Inspection Results by Region of the Generator

Data Acquisition and Analysis Round Robin

	Type of Defect(a)	Team				
		A	B	C	D	E
Number of specimens		484	488	494	487	481
Number of wall-loss defects		312	317	324	316	314
TTS						
Detections	L	10	4	13	26	9
	M	38	31	41	43	42
	H	49	45	48	50	50
	K	0	0	0	0	0
False Calls		0	0	0	1	0
Nondetections	L	110	116	107	94	110
	M	17	25	15	13	14
	H	2	6	3	1	1
	K	0	0	0	0	0
TSP						
Detections	L	1	0	0	0	0
	M	0	0	0	0	0
	H	0(1)	0(1)	0(1)	0(1)	0(1)
	K	0	0	0	0	0
False Calls		0(4)	0(2)	1(1)	0(1)	0
Nondetections	L	65(1)	69(1)	75(1)	68(1)	67(1)
	M	1	1	1	1	1
	H	0(1)	0(1)	0(1)	0(1)	0(1)
	K	1	2	3	2	2
U-bend						
Detections	L	0	0	0	0	0
	M	0	0	0	0	0
	H	0(2)	0(2)	0(1)	0(2)	0(2)
	K	0	0	0	0	0
False Calls		0	0	0	0	0
Nondetections	L	12	12	12	12	12
	M	1	1	1	1	1
	H	0	0	0(1)	0	0
	K	0	0	0	0	0

(a) L = Light, M = Medium, H = Heavy, K = Crack.

TABLE 3.18. (cont'd)

Base-Line EC Inspections

	Type of Defect[a]	Team	
		X	Y
Number of specimens		497	488
Number of wall-loss defects		319	316
TTS			
Detections	L	7	34
	M	35	45
	H	47	46
	K	0	0
False Calls		0	0
Nondetections	L	112	86
	M	21	11
	H	4	4
	K	0	0
TSP			
Detections	L	0	0
	M	0	0
	H	0(2)	0(1)
	K	0	0
False Calls		0(7)	0(9)
Nondetections	L	72(1)	70
	M	1	1
	H	0	0
	K	2	3
U-bend			
Detections	L	0	0
	M	0	0
	H	0(2)	0(2)
	K	0	0
False Calls		0(8)	0(14)
Nondetections	L	12	12
	M	1	1
	H	0	0
	K	0	0

(a) L = Light, M = Medium, H = Heavy, K = Crack.

TABLE 3.18. (cont'd)

Advanced/Alternate Techniques Round Robin

	Type of Defect[a]	Team U	UU	V	VV	W
Number of specimens		128	172	392	172	22
Number of wall-loss defects		70	131	245	131	20
TTS						
Detections	L	31	9	25	11	0
	M	12	15	48	17	9
	H	8	26	51	24	7
	K	0	0	0	0	0
False Calls		0	4	2	1	0
Nondetections	L	7	72	63	70	0
	M	4	6	8	4	2
	H	0	3	0	5	2
	K	0	0	0	0	0
TSP						
Detections	L	0	(b)	0	(b)	(c)
	M	0	(b)	0	(b)	(c)
	H	0	(b)	0	(b)	(c)
	K	0	(b)	0	(b)	(c)
False Calls		0(3)	(b)	5(12)	(b)	(c)
Nondetections	L	8	(b)	34(1)	(b)	(c)
	M	0	(b)	0	(b)	(c)
	H	0	(b)	0(1)	(b)	(c)
	K	0	(b)	2	(b)	(c)
U-bend						
Detections	L	0	(b)	0	(b)	(c)
	M	0	(b)	0	(b)	(c)
	H	0	(b)	0	(b)	(c)
	K	0	(b)	0	(b)	(c)
False Calls		0(3)	(b)	0	(b)	(c)
Nondetections	L	0	(b)	11	(b)	(c)
	M	0	(b)	1	(b)	(c)
	H	0	(b)	0	(b)	(c)
	K	0	(b)	0	(b)	(c)

(a) L = light, M = medium, H = heavy, K = crack.
(b) Not analyzed because the extent of the inspection was uncertain at the time.
(c) Not inspected.

There were numerous false calls in the support-plate region, only one of which was at a support-plate intersection. The two base-line teams had more nondetections than any of the other teams. The majority of the nondetections were reported as small defects (<20%).

There were very few wall-loss defects found in the U-bend region. With the exception of the two grinder marks found by all but one team, the defects were mostly light fretting wastage at the AVB contact points (one was classified as medium wall-loss). Since they were the earliest inspections, Teams X and Y had a tendency to report the small volume indications in the U-bend as small defects that later proved to be gaps in the copper-rich deposits on the tubes. All of the Team Y indications called were less than 25% wall-loss. Team X's indications, on the other hand, were sized larger; the largest indication was reported as 55% wall-loss. None of the false positives were in the same specimens.

With the exception of Team V, the conclusions that can be drawn from the AATRR results are limited, since so few of the specimens were inspected by these teams. Team W did not inspect beyond the TTS. For Teams UU and VV, the extent of the individual inspections was not given, so the decision was to report information only for the TTS. Team V's results are similar to those of the base-line and DAARR teams. However, they reported fourteen 50% through-wall ID defects outside support-plate intersections that turned out to be false calls.

The probability of detection was determined for both the visual wall-loss estimates and the metallography data. The visual data provided a larger number of specimens, while a more precise estimate of wall-loss was obtained by metallography. Similar POD responses were observed for the Base-Line and DAARR inspection teams. A plot of the median POD from these seven inspection teams as function of visual wall-loss is shown in Figure 3.36.

As expected, the median POD for TTS specimens increased with wall-loss and was 0.94 for specimens in the heavy category, which corresponds to estimated wall-losses greater than 40%. The POD from the seven teams ranged from 0.88 to 0.98 for this specimen category, while somewhat greater variations were observed for the light and medium categories. A slight decrease in POD was observed when specimens from all regions of the generator were included in the calculations. However, the magnitude of the decrease may be misleading since the vast majority of defects in the medium and heavy categories were found at the TTS. It should also be noted that almost all of the data pertain to pitting or wastage type defects and the PODs may not be appropriate for other defect types such as SCC or IGA.

The PODs calculated from the metallography data show similar trends to those from the visual estimates of wall-loss. Figure 3.37 shows the median POD from the Base-Line and DAARR inspection teams; the metallography data are grouped into increments of 10% wall-loss. As before, the POD increased with wall-loss and the average POD for wall-loss more than 40% was greater than 0.9. Below 40% wall-loss, definite team-to-team variations in the POD curves were observed. However, there are inadequate data in each size category to

3.76
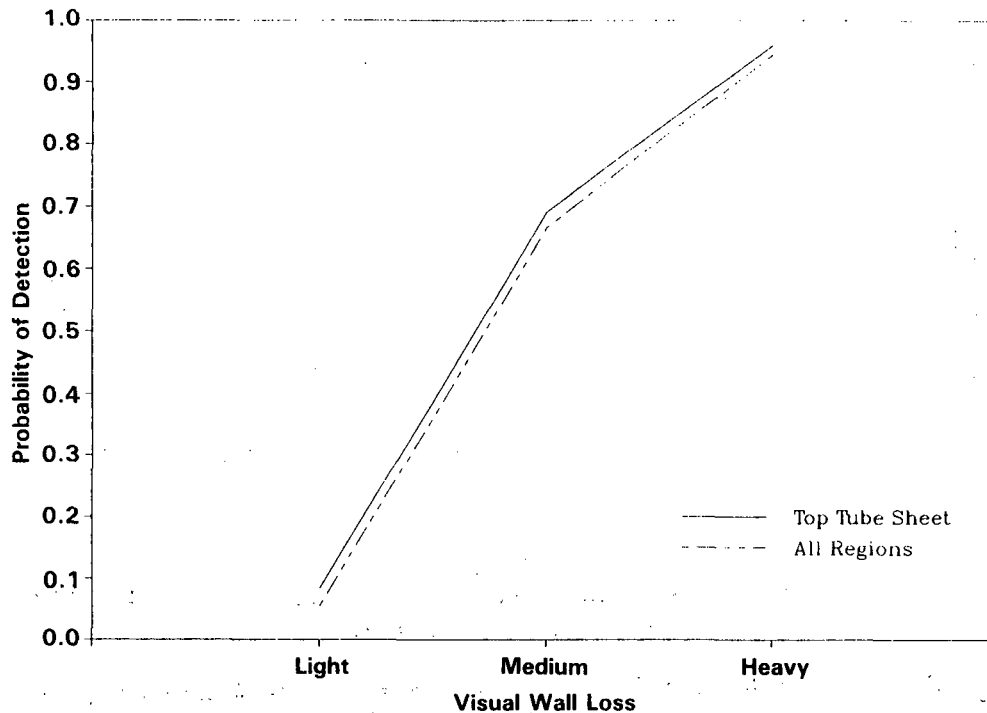
FIGURE 3.36. Median Probability of Detection of DAARR and Base-Line Inspection Teams Based on Visual Determination of Wall-Loss

assess the statistical significance of these variations. An apparent improvement in the POD curve of one AATRR inspection team was observed, as shown in Figure 3.38. The POD curve increased more rapidly than the typical Base-Line or DAARR team and the average POD was higher above 40% wall-loss. This team utilized an automated data screening system to sort through their data prior to analysis by a human. This was probably, in part, responsible for the better POD performance.

Figure 3.39 gives a plot of the individual POD performance for the DAARR and Base-Line teams for each 10% wall-loss increment. To estimate the lower bound POD, an approximate 90/90 lower tolerance limit (LTL) was computed (curve in Figure 3.39) from the teams participating in the DAARR and Base-Line inspections. These teams are assumed to be typical of the total population of teams performing ISI; therefore, if each team in this population had inspected the same set of tubes, we can be about 90% confident that about 90% of the individual team POD values would be above this LTL. The dashed segment of the curve indicates that the number of specimens with deep through-wall degradation was inadequate to provide a meaningful estimate of the LTL. Thus, the LTL at 65% wall loss is extended as a conservative approximation of the LTL (i.e., the POD is assumed to either increase or stay the same as wall-loss increases). This information was developed as an appropriate lower bound estimate of POD for field EC inspection and was used to validate the selection POD curves used in the evaluation of various sampling/inspection schemes described in Section 3.6.

3.77
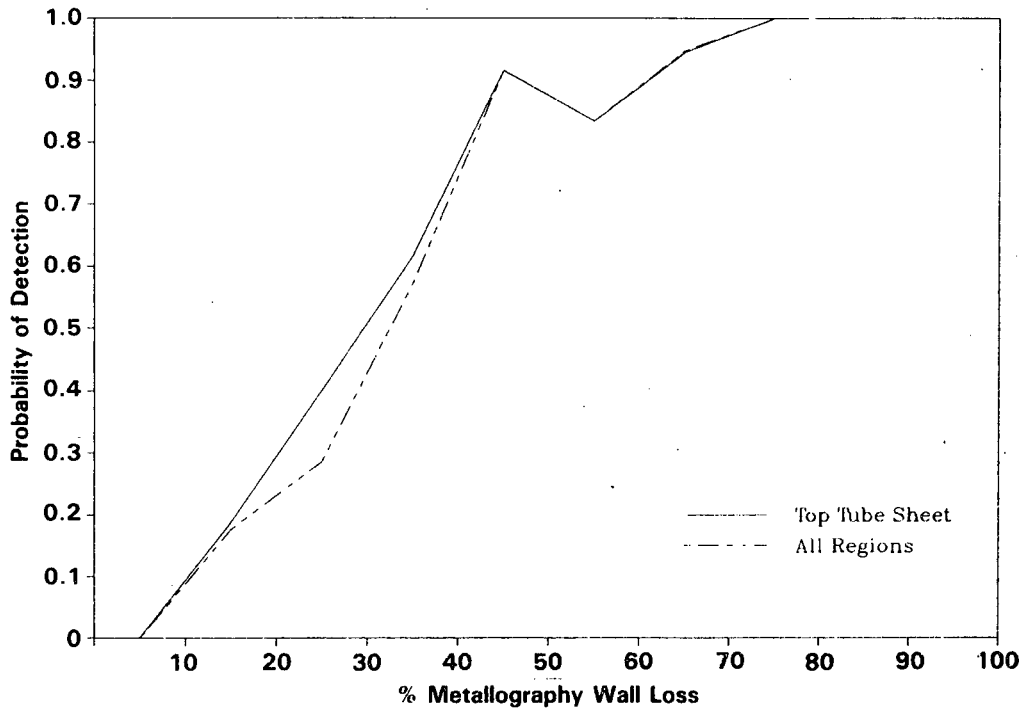
FIGURE 3.37. Median Probability of Detection of DAARR and Base-Line Inspection Teams Based on Metallographic Determination of Wall Loss
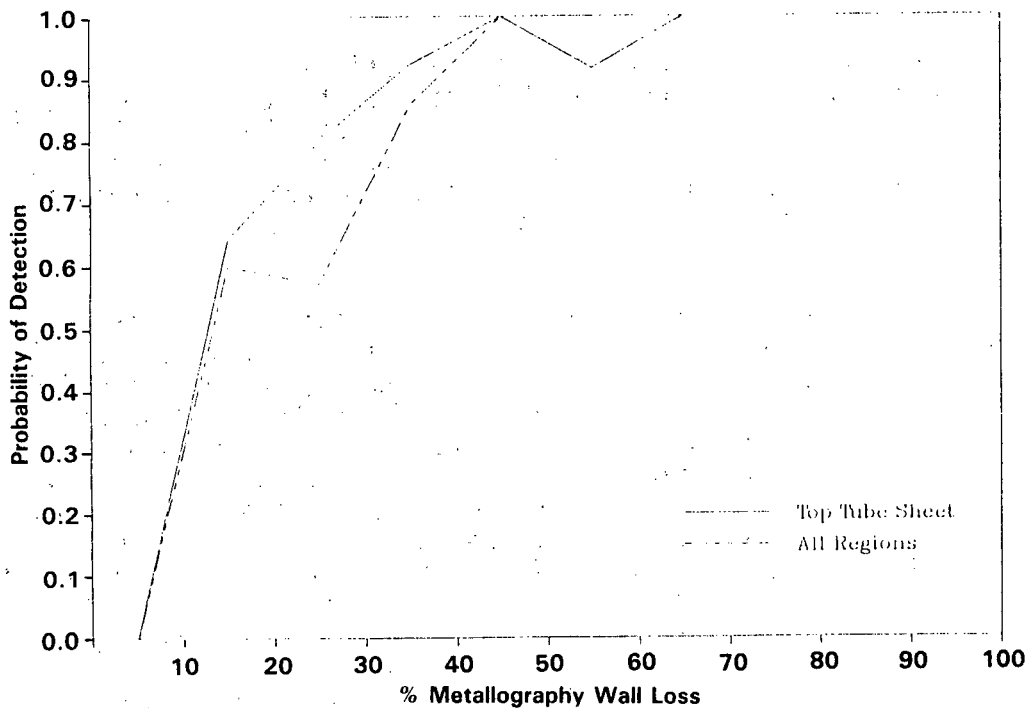
FIGURE 3.38. Probability of Detection of an AATRR Inspection Team Based on Metallographic Determination of Wall Loss

3.78
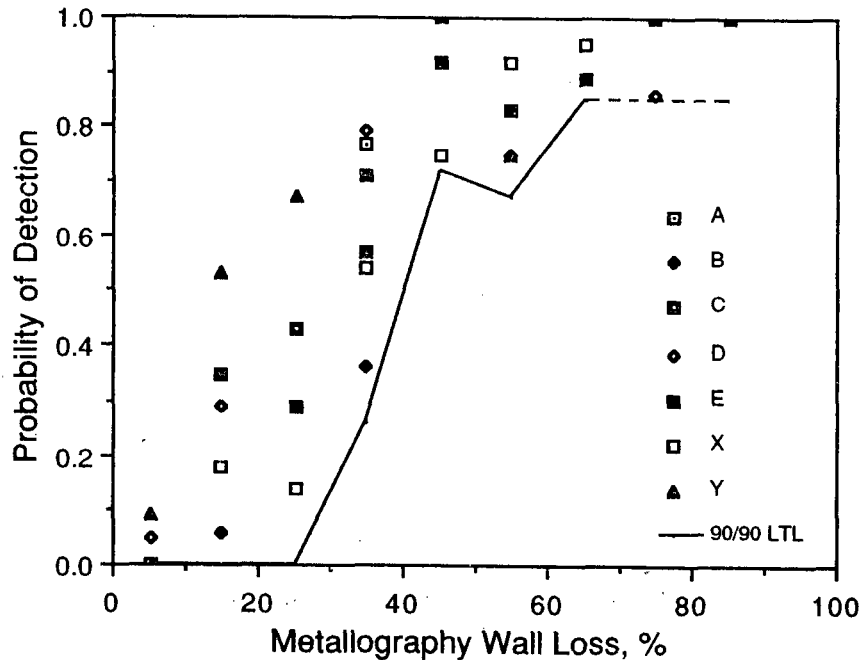
FIGURE 3.39. Individual POD Performance for the DAARR and
Base-Line Teams for Each 10% Wall-Loss Increment

Comparing the EC and metallography data shows that EC generally tended to underestimate the defect depth as measured by metallography, especially for the more severely-degraded specimens. Figure 3.40 shows the relationship between the EC and metallographic results for a typical inspection team using standard bobbin-coil techniques. Points plotted along the horizontal axis are nondetections and points shown on the vertical axis are false calls. Team-to-team variations were observed, but the general tendencies shown in Figure 3.40 were apparent for all of the Base-Line and DAARR inspections. Wide variations in the EC depth estimates were reported for specimens with similar wall-loss and also for the same specimen but from different teams. A better correlation between the EC and metallography wall-loss was observed for one of the AATRR teams, as shown in Figure 3.41.

Linear models were fit to the team's sizing data using an algorithm designed for truncated data (Aitkin 1981). The perfect sizing relationship is described by an intercept of 0.0 and a slope of 1.0. A measure of how well the model fits the data is obtained from the correlation coefficient, R^2. Summary statistics for the linear sizing model for all teams is given in Table 3.19. The intercept, slope, sizing error estimate, number of defects and R^2 are listed.
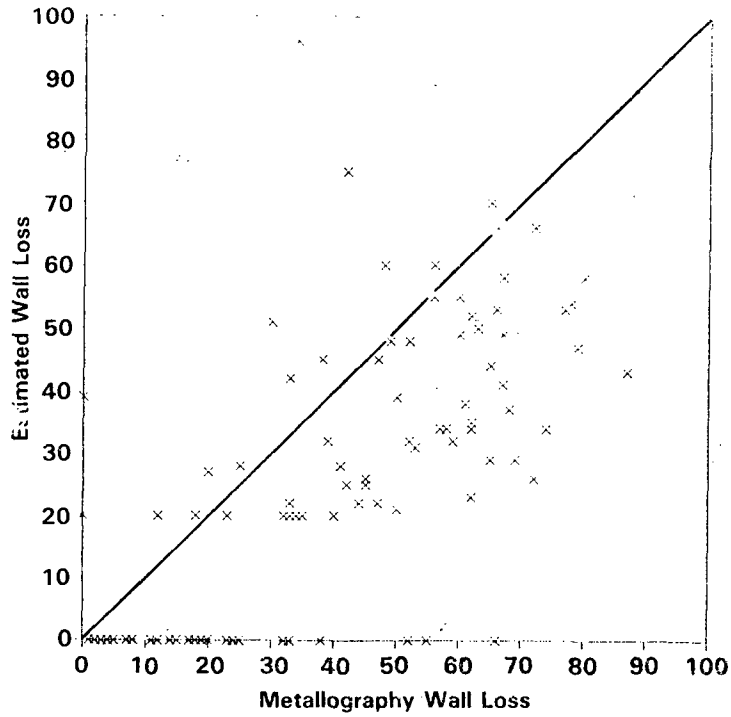
FIGURE 3.40. Typical Plot of EC Estimated Flaw Depth Versus
Actual Depth from Metallographic Analysis
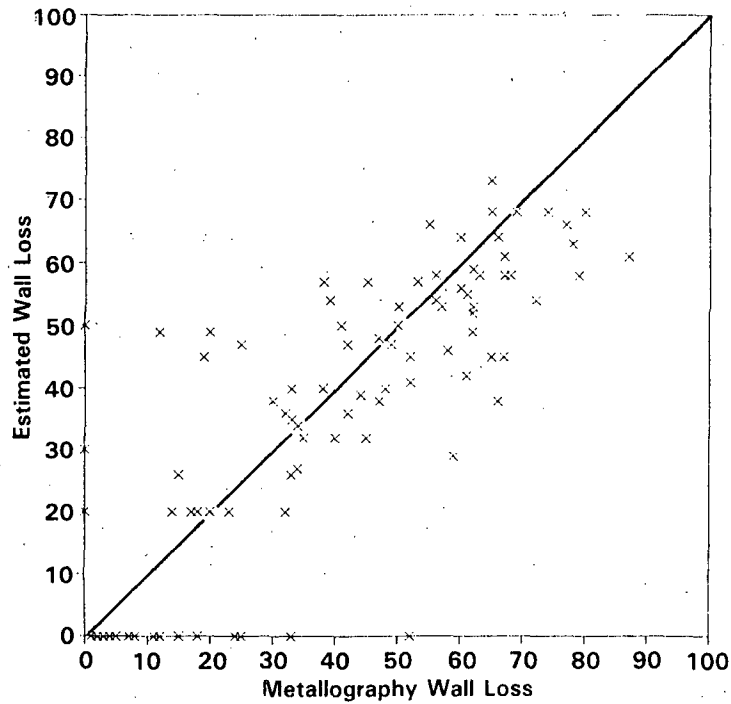
FIGURE 3.41. Plot of Best Observed EC Estimated Flaw Depth
Versus Actual Depth from Metallographic Analysis

3.80

Table 3.19 shows little consistency in the estimates of the intercept. For the Base-Line and DAARR teams, it varies from 6% to 24%, which represents a significant sizing bias. The slopes, varying from 0.38 to 0.61, are reasonably consistent. The sizing errors are also consistent, 14.67% to 16.69%, with the exception of Team Y at 21.11%. These errors are large; a one standard deviation (error estimate) range about a defect size estimate is at minimum 30% of wall thickness. Although Team V's fitted intercept and slope were not significantly different from some of the other teams, their dispersion was the lowest (except for Team U with only 13 defects >20%) and their R^2 value was the highest of any team. Team V employed two inspection techniques that probably explain, in part, their improved sizing performance. First, special frequency mixes were developed specifically for the Surry generator and used to enhance the signal-to-noise ratio by suppressing the effects of dents, support plates, and copper deposits. Second, rotating EC and focused ultrasonic probes were used to reinspect 22 of the tubes previously inspected by conventional bobbin-coil EC. The wall-loss determined from the supplemental inspection was then compared to the bobbin-coil results and a correction factor computed. In this case the bobbin-coil data was adjusted by +15% to correct for an apparent underestimate of defect depth. Both of these factors, namely, special frequency mixes and augmentation of the EC/bobbin-coil data, apparently were responsible for the improved sizing accuracy.

TABLE 3.19. Sizing Regression Summary Statistics

Team	Intercept, %	Slope	Error, %	n	R^2	Measurement Truncation, %
A	12.05	0.49	16.48	64	0.21	20
B	17.58	0.38	14.67	52	0.13	20
C	24.17	0.40	15.60	62	0.16	20
D	8.96	0.61	16.69	66	0.31	20
E	20.27	0.45	14.81	64	0.24	20
X	9.43	0.49	15.82	58	0.21	0
Y	5.98	0.61	21.11	69	0.26	10
U	-4.21	0.84	7.62	19	0.85	20
UU	35.33	0.19	17.80	31	0.04	20
V	14.30	0.64	10.59	73	0.57	20
VV	19.76	0.29	17.94	33	0.09	0
W	-33.26	1.40	23.34	14	0.33	10

3.5.3.3 Factors Influencing EC Inspection Reliability

The EC data and reports obtained from the various inspection teams were examined to determine the cause of the lack of detection for some severely damaged specimens and the wide variations in sizing. Defect indications that were missed by one or more of the inspection teams were subsequently found on the EC data tapes when reanalyzed by a PNL analyst (Bradley et al. 1988). This indicates that the analysts either bypassed the indication or, for some reason, did not interpret the generally complex EC signals to be defects. Interpretation of the complex EC signals also appears to be the primary source

of the large variations in reported defect depths for the same specimen. Specific causes that were identified include: 1) multiple defect signals within the degraded region, 2) different procedures and locations used to measure the phase angle within distorted signals; and 3) the frequency used to measure the defect depth. Most of the large variations in reported defect depth for a given specimen could be individually explained by one or more of the above causes.

It was also noted that complex EC signal shapes usually coupled with a low signal-to-noise ratio were general characteristics of specimens with large variations in the reported defect depths.

The EC data from TTS specimens with metallographic data available were reanalyzed to determine if a consistent analysis method and or frequency would improve the correlation between EC and metallography wall-loss. The EC data tapes from one of the DAARR inspection teams were analyzed at 400 kHz, 100 kHz, and a 400/100 kHz mix. The defect signals were measured at all three channels by always taking the location within the signal which produced the deepest wall-loss. This location usually was a tangent point of a deflection on the vertical channel of each output. A comparison of the resulting EC depth estimates with the metallographic data is shown in Figure 3.42. No definite improvement in the variability of the EC depth estimates is seen in the three sets of data, although a consistent analysis method was employed.

The effect of defect type and distribution on the EC sizing variability was evaluated by dividing the TTS specimens into defect categories consisting of wastage, pitting and wastage, and isolated pitting. The pitting and wastage specimens were subdivided into two categories depending on the circumferential extent of the defects in the transverse sections. Degraded regions (not necessarily continuous) were distributed around more than one-half of the tube circumference for Category 1 and less than one-half of the tube circumference for Category 2. The resulting correlations between the reported EC wall-loss from the Base-Line and DAARR inspections and the metallographic data are shown in Figures 3.43 and 3.44. As can be seen, definite improvements in the correlations were not obtained. The simple defect types, wastage and isolated pitting, appear to provide a slightly improved EC estimate of wall-loss. However, the number of specimens in these categories is limited and the differences may not be significant.

Deposits on the OD surfaces were found to be the primary cause of the false positive calls made by the inspection teams. Most of the false calls were located in the U-bend and TSP regions of the generator, and tubes from these locations were generally coated with a Cu-rich deposit described above. Examination of the EC data showed that two types of defect indications were responsible for the false calls. The first type of indication appeared as a shallow OD defect and was most easily detected at 100 kHz frequency. After removal from the generator, correlations were observed between this type of EC signal and locations where there was a lack of, or an interruption in the deposit (Bradley et al. 1988). The second type of indication was characteristic of a permeability variation (PV) signal and was reported as an ID defect. Removing the deposits by chemical cleaning eliminated both signal types from most of the specimens, although a small residual PV-type signal
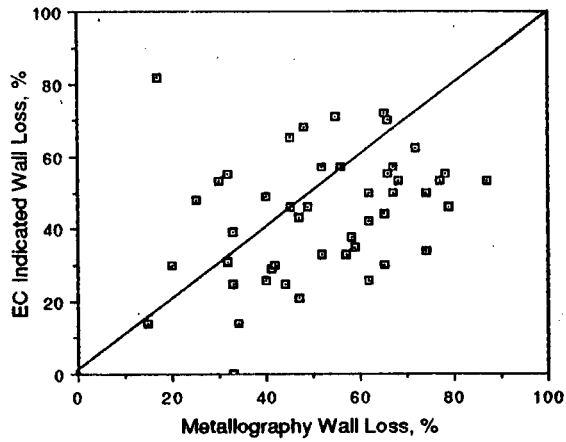
a) 400 kHz
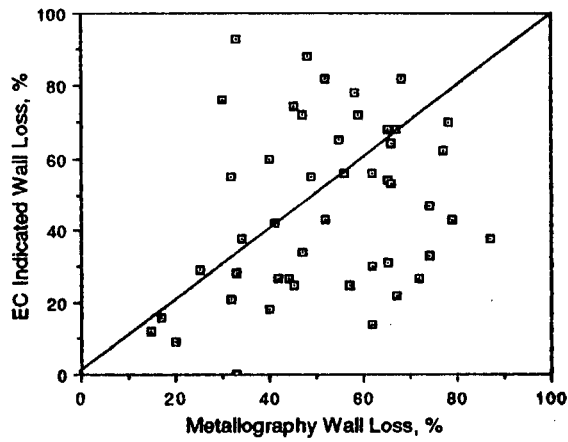
b) 100 kHz
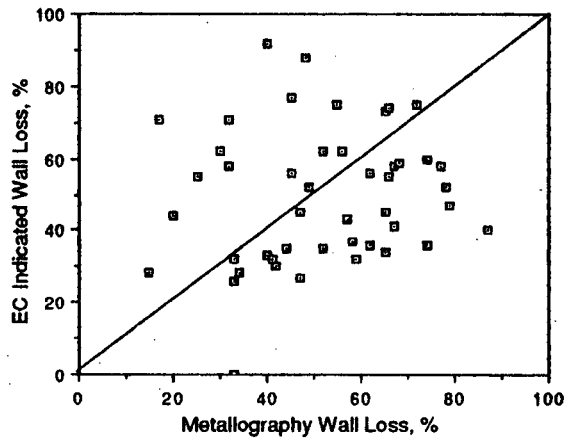
c) 100/400 kHz

FIGURE 3.42. Comparison EC Data Reanalyzed at Various Frequencies With Metallography

3.83
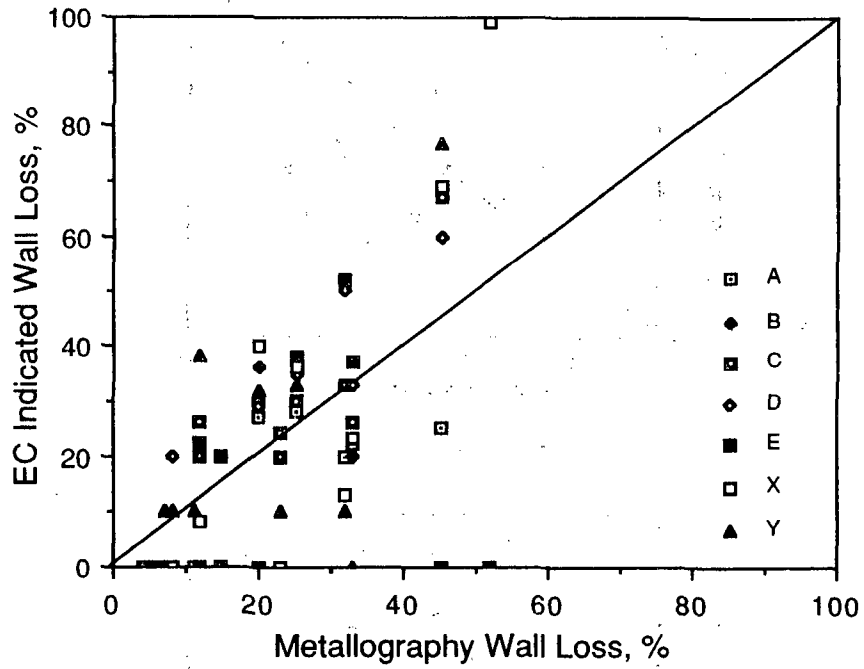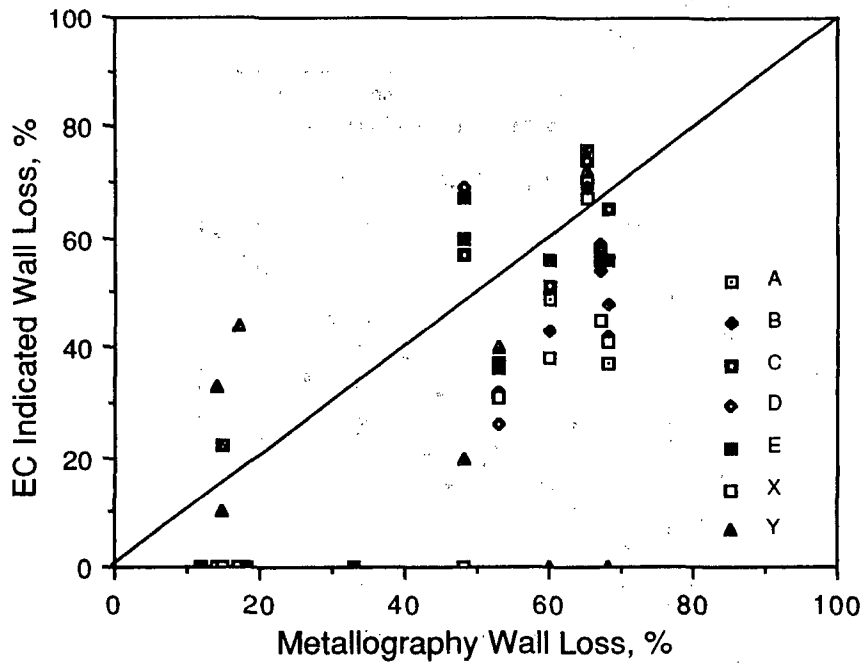
a) Wastage Defects

b) Pitting Defects

FIGURE 3.43. Correlation of EC Estimated Wall-Loss (Base-Line
and DAARR Teams) With Metallography

3.84
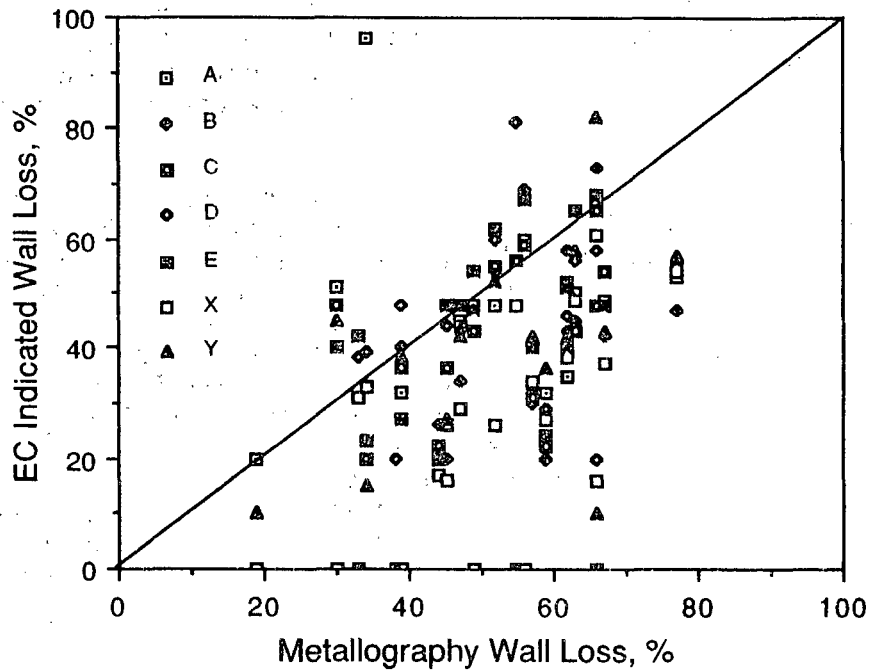
a) Pitting/Wastage Less Than Half Circumference
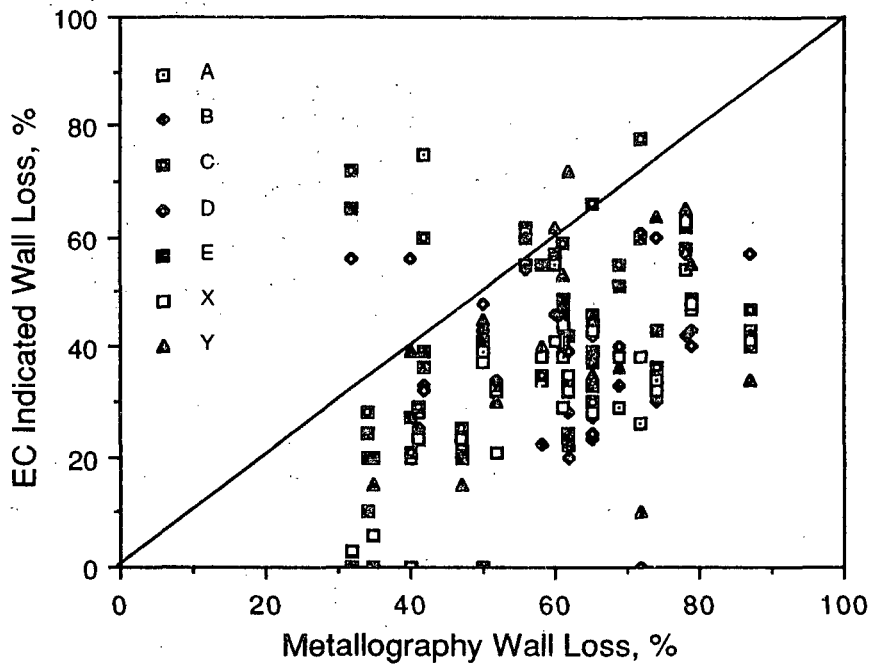
b) Pitting/Wastage More Than Half Circumference

FIGURE 3.44. Correlation of EC Estimated Wall-Loss (Base-Line and DAARR Teams) With Metallography

3.85

remained in a few specimens. Visual inspection of all specimens and metallography on selected specimens found no evidence of defects. Superficial fabrication marks and spots without the thin oxide coating on the tube OD were noted in the inspection data because of possible correlations with interruptions in the Cu-rich deposits.

A large number of the EC signals observed on the inspection data tapes were due to interruptions in the Cu-rich surface deposits. These signals tended to be classified as defect indications by inspection teams depending upon their amplitude, shape and location within the generator. Figure 3.45 provides a typical example of an EC signal caused by the Cu deposits. The signal shown in Figure 3.45 was interpreted by an inspection team as a defect. After removal from the steam generator, this specimen was EC inspected and then chemically cleaned to remove the Cu-rich deposits. Following chemical cleaning, another EC inspection was performed. In all cases, the EC signals that could have been interpreted as a defect were no longer visible. Figure 3.46 shows the post-cleaning EC inspection results for the specimen in Figure 3.45; note the defect indication has disappeared. Destructive examination of some specimens with these types of signals confirmed the absence of defects.

3.5.4 Burst Testing of Service-Degraded Tubes

The objective of the burst-test work was to validate empirical models of remaining tube integrity developed during Phase I of this program (Alzheimer et al. 1979). Burst tests were performed on tubes removed from the steam generator with pitting/wastage type defects. The results of these tests are described below.

Twenty specimens removed from the hot-leg TTS region of the steam generator were burst tested to measure remaining tube integrity. Seventeen specimens with visually-severe pitting/wastage type defects from above the TTS were tested as well as three specimens taken from the TS crevice with no observable defects. Undefected portions of tubing were tested so that the normalized burst pressure of defected specimens could be computed. This was done to minimize the influence of material property and tube dimensional variations on burst strength. Thus, the dependence of tube integrity on just defect severity could be determined.

Prior to testing, specimens were cleaned to remove residual radioactive contamination, photographed, and dimensionally characterized. A wall thickness gage was used to estimate the amount of remaining wall thickness for the most severely-degraded regions of each tube. The wall-thickness measurements were recorded on the specimen photographs.

After burst testing, the length and depth of defect that caused each specimen to fail was estimated by comparing the failed tube with the pretest photographs that show the remaining wall-thickness measurements. In most instances, the depth of defect causing tube failure corresponds to the region of maximum pitting/wastage. The burst-test results (see Table 3.20) show that even deep pitting/wastage did not significantly reduce tube strength. All tubes leaked or burst at levels several times the highest pressure

Panel 1 (top):

| CH 1 VERT | CH 2 VERT | CHANNEL NO — 1 | ID 0 ROW 4 COL 3 |

```
CHANNEL 1    DIFF
  FREQ ——— 400 kHz
  SPAN ——— 564
  ROTATION -   2 DEG
CHANNEL 2    DIFF
  FREQ ——— 100 kHz
  SPAN ——— 554
  ROTATION -  16 DEG
CHANNEL 3    DIFF
  FREQ ——— 240 kHz
  SPAN ——— 634
  ROTATION -   7 DEG
CHANNEL 4    DIFF
  FREQ ——— 500 kHz
  SPAN ——— 384
  ROTATION -   6 DEG
MIX 1 (5)   <—
  CHANNELS    12
  SPAN ——— 1024
  ROTATION -   0 DEG
MIX 2 (6)   <—
  CHANNELS    13
  SPAN ——— 1024
  ROTATION -   0 DEG
```

0.96 VOLTS   196 DEG   0

Panel 2 (bottom):

| CH 1 VERT | CH 2 VERT | CHANNEL NO — 2 | ID 0 ROW 4 COL 3 |

```
CHANNEL 1    DIFF
  FREQ ——— 400 kHz
  SPAN ——— 564
  ROTATION -   2 DEG
CHANNEL 2    DIFF
  FREQ ——— 100 kHz
  SPAN ——— 554
  ROTATION -  16 DEG
CHANNEL 3    DIFF
  FREQ ——— 240 kHz
  SPAN ——— 634
  ROTATION -   7 DEG
CHANNEL 4    DIFF
  FREQ ——— 500 kHz
  SPAN ——— 384
  ROTATION -   6 DEG
MIX 1 (5)   <—
  CHANNELS    12
  SPAN ——— 1024
  ROTATION -   0 DEG
MIX 2 (6)   <—
  CHANNELS    13
  SPAN ——— 1024
  ROTATION -   0 DEG
```

2.13 VOLTS   102 DEG   0

FIGURE 3.45   U-Bend Specimen 568 (R4 C3) Showing a Defect-Called Signal in U-Bend Area Which Turned Out to be an Interruption in the Copper-Rich Surface Deposits

3.87
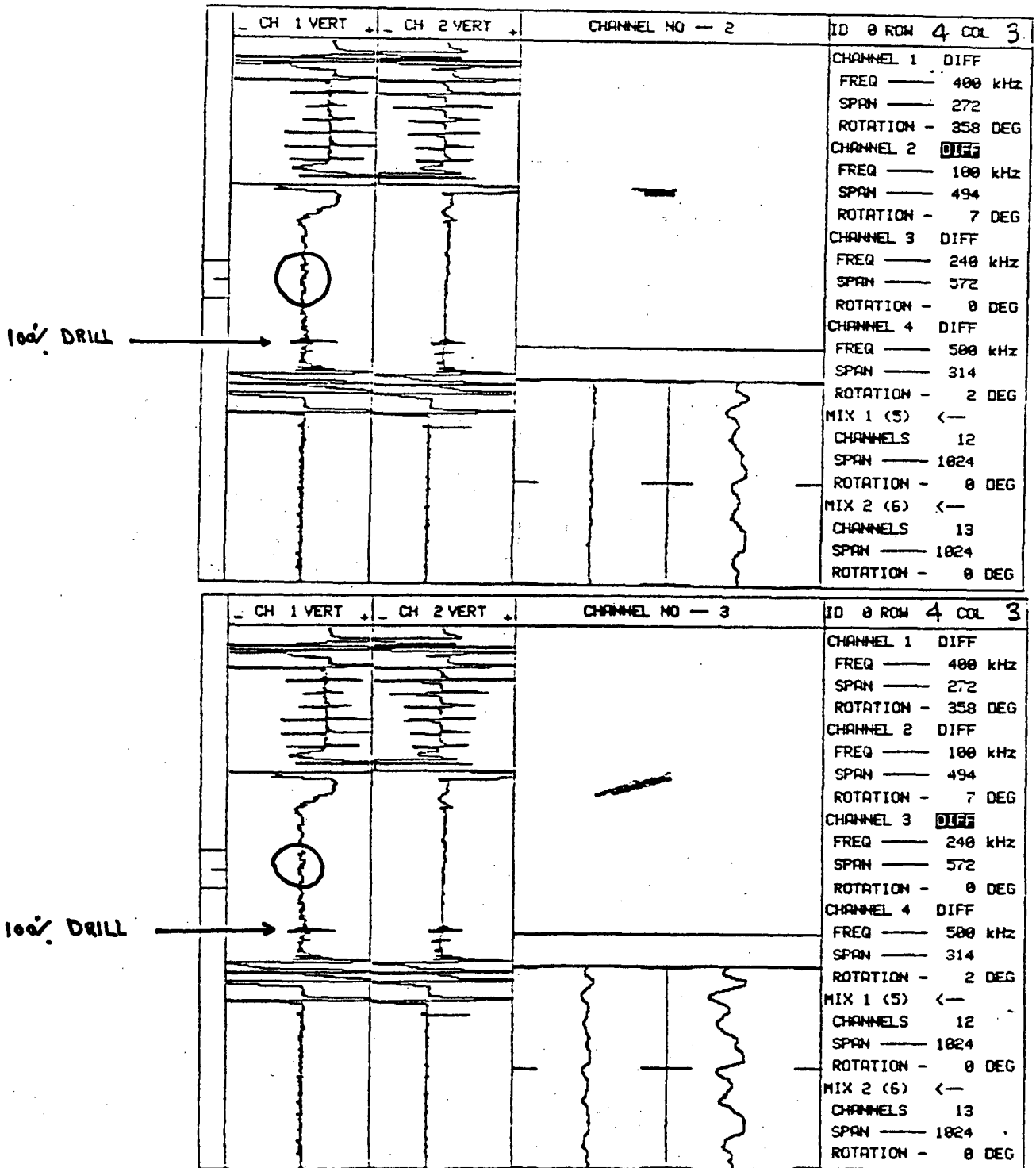
FIGURE 3.46. Specimen 568 (R4 C3) After Cleaning

TABLE 3.20. Surry Tube Burst Data

Specimen No.	Test Temp., °F	Max. P/W Depth, %	Max. Flaw[a] Depth, %	Max. Flaw[a] Length, in.	Burst Pressure, psig	Normalized Burst Pressure, $\Delta P/\Delta P_0$
657B	550	--	--	--	11,165	1.00
794B	550	--	--	--	10,720	1.00
797B	550	--	--	--	11,765	1.00
601C	550	49	24	0.06	10,540	0.94
603C	550	55	55	0.15	9,790	0.87
635C	600	51	43	0.10	10,825	0.97
657C	550	69	69	0.15	8,835	0.79
794C	600	78	78	0.17	7,175	0.67
797C	550	50	50	0.10	11,110	0.94
615C	600	37	24	0.06	10,152	0.91
628C	600	65	52	0.10	10,078	0.90
642C	600	36	36	0.04	10,498	0.94
661C	600	75	75	0.11	9,195	0.82
712C	600	38	38	0.06	10,652	0.95
790C	600	57	57	0.05	10,300	0.92
792C	600	38	38	0.07	10,128	0.90
795C	600	29	29	0.04	10,800	0.96
799C	600	51	80[b]	0.53[b]	6,930	0.62
812C	600	44	22	0.08	9,988	0.89
826C	600	57	43	0.10	10,485	0.94

(a) Corresponds to max. depth and length of P/W at failure location.
(b) Max. depth and length of an axial crack.

attainable in a main-steam-line-break accident (about 2600 psi). This was because of the short length of these defects both axially and circumferentially.

Figure 3.47 shows a plot of the calculated normalized burst pressure against measured values. Excellent agreement was obtained between calculated and measured values for the Phase I EDM notch empirical model. Similar results were obtained for the uniform-thinning model, but the elliptical-wastage model predicted burst pressures substantially below actual values. This model tended to overpredict burst pressure because it was developed from burst-test results on tubes with long axial elliptical wastage. All data points, except one, were within ±10% of perfect agreement. The one data point outside the ±10% range was from a tube in which failure was caused by an OD initiated SCC. The actual burst pressure of this tube was about 20% greater than the predicted value. This result was partially due to the method employed for characterizing the crack dimensions. The cracked portion of the tube was, in fact, composed of several small closely spaced cracks. To conservatively characterize the flawed area, an overall crack length consisting of the sum of the smaller cracks was used. The crack depth was estimated from post-test fracture surface measurements and a metallographic section taken through the center point where the crack had penetrated the tube wall. It is clear that the EDM notch empirical equation gave conservative results for the axial SCC when bounding dimensions were used to characterize its size.

The burst-test results illustrate how bobbin-coil EC depth measurements provided a conservative estimate of remaining tube integrity even with significant undersizing. Figure 3.48 gives a plot of burst pressure versus median EC estimated defect depth for the Base-Line and DAARR teams. The boxed area in the lower left-hand corner of Figure 3.48 defines a zone bounded by the present 40% plugging limit and three (the present factor of safety specified in Regulatory Guide 1.121) times normal operating pressure differential. Note that none of the data fall within the nonconservative zone. This was because of the short axial extent of the pitting/wastage. Large uncertainty in the EC depth estimate can be tolerated when the true defect length is short (<0.25 in.). Thus, the 40% plugging limit is conservative for these defect types. Accurate measurement of defect depth becomes much more important when the defect length is greater than about one tube diameter.

3.6 INSERVICE INSPECTION SAMPLING PLAN EVALUATION

A major objective of the statistical work was to evaluate and compare candidate sampling/inspection schemes for ISI of steam generator tubes. One criterion for comparing sampling/inspection schemes is the probability of detecting and plugging a tube that has a flaw with a specified through-wall depth. For a single tube, this probability is a function of two other probabilities: (1) the probability of detection, which is the probability of observing a positive eddy-current reading, and (2) the probability of plugging (POP), which is the conditional probability that a positive EC reading will exceed the plugging limit and result in plugging or repairing the tube. Both the POD and POP are functions of the true size and type of flaw. They also depend upon the capability and reliability of the inspectors and their equipment.
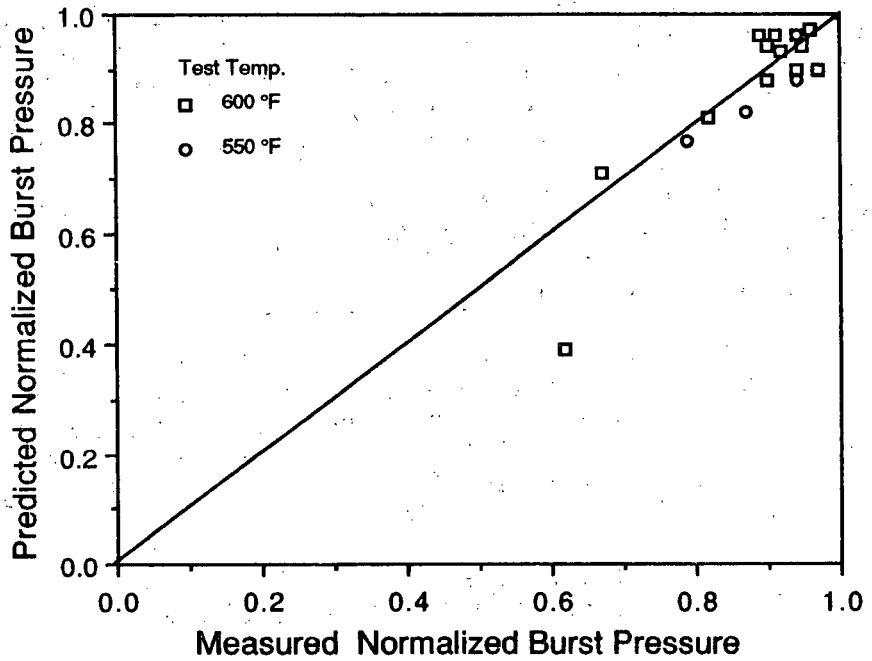
FIGURE 3.47. Calculated Normalized Burst Pressure From EDM Slot Equation
vs Measured Normalized Burst Pressure for Tubes
Removed From the HLTTS Region With P/W Defects
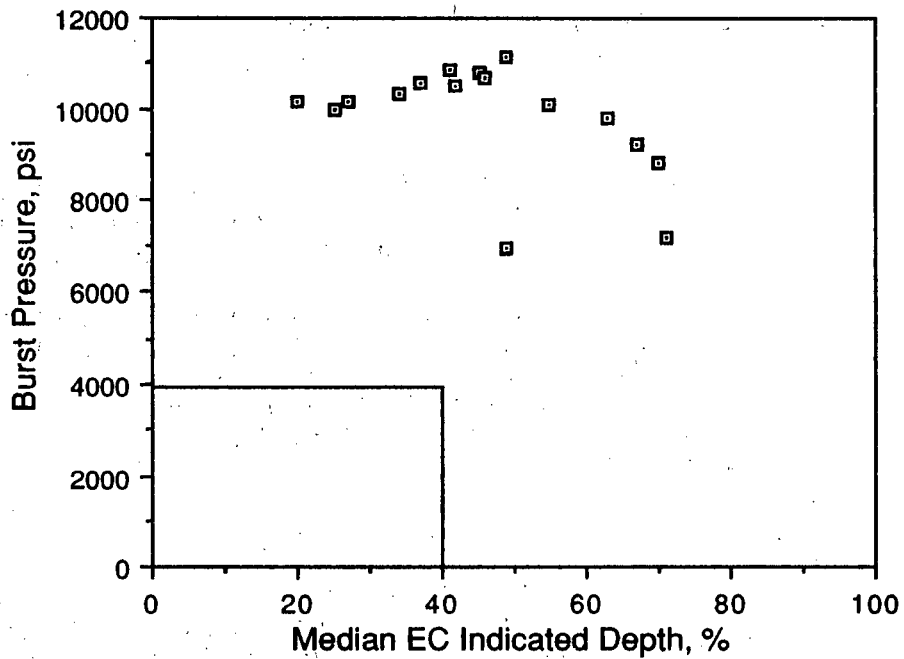
FIGURE 3.48. Burst Pressure vs Median Eddy-Current Depth for
Tube Segments From the Surry Steam Generator

3.91

The Surry generator inspection data were used to develop statistical models of POD and POP as functions of true flaw size for flaws due to wastage and pitting. Because multiple inspection teams were involved, the statistical modeling yielded a range of estimated POD and POP values for each specified flaw size. These ranges of values were utilized with probability theory and Monte Carlo simulation techniques to evaluate and compare sampling/inspection schemes. This section provides a brief overview of the statistical approach, results, and conclusions. A comprehensive report has been prepared (Bowen et al. 1989) that provides a detailed account of this work.

3.6.1 EC Sizing Error and Probability of Plugging

For the purpose of characterizing EC sizing error and estimating POP values, results from the destructive metallographic analyses were matched with the EC inspection results for Surry generator tube segments. EC inspection data are present for 12 teams. Because POP is conditional upon a positive EC indication, the data set for each team was reduced by removing data pairs with no positive EC indication.

The statistical methodology used to model EC sizing error is based on the following definitions and assumptions. For a particular team and a particular "flaw," define

X = "True" Maximum Flaw Depth Determined from
    Destructive Metallographic Analysis (DMA)

Y = Observed Flaw Depth as Determined from
    EC Inspection

Assume that Y can be modeled as a simple linear function of X but with random measurement error e, so that

$$Y = a + bX + e \qquad\qquad (3.1)$$

That is, at a specified value of X, the distribution of Y is assumed to have true mean a + bX and variance Var(e), where a, b, and Var(e) are unknown parameters that must be estimated for each team from the inspection data.

The iterative algorithm presented by Aitkin (1981) was used to fit the model in Equation (1) to the inspection data for each team. This technique for fitting models to data with some censored observations produces estimates of a, b, and Var(e) with desirable statistical properties. Also, a more sophisticated model was fitted to the combined data from the five DAARR teams that incorporates team-to-team variability into the estimate of "Var(e)."

3.6.2 Probability of Exceeding EC Plugging Limit (PEL)

It is of interest to estimate the probability that a non-zero EC value will exceed a specified "plugging limit" T for a flaw with "true" depth X. It is also of interest to determine an EC plugging limit such that the probability of plugging or repairing defective tubes is acceptably high. The

fitted linear models described previously provide a means for achieving these objectives.

For a particular fitted model and a specified EC plugging limit T, the probability of exceeding the EC plugging limit for a tube with a positive EC indication and a flaw with "true" DMA depth X can be evaluated as follows. The predicted mean EC value is computed from the formula $Y = a + bX$ with estimates of a and b substituted. The variance of the distribution of EC values at X is the sum of the estimate of Var(e) and the variance of the predicted EC mean value. The probability that an observed EC value will exceed T is estimated from the normal distribution with mean and variance set equal to their estimated values.

In this study, a defective tube was defined as one having a flaw with true through-wall depth of at least 75%. If it is assumed that the EC plugging limit is 40%, the estimated PEL values (probability that Y >40% given that Y >0%) for six of the fitted models are displayed in Table 3.21. For example, when a tube has a flaw with true depth X = 75%, and a non-zero EC value has been observed by a team like one of the DAARR teams, the probability is 0.73 that the observed EC value will be greater than T = 40%. Clearly, a range of sizing capabilities is represented by the six models.

TABLE 3.21. Estimates of PEL for X = 75% and T = 40%

Round Robin	0.733	Team UU	0.695
Team Y	0.709	Team X	0.644
Team V	0.986	Team VV	0.471

It is also of interest to determine for each model the value of the EC plugging limit T required to achieve a specified PEL when X = 75%. For example, suppose that it is desirable to have PEL = 0.9 when X = 75%. The required T values, estimated from the normal distribution, are displayed in Table 3.22 for the six models. If, for example, the DAARR Teams or teams UU, X, or Y are representative of the teams that currently perform inservice inspections, then the EC plugging limit would have to be lowered to about 25%.

TABLE 3.22. Plugging Limit T Required for PEL = 0.9 When X = 75%

Round Robin	29.2	Team UU	25.2
Team Y	26.6	Team X	25.5
Team V	49.8	Team VV	14.2

If Team VV is the "norm," then a plugging limit at about 14% would be required. However, if all teams could perform like Team V, the plugging limit could be increased to 50%.

The sizing capabilities of the teams can be compared by comparing the fitted models or by comparing PEL values. For example, Table 3.23 displays PEL values for three of the models with plugging limit values T = 30%, 40%, and 50%.

TABLE 3.23. Estimated PEL Values for Three Plugging Limits

Plugging Limit, %	True Depth, %	Round Robin Teams	Team UU	Team V
T = 30	0	0.23	0.65	0.05
	20	0.41	0.72	0.36
	30	0.51	0.75	0.61
	50	0.72	0.80	0.94
	75	0.89	0.85	1.00
T = 40	0	0.09	0.47	0.01
	20	0.20	0.53	0.09
	30	0.28	0.56	0.25
	50	0.48	0.63	0.73
	75	0.73	0.70	0.99
T = 50	0	0.03	0.29	0.00
	20	0.08	0.33	0.01
	30	0.12	0.36	0.05
	50	0.26	0.42	0.36
	75	0.51	0.50	0.90

Note that Team UU always has higher PEL values for nondefective tubes (X <75%) than the other teams. If the plugging limit is set at T = 30% so that the DAARR teams and Team UU have a high PEL when X = 75%, all teams have PEL >0.5 when X >30%; and Team UU would tend to plug most of the tubes with positive EC indications. If T is increased to 50%, Team V has a high PEL when X = 75%, and would not be likely to plug tubes with true flaw depth X <50%; but the DAARR teams and Team UU have low PEL values when X = 75%.

3.6.3 Probability of Detection (POD)

Estimates of POD were computed by matching EC inspection results with the results from both the visual inspections and destructive metallographic analyses. For each "true flaw size" category, the number of non-zero EC indications divided by the total number of flaws was used as a POD estimate. A POD curve (i.e., a plot of estimated POD vs "true size") was constructed for each inspection team, and an overall POD curve was constructed by combining the data from all teams. Some of these curves were presented in Section 3.5.3.2, and the ranges of estimated POD values were used as a basis for evaluating and comparing the performance of sampling/inspection schemes.

3.6.4 Evaluation and Comparison of Sampling/Inspection Schemes

There are two basic strategies for selecting tubes from a generator for inservice inspection. Either all tubes are inspected (100% inspection) or a sample of the tubes is selected for inspection. Although there are many possible sampling schemes that could be applied, one particular type of sequential sampling/inspection was identified as most appropriate and was evaluated and compared with 100% inspection.

With 100% inspection, all defective tubes in a generator will be inspected, and the joint probability, p, of detecting and plugging an individual defective tube is the product of the POD and the PEL for a defective tube. That is,

$$p = POD(PEL) = Pr(Detect \text{ and } Plug \mid Defective) \qquad (3.2)$$

To be conservative in this study, POD = 0.9 was assumed for flaws large enough to classify a tube as defective. Thus, p can be computed from Equation (2) for a specified PEL value. When there are n defective tubes in the generator, the probability that k or more defective tubes are plugged after inspection is computed from the cumulative binomial distribution with parameters n and p.

When a sampling scheme is applied to select tubes for inspection, there is no guarantee that all defective tubes in a generator will be inspected. Thus, the probability of detecting and plugging a defective tube is a function of the probability that the defective tube will be inspected. Without further assumptions about the distribution of defective tubes in a generator or supplementary sampling/inspection, Equation (2) would be multiplied by the probability of inspection. For example, if POD = 0.9, PEL = 0.7, and if 3% of the tubes are randomly selected for inspection, then the probability of inspecting, detecting, and plugging an individual defective tube is p = 0.9(0.7)(0.03) = 0.0189. With 50% random sampling, p = 0.9(0.7)(0.5) = 0.315. These values compare with p = 0.9(0.7) = 0.63 for 100% inspection. By making assumptions about the distribution of defective tubes and by considering a particular type of sequential sampling/inspection scheme, the effectiveness of sampling/inspection relative to 100% inspection can be improved considerably over the completely random sampling implied above.

In the analytical portion of this study, it was assumed that defective tubes tend to occur in "clusters," which are groups of defective and degraded tubes. For the purpose of evaluating and comparing sampling/inspection schemes, a "minimum" cluster was assumed, which is a defective tube surrounded by degraded but not defective tubes in the following pattern:

$$\begin{matrix} & 0 & \\ 0 & X & 0 \\ & 0 & \end{matrix}$$

where X denotes a defective tube and 0 denotes a degraded but not defective tube.

It is recognized that in a real generator, clusters could be shaped differently than the one shown above, and could be different sizes, and could include more than one defective tube. The above cluster configuration was selected for evaluation purposes because it would be harder to detect than a larger cluster or a cluster with more than one defective tube. It is also recognized that in some cases defective tubes may be isolated. As a result, in the simulation analysis portion of the study (see Section 3.6.5), various distributions of degraded and defective tubes were examined to evaluate other conditions of clustering ranging from nearly isolated defectives up to a single large cluster.

The sequential sampling/inspection scheme that was chosen for evaluation is assumed to proceed as follows:

a)   The initial sample is selected according to a systematic sampling plan that consists of a specified percentage of the tubes in a generator, and each tube in the sample is inspected.

b)   When a positive EC indication is observed, inspection continues in the region immediately surrounding the suspect tube until a 2-tube wide "buffer zone" is observed, which is composed of tubes with no positive EC indication, and which completely surrounds the tube(s) with positive EC indication(s).

c)   In steps a and b, each tube with an EC indication that exceeds the plugging limit will be plugged or repaired.

By assuming the above cluster configuration, it is possible to define a 20% systematic sampling plan for step (a) that would include exactly one tube from each cluster. It is also possible to define a 40% systematic sampling plan that would include exactly two tubes from each cluster. Then, if the defective tube in a cluster is not included in the initial sample, there is a chance that the degraded tube(s) will produce a positive EC indication that will trigger additional inspection (step b), which will include the defective tube.

Thus, the probability of inspecting and detecting the defective tube, denoted by PI&D, is a function of the POD for degraded but not defective tubes, denoted by POD(deg), as well as the POD for defective tubes (which is assumed to be 0.9). Specifically, with 20% systematic sampling at the first stage,

$$PI\&D = 0.18 + 0.72 \ POD(deg) \tag{3.3}$$

and with 40% systematic sampling at the first stage,

$$PI\&D = 0.36 + 1.116 \ POD(deg) - 0.54 \ [POD(deg)]^2 \tag{3.4}$$

The joint probability of detecting and plugging a defective tube is given by

$$p = PI\&D(PEL) \tag{3.5}$$

If there are n defective tubes (n clusters as defined above) in a generator, and if the clusters are assumed to be far enough apart so that the inspection results from one cluster do not affect those of other clusters, the probability that k or more defective tubes are plugged after inspection is computed from the cumulative binomial distribution with parameters n and p.

For evaluating and comparing the sequential sampling/inspection schemes and 100% inspection, PEL values ranging from 0.50 to 1.0 were considered (the PEL estimates from the six fitted models range from 0.471 to 0.986), together with values of POD(deg) ranging from 0.5 to 0.7. For the sequential sampling/inspection schemes with 20% or 40% initial sampling, values of p were computed from Equation (3.5). The resulting values of p are displayed in Table 3.24. For 100% inspection, values of p were computed from Equation (3.2) by assuming POD = 0.9.

TABLE 3.24. Values of p Computed for a Range PEL and POD(deg) Values Assuming That POD = 0.9 for Defectives

| | | PEL | | | | | | | |
		0.50	0.60	0.70	0.80	0.85	0.90	0.95	1.00
		20% Sequential							
POD(deg)	0.50	0.2700	0.3240	0.3780	0.4320	0.4590	0.4860	0.5130	0.5400
	0.60	0.3060	0.3672	0.4284	0.4896	0.5202	0.5508	0.5814	0.6120
	0.70	0.3420	0.4104	0.4788	0.5472	0.5814	0.6156	0.6498	0.6840
		40% Sequential							
POD(deg)	0.50	0.3915	0.4698	0.5481	0.6264	0.6656	0.7047	0.7439	0.7830
	0.60	0.4176	0.5011	0.5846	0.6682	0.7099	0.7517	0.7934	0.8352
	0.70	0.4383	0.5260	0.6136	0.7013	0.7451	0.7889	0.8328	0.8766
		100% Inspection							
		0.45	0.54	0.63	0.72	0.765	0.81	0.855	0.90

Note in Table 3.24 that when POD(deg) = 0.7, the sequential sampling/ inspection scheme with 40% systematic sampling at the initial stage yields values of p that are close to those obtained for 100% inspection. In fact, by setting Equations (3.3) and (3.4) equal to 0.9 and then solving for POD(deg), a value of POD(deg) = 1.0 would be required for the 20% sequential plan to perform exactly like 100% inspection, whereas POD(deg) = 0.77 would be required for the 40% sequential plan to perform exactly like 100% inspection. Numerous tables were computed for each of the three plans which display the probability of leaving a specified number of defective tubes unplugged after inspection when there are n (n ranged from 2 to 20) defective tubes in the generator prior to inspection. These results indicate that when POD(deg) is approximately 0.7, the 40% sequential plan nearly duplicates the performance

3.97

of 100% inspection (Bowen et al. 1989). It must be emphasized, however, that these results are dependent upon the cluster assumption discussed previously.

3.6.5 Monte Carlo Simulation Analysis

To supplement the analytical results, it was desirable to evaluate the performance of the sampling/inspection schemes when the assumption of isolated, perfectly-shaped-cluster sets does not hold. This was accomplished by application of Monte Carlo simulation techniques. A computer program was developed that simulates 100% inspection and the sequential sampling/inspection scheme with 20% or 40% systematic sampling at the initial stage.

A generator with the same number of tubes as the Surry generator (i.e., 3,388) was assumed, and five different tube maps (shown in Figures 3.49 to 3.53) were considered. As shown in the analytical evaluation, the effectiveness of a sampling/inspection scheme depends on probability of detection (POD), sizing capability, and plugging limit. Thus, to simulate the inspection of a tube, it was necessary to input: 1) a POD model that expresses POD as a function of true flaw size X, 2) an EC sizing model that expresses the expected (or mean) EC size as a function of true flaw size X and also provides the standard deviation of individual EC values about the mean value, and 3) an EC plugging limit such that a tube with an EC reading that exceeds the plugging limit will be "plugged." It was of interest to study how changes in any or all of these factors would affect the performance of each sampling/inspection scheme. To accomplish this, several different POD curves were considered. Figures 3.54 and 3.55 show the most important POD curves utilized.

Each POD curve defines a POD value for any true flaw size from X = 0 to X = 100% through-wall. The POD Curves 1 and 2 in Figure 3.54 were chosen to represent lower (Curve 1) and upper (Curve 2) bounds on the POD estimates obtained from the Surry inspection data prior to the final POD analysis presented in the Task 13 Report (Bradley et al. 1988). Note, however, that Curves 1 and 2 do not include a false call probability; that is, in Figure 3.54 both curves have POD = 0 when the true flaw depth is X = 0. Although this zero false call probability is not realistic, false calls can only improve the effectiveness of the sequential sampling/inspection scheme. Thus, an evaluation of effectiveness with a zero false call probability will tend to be conservative.

The POD Curves 4 and 5 in Figure 3.55 are refinement of Curves 1 and 2 based on later (but not the final) POD estimates. The differences are as follows. Curve 4 rises from POD = 0.10 to POD = 0.90 on the interval X = 20 to X = 60; whereas Curve 1 does not reach POD = 0.90 until X = 75. On the interval X = 0 to X = 40, Curves 2 and 5 are identical. For X > 40, however, Curve 5 reaches a maximum POD = 0.95 at X = 75 and then remains at POD = 0.95 for X > 75; whereas Curve 2 increases faster than Curve 5 and reaches a maximum POD = 1.0. Thus, Curve 5 is a less optimistic lower bound on POD than Curve 1. Note also that Curves 4 and 5 have a zero false call probability; that is, POD = 0 at X = 0.

Percent Flaw Depth

- ⊙   < 20
- ●   20 - 49
- ●   50 - 74
- ●   75 - 100

3.99
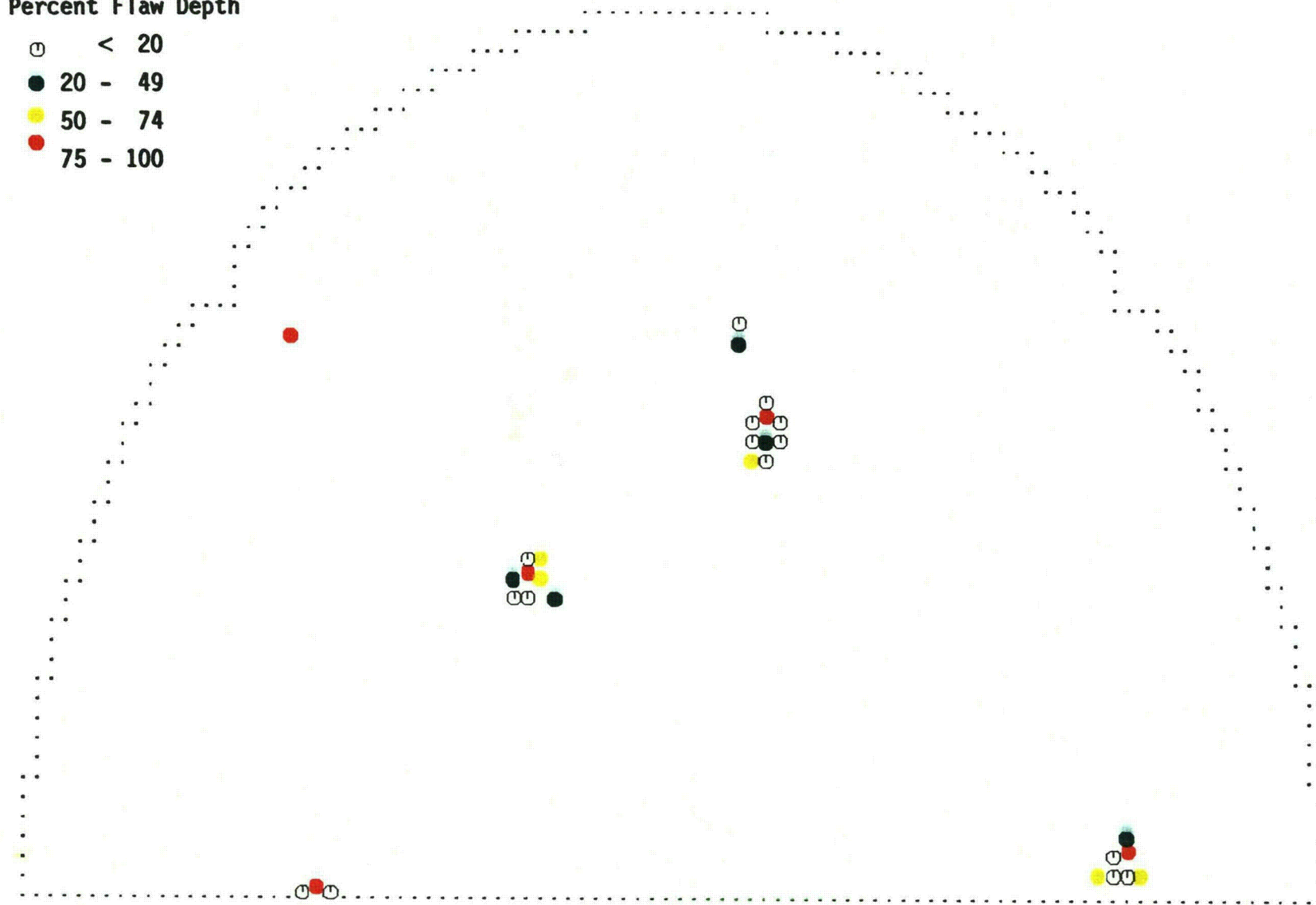
—NOZZLE   FIGURE 3.49.   Tube Map 1   MANWAY—

Percent Flaw Depth

- ⊙ < 20
- ● 20 - 49
- ● 50 - 74
- ● 75 - 100

3.100
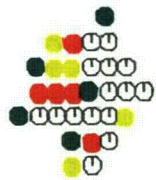
−NOZZLE

FIGURE 3.50. Tube Map 3

MANWAY−

Percent Flaw Depth

- ⊙   < 20
- ●   20 - 49
- ●   50 - 74
- ●   75 - 100
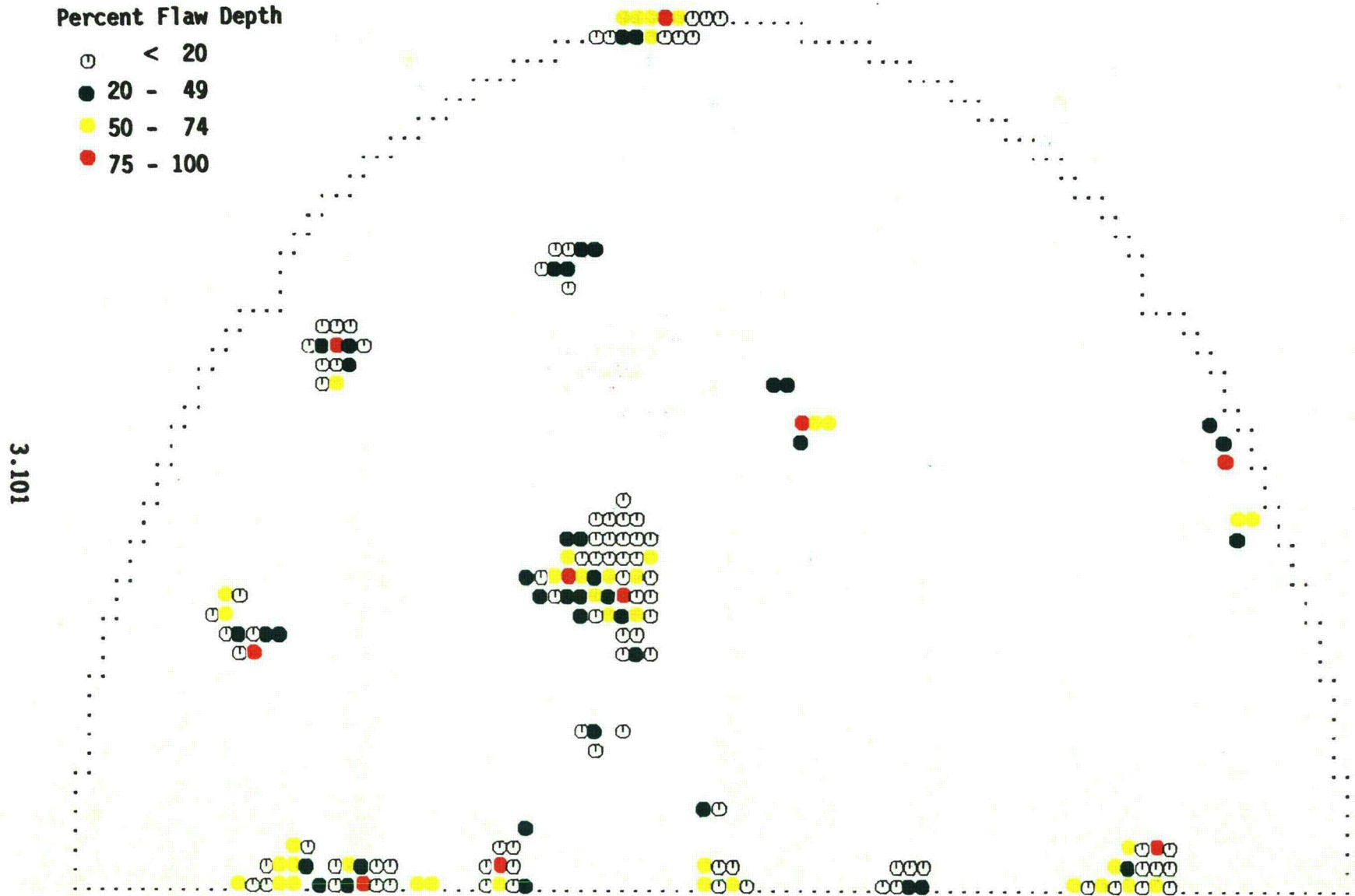
−NOZZLE

FIGURE 3.51. Tube Map 6

MANWAY−

Percent Flaw Depth

- ○ < 20
- ● 20 - 49
- ● 50 - 74
- ● 75 - 100

3.102
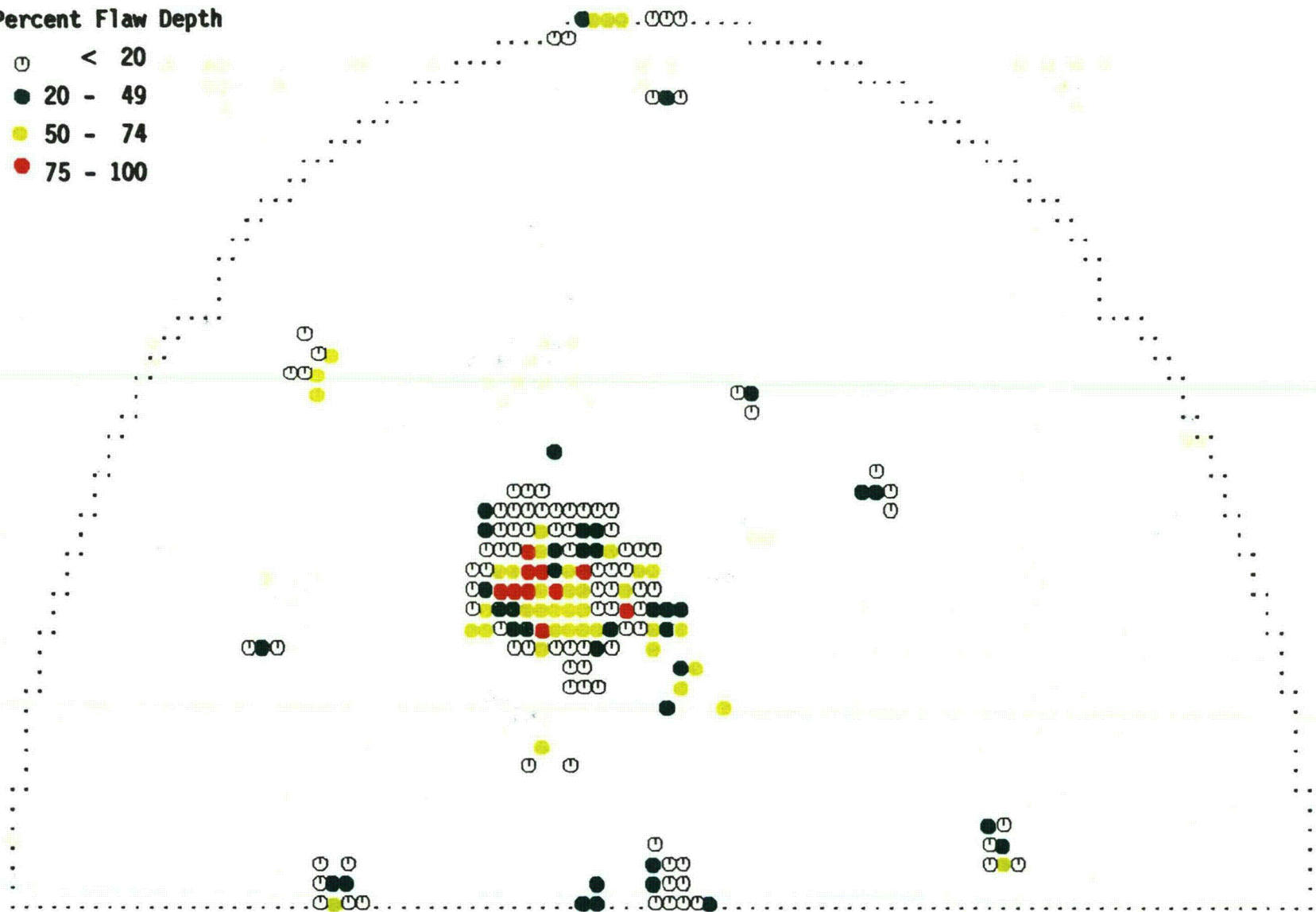
FIGURE 3.52.   Tube Map 8

Percent Flaw Depth

- ⊙   < 20
- 🟢   20 - 49
- 🟡   50 - 74
- 🔴   75 - 100
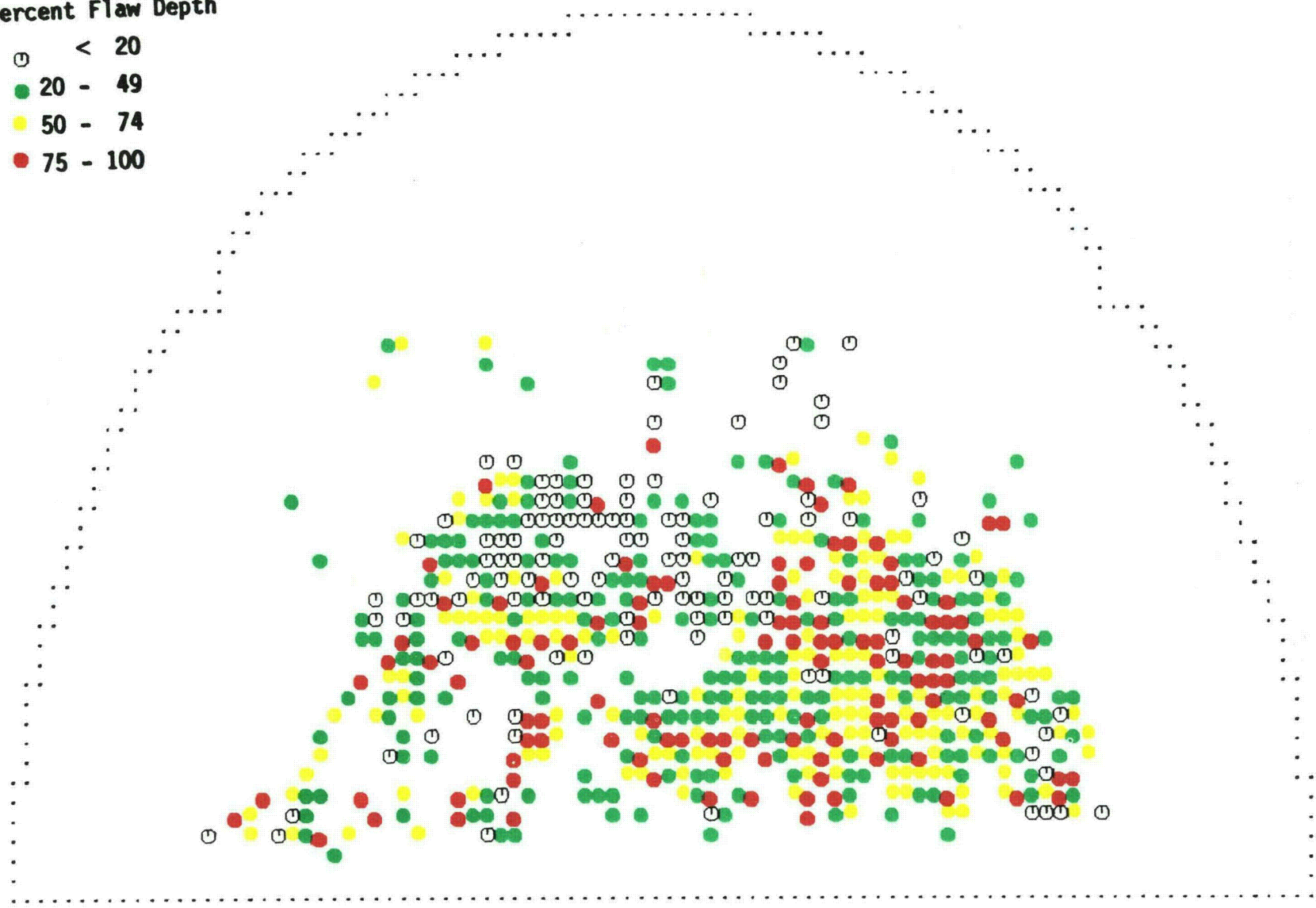
FIGURE 3.53.   Tube Map 13 Predicted Surry "True State"
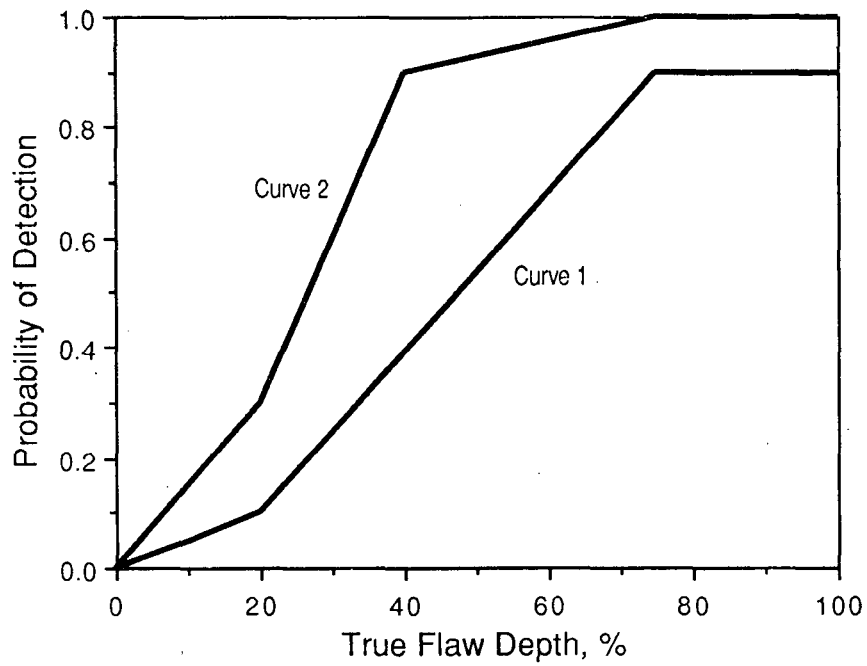
FIGURE 3.54. Simulation POD Curves 1 and 2
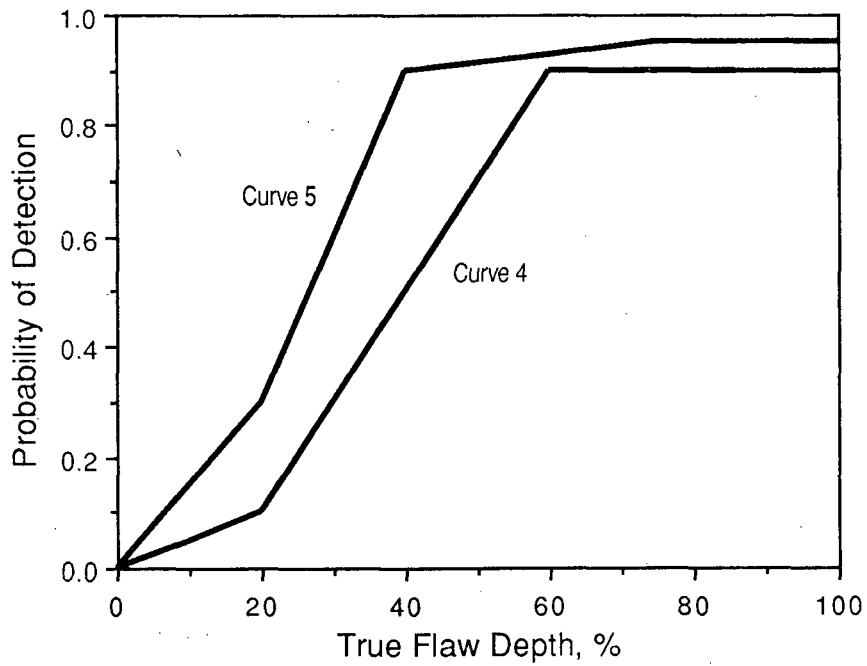
FIGURE 3.55. Simulation POD Curves 4 and 5

To study the effect of sizing capability on the effectiveness of the sampling/inspection schemes, two EC sizing models were considered. Model 1 in Table 3.25 is intended to represent the "average" sizing capability of U.S. inspection teams. Specifically, the parameters a and b were estimated by averaging the values of a and b (see Equation 3.1) for Teams A, B, C, D, and X. The standard deviation, SD, was estimated by first averaging the Var(e) values for these teams and then taking the square root of the average. Model 2 in Table 3.25 is the fitted model for Team V and is intended to represent an achievable level of sizing performance.

TABLE 3.25. EC Sizing Models Used in Simulations

Model	Equation	SD*	Description
1	14.5 + 0.46(X)	16	Average US Team
2	12.6 + 0.68(X)	10	Team V

*SD = Standard Deviation

The simulation analysis strategy was to consider various combinations of tube map, POD curve, EC sizing model, and plugging limit. For a given combination of these parameters, 25 independent applications of all three sampling/inspection schemes were simulated. For each combination, results from the 25 simulated inspections were summarized in tables and plots.

The principal measure of sampling plan performance for detecting and plugging defective tubes was the sampling effectiveness. The sampling plan effectiveness was defined as the ratio of the average number of defective tubes plugged to the total number of defective tubes in the tube map. The effectiveness parameter provided a means for comparing the plugging capability of various sampling plans across the different tube maps.

The results of the Monte Carlo simulation analysis (see Figures 3.56 to 3.59) support the conclusions reached from the analytical evaluation and provide some valuable additional insights. When the isolated clustering assumption discussed in Section 3.6.4 is approximately valid, the sequential/40% scheme tends to be nearly as effective as 100% inspection, but requires substantially less inspection. Note that for conditions of small to almost no clustering (tube maps 1 and 6), 40% sampling plan is significantly better than 20% sampling. However, when the defective tubes are in one large cluster with degraded tubes, all three sampling/inspection schemes are equally effective for detecting and plugging defective tubes (Figures 3.56 and 3.57). For the single large cluster cases, the results imply that a sequential scheme with less than 20% initial sampling might be adequate; however, no simulations were performed to determine how small the initial sample could be before the effectiveness is significantly decreased.
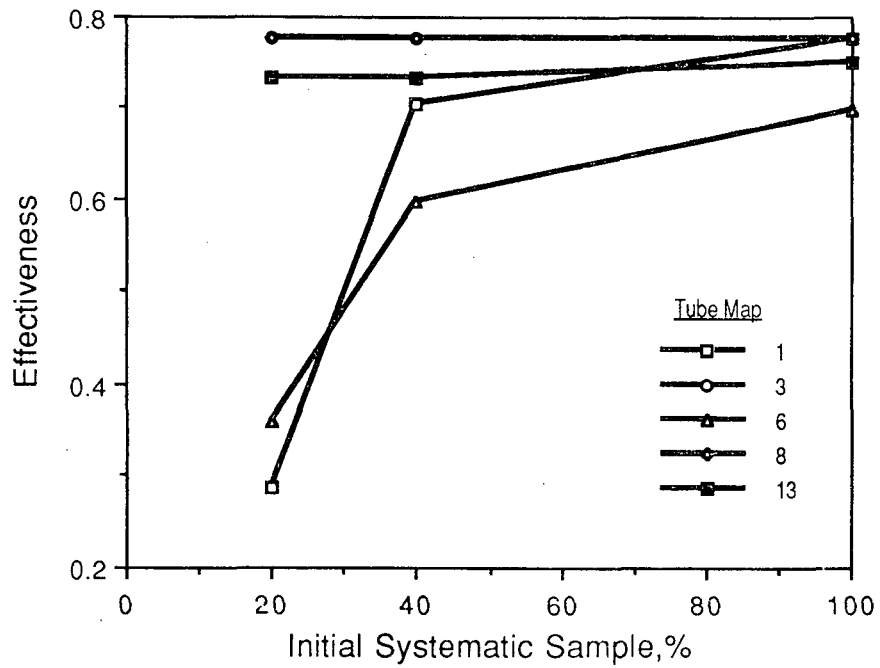
FIGURE 3.56. Sampling Plan Effectiveness Versus Systematic Sample Size for Various Tube Maps - POD Curve 1/Sizing Model 1
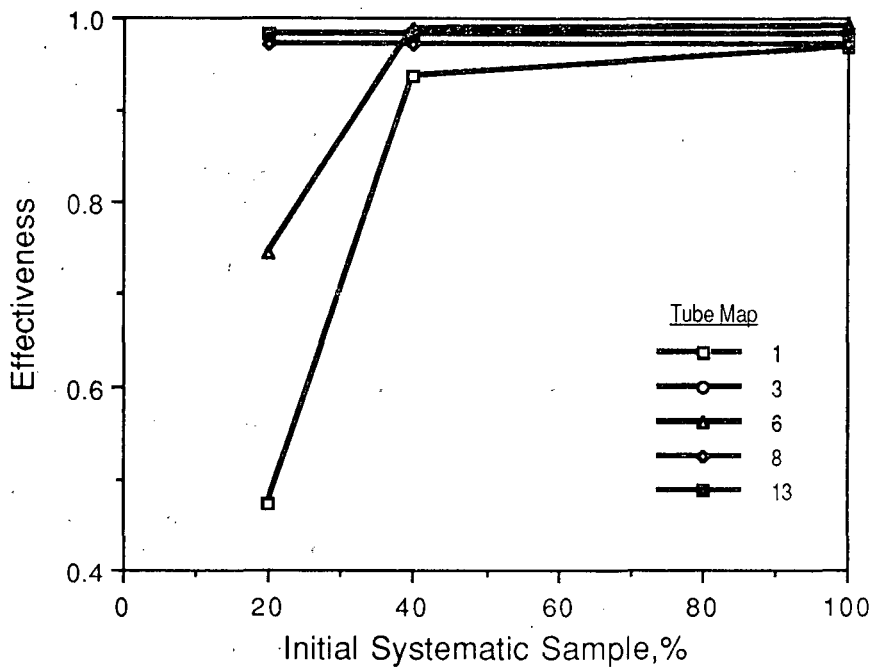
FIGURE 3.57. Sampling Plan Effectiveness Versus Systematic Sample Size for Various Tube Maps - POD Curve 2/Sizing Model 2
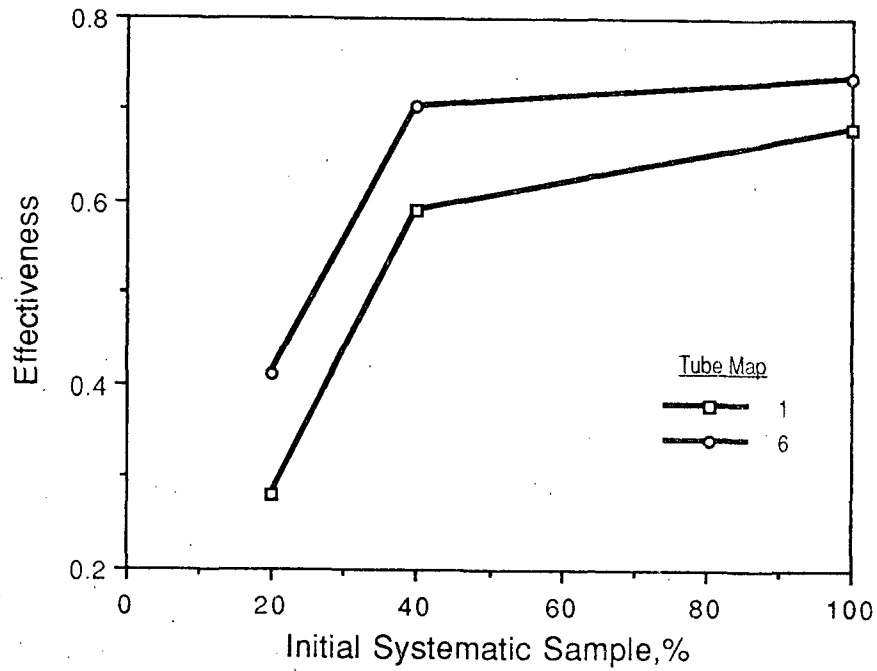
FIGURE 3.58. Sampling Plan Effectiveness Versus Systematic Sample Size for Tube Maps 1 and 6 - POD Curve 4/Sizing Model 1
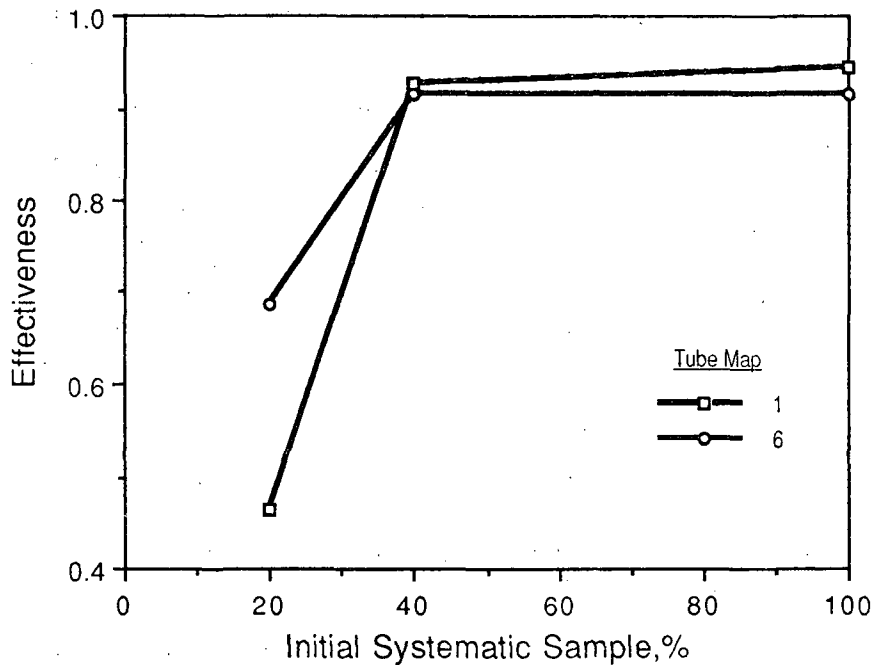
FIGURE 3.59. Sampling Plan Effectiveness Versus Systematic Sample Size for Tube Maps 1 and 6 - POD Curve 5/Sizing Model 2

3.107

Improving the defect sizing capability to the best observed in the Surry inspection data yields improved effectiveness of all three sampling/inspection schemes. (Compare Figure 3.57 to 3.56 and Figure 3.59 to 3.58). Also, with the improved defect sizing capability, increasing the EC plugging limit from 40 to 50 has little impact on the effectiveness of each sampling/inspection scheme for plugging defective tubes, but it minimizes the probability of plugging nondefective tubes. Whereas if the "average U.S. team" sizing capability observed in the Surry inspection data is assumed, increasing the plugging limit from 40 to 50 significantly decreases the effectiveness of all sampling/inspection schemes. (Results not presented here; see Bowen et al. 1989.)

Improving the POD enhances the effectiveness of all sampling/inspection schemes, and the best performance is achieved when the best POD curve and sizing model are assumed. However, for the cases and the POD curves considered, flaws with true sizes less than 20% through-wall do not significantly contribute to the effectiveness of the sequential schemes (see Bowen et al. 1989).

The final issue studied in the simulation analysis is the impact of a 0.05 false call probability on the total number of tubes inspected with either sequential scheme, and whether the additional inspections triggered by false calls enhance the effectiveness of the sequential schemes. For the sequential schemes, the resulting false calls triggered inspection of an additional 19% to 26% of the 3388 tubes in the generator. However, a 0.05 false call probability does not cause either the 20% or 40% sequential scheme to increase to 100% inspection. Also, for the cases considered, there is no firm indication that the false calls improve the effectiveness of the sequential schemes (see Bowen et al. 1989).

3.7 INTERGRANULAR STRESS CORROSION CRACK ROUND ROBIN

To supplement the NDE validation data obtained from the SGGP, an additional round robin was performed to provide information on the reliability of EC techniques to detect and size SCC under simulated service conditions. Fifteen tubes with laboratory produced SCC, along with one tube containing a through-wall SCC that had been previously leak-rate tested, one blank tube and an ASME flat-bottom hole standard, were assembled into a bundle and sent sequentially to the J. A. Jones Applied Research Center, Universal Testing Laboratories/(KWU), Zetec, and Combustion Engineering. It is important to note that three of these firms routinely conduct inservice inspections of steam generators. Thus, the results of this round robin should provide an estimate of field inspections to detect and size SCC. Some of the tubes were coated with a 1- to 2-mil nonuniform layer of copper to simulate the type of deposits observed on tubes removed from the Surry generator. In other cases the cracked portion of the tube was covered either partially or completely by an 0.75-in. thick carbon steel support plate. In these instances the tube-to-tube support-plate crevice was not filled with magnetite or other typical crevice deposits, nor was the tube dented in any way. Each participant in the round robin was required to perform a standard bobbin-coil inspection with 100 kHz and 400 kHz frequencies and any other frequencies of their choice. Each was also permitted to inspect the tube bundle with any alternative method desired.

Typically, segmented bobbin-coil and rotating pancake-coil probes were used for the alternate inspections.

Figure 3.60 summarizes the POD results for the fourteen teams/techniques that inspected the tube bundle blind. Due to the limited amount of data, no attempt was made to determine POD as a function of crack dimensions. However, it should be noted that in 12 of the 16 tubes the crack depth was greater than 40% through-wall. To summarize, the average probability of detection of SCC for teams using bobbin-coil techniques was 0.5. Surprisingly, the alternate bobbin-coil techniques performed significantly below techniques using the conventional bobbin-coil probe. The best detection was obtained from teams utilizing rotating pancake-coil (RPC) or array-coil techniques either alone or as a supplemental technique for conventional bobbin-coil inspection. The average POD for teams using rotating pancake-coil techniques was 0.63.
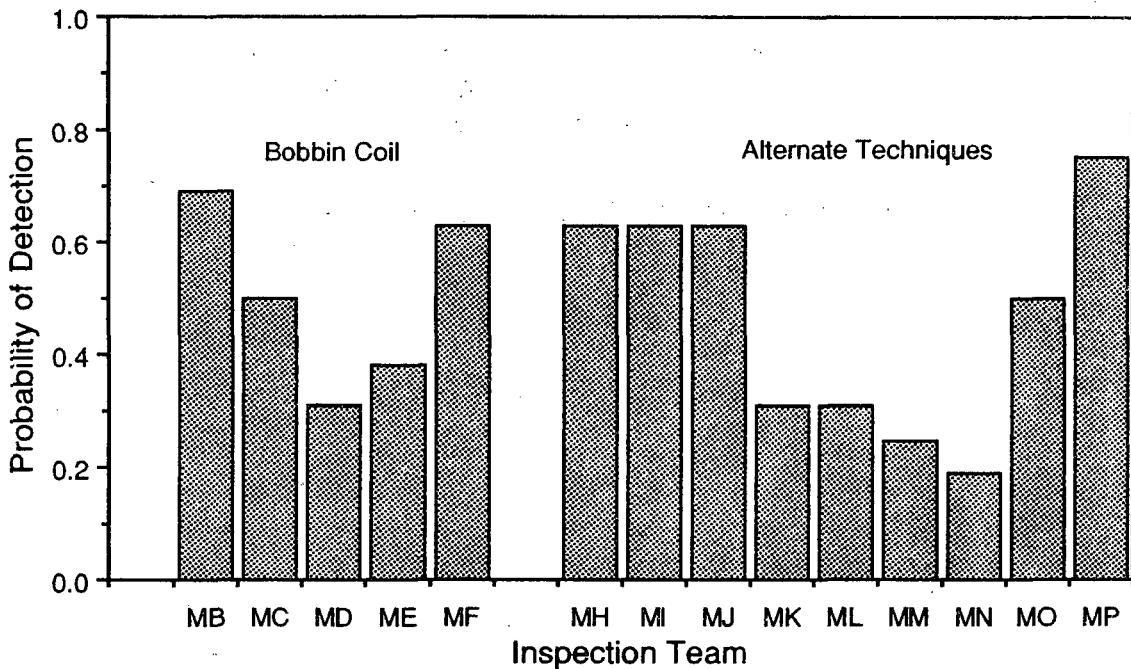
FIGURE 3.60. Summary of POD Results for IGSCC Round Robin Teams

Teams were asked to characterize detected SCC and provide estimates of the crack depth and length. Although the amount of data collected during the mini-round robin was limited, typical results for EC estimated crack depth and length versus destructive measurements are shown in Figures 3.61 to 3.68. It is evident from these graphs that the reliability of EC for crack depth and length was not very accurate or precise. Some teams tended to undersize, while other teams oversized. Another observation from this exercise was that the alternate inspection techniques were not significantly better at sizing SCC then the conventional NDE methods. As a final note, the reader should be
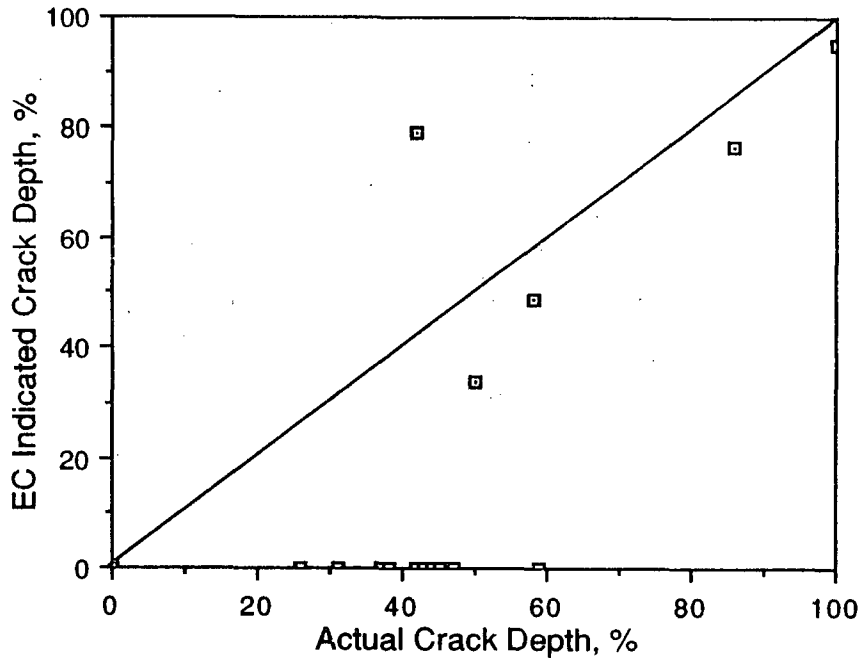
FIGURE 3.61. EC Indicated vs. Actual SCC Depth for Team MD - Bobbin
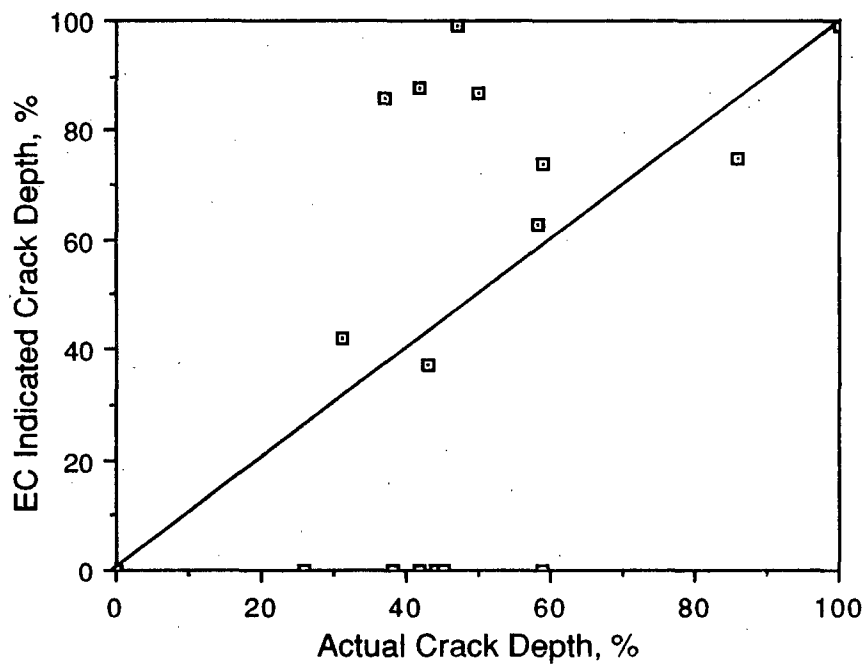
FIGURE 3.62. EC Indicated vs. Actual SCC Depth for Team MF - Bobbin
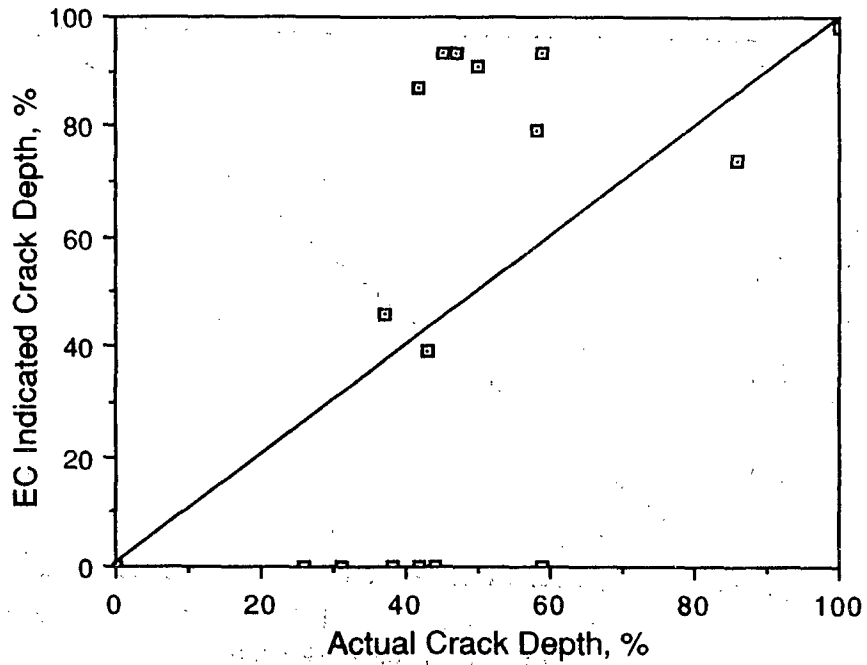
FIGURE 3.63. EC Indicated vs. Actual SCC Depth for Team MH - RPC
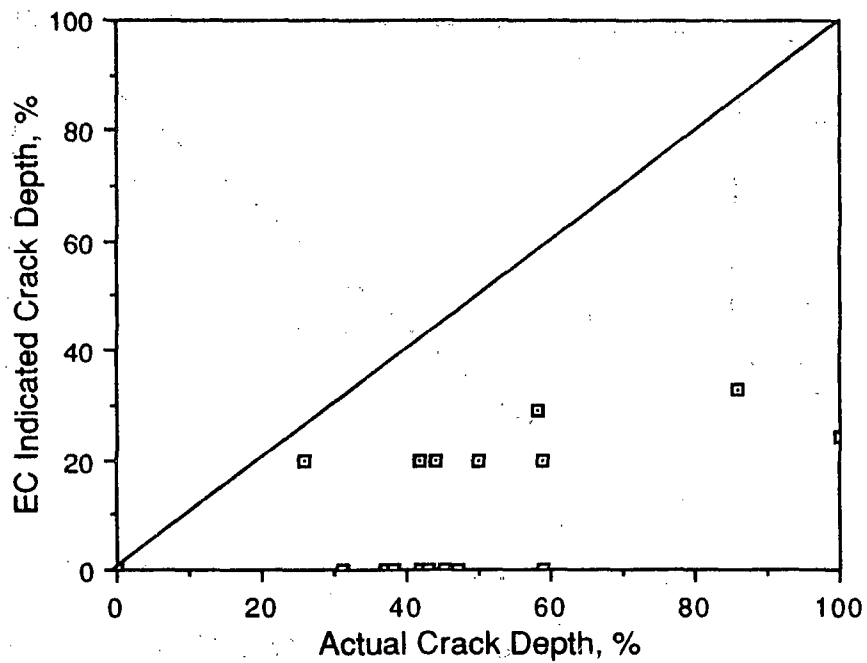
FIGURE 3.64. EC Indicated vs. Actual SCC Depth for Team MO - Array Coil

3.111
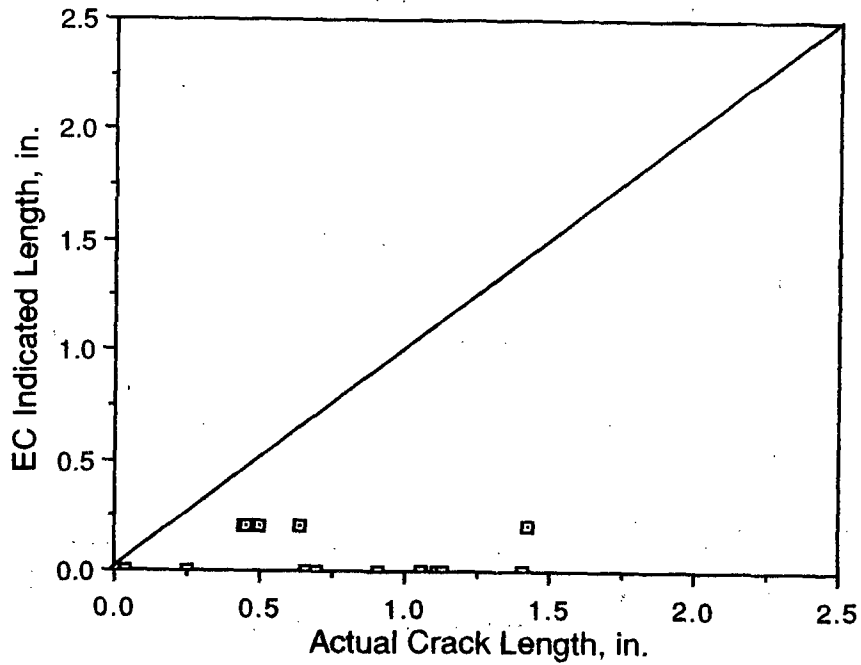
FIGURE 3.65. EC Indicated vs. Actual SCC Length for Team MD - Bobbin
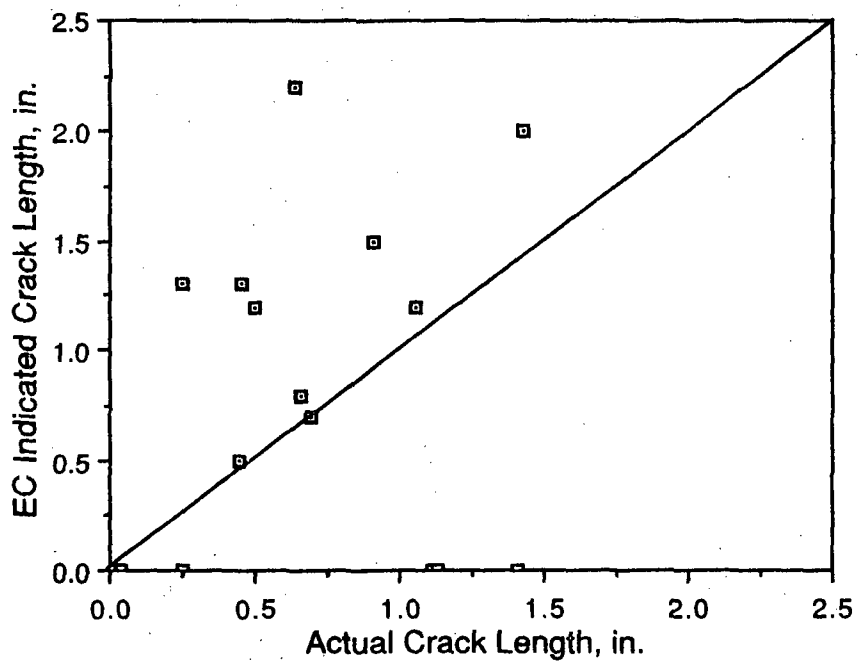
FIGURE 3.66. EC Indicated vs. Actual SCC Length for Team MF - Bobbin
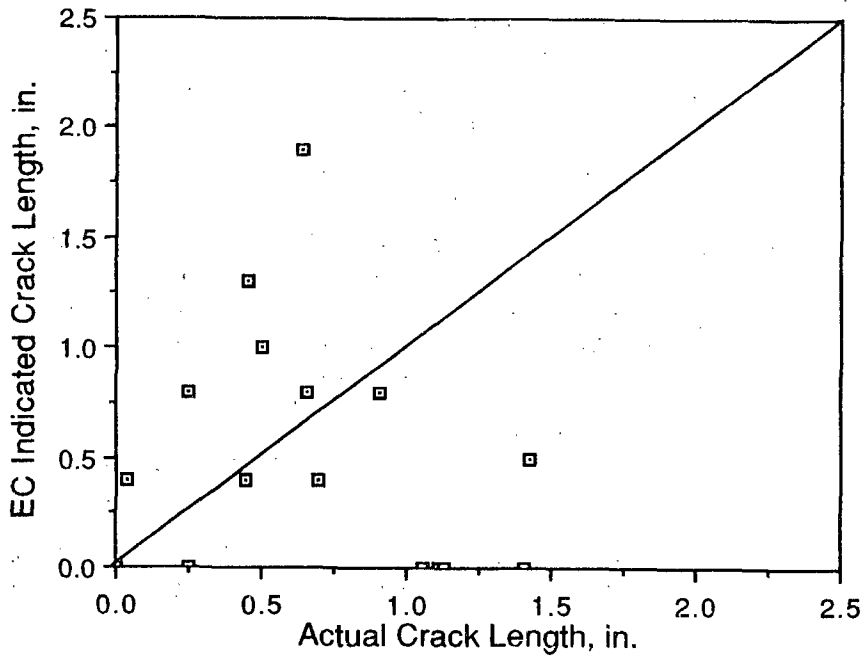
FIGURE 3.67. EC Indicated vs. Actual SCC Length for Team MH - RPC
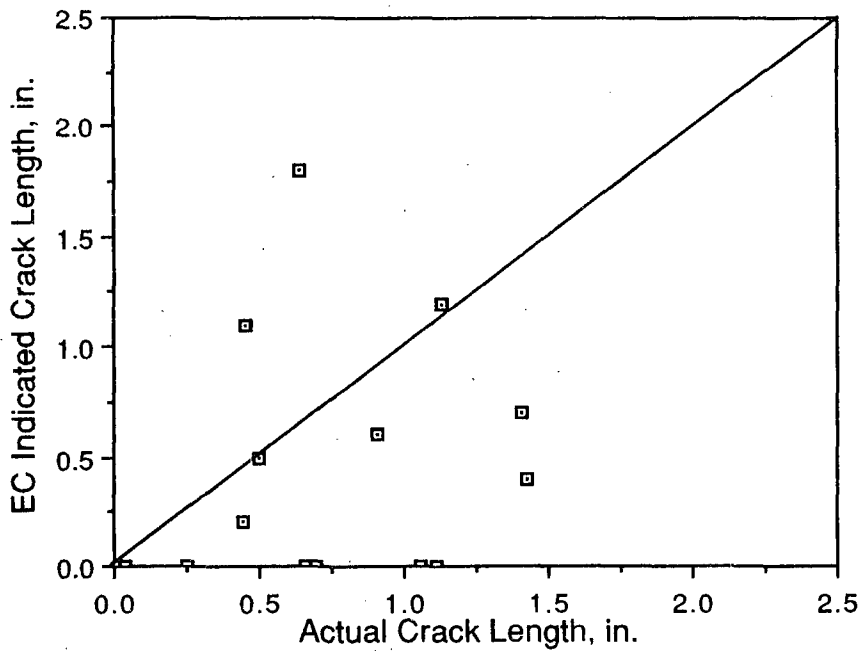
FIGURE 3.68. EC Indicated vs. Actual SCC Length for Team MO - Array Coil

cautioned that this round robin was obviously not designed to be a definitive study, but rather to indicate trends. Too few specimens were employed to permit firm conclusions about the capability of any given team to detect and size SCC, or allow team-to-team comparisons.

3.8 COOPERATIVE RESEARCH NOT FUNDED BY PROJECT

The service-degraded Surry steam generator, located in a research facility, presented a unique opportunity for testing and development of new technology for application in the field. While the SGGP did not have program goals related to the development of new technology, the Project made facilities available, on a cost-reimbursement basis, for research, development, and demonstration activities using the Surry generator. Such additional activities, subject to SGGP sponsor acceptance, were only undertaken if they did not interfere with the progress or goals of the SGGP. The results were communicated to the SGGP sponsors, although specific details concerning the nature of the new technology remained the property of the companies conducting the work. An advantage of using the Surry generator and the SGEF was an ability to conduct the work in a semi-realistic environment, including radiation exposure and service-degraded materials.

As mentioned previously, several SGGP subcontractors entered into cost sharing arrangements, allowing demonstration of their technology during use on the Surry generator to perform needed tasks. This included the two dilute chemical techniques demonstrated during the channel-head decontamination task, and the development of automated equipment for tube plug removals. Most non-Project developmental activities involved the demonstration of repair techniques or maintenance procedures which had been previously developed and tested in a laboratory environment.

The maintenance procedures demonstrated included techniques to internally sleeve damaged steam generator tubes, by brazing or welding an ID insert into the affected tube region. Replacement of damaged tubing below the first support plate was demonstrated. This involved internally cutting the tube above the damaged region and then removing the damaged tube section through the tube sheet by using normal tube-pulling techniques. The hole in the tube sheet was then cleaned out and the cut stub of the undamaged portion of tube was cleaned and a smooth end-finish machined. A matched section of new tubing was next welded in the generator onto the old tubing. This required maintaining an inert atmosphere in the generator. Final operations were expanding the new tube section into the tube sheet and welding the end of the tube to the tube sheet. Quality control consisted of NDE inspections using ultrasonics, along with visual inspection.

Another maintenance operation demonstrated was the replacement of corrosion damaged antivibration bars. This involved cutting the old bars, extracting them from the tube bundle, then replacing the AVBs with new ones designed to assist the replacement activity. The Surry demonstration helped to determine the forces necessary to remove partially corroded bars, and allowed evaluation of the effect of adjacent tubes of pulling the AVBs out. The demonstration also permitted testing and refinement of the AVB replacement procedure and an evaluation of the time and exposure required to perform this operation.

3.114

4.0 CONCLUSIONS

This section reviews the significant results and conclusions from all phases of the SGTIP. The conclusions presented here served as the bases for recommendations for improved inservice inspection procedures and methods for maintenance of steam generator tube integrity presented in Section 5.0.

4.1 TUBE INTEGRITY

Burst testing of steam generator tubes with artificial and service-induced degradation indicated that tube failure was governed by yielding of the undegraded ligament. The basis for this conclusion is the fact that the burst pressure of degraded steam generator tubes is, in most instances, conservatively predicted by the axial flaw tables given in Section XI, Subsection IWB-3640 of the ASME Code. This tables were derived from net section collapse theory and validated through tests on flawed stainless steel piping. Since it is generally accepted that stainless steel pipes fail by net section collapse, it seems reasonable to postulate that Inconel 600 steam generator tubes would behave similarly.

The burst test results also indicated that the most severe flaw types are axial cracks and uniform thinning. These flaws caused a larger decrease in burst strength compared to elliptical wastage of similar dimensions.

Because of the high mechanical strength, ductility, and inherent overdesign of steam generator tubing, long (> one tube diameter) axial flaws up to 80% through-wall did not rupture at pressures that would be experienced during a main-steam-line-break (MSLB) accident. Burst pressures several times the normal operating or main-steam-line-break pressure differential were measured for tubes with short axial artificial flaws (i.e., <0.25 in.). This result was validated by testing of tube segments with pitting/wastage type defects removed from the Surry generator. The Phase I empirical relationships predicted the burst strength of service-degraded tubes with pitting/wastage degradation to within ±10% of measured values. Even through-wall flaws of this length would not burst under MSLB loading conditions. The test results also showed that the tube burst strength did not decrease significantly with increasing axial flaw length for lengths greater than about one tube diameter. For flaw lengths greater than this level, the burst pressure was controlled by the flaw depth.

All of the collapse pressures for specimens with machined flaws were higher than would be experienced during a loss-of-coolant-accident, which is the worst credible collapse mode accident condition. EDM slots of any size had very little effect on the collapse pressure. For all heats and sizes of tubing with EDM slots up to 80% through-wall, the maximum decrease in collapse pressure was 23%. The lowest collapse pressure of any EDM slot specimen was 3.6 times higher than the most severe pressure attainable during a LOCA. For uniform-thinning and elliptical-wastage specimens, the collapse pressure decreased with increasing flaw length and depth. Even for tubes with 75% uniform thinning or elliptical wastage, the worst collapse pressure measured was still appreciably higher than the expected LOCA collapse pressure.

Empirical equations were developed from the Phase I and Phase II pressure test data by least squares regression techniques. The equations may be used to predict the percent reduction in the strength of flawed steam generator tubes of any geometry. Only the unflawed burst or collapse strength must be known. The equations relate flaw size and orientation to remaining tube strength and were validated by burst testing service-degraded tubes removed from the Surry generator. The ASME IWB-3640 axial flaw tables bound most of the SGTIP data and suggests that failure of steam generator tubes is governed by net section collapse of the undefected ligament. Application of all the IWB-3640 tables for axial and circumferential flaws to steam generator tubing would extend the range of loading conditions and flaw geometries that could be evaluated. For example, this would permit bending loading conditions to be evaluated.

The main conclusion of the evaluation of leak rate data is that leak rates measured from laboratory tests can be highly variable. These leak rates can be influenced by "random" variables that are not addressed in the predictive models. Measured leak rates are sometimes as much as a factor of ten less than predicted rates. This suggests that conservatism should be applied in calculations used to establish leak detection limits for detection systems.

It is concluded that the prediction of leak rates under ideal conditions of crack opening behavior is a relatively straightforward calculation. Differences in predictions from independently developed models were small compared with the variability in the test data. Continued efforts to refine the predictive models do not appear warranted, since it is likely that more refined models would still not adequately treat the factors that give rise to the variability in measured leak rates in test specimens. The recommended approach would be to recognize the uncertainties in predictions of leak rates, and to use conservative margins in the applications of calculated leak rates.

The available leak rate data should also be viewed in a positive perspective, since in most (but not all) tests the measured leak rates approached or even exceeded the predicted rates. This clearly shows the value of leak detection systems as a means to detect tube degradation prior to failure of tube by rupture. Operating histories of reactors include numerous cases of successful leak detection. The data base addressed in the present study included many tests of tubes at pressures corresponding to a MSLB accident. It is encouraging to note that none of this limited sample of tubes experienced what could be called a rupture, whereas in most cases the measured leak rates at normal operating pressures would have been detectable and exceeded plant technical specification limits.

Deep axial SCC were found in tubes removed from the Surry generator with calculated strains as low as 10%. This indicates a strain-based plugging criterion of 17% to 25% may be too high and that 10% is more appropriate.

4.2 NDE RELIABILITY

Laboratory measurements (under non-blind test conditions) of EC sizing capability of precision-machined flaws indicated that sizing accuracy and precision depended on the degradation volume. The depths of flaws such as EDM notches and elliptical wastage were overestimated when the depth of penetration was between 20% and 35%. On the other hand, EC underestimated the depth for these flaw types when the depth of penetration was more than 50%. In addition, the degree of undersizing increased with increasing flaw depth. The magnitude of the undersizing and scatter in the EC data increased as the volume of metal removed decreased. For degradation, such as uniform thinning, EC estimated depths were very precise, with a trend towards oversizing at all flaw depths. Estimates of length sizing capability for EDM slots and uniform-thinning flaws indicated that sizing accuracy was similar, but that sizing precision depended on the volume of metal removed. As with the depth sizing results, the length sizing precision was better for flaw morphologies in which more of the tube wall was removed.

The POD for machined flaws also depended on volume of metal removed. The POD increased with increasing volume of metal removed for flaws in the 20% to 35% depth range. EDM slots between 20% and 31% had a POD of 0.13, whereas for elliptical-wastage and uniform-thinning specimens the POD was 0.8 and 1.0, respectively. When the flaw depth was greater than 50%, the POD was 1.0 for all flaw types.

The single-frequency EC results for tubes with chemically-induced degradation were similar to the trends observed for specimens with machined degradation. As with the EC sizing capability studies conducted on precision-machined flaws, these tests were performed under non-blind laboratory conditions. Single-frequency EC measurements of laboratory SCC depth indicated that this type of degradation was, on the average, undersized. The mean error was found to be -1.3% of wall. Data scatter for this defect type was quite high, with a standard deviation of 17.1. (For additional conclusions regarding EC sizing reliability of SCC, see discussion below on SCC mini-round robin results.) Specimens with chemically-produced elliptical wastage also tended to be undersized in depth (-5.3% of wall mean error), but data scatter was much less than for the SCC-degraded tubes, with a standard deviation of only 3.8. Similar to the Phase I results, the tubes with chemically-produced uniform thinning were conservatively oversized, with a mean error of about 9%. The standard deviation for this flaw type was comparable to the elliptical-wastage specimens at about 4.0.

The single-frequency EC results discussed above should be considered only as a rough indicator of EC capability, since 1) the tests were conducted under non-blind laboratory conditions and 2) the test specimens all had idealized flaws and no complicating factors to simulate real-world conditions, such as copper deposits, denting, support plates, and antivibration bars. In addition, the tests were performed so that inspectors were aware of the type of degradation being examined. The Surry investigation provided a unique opportunity to gather NDE reliability information on tubes with service-induced degradation and extraneous effects under simulated field conditions using multifrequency EC equipment. Thus, the information developed more closely

represents the reliability of actual inservice EC inspections rather than a measure of the capability of the equipment to detect and size degradation in ideal situations. Significant findings from the numerous round robins performed on the Surry generator are summarized below.

Metallurgical and visual examination of specimens from all regions of the Surry 2A steam generator identified a variety of defect types at specific locations. Pitting and wastage were the predominant defects present. These defects were located in the sludge pile region above the TTS, within the crevice region between the tube and support plates, and, to a lesser extent, at antivibration bar contact areas. The severity of the pitting/wastage degradation was generally <20% through-wall except for specimens from the sludge pile region above the TTS where the wall-loss ranged up to 87%. Sufficient numbers of specimens with other types of degradation were not found, and thus the following conclusions regarding the reliability of EC inspections in detecting and sizing flaws relates primarily to pitting/wastage type degradation.

The probability of detecting service-induced flaws increased with increasing wall-loss and approached 0.9 for pitting/wastage degradation more than 40% through-wall. An automated data screening technique employed by one team that inspected the Surry generator appeared to improve the probability for detecting pitting/wastage degradation over conventional EC analysis methods.

Eddy-current estimates of the through-wall depth of service-induced pitting/wastage degradation showed wide variations between teams for the same flaw indication and also between specimens with similar wall losses. The team-to-team variations from a given specimen appeared to result from differences in analysis procedures and analyst interpretation. This team-to-team variance could not be significantly reduced by using consistent analysis procedures. The specimen-to-specimen variations appeared to be related to the complex flaw morphology which produces complex EC signals.

Conventional EC tended to underestimate the depth of service-induced pitting/wastage degradation. Sizing accuracy of this type of degradation decreased as the complexity of its morphology and through-wall depth increased. Improved sizing accuracy on service-induced degradation was obtained for one team that employed special frequency mixes to enhance the signal-to-noise ratio by suppression of signals due to denting, copper deposits, and support plates. Also, ultrasonic and rotating EC probes were successfully used to augment conventional EC/bobbin-coil data and provide an improved estimate of pitting/wastage depth.

Denting at tube support plate intersections in the Surry Generator interfered with the EC inspections and made flaw detection and sizing nearly impossible at these locations.

Copper-rich deposits found on the OD surfaces of tubes removed from the Surry Generator produced EC signals, which resulted in false calls being made in the U-bend and support-plate regions of the generator. Flaw-like EC signals were produced at regions where there was an interruption in the Cu-rich deposits.

To supplement the NDE validation data obtained from the SGGP and obtain a more realistic assessment of the reliability of NDE techniques to detect and size SCC in steam generator tubes under simulated service conditions, an additional mini-round robin was performed. The results from the mini-round robin using a limited number of tubes from the Phase II specimen inventory, with laboratory-produced SCC, indicated that the average POD by conventional multifrequency EC using bobbin-coil probes was only 0.5. Alternate inspection techniques using rotating pancake-coil, array-coil and segmented bobbin-coil probes also showed a low POD for SCC, with an average of 0.63. The reliability of both conventional bobbin-coil and alternate EC techniques to size laboratory-produced SCC length and depth was not very accurate or precise. The reader should be cautioned that this round robin was not designed to be a comprehensive study, but rather to indicate trends.

4.3 EVALUATION OF SAMPLING PLANS FOR ISI

The analytical evaluation of 100% inspection indicated that, on the average, most teams that inspected the steam generator would identify only about 65% of the defective tubes (defined as tubes with >75% through-wall degradation). In contrast, the best performing team could be expected to identify about 95% of the defective tubes.

The results of the analytical evaluation also demonstrated that if the clustering assumption holds, and if the POD for degraded but not defective tubes was at least 0.7, then the sequential sampling plan with 40% systematic sampling at the initial stage was nearly as effective as 100% inspection for detecting and plugging defective tubes. This was true for any PEL value. However, the 20% systematic sampling at the initial stage was significantly inferior to both 100% inspection and the 40% systematic sampling plan.

The results of the Monte Carlo simulation analysis supported the conclusions reached from the analytical evaluation and provided some valuable additional insights. When the isolated clustering assumption discussed in Section 3.6.4 was approximately valid, the 40% sequential scheme tended to be nearly as effective as 100% inspection, but required substantially less inspection. However, when the defective tubes were in one large cluster with degraded tubes, all three sampling plans were equally effective for detecting and plugging defective tubes.

Improving the sizing capability to that demonstrated by Team V resulted in improved effectiveness of all three inspection plans. Also, with the improved sizing capability, increasing the EC plugging limit from 40% to 50% had little impact on the effectiveness of each sampling plan for plugging defective tubes, but it minimized the probability for plugging nondefective tubes. Whereas, if the "Average U.S. Team" sizing capability was assumed, increasing the plugging limit from 40% to 50% significantly decreased the effectiveness of all sampling plans for plugging defective tubes.

Improving the POD enhances the effectiveness of all inspection plans, and the best performance was achieved when the better POD curve and the better sizing model were assumed. For the POD curves considered, flaws with true

sizes less than 20% through-wall did not significantly improve the effectiveness of the sampling plans because these flaws had a very low POD.

4.4 STEAM GENERATOR PREPARATORY TASKS AND INITIAL INSPECTIONS

Secondary-side examinations conducted on the Surry Generator were useful for qualitatively identifying conditions that could lead to loss of steam generator integrity. These examinations did not provide quantitative tube degradation information usable for assessing remaining tube integrity.

Dilute chemical decontamination such as by the LOMI or CAN-DECON techniques (modified for PWRs) provided decontamination factors up to ten in the channel-head region on the Surry Generator. No significant corrosion effects were observed from these decontamination processes. In addition, the volume of liquid waste could be minimized through the use of ion exchange resins.

Radiation monitoring of channel-head workers during the tube unplugging task indicated that exposure to the eyes was the limiting exposure. Thus, badging of the forehead and chest was determined to be the most effective for ensuring adequate personnel dosimetry.

5.0 RECOMMENDATIONS FOR IMPROVED ISI AND TUBE PLUGGING LIMITS

This section presents recommendations for improved ISI and tube plugging limits based on the research results of the SGTIP/SGGP.

5.1 RECOMMENDATIONS FOR IMPROVED ISI

5.1.1 Full-Length Tube Inspection

It is recommended that tubes should be inspected full length, from tube end to tube end. This recommendation is based on observation of significant degradation on the cold-leg portion of Surry tubes and occurrences of tube rupture events in this region of the generator.

5.1.2 Screening of Data Prior to Analysis

All data should be screened prior to analysis. An automated data screening system may be used, but it should be established via performance demonstrations that it is capable of detecting all flaws including small-volume degradation such as IGA, SCC, and fatigue cracking. The basis for this recommendation is in the superior POD performance of one of the teams that inspected the Surry Generator. By employing an automated data screening system to filter the vast number of EC signals, this team had the highest overall POD performance.

5.1.3 Independent Data Analysis

As an additional aid towards improved flaw detection and characterization, it is recommended that an independent review of the EC inspection data be performed. Although independent reviews of the data were not done during the inspections of the Surry 2A Steam Generator, there were several instances in which a review of the data could have helped avoid missed flaws. There were several instances noted during the validation in which one team missed a flaw that other teams detected. In addition, the team-to-team variation in flaw sizing was substantial for specimens with similar wall losses. It is recommended that accord be reached between the principal and independent analyst regarding the nature and categorization of the eddy-current data. If accord cannot be reached, then conservative practice would be to reinspect the tube with supplemental inspection methods or plug/repair the tube.

5.1.4 Sampling Plan

Based on a statistical evaluation and Monte Carlo studies of different flaw distributions and different inspection plans and using the Surry round-robin results, the recommended minimum sampling scheme should be a systematic sequential sample with 40% sampling at the first stage. During each inservice inspection, a sample of tubes should be selected according to a 40% systematic sampling grid. An example of a 40% systematic sampling grid pattern is illustrated in Figures 5.1 to 5.3, where sampled tubes are denoted by X. Each tube in the inspection sample plan should be inspected over its full length from tube end to tube end. For each tube in the sample with an

```
 ABCDEFGHIJKLMNOPQRSTUVWXY

 1 XX000XX000XX000XX000XX000
 2 00XX000XX000XX000XX000XX0
 3 X000XX000XX000XX000XX000X
 4 0XX000XX000XX000XX000XX00
 5 000XX000XX000XX000XX000XX
 6 XX000XX000XX000XX000XX000
 7 00XX000XX000XX000XX000XX0
 8 X000XX000XX000XX000XX000X
 9 0XX000XX000XX000XX000XX00
10 000XX000XX000XX000XX000XX
```

FIGURE 5.1.   40% Systematic Sampling
              Grid Pattern for First
              Inservice Inspection

```
 ABCDEFGHIJKLMNOPQRSTUVWXY

 1 00XX000XX000XX000XX000XX0
 2 X000XX000XX000XX000XX000X
 3 0XX000XX000XX000XX000XX00
 4 000XX000XX000XX000XX000XX
 5 XX000XX000XX000XX000XX000
 6 00XX000XX000XX000XX000XX0
 7 X000XX000XX000XX000XX000X
 8 0XX000XX000XX000XX000XX00
 9 000XX000XX000XX000XX000XX
10 XX000XX000XX000XX000XX000
```

FIGURE 5.2.   40% Systematic Sampling
              Grid Pattern for Second
              Inservice Inspection

```
 ABCDEFGHIJKLMNOPQRSTUVWXY

 1 X000XX000XX000XX000XX000X
 2 0XX000XX000XX000XX000XX00
 3 000XX000XX000XX000XX000XX
 4 XX000XX000XX000XX000XX000
 5 00XX000XX000XX000XX000XX0
 6 X000XX000XX000XX000XX000X
 7 0XX000XX000XX000XX000XX00
 8 000XX000XX000XX000XX000XX
 9 XX000XX000XX000XX000XX000
10 00XX000XX000XX000XX000XX0
```

FIGURE 5.3.   40% Systematic Sampling
              Grid Pattern for Third
              Inservice Inspection

eddy-current indication due to degradation (of any size), further inspection should be performed by testing tubes immediately surrounding the tube with the eddy-current degradation indication. This additional inspection should continue until two-tube-wide "buffer zone" is observed, which is composed of tubes with no eddy-current degradation indications and which completely surrounds the tube(s) with eddy-current degradation indications. In implementing this sampling scheme, the initial systematic sampling grid should be "shifted" at each inservice inspection so that every tube in a generator will be inspected at least once during the course of three consecutive inservice inspections and at least twice during the course of five inservice inspections. In addition, since inspection results from one steam generator are not always reliable indicators of the condition of other steam generators in the plant, it is also recommended that every steam generator be inspected at each inservice inspection.

5.1.5 Application of Frequency Mixes for Noise and Foreign Deposit Suppression

Analysis of the Surry round-robin data indicated that special frequency mixes designed to suppress the effects of internal support structure, denting, and copper deposits was successfully used by one team. This team exhibited the highest POD and flaw sizing accuracy of all the teams inspecting the Surry Generator. The use of frequency mixes specially developed for the Surry Generator improved the signal-to-noise ratio over that attainable with conventional inspection procedures, and provided enhanced flaw detection and sizing capability. The teams participating in the Base-line and DAARR round robins used multifrequency eddy-current inspection equipment, but during data evaluation only a single frequency (400 kHz) tended to be used (Doctor et al. 1986b). Thus, much of the capability of multifrequency inspection was not utilized in evaluating the inspection results.

5.1.6 Development of Performance Demonstrations for Personnel, Equipment and Procedures

The foregoing research results indicate that existing requirements for qualifying personnel, equipment and procedures for eddy-current inspection of nuclear steam generators may not be adequate to ensure reliable inspection performance. In order to obtain effective inservice inspection, an NDE system qualification covering the personnel, equipment and inspection procedure is recommended. In this context, personnel qualification consists of training, qualification and certification. The inspection personnel, equipment and the inspection procedure should be qualified in combination through performance demonstrations. One possible performance demonstration program might consist of two components: a generic qualification, and a plant-specific qualification. A generic performance demonstration is needed to ensure that inservice inspections are effective at detecting any type of degradation that may occur in any steam generator. On the other hand, because different plants often exhibit different degradation mechanisms and conditions, it is important that inspection personnel should also be qualified to perform inspections on that particular plant.

5.1.7 Improved Techniques for Crack Detection

Results from the SCC mini-round robin suggest that crack detection and sizing may be a significant problem. These types of flaws had the lowest POD and among the worst sizing accuracy for any of the types of degradation investigated. It was also concluded that along with uniform-thinning degradation, this class of defects caused the largest decrease in tube burst strength. Further, as noted from the survey of laboratory data summarized in Appendix A, crack-type flaws can grow at very high rates, potentially from initiation to leakage in less than one operating cycle. In consideration of these concerns, it is recommended that if cracking degradation is known or suspected, then NDE techniques optimized for crack detection be employed.

5.2 RECOMMENDATIONS FOR IMPROVED TUBE PLUGGING LIMITS

5.2.1 Through-Wall Flaws

It is recommended when the plant is shut down that all tubes with through-wall flaws discovered during operation, or found during inservice inspection, should be plugged or repaired. This recommendation stems from the evaluation of the publicly available leak-rate data. This evaluation showed that through-wall flaws, in some cases, leaked significantly less than predicted from model calculations. The lower than expected leakage may have been caused by the complex interaction of "random" variables such as 1) residual stresses which hold the crack closed, 2) crack roughness leading to increased fluid flow resistance, or 3) crack plugging by impurity or corrosion product build-up on fracture faces. Any or all of these effects could have influenced the measured leakage and might also be operative for inservice cracks. Given the unpredictability of leak rates from cracks in steam generator tubes, the conservative approach to management of known through-wall flaws would be to plug or repair the tube.

5.2.2 Disposition of Crack-Type Flaw Indications

Based on the above discussion and a cursory literature search to document flaw growth rates (see Appendix A), it is recommended that all tubes with indications of cracking should be plugged or repaired. It is recognized that under some conditions the return to service of a cracked tube may be justified. For example, there are many examples of tube cracking within the tubesheet where the tube is restrained by frictional forces caused by tube expansion. Thus, if compelling engineering evidence can be developed to demonstrate that reliable NDE techniques and procedures are available for crack detection and sizing, and that reliable and conservative data on expected crack growth until the next inspection is also available, then it is recommended that case-by-case exceptions to plugging of all tubes with crack-type indications be considered.

5.2.3 Flaw Characterization and Consideration of Inspection Uncertainties

Based on the pressure test results and a review of the flaw growth rate literature, it is evident that degradation type can significantly affect proper flaw evaluation. In other words, flaw type (i.e., cracks, pits, wastage,

5.4

erosion-corrosion, etc.), geometry and orientation were found to be the most important variables in determining the burst or collapse pressure of a degraded tube. In addition, flaw growth rates depend largely on the type of flaw under consideration. In order to perform the most accurate flaw evaluation possible, it is desirable to obtain specific knowledge of the type of degradation afflicting a particular tube. Thus, it is recommended that other types of information such as tube pulls and secondary-side inspections be used to supplement conventional eddy-current inspection results to permit improved characterization of tube degradation. The locations of indications relative to support plates, tube sheets, and U-bends can also provide useful information for establishing the likely modes of degradation. Past service histories for the particular steam generator and for other generators of similar design and operating conditions may also be useful for establishing the degradation type.

The NDE flaw-sizing error is also an important consideration in determining an appropriate tube plugging limit. An accurate estimate of the degradation size in terms of depth, length, orientation and proximity to other degraded regions is needed in order to arrive at a realistic estimate of remaining tube integrity. It is recommended that the degraded region should be characterized by bounding dimensions so that it can be described by parameters of depth, orientation, and a length dimension as measured along the axial and circumferential directions of the tube.

A considerable body of EC sizing error data was developed during the SGTIP on typical steam generator tubes with both natural and artificial flaws. This extensive information base indicates that the EC sizing error depends strongly on the type of degradation, the inspection equipment and procedure, and the presence of extraneous conditions such as surface deposits. Even though the SGTIP data provides useful estimates of the EC sizing error in the absence of more definitive information, it is recommended that specific allowances for flaw sizing uncertainty be developed from NDE performance demonstrations (see discussion in 5.1.6 above). Such performance demonstrations should be based on a statistically significant number of samples for the relevant type of degradation and NDE method employed. Since the SGTIP pressure test results show that relatively deep but short degraded regions have little effect on burst pressures, reductions in uncertainties in length measurements should be given equal priority to improved accuracy of depth measurements.

5.2.4 Methods for Flaw Evaluation

An extensive amount of information on the effect of flaw type and severity on remaining tube integrity was developed during the SGTIP. Empirical equations were developed relating the extent of degradation to remaining tube integrity. It is recommended that evaluations of the effect of degradation on tube integrity should be based on the empirical equations of burst tests of tubes with artificial and/or service-induced degradation. Since the empirical data on tube failure are limited to pressure loadings, the effects of bending loads need to be addressed by predictive models. If ductile fracture is assumed, then the net section collapse of the remaining cross section of the tube as presented in Section XI, Subsection IWB-3640, of

the ASME Code, 1986 Edition, is recommended as a suitable model for evaluating these conditions. The bounding trends of tube burst tests are summarized in Figure 5.4 for degradation geometries and loads such that the circumferential stress governs predictions of tube integrity. This figure is an example of the data recommended for predicting the integrity of degraded tubes. The curves indicate percentage reductions in allowable pressure as a function of both degradation depth and length. Figure 5.5 gives curves that are recommended for evaluating circumferentially-oriented degradation for which the critical stress is in the axial direction. These curves are purely for pressure loading. Limited tube burst tests served to confirm the trends of these curves. The technical basis for generating these curves was the IWB-3640 tables for net section collapse of the remaining wall cross section of the degraded tube. Extension of these results to account for bending loads could be made using the net section collapse methodology.
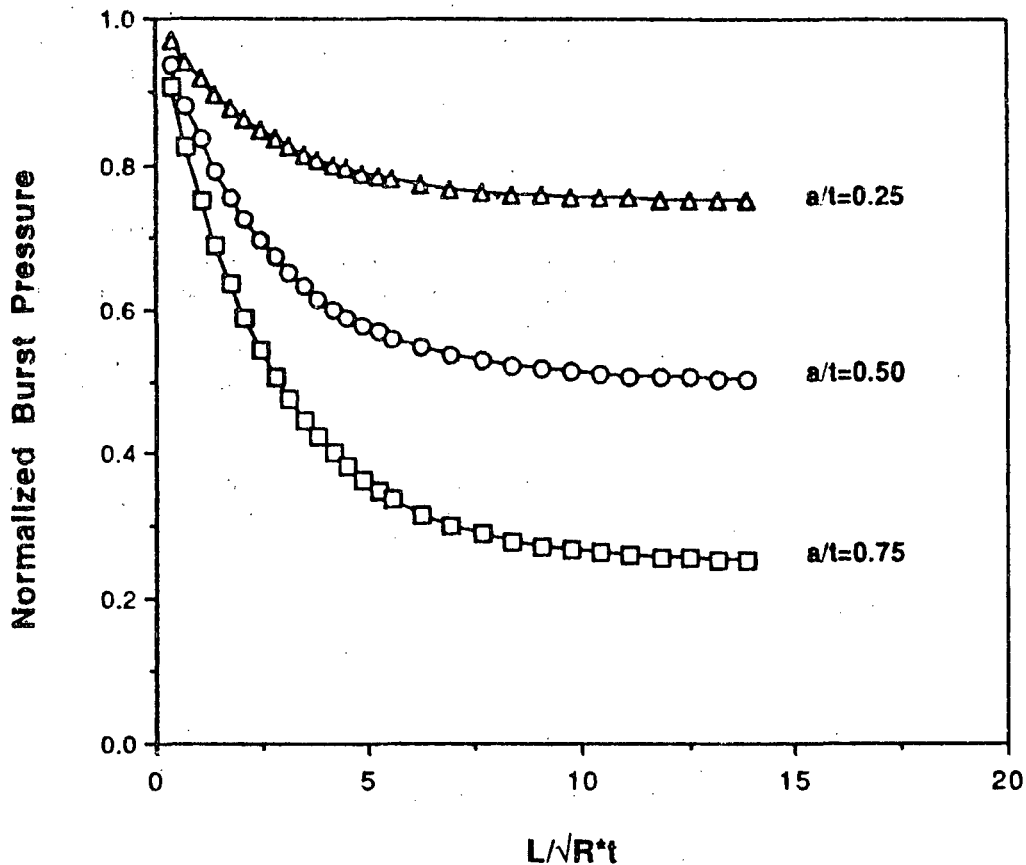
FIGURE 5.4. Burst Parameter Prediction Curves for Axially Oriented EDM Notches in Steam Generator Tubes. L = Degradation Length, a = Degradation Depth, R = Tube Inner Radius, and t = Tube Wall Thickness
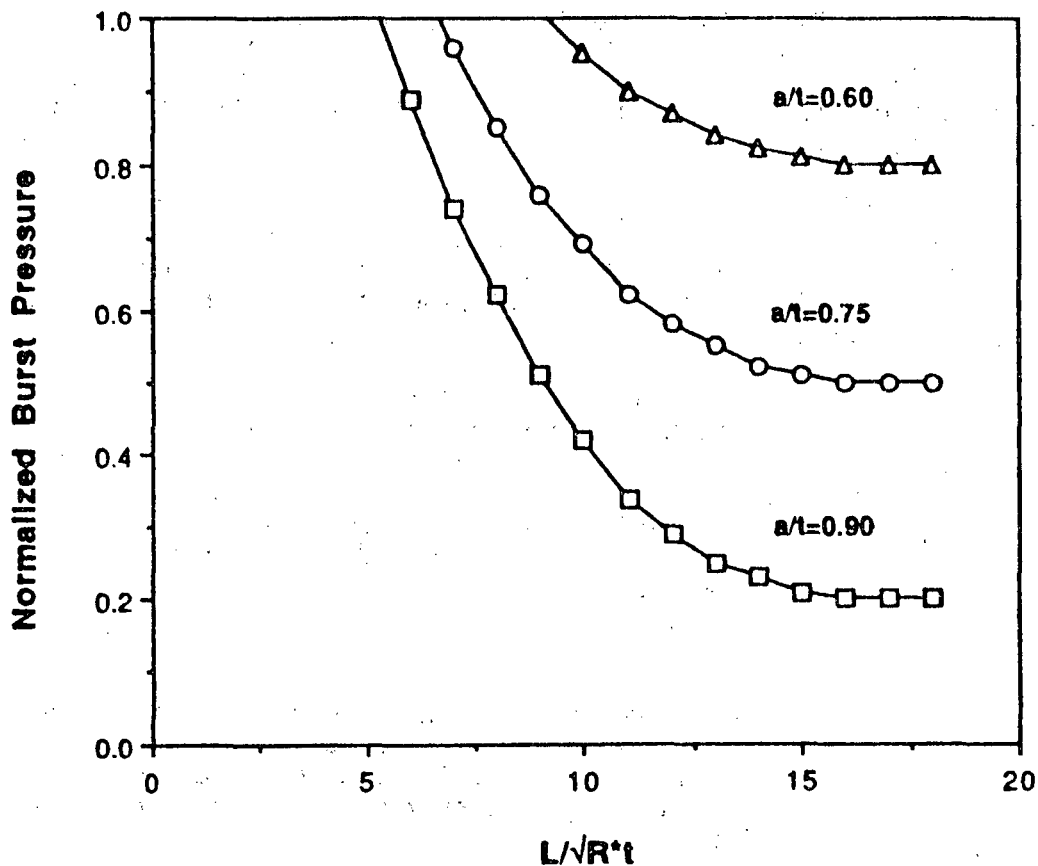
FIGURE 5.5. Burst Parameter Prediction Curves for Circumferentially
Oriented Cracks (based on IWB-3640). L = Degradation
Length, a = Degradation Depth, R = Tube Inner Radius,
and t = Tube Wall Thickness

5.2.5 Repair Versus Plugging

As an alternative to plugging of defective tubes, it is recommended that
repair be considered a viable option for maintaining steam generator
integrity. The repair should meet the same performance requirements (i.e.,
ASME Code) as the original tube, including structural integrity and leak
tightness. The repaired tube should be inspectable both for the repaired
area and for continued inspection of the unrepaired length of the tube.
Activities in the QC/QA area should assure that all defective tubes have
actually been repaired. Accurate documentation through photographs, video
tapes, or other methods should be utilized.

5.2.6 Plugging Limit for Allowable Denting

Operating experience with steam generators at a number of plants has
resulted in severe build-up of corrosion products in the tube-to-tube
support-plate crevice region, resulting in denting of the tube. While this

reduction in tube diameter does not by itself constitute a problem to tube integrity, it has resulted in initiation and growth of stress corrosion cracks that may lead to leakage and rupture. In addition, the reduction in tube diameter could prevent the passage of appropriately-sized NDE probes, making inservice inspections unreliable or impossible.

It is recommended that plugging limits for dented tubes be based on either reduction in tube diameter or on peak strain at the dented location of the tube. Peak strains can be calculated from measurements of the profile of the dented tube as demonstrated during the PROFILE-360 examination of selected tubes from the Surry Generator.

Based on the work, an appropriate strain limit for plugging of dented tubes would be 10%. It is recognized that the susceptibility of tubes to SCC is governed by factors such as strain rate, material microstructure, and plant water chemistry. Thus, strain-based plugging limits lower than 10% may be needed for particular plants. Development of an alternate plugging limit should seek to preclude crack initiation and limit denting severity such that effective tube inspection is possible.

5.2.7 Flaw Growth Allowance

One of the considerations in determining tube plugging limits is an allowance for degradation growth until the next scheduled inservice inspection. The rationale for including this allowance is to 1) ensure that no degradation grows through-wall, and 2) that all degradation remains at an acceptable size consistent with required safety margins.

Based on the cursory literature review given in Appendix A, it is evident that predictions of degradation growth are subject to considerable uncertainty, and, therefore, it is not possible to recommend precise methods or supporting data for this purpose. A practical method for determining this allowance that would be relevant to specific plants is the application of historical service experience and results from inservice inspections. In addition, observed growth rates for plants with similar operating histories should be considered. Since the laboratory data indicates there are vast differences in growth rates for different degradation mechanisms, the growth for the specific mechanism should be determined. If knowledge of the degradation mechanism is lacking, then growth rates for the most rapidly propagating degradation mechanism should be applied.

Growth allowances based on observed plant-specific rates should be subject to conservative assumptions about future service conditions and to confirmation of degradation extent during scheduled inspections. Growth rates less than projections based on the prior observed rates should be used only if substantial reductions in the severity of the operating environment can be assured. If methods other than linear projections of observed growth rates are used, then predictions of these other methods should be checked for consistency with the observed rates of growth.

6.0 REFERENCES

Aitkin, M. 1981. "A Note on the Regression Analysis of Censored Data." Technometrics 23(2):161-163.

Allen, R. P., R. L. Clark, and W. D. Reece. 1984. Steam Generator Group Project Task 6 - Channel Head Decontamination. NUREG/CR-3841, PNL-4712, Pacific Northwest Laboratory, Richland, Washington.

Alzheimer, J. M., R. A. Clark, C. J. Morris, and M. Vagins. 1979. Steam Generator Tube Integrity Program - Phase I Report. NUREG/CR-0718, PNL-2937, Pacific Northwest Laboratory, Richland, Washington.

American Society of Mechanical Engineer's Boiler and Pressure Vessel Code. Section XI Rules for In-Service Inspection of Nuclear Power Plant Components. 1986 Edition. ASME, New York, New York.

Angwin, M. J. et al. 1985. Steam Generator Reference Book. Electric Power Research Institute, Palo Alto, California.

Aspden, R. G. 1986. "Background Reporting and IGA Screening in Static Test Devices." In Proceedings: 1984 Workshop on Secondary Side Stress Corrosion Cracking and Intergranular Corrosion of PWR Steam Generator Tubing. EPRI NP-4478, Electric Power Research Institute, Palo Alto, California.

Bandy, R. and D. Van Rooyan. 1984. "Stress Corrosion Cracking of Inconel Alloy 600 in High Temperature Water - An Update." Corrosion 40(8):425-430.

Baum, A. J., C. Dangelo, P. J. Kuchirka, N. Singleton, and M. J. Sredzienski. 1987. Steam Generator Cold Leg Thinning in Operating Plants. EPRI NP-5140, Electric Power Research Institute, Palo Alto, California.

Berge, J. P. 1986. "Questions on U-Bend Cracking." In Proceedings: 1984 Workshop on Secondary Side Stress Corrosion Cracking and Intergranular Corrosion of PWR Steam Generator Tubing, EPRI NP-4478, Electric Power Research Institute, Palo Alto, California.

Berge, J. P. 1987. "Overview of Primary Side Stress Corrosion Cracking SG Tubes of Electricite de France." In Proceedings: 1985 Workshop on Primary-Side Corrosion Cracking of PWR Steam Generator Tubing, EPRI NP-5158, Electric Power Research Institute, Palo Alto, California.

Bickford, R. L., R. A. Clark, P. G. Doctor, H. E. Kjarmo, and C. A. LoPresti. 1984. Eddy-Current Round Robin Test on Laboratory Produced Intergranular Stress Corrosion Cracked Inconel Steam Generator Tubes. NUREG/CR-3561, PNL-4695, Pacific Northwest Laboratory, Richland, Washington.

Bowen, W. M., P. G. Heasler, and R. B. White. 1989. Evaluation of Sampling Plans for In-Service Inspection of Steam Generator Tubes: Part I. NUREG/CR-5161, PNL-6462, Pacific Northwest Laboratory, Richland, Washington.

Bradley, E. R., P. G. Doctor, R. H. Ferris, and J. A. Buchanan. 1988. Steam Generator Group Project Task 13 Final Report - NDE Validation. NUREG/CR-5185, PNL-6399, Pacific Northwest Laboratory, Richland, Washington.

Brown, S. D. 1985. PWR Steam Generator Tubing Inspection Guidelines. Electric Power Research Institute, Palo Alto, California.

Clark, R. A. and M. Lewis. 1984. Steam Generator Group Project Annual Report - 1982. NUREG/CR-3581, PNL-4693, Pacific Northwest Laboratory, Richland, Washington.

Clark, R. A. and M. Lewis. 1985. Steam Generator Group Project Annual Report - 1984. NUREG/CR-4362, PNL-5417, Pacific Northwest Laboratory, Richland, Washington.

Davis, C. S., J. M. Thomas, S. W. Winder, and D. E. Allison. 1983. An Engineering and Probabilistic Analysis of Tube Cracking Performance in Once-Through Steam Generators. EPRI NP-3065, Electric Power Research Institute, Palo Alto, California.

DeRosa, P., W. Rinne, H. W. Massie, and P. Mitchell. 1973. Evaluation of Steam Generator Tube, Tube Sheet and Divider Plate Under Combined LOCA Plus SSE Conditions. WCAP-7832, Westinghouse Electric Corp., Pittsburgh, Pennsylvania.

Doctor, P. G., J. M. McIntyre, P.K. Alley, L. R. DesCamp, J. S. Littlefield, C. A. LoPresti, and J. A. Buchanan. 1983. The In-Service History of The Surry Unit 2A Steam Generator. PNL-4880, Pacific Northwest Laboratory, Richland, Washington.

Doctor, P. G., A. S. Birks, R. H. Ferris, H. Harty, and G. E. Spanner. 1988a. Steam Generator Group Project Task 7 Final Report - Post Service Baseline Eddy-Current Examination. NUREG/CR-5087, PNL-5940, Pacific Northwest Laboratory, Richland, Washington.

Doctor, P. G., H. Harty, R. H. Ferris, and A. S. Birks. 1989. Steam Generator Group Project Task 9 Final Report - Nondestructive Evaluation Round, Vol. 1: Description and Summary Data. NUREG/CR-4849, PNL-5868, Pacific Northwest Laboratory, Richland, Washington.

Hall, J. F. 1984. "Pitting in the Laboratory at Combustion Engineering." In Workshop Proceedings: Pitting in Steam Generator Tubing. EPRI NP-3574-SR, Electric Power Research Institute, Palo Alto, California.

Hall, J. F., R. S. Frisk, K. E. Marugy, and A. S. O'Neill. 1987. Investigation of Causes and Corrective Actions for Pitting in Steam Generator Tubes: Prototypic Tests. EPRI NP-5248, Electric Power Research Institute, Palo Alto, California.

Hermer, R. E. and C. R. Wolfe. 1986. "Alloy 600 Intergranular Corrosion in Alkaline Environments." In Proceedings: 1984 Workshop on Secondary Side Stress Corrosion Cracking and Intergranular Corrosion of PWR Steam Generator Tubing. EPRI NP-4478, Electric Power Research Institute, Palo Alto, California.

Jacko, R. J. 1986. "IGSCC and IGA Behavior of Inconel 600." In Proceedings: 1984 Workshop on Secondary Side Stress Corrosion Cracking and Intergranular Corrosion of PWR Steam Generator Tubing. EPRI NP-4478, Electric Power Research Institute, Palo Alto, California.

Kurtz, R. J., R. L. Bickford, R. A. Clark, C. J. Morris, F. A. Simonen and K. R. Wheeler. 1988. Steam Generator Tube Integrity Program - Phase II Final Report. NUREG/CR-2336, PNL-4008, Pacific Northwest Laboratory, Richland, Washington.

Kurtz, R. J., M. Lewis and R. A. Clark. 1987. Steam Generator Group Project Annual Report - 1985. NUREG/CR-4848, PNL-5771, Pacific Northwest Laboratory, Richland, Washington.

Miglin, B. P. 1987. Production of Eddy-Current Standards for Caustic Intergranular Corrosion. EPRI NP-5109, Electric Power Research Institute, Palo Alto, California.

Newman, J. R., P. McIntyre, and S. M. Payne. 1987. "Effect of Thermal Treatment and Impurity Segregation on the Kinetics of IGA in Inconel 600." Presented at EPRI Workshop on IGA and SCC Mechanisms, Electric Power Research Institute, Palo Alto, California.

Partridge, M. J. 1987. "Effect of Temperature and Caustic on IGA and IGSCC Corrosion Rates." Presented at EPRI Workshop on IGA and SCC Mechanisms, Electric Power Research Institute, Palo Alto, California.

Pathania, R. S. and P. V. Balakrishnan. 1986. Correlation of Tube Support Structure Studies. EPRI NP-4672, Electric Power Research Institute, Palo Alto, California.

Powell, D. E. and J. F. Hall. 1987. "Experimental Measurements of Leak Rates and Burst Pressures for Cracked Alloy 600 Tubes Under Steam Generator Conditions." In Proceedings: 1985 Workshop on Primary-Side Corrosion Cracking of PWR Steam Generator Tubing, EPRI NR-5158, Electric Power Research Institute, Palo alto, California.

Reece, W. D. and R. Harty. 1983. Dosimeter Placement and Interpretation for Determination of Dose to the Extremities and the Head. PNL-4967, Pacific Northwest Laboratory, Richland, Washington.

Sawsochka, S. G., K. D. Friedman, S. S. Choi, and J. K. Pyo. 1986. Correlation of Tube Support Corrosion Studies. EPRI NP-4818, Electric Power Research Institute, Palo Alto, California.

Schwenk, E. B. and K. R. Wheeler. 1984. Steam Generator Group Project Task 10 - Secondary Side Examination. NUREG/CR-3843, PNL-5033, Pacific Northwest Laboratory, Richland, Washington.

Schwenk, E. B. 1987. Steam Generator Group Project Task 10 - Secondary Side Examination. NUREG/CR-4850, PNL-6045, Pacific Northwest Laboratory, Richland, Washington.

Simonen, F. A. et al. 1986. Reactor Pressure Vessel Failure Probability Following Through-Wall Cracks Due to Pressurized Thermal Shock Events, NUREG/CR-4483, Pacific Northwest Laboratory, Richland, Washington.

Sinclair, R. B. 1984. Secondary Side Photographic Techniques Used in Characterization of Surry Steam Generator. NUREG/CR-3094, PNL-5053, Pacific Northwest Laboratory, Richland, Washington.

Theus, G. J. 1981. "Stress Corrosion Cracking Tests of Alloy 600." In Workshop Proceedings: U-Bend Tube Cracking in Steam Generators, EPRI WS-80-136, Electric Power Research Institute, Palo Alto, California.

Wheeler, K. R. 1984. Initial Inspection of the Service Degraded Surry 2A Steam Generator, June 1982. PNL-5268, Pacific Northwest Laboratory, Richland, Washington.

Wheeler, K. R., P. G. Doctor, L. K. Fetrow, and M. Lewis. 1984. Steam Generator Group Project Task 8 - Selective Tube Unplugging. NUREG/CR-3842, PNL-4876, Pacific Northwest Laboratory, Richland, Washington.

APPENDIX A

COMPENDIUM OF DEFECT GROWTH RATES

APPENDIX A

COMPENDIUM OF DEFECT GROWTH RATES

1.0 INTRODUCTION

The information in this appendix summarizes much of the currently available data on the growth rate of the common defects found in steam generator tubing. This information was compiled to assist the determination of appropriate degradation allowances for evaluation of degraded steam generator tubing. Most of the data was obtained from recently published research reports and for the most part represents the results of laboratory investigations conducted under severe test conditions (e.g., high applied stresses and aggressive environments). In some cases, field data was available for comparison with the laboratory produced data.

2.0 THINNING (WASTAGE)

Very little data on the growth rate of wastage is available. With no plants in the U.S. presently using phosphate secondary water chemistry, this problem is not a major concern. Most recent occurrences of wastage have been observed at the periphery of the first or second tube support plate on the cold leg side of the generator. Limited data on the progression of cold leg thinning was reported by Baum et al. (1987). These data were obtained by monitoring the change in the eddy-current measurements on a given tube during successive inspections and dividing by the elapsed time. Corrosion rates were based on data from tubes with indications having reported depths 20% or greater in two successive inspections. The calculations were based on a total of 489 tubes in 18 steam generators. An overall degradation rate of 3 mils/y was estimated from these data.

Other published data (Angwin et al. 1985) plotted in Figures A.1 and A.2 show that the corrosion rate depends upon the Na/PO_4 molar ratio and temperature, but maximum corrosion rates never exceeded about 5.5 mils/y.

Estimates were also obtained from evaluation of Surry metallographic data presented by Bradley et al. (1988). Maximum wall penetration of pure wastage was measured on tubes removed from both the hot and cold leg sides of the Surry generator. Table A.1 gives the minimum, average, and maximum percent wall-loss measured.

The data in Table A.1 can be used to estimate growth rates by dividing by the duration the defect mechanism is operative. The Surry generator was in service for slightly less than six years, from March 1973 to January 1979.

FIGURE A.1. Average Corrosion Penetrations of Alloy 600 in Deaerated Sodium Phosphate Solutions at 615°F as a Function of the Na/PO₄ Molar Ratio (Angwin et al. 1985).

Table A.1. Maximum Percent Wall-Loss for Wastage Degraded Surry Tubes

Leg	Min	Ave	Max
CL**	4	11	24
HL	12	30	52
HL*	12	22	32
HL**	20	35	52

*Tubes never plugged during service
**Tubes plugged during service

FIGURE A.2. Temperature Dependence of the Corrosion Rate of Alloy 600 Tubing Exposed to Deaerated Phosphate Solutions (Angwin et al. 1985).

Secondary water chemistry was changed from phosphate to AVT after approximately two years of operation. Table A.2 gives the number of tubes plugged for wastage degradation from 1974 through 1977 (no tubes were plugged for wastage after 1977).

Table A.2. Number of Tubes Plugged for Wastage Degradation

Year	No. of Tubes
1974	14
1975	34
1976	19
1977	7

A.3

The data in Table A.2 suggests that time-to-initiation for phosphate wastage was very short and growth was not immediately arrested after conversion to AVT. As a first approximation, wastage growth rates were estimated by dividing the numbers in Table A.1 by four years. Performing this calculation yields the growth rates presented in Table A.3.

As expected, cold leg wastage grows more slowly than hot leg wastage. Removal of tubes from service by plugging did not reduce the growth rate below the rate observed in never-plugged tubes (limited data, however). Further, the results correlate well with the other published data.

Table A.3. Estimated Growth Rates for Surry Generator
Wastage Degradation (mils/yr)

Leg	Min	Ave	Max
CL**	.5	1.3	3
HL	1.5	3.8	6.5
HL*	1.5	2.8	4
HL**	2.5	4.4	6.5

*Tubes never plugged during service
**Tubes plugged during service

3.0 PITTING

Limited laboratory data has been developed by Combustion Engineering under a variety of conditions (Hall 1984). Figure A.3 gives a plot of pit depth versus exposure time for various test conditions. Table A.4 lists pit growth rates in mils/yr calculated from the data in Figure A.3. The average pit growth rate for all conditions was about 7.7 mils/yr.

Table A.5 shows maximum wall-loss measured from pitted (no wastage) and pitted/wastage degraded tubes from the Surry generator.

Since the in-service inspection and tube plugging history for the Surry generator did not identify tubes degraded by pitting, it was difficult to determine the pit growth rate. NDE detection of pitting is masked by copper deposits, so determination of pit growth from field NDE data is not reliable. One possible assumption might be one year for pit initiation followed by five years of growth. This assumption yields the results shown in Table A.6. These results compare reasonably well with the laboratory results given above. On the other hand, much of the recent laboratory data suggests that pit growth rates are highly nonlinear. Model boiler test results reported by Hall, et al. (1987), indicated that pit growth rates were initially rapid but were followed by stifling of further growth due to the formation of corrosion products that covered the outer surface of the pit.

A.4

FIGURE A.3. Pit Depth Versus Exposure Time in Alloy 600 Tubes in Model and Pot Boiler Tests (Hall 1984)

38712-170.4M

Table A.4. Laboratory Pit Growth Rates (mils/yr)

Environ.	Min	Ave	Max
Fresh	1.5	8.0	25.3
Sea	2.4	8.9	26.1
CP	1.1	4.0	6.8
AVT(1 pt)	4.0	4.0	4.0

Table A.5. Maximum Percent Wall-Loss for Hot Leg Pitting
and Pitting/Wastage Degradation of Surry Tubes

Mech.	Min	Ave	Max
P**	14	42	68
P/W*	15	53	87
P/W**	34	48	67
P/W	15	52	87

*Tubes never plugged during service
**Tubes plugged during service

Table A.6 Estimated Pitting and Pitting/Wastage
Growth Rates from Surry Tubes

Mech.	Min	Ave	Max
P**	1.4	4.2	6.8
P/W*	1.5	5.3	8.7
P/W**	3.4	4.8	6.7
P/W	1.5	5.2	8.7

*Tubes never plugged during service
**Tubes plugged during service

4.0 DENTING

The phenomenon of denting has been arbitrarily divided into two phases; the time to fill the tube/TSP crevice gap with magnetite (dent initiation), and the rate of dent progression. Correlations have been developed by two investigators (Sawsochka et al. 1986; Pathania and Balakrishnan 1986) that relate the bulk chloride concentration measured in the blowdown water, with time to initiate a dent. These are given as equations (1) and (2) below:

$$T_d = 41.1 \, [Cl]^{-.928} \tag{1}$$

where T_d is the time to dent initiation in years and $[Cl]$ is the chloride concentration in ppb, and

$$Y' = 1.99 \, [Cl]^{.296} \tag{2}$$

APPENDIX A

COMPENDIUM OF DEFECT GROWTH RATES

APPENDIX A

COMPENDIUM OF DEFECT GROWTH RATES

1.0 INTRODUCTION

The information in this appendix summarizes much of the currently available data on the growth rate of the common defects found in steam generator tubing. This information was compiled to assist the determination of appropriate degradation allowances for evaluation of degraded steam generator tubing. Most of the data was obtained from recently published research reports and for the most part represents the results of laboratory investigations conducted under severe test conditions (e.g., high applied stresses and aggressive environments). In some cases, field data was available for comparison with the laboratory produced data.

2.0 THINNING (WASTAGE)

Very little data on the growth rate of wastage is available. With no plants in the U.S. presently using phosphate secondary water chemistry, this problem is not a major concern. Most recent occurrences of wastage have been observed at the periphery of the first or second tube support plate on the cold leg side of the generator. Limited data on the progression of cold leg thinning was reported by Baum et al. (1987). These data were obtained by monitoring the change in the eddy-current measurements on a given tube during successive inspections and dividing by the elapsed time. Corrosion rates were based on data from tubes with indications having reported depths 20% or greater in two successive inspections. The calculations were based on a total of 489 tubes in 18 steam generators. An overall degradation rate of 3 mils/y was estimated from these data.

Other published data (Angwin et al. 1985) plotted in Figures A.1 and A.2 show that the corrosion rate depends upon the Na/PO4 molar ratio and temperature, but maximum corrosion rates never exceeded about 5.5 mils/y.

Estimates were also obtained from evaluation of Surry metallographic data presented by Bradley et al. (1988). Maximum wall penetration of pure wastage was measured on tubes removed from both the hot and cold leg sides of the Surry generator. Table A.1 gives the minimum, average, and maximum percent wall-loss measured.

The data in Table A.1 can be used to estimate growth rates by dividing by the duration the defect mechanism is operative. The Surry generator was in service for slightly less than six years, from March 1973 to January 1979.

	Initial	Time of Exposure
r	Molality	Hours
1.0	6	387
1.35	6	312
1.6	6	480
2.0	5.2	504
2.3	5	451
2.7	5	432

38712-170.1M

FIGURE A.1. Average Corrosion Penetrations of Alloy 600 in Deaerated Sodium Phosphate Solutions at 615°F as a Function of the Na/PO4 Molar Ratio (Angwin et al. 1985).

Table A.1. Maximum Percent Wall-Loss for Wastage Degraded Surry Tubes

Leg	Min	Ave	Max
CL**	4	11	24
HL	12	30	52
HL*	12	22	32
HL**	20	35	52

  *Tubes never plugged during service
**Tubes plugged during service

A.2

FIGURE A.2. Temperature Dependence of the Corrosion Rate of Alloy 600 Tubing Exposed to Deaerated Phosphate Solutions (Angwin et al. 1985).

Secondary water chemistry was changed from phosphate to AVT after approximately two years of operation. Table A.2 gives the number of tubes plugged for wastage degradation from 1974 through 1977 (no tubes were plugged for wastage after 1977).

Table A.2. Number of Tubes Plugged for Wastage Degradation

Year	No. of Tubes
1974	14
1975	34
1976	19
1977	7

A.3

The data in Table A.2 suggests that time-to-initiation for phosphate wastage was very short and growth was not immediately arrested after conversion to AVT. As a first approximation, wastage growth rates were estimated by dividing the numbers in Table A.1 by four years. Performing this calculation yields the growth rates presented in Table A.3.

As expected, cold leg wastage grows more slowly than hot leg wastage. Removal of tubes from service by plugging did not reduce the growth rate below the rate observed in never-plugged tubes (limited data, however). Further, the results correlate well with the other published data.

Table A.3. Estimated Growth Rates for Surry Generator
Wastage Degradation (mils/yr)

Leg	Min	Ave	Max
CL**	.5	1.3	3
HL	1.5	3.8	6.5
HL*	1.5	2.8	4
HL**	2.5	4.4	6.5

*Tubes never plugged during service
**Tubes plugged during service

3.0 PITTING

Limited laboratory data has been developed by Combustion Engineering under a variety of conditions (Hall 1984). Figure A.3 gives a plot of pit depth versus exposure time for various test conditions. Table A.4 lists pit growth rates in mils/yr calculated from the data in Figure A.3. The average pit growth rate for all conditions was about 7.7 mils/yr.

Table A.5 shows maximum wall-loss measured from pitted (no wastage) and pitted/wastage degraded tubes from the Surry generator.

Since the in-service inspection and tube plugging history for the Surry generator did not identify tubes degraded by pitting, it was difficult to determine the pit growth rate. NDE detection of pitting is masked by copper deposits, so determination of pit growth from field NDE data is not reliable. One possible assumption might be one year for pit initiation followed by five years of growth. This assumption yields the results shown in Table A.6. These results compare reasonably well with the laboratory results given above. On the other hand, much of the recent laboratory data suggests that pit growth rates are highly nonlinear. Model boiler test results reported by Hall, et al. (1987), indicated that pit growth rates were initially rapid but were followed by stifling of further growth due to the formation of corrosion products that covered the outer surface of the pit.
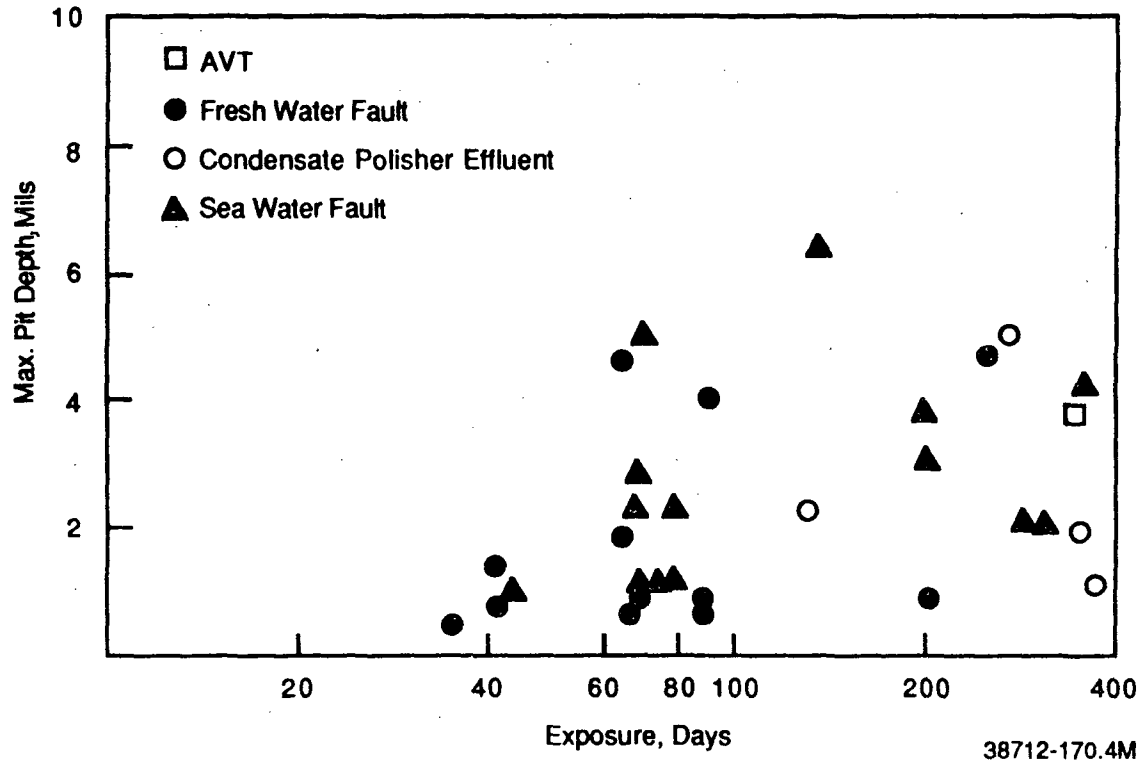
FIGURE A.3. Pit Depth Versus Exposure Time in Alloy 600 Tubes in Model and Pot Boiler Tests (Hall 1984)

Table A.4. Laboratory Pit Growth Rates (mils/yr)

Environ.	Min	Ave	Max
Fresh	1.5	8.0	25.3
Sea	2.4	8.9	26.1
CP	1.1	4.0	6.8
AVT(1 pt)	4.0	4.0	4.0

Table A.5. Maximum Percent Wall-Loss for Hot Leg Pitting and Pitting/Wastage Degradation of Surry Tubes

Mech.	Min	Ave	Max
P**	14	42	68
P/W*	15	53	87
P/W**	34	48	67
P/W	15	52	87

*Tubes never plugged during service
**Tubes plugged during service

Table A.6 Estimated Pitting and Pitting/Wastage Growth Rates from Surry Tubes

Mech.	Min	Ave	Max
P**	1.4	4.2	6.8
P/W*	1.5	5.3	8.7
P/W**	3.4	4.8	6.7
P/W	1.5	5.2	8.7

*Tubes never plugged during service
**Tubes plugged during service

4.0 DENTING

The phenomenon of denting has been arbitrarily divided into two phases; the time to fill the tube/TSP crevice gap with magnetite (dent initiation), and the rate of dent progression. Correlations have been developed by two investigators (Sawsochka et al. 1986; Pathania and Balakrishnan 1986) that relate the bulk chloride concentration measured in the blowdown water, with time to initiate a dent. These are given as equations (1) and (2) below:

$$T_d = 41.1 \; [Cl]^{-.928} \tag{1}$$

where T_d is the time to dent initiation in years and [Cl] is the chloride concentration in ppb, and

$$Y' = 1.99 \; [Cl]^{.296} \tag{2}$$

A.6

where Y' is the corrosion rate in mils/y. Equation (2) can be rearranged to give an equation of the same form as equation (1):

$$T_d = .503 \ Y_r \ [Cl]^{-.296} \qquad\qquad (3)$$

where Y_r is the crevice gap in mils.

These correlations are only applicable to plants that are sea/brackish water cooled and with AVT secondary water chemistry. In the development of equation (1) the crevice gap was assumed to be 7.5 mils. Substituting this value into equation (3) yields a coefficient of 3.77. For a chloride concentration of 200 ppb (represents a crude estimate of the low end of Surry conditions), equation (1) predicts a time-to-denting of about 4 months and equation (2) predicts about 9 months. These values seem reasonable given the experience at Surry (Doctor et al. 1983).

Of course, the time-to-denting depends on factors in addition to the bulk chloride concentration. The presence of copper in the secondary water has been observed to increase corrosion by lowering the crevice pH. Heat transfer test results clearly show the corrosion rate and hence time-to-denting strongly depend on the crevice superheat. In addition, tube support plate design and material of construction can change the corrosion rate. More open geometries such trefoil, quatrefoil, 'egg crate' and lattice bars are less susceptible to accelerated corrosion compared with the cylindrical annuli in drilled support plates. This may be explained by the lower crevice superheat in the more open geometries which results in lower concentrations of contaminants in the crevice and hence lower corrosion rates. Support plates made from Type 405 stainless steel are more corrosion resistant than carbon steel. Data from single tube model boiler tests in sea water indicated that the corrosion rate of Type 405 stainless steel support plates was about 5-10 times lower than carbon steel. However, at high bulk chloride concentrations (30 ppm) Types 405 and 409 tube supports corroded at rates comparable to carbon steel.

The available evidence on dent progression suggests the corrosion rate decreases once the crevice gap is filled. Reductions in corrosion rate ranging from 3 to 10 have been observed. Thus radial dent progression for a given chloride concentration may be predicted by multiplying the initial corrosion rates by a factor between 0.1 to 0.3. If a chloride concentration of 200 ppb is substituted into equation (2), then corrosion rates of about 9.4 mils/yr are predicted. This translates to dent progression rates of about 1 to 3 mils/yr.

The Surry plant was on AVT chemistry for four years. If the crevice gap filled within 4 to 9 months following conversion to AVT, then between 3 and 11 mils of radial denting would be predicted (assuming a constant denting rate). This would result in tube diameter changes of between 6 and 22 mils. Eddy-current profilometry measured an average diameter decrease of approximately 15 mils on the cold leg side and about 45 mils on the hot leg side. These results are in fair agreement with the predicted values from the bulk blowdown chemistry correlations. Better agreement would not be expected since it is difficult to derive a single chloride concentration that

represents Surry operating history. It was not uncommon for the blowdown chemistry to exhibit large periodic increases in chloride. In one transient up to 50,000 ppb was measured (Doctor et al. 1983).

4.1 CORRELATION OF DENTING STRAIN WITH IGSCC INITIATION

Electromechanical profilometry measurements were made on 101 tubes on the hot leg side of the Surry generator. The maximum principal strain was computed from these data by analyzing the shape of the dented tube cross section. A histogram of the strain measurement results is given in Figure A.4. The average measured strain was about 7.4% for the entire generator. If the denting at the top of tube sheet is excluded, then the average increases to 8.1%. Assuming that denting initiated within 4 to 9 months after conversion to AVT chemistry, the average strain rate would be about 7×10^{-10} sec^{-1}. Constant extension rate tests (CERT) conducted by Bandy and Van Rooyan (1984) at a strain rate of 2×10^{-7} sec^{-1} have shown decreasing plastic strain required for SCC initiation with increasing temperature, Figure A.5. By extrapolating Van Rooyan's data to 288°C (550°F) and 316°C (600°F), estimates of about 12% and 7.5% plastic strain are obtained for operating conditions.

Thirty tubes with calculated strains ranging from 4.2% to 88.3% were removed from the hot leg side of the Surry generator to determine the frequency of SCC with increasing strain. These tubes were examined visually and in some cases metallographically. Results of these examinations can be divided into three strain regions: 0% to 10%, 10% to 20% and greater than 20%. No cracking was observed below 10%, while approximately one-third of the specimens with calculated strain levels between 10% and 20% exhibited ID cracking. All of the specimens above 20% were found to contain ID cracks. These results compare reasonably well with the predicted values based on the CERT data. These comparisons are only semi-quantitative, since material susceptibility, temperature and strain rate all play an important role in determining the propensity for SCC.

5.0 INTERGRANULAR ATTACK AND STRESS CORROSION CRACKING

Intergranular attack (IGA) and secondary water stress corrosion cracking (SWSCC) have been observed in at least 30 domestic and foreign reactors. SWSCC is characterized by single or multiple major cracks that affect only a few grain boundaries. In contrast, volumetric IGA affects all the grain boundaries and may be accompanied by deeper SWSCC-type penetrations.

A significant number of plants have also been affected by primary water stress corrosion cracking (PWSCC). High stress, either applied, residual or a combination of the two appears to be a necessary condition for PWSCC. Cyclic load and the associated strain rate may reduce the level of stress required for cracking. Higher temperature tends to increase cracking rates.

The bulk of the laboratory data for Alloy 600 in PWR environments is related to crack initiation. Most investigations have utilized specimens such as tensile bars (CERT), bent beams, U-bends or C-rings. Typically, these specimens have been loaded or bent, exposed in a controlled environment

500

428

400

Occurrences

300

262

200

100

69

14   8   9   4   3   1   3   3   2   1   1

0

0   5   10   15   20   25   30   35   40   45   50   55   60   65   70   75   80   85   90   95   100

Percent Strain at Tube Sheet/Support Plates
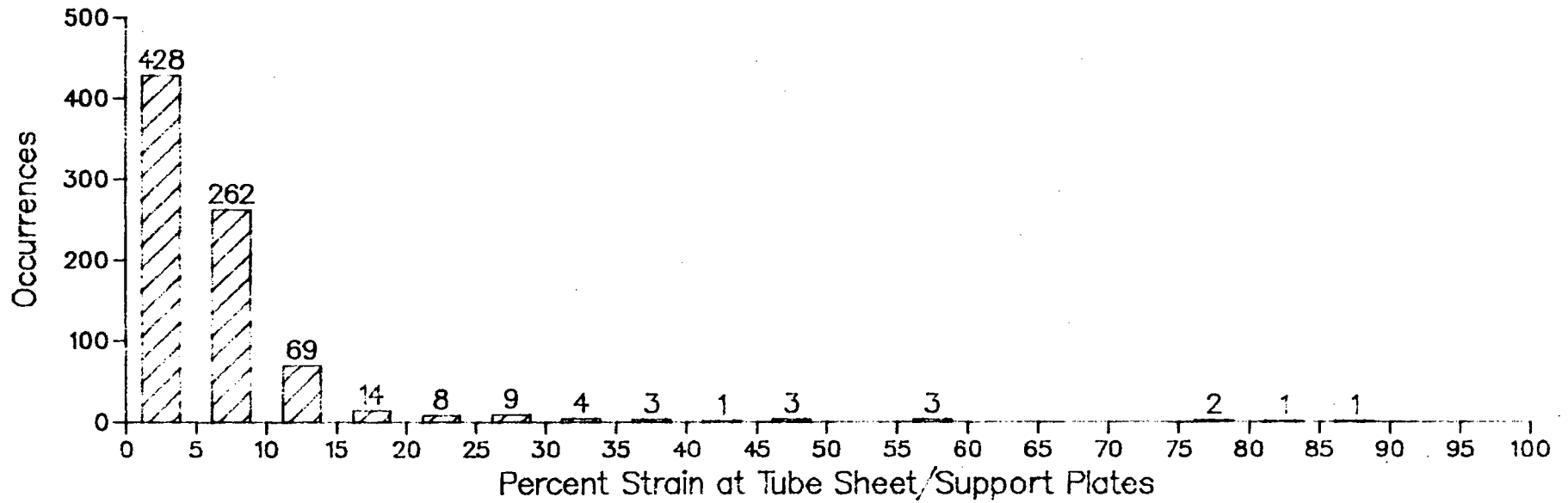
FIGURE A.4. Histogram Showing Strain Measurements From the PROFIL-360 Inspection (Doctor et al. 1988b)
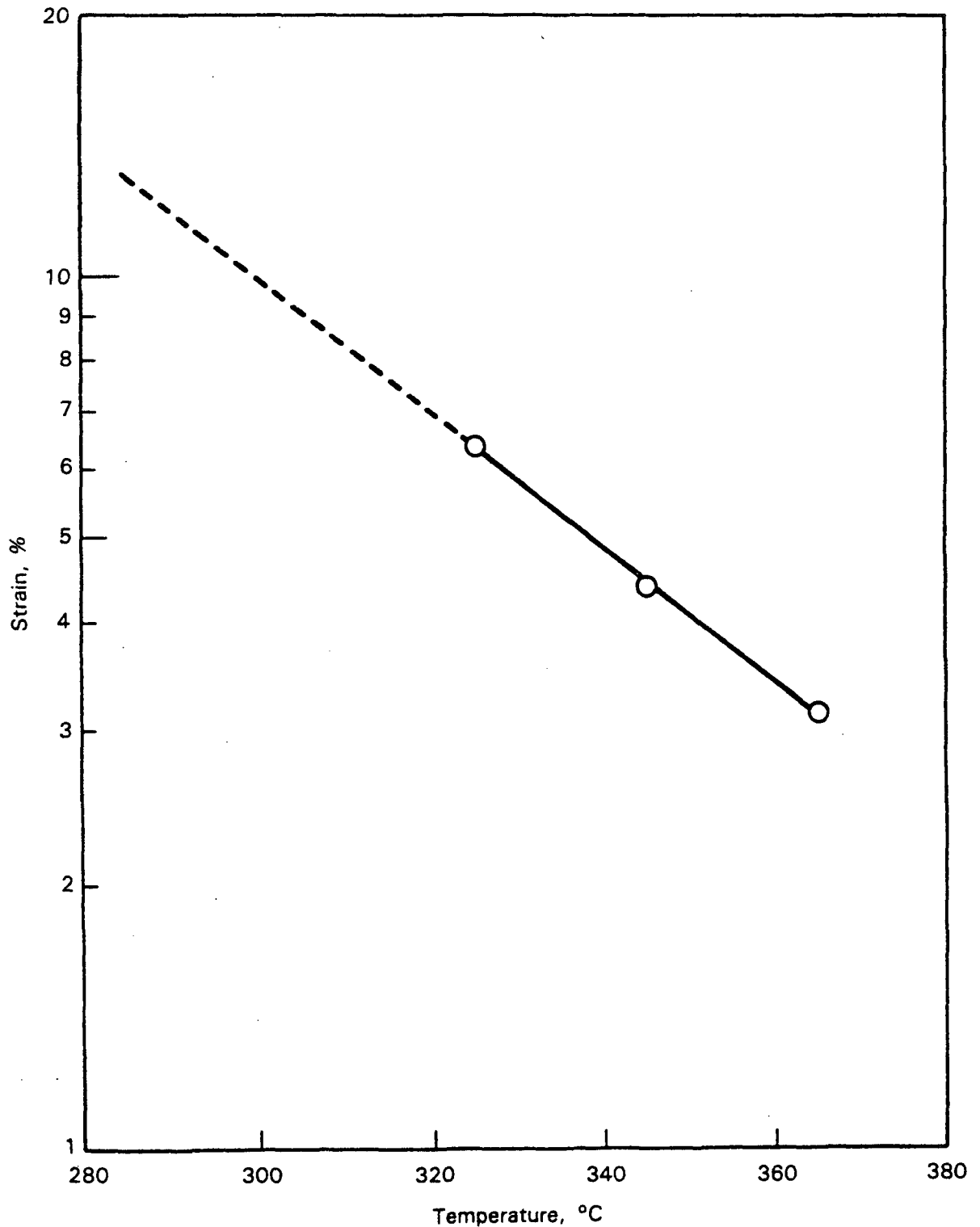
FIGURE A.5. Temperature Dependence of SCC Initiation Strain for CERT Tests at $\dot{e}$ = 2 x 10^{-10} sec^{-1}. (Reprinted with permission from Corrosion, Vol. 40, No. 8, "Stress Corrosion Cracking of Inconel Alloy 600 in High Temperature Water - An Update." Bandy and Van Rooyan, National Association of Corrosion Engineers, Houston, Texas.)

and periodically removed from the environment for examination. The results of these tests are usually the time-to-crack or time-to-failure. In some cases, estimates of the crack growth rate were obtained. Very few studies employed fracture mechanics type specimens, with sharp starter notches for measuring crack growth. Usually temperature, stress, or strain rate are used as accelerating parameters. Often, the test conditions were severe compared to expected service conditions.

The growth rates of IGA and SCC can only be estimated approximately for the reasons noted above. Figures A.6 and A.7 summarize the available data (Bandy and Van Rooyan 1984; Partridge 1987; Hermer and Wolf 1986; Aspden 1986; Newman et al. 1987; Theus 1981; Jacko 1986) on growth of IGA and SCC (both primary and secondary) as a function of temperature. Note the strong temperature dependence of all three forms of cracking. Another interesting observation is that SCC is more rapid in primary than in secondary water. Although not shown in Figures A.6 and A.7, both IGA and SWSCC appear to be insensitive to caustic concentration over the range 10 to 40%. Below 10% caustic, the growth rate decreases with decreasing concentration. Two additional observations not explicitly depicted in Figure A.7 are that different heats of material behave differently and little difference is observed in the PWSCC growth rate in pure water, primary water, or AVT treated water. Also shown in Figure A.7 is the decreased rate of SWSCC for thermally treated (TT) Alloy 600 relative to mill annealed (MA) material. Corrosion resistance to IGA is improved by thermal treatment by a factor of about 1.6.

Figures A.8 and A.9 show the limited amount of data (Newman et al. 1987 and Berge 1986) suggesting a relationship between applied stress (or stress intensity) and growth rate for IGA and SWSCC respectively. For SWSCC at high applied stress levels, the curves in Figure A.8 suggest a saturation of crack growth rate. Also a significant dependence on caustic concentration was observed over the full range of stress intensity factors investigated. In addition, the results in Figure A.8 suggest a threshold below which no significant SWSCC is expected.

Upper bound estimates for growth rates at 550°F and 600°F obtained from Figures A.6 and A.7 are listed in Table A.7.
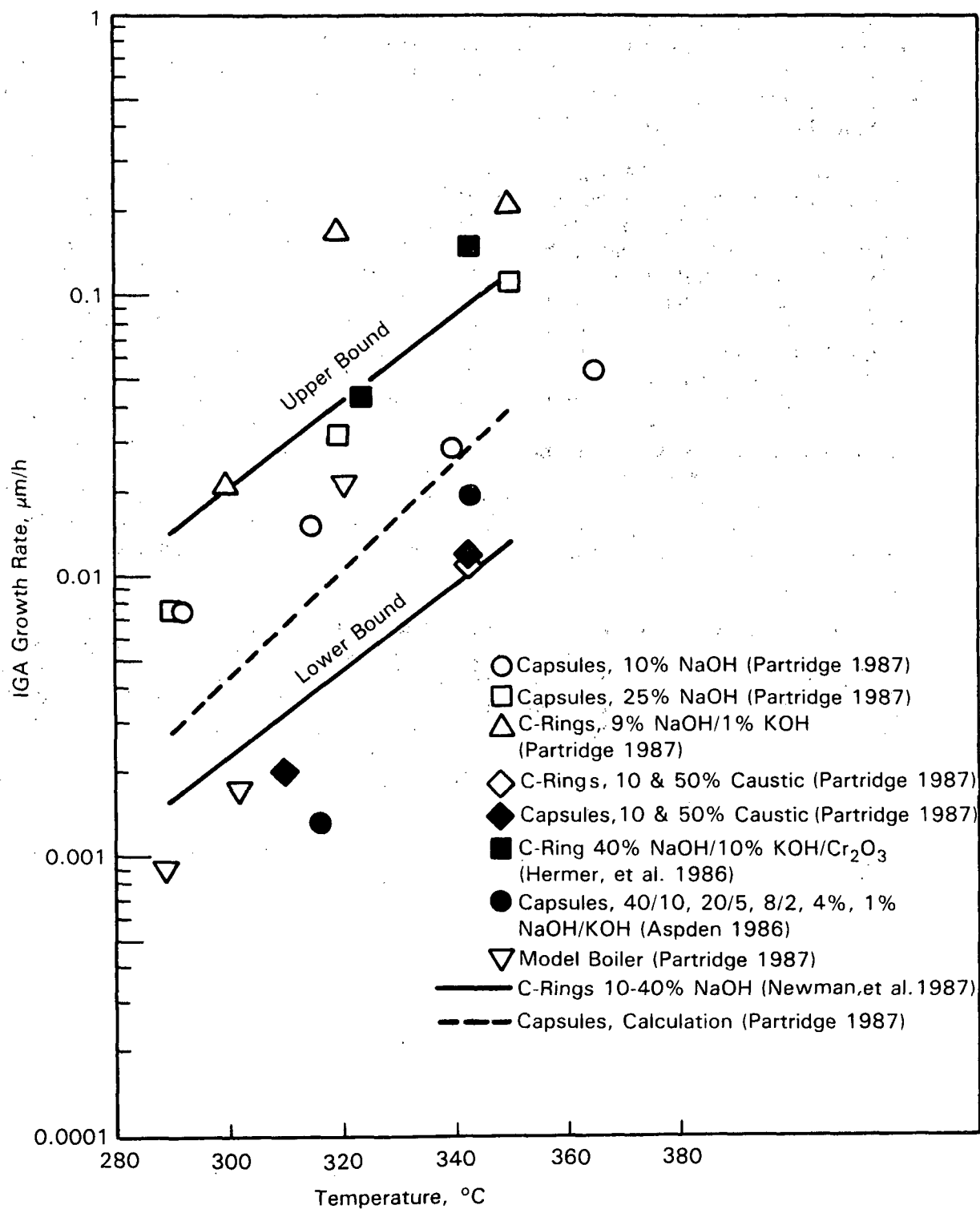
FIGURE A.6. Temperature Dependence of IGA Growth Rate

A.12
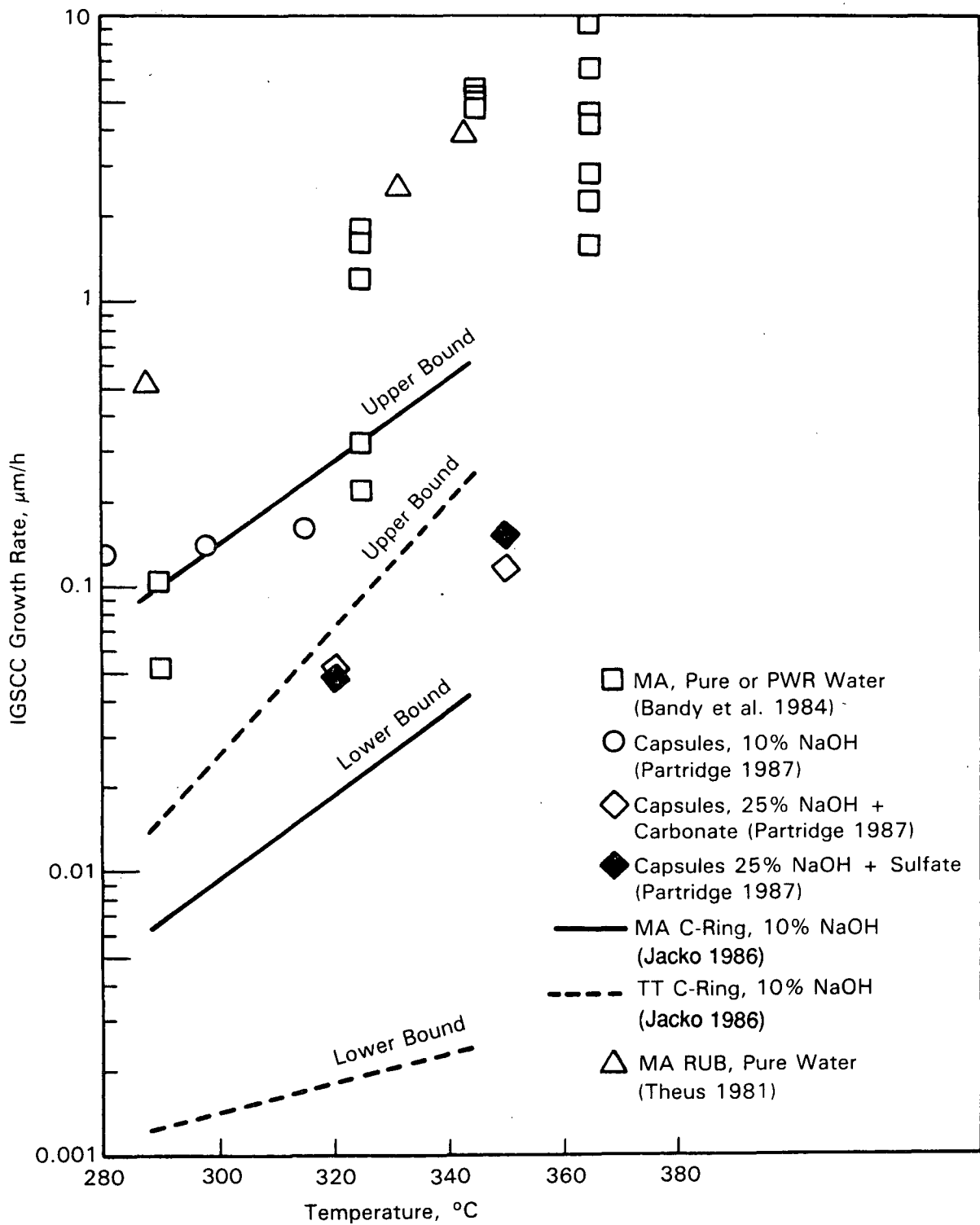
FIGURE A.7. Temperature Dependence of SCC Growth Rate

Stress, MPa
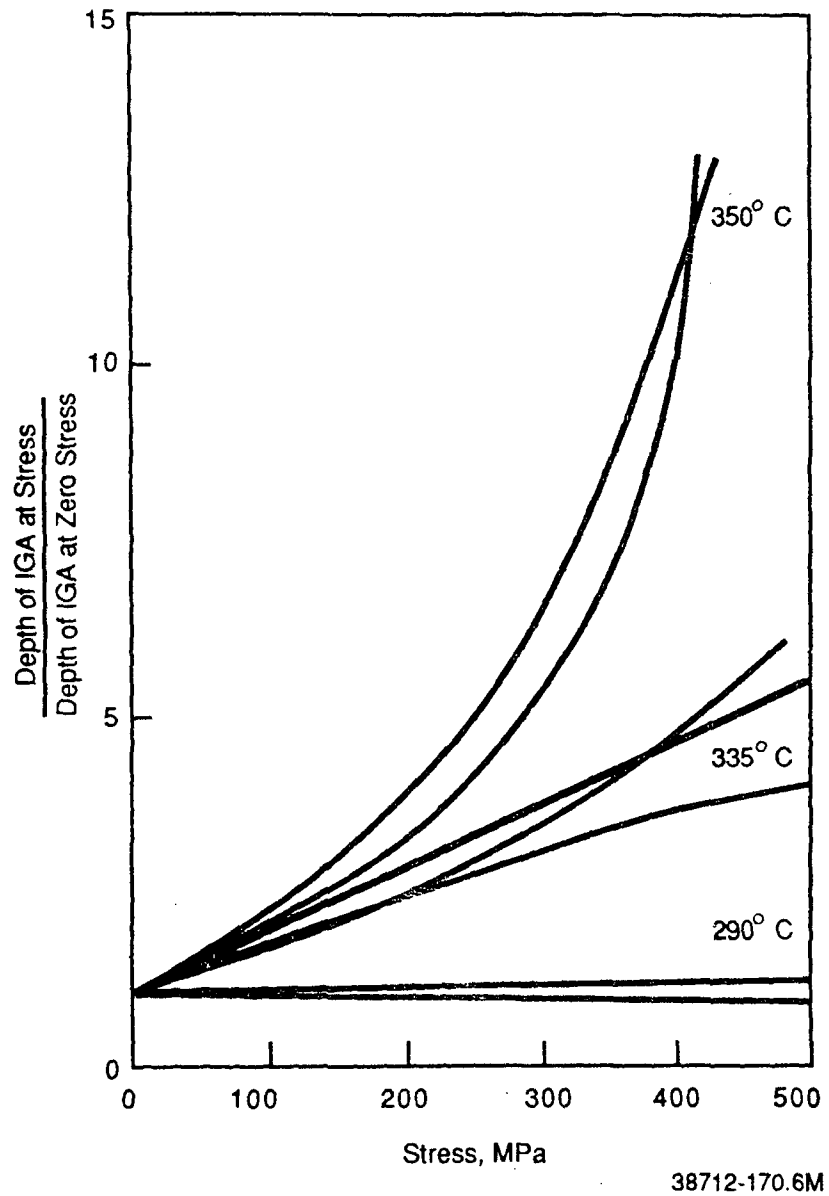
38712-170.6M

FIGURE A.8. Influence of Stress on IGA as a Function
of Temperature (Newman et al. 1987).

Table A.7. Estimated Upper Bound Growth Rates
for Cracking Mechanisms (mils/yr)

Mechanism	550°F	600°F
IGA	5	30
SWSCC	50	85
PWSCC	170	600

A.14

MA: Mill Annealed
HT: Heat Treated 16h at 700 °C
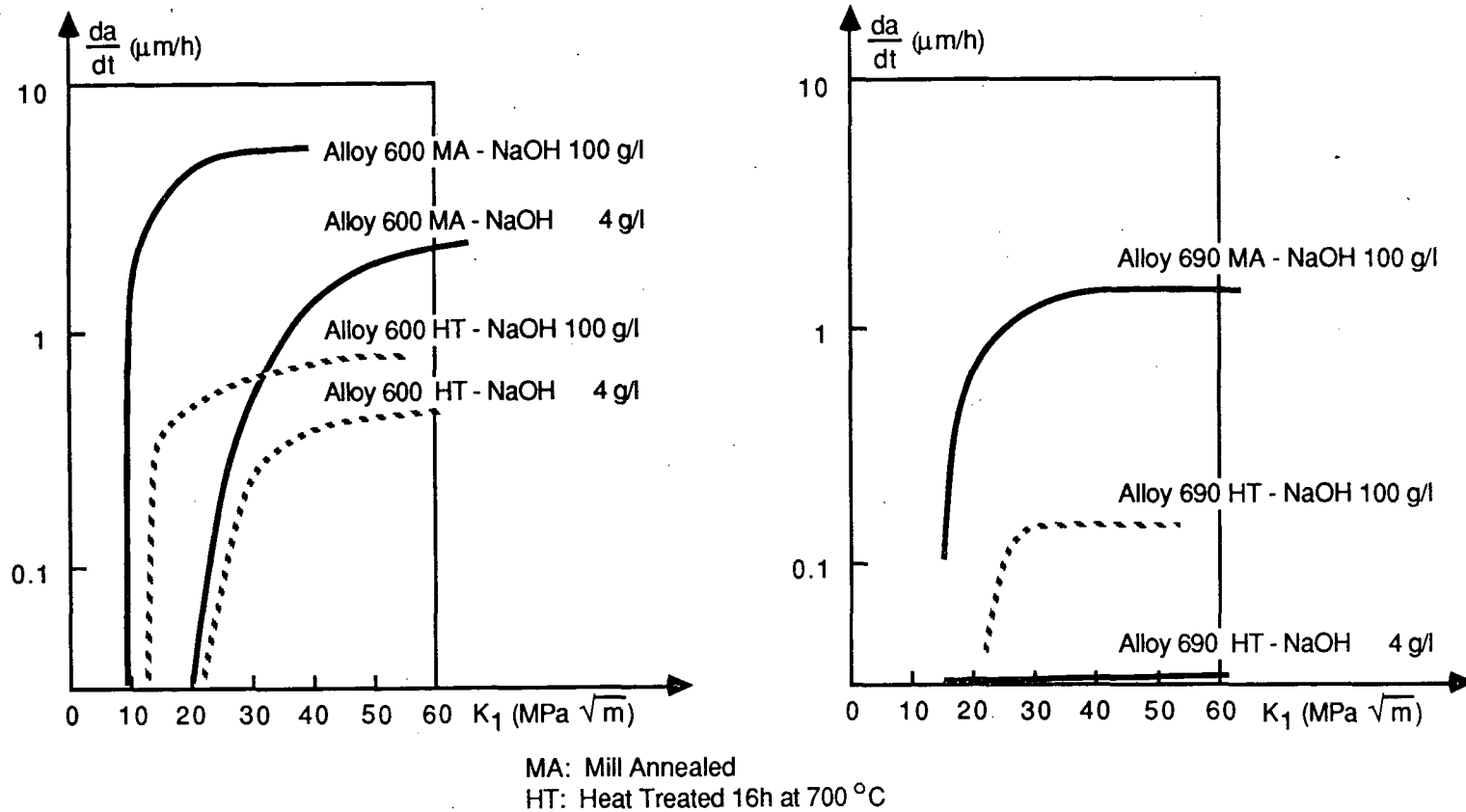
38712-170.5M

FIGURE A.9. Stress Corrosion Tests in Deaerated Sodium Hydroxide at 350°C on Fracture Mechanics
Type Specimens: Comparison of Alloy 600 and 690 Behavior. Effect of Heat Treatment
at 700°C. (Berge 1986)

6.0 CORROSION FATIGUE

For corrosion fatigue conditions the material property needed is the cyclic crack growth rate, da/dN. The data on Alloy 600 in typical PWR environments is limited. Furthermore, for the low K regime, there are few da/dN data in any environment. Figure A.10 (Davis et al. 1983) shows a summary of the crack growth rate results for Alloy 600 in air and water environments. These data combined with appropriate stress analyses can be used to estimate crack growth for tubes in OTSGs affected by this damage mechanism.

7.0 SUMMARY

The foregoing material briefly presented much of the publicly available information on growth rates of various damage mechanisms for steam generator tubing. The information is sparse in most instances and nonexistent in other cases. Table A.8 provides upper bound growth rate estimates at 600°F for the major damage mechanisms of concern.

Table A.8. Upper Bound Growth Rates (600°F) for Principal Steam Generator Tube Damage Mechanisms (mils/yr)

Mechanism	Rate
Thinning	6
Pitting	25
IGA	30
SWSCC	85
PWSCC	600

It is clear the damage mechanism most likely to penetrate the tube wall between inspection outages is primary side cracking. However, all damage forms (except for thinning) potentially grow at rates that could penetrate the tube wall during a typical eighteen month period between inservice inspections. This assumes that a particular damage mechanism operates at a constant rate with time, which as Figure A.11 illustrates may not be the case for IGA (Miglin 1987). It is typical of non-stress-assisted corrosion mechanisms to exhibit decreasing rate with time. However, not enough data exists to permit more accurate defect growth rate estimates for many of the damage mechanisms discussed here.
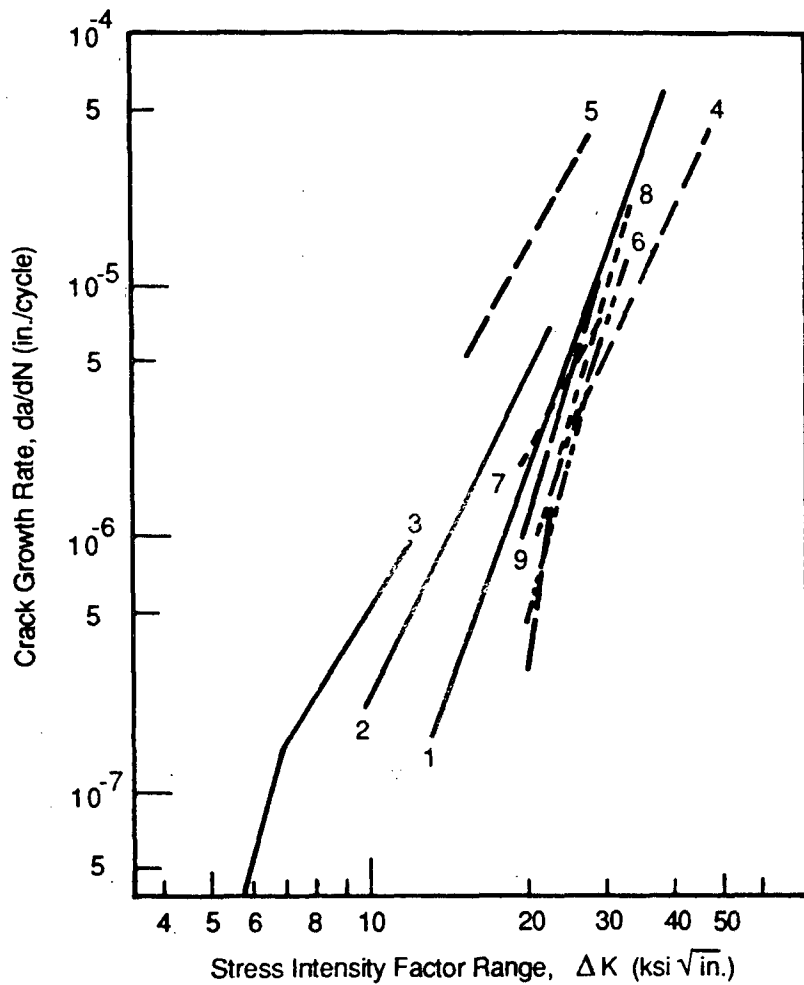
Key to crack growth test conditions:

1   400 cpm in air at 300 °F, R = .05
2   400 cpm in air at 800 °F, R = .333
3   400 cpm in air at 300 °F, R = .6
4   40 cpm in air at 75°F, R = .05
5   40 cpm in air at 1200 °F, R = .05
6   900 cpm in pure water at 185 °F, 15 ppm O_2, R = 0, solution annealed in air
7   1 cpm in pure water at 185 °F, 15 ppm O_2, R = 0, solution annealed
8   1 cpm in pure water at 185 °F, 15 ppm O_2, R = 0, sensitized 24h at 650 °C
9   1 cpm in pure water at 185 °F, 15 ppm O_2, R = 0, sensitized 1000h at 650 °C

38712-170.2

FIGURE A.10.   Summary of Corrosion Fatigue Crack Growth
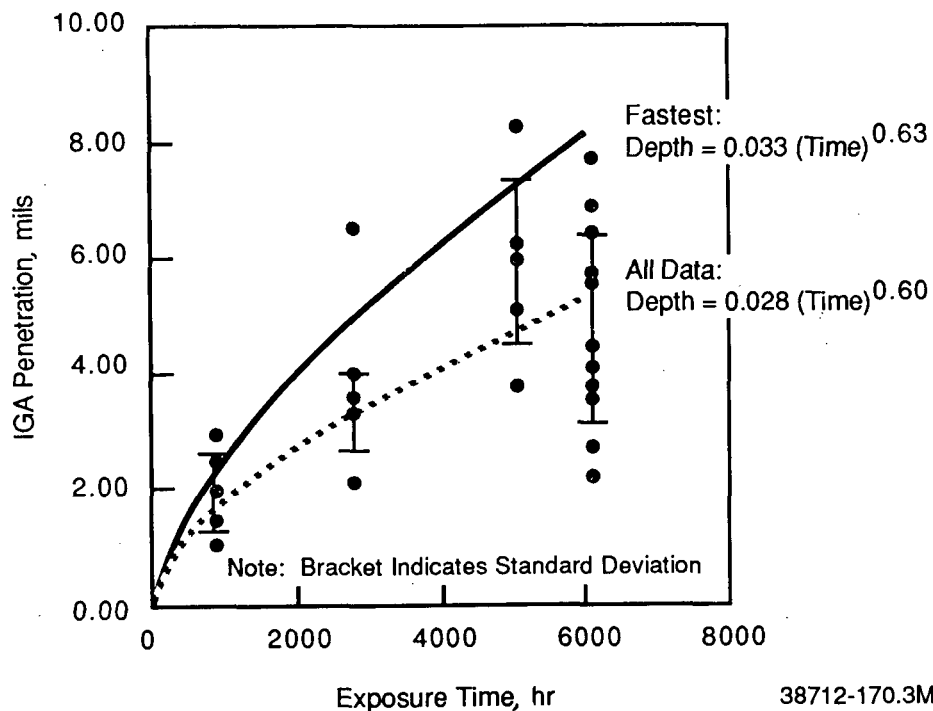Results for Inconel 600 (Davis 1983)

A.17

FIGURE A.11. Depth of IGA Penetrations on Mill-Annealed Alloy 600 Tubing (Heat NX3335) as a Function of Exposure Time (Miglin 1987)

8.0 REFERENCES

Angwin, M. J. et al. 1985. Steam Generator Reference Book. Electric Power Research Institute, Palo Alto, California.

Aspden, R. G. 1986. "Background Reporting and IGA Screening in Static Test Devices." In Proceedings: 1984 Workshop on Secondary Side Stress Corrosion Cracking and Intergranular Corrosion of PWR Steam Generator Tubing. EPRI NP-4478, Electric Power Research Institute, Palo Alto, California.

Bandy, R. and D. Van Rooyan. 1984. "Stress Corrosion Cracking of Inconel Alloy 600 in High Temperature Water - An Update." Corrosion 40(8):425-430.

Baum, A. J., C. Dangelo, P. J. Kuchirka, N. Singleton, and M. J. Sredzienski. 1987. Steam Generator Cold Leg Thinning in Operating Plants. EPRI NP-5140, Electric Power Research Institute, Palo Alto, California.

Berge, J. P. 1986. "Questions on U-Bend Cracking." In Proceedings: 1984 Workshop on Secondary Side Stress Corrosion Cracking and Intergranular Corrosion of PWR Steam Generator Tubing, EPRI NP-4478, Electric Power Research Institute, Palo Alto, California.

Bradley, E. R., P. G. Doctor, R. H. Ferris, and J. A. Buchanan. 1988. _Steam Generator Group Project Task 13 Final Report - NDE Validation._ NUREG/CR-5185, PNL-6399, Pacific Northwest Laboratory, Richland, Washington.

Davis, C. S., J. M. Thomas, S. W. Winder, and D. E. Allison. 1983. _An Engineering and Probabilistic Analysis of Tube Cracking Performance in Once-Through Steam Generators._ EPRI NP-3065, Electric Power Research Institute, Palo Alto, California.

Doctor, P. G., J. M. McIntyre, P.K. Alley, L. R. DesCamp, J. S. Littlefield, C. A. LoPresti, and J. A. Buchanan. 1983. _The In-Service History of The Surry Unit 2A Steam Generator._ PNL-4880, Pacific Northwest Laboratory, Richland, Washington.

Doctor, P. G., H. Harty, R. H. Ferris, and A. S. Birks. 1989. _Steam Generator Group Project Task 9 Final Report - Nondestructive Evaluation Round, Vol. 1: Description and Summary Data._ NUREG/CR-4849, PNL-5868, Pacific Northwest Laboratory, Richland, Washington.

Hall, J. F. 1984. "Pitting in the Laboratory at Combustion Engineering." In _Workshop Proceedings: Pitting in Steam Generator Tubing._ EPRI NP-3574-SR, Electric Power Research Institute, Palo Alto, California.

Hall, J. F., R. S. Frisk, K. E. Marugy, and A. S. O'Neill. 1987. _Investigation of Causes and Corrective Actions for Pitting in Steam Generator Tubes: Prototypic Tests._ EPRI NP-5248, Electric Power Research Institute, Palo Alto, California.

Hermer, R. E. and C. R. Wolfe. 1986. "Alloy 600 Intergranular Corrosion in Alkaline Environments." In _Proceedings: 1984 Workshop on Secondary Side Stress Corrosion Cracking and Intergranular Corrosion of PWR Steam Generator Tubing._ EPRI NP-4478, Electric Power Research Institute, Palo Alto, California.

Jacko, R. J. 1986. "IGSCC and IGA Behavior of Inconel 600." In _Proceedings: 1984 Workshop on Secondary Side Stress Corrosion Cracking and Intergranular Corrosion of PWR Steam Generator Tubing._ EPRI NP-4478, Electric Power Research Institute, Palo Alto, California.

Miglin, B. P. 1987. _Production of Eddy-Current Standards for Caustic Intergranular Corrosion._ EPRI NP-5109, Electric Power Research Institute, Palo Alto, California.

Newman, J. R., P. McIntyre, and S. M. Payne. 1987. "Effect of Thermal Treatment and Impurity Segregation on the Kinetics of IGA in Inconel 600." Presented at _EPRI Workshop on IGA and SCC Mechanisms,_ Electric Power Research Institute, Palo Alto, California.

Partridge, M. J. 1987. "Effect of Temperature and Caustic on IGA and IGSCC Corrosion Rates." Presented at _EPRI Workshop on IGA and SCC Mechanisms,_ Electric Power Research Institute, Palo Alto, California.

Pathania, R. S. and P. V. Balakrishnan. 1986. Correlation of Tube Support Structure Studies. EPRI NP-4672, Electric Power Research Institute, Palo Alto, California.

Sawsochka, S. G., K. D. Friedman, S. S. Choi, and J. K. Pyo. 1986. Correlation of Tube Support Corrosion Studies. EPRI NP-4818, Electric Power Research Institute, Palo Alto, California.

Theus, G. J. ,1981. "Stress Corrosion Cracking Tests of Alloy 600. In Workshop Proceedings: U-Bend Cracking in Steam Generators, EPRI WS-80-136, Electric Power Research Institute, Palo Alto, California.

APPENDIX B

STEAM GENERATOR TUBE INTEGRITY PROGRAM/STEAM GENERATOR GROUP PROJECT
REPORTS AND PUBLICATIONS

STEAM GENERATOR TUBE INTEGRITY PROGRAM/STEAM GENERATOR GROUP PROJECT
REPORTS AND PUBLICATIONS

Alzheimer, J. M., R. A. Clark, W. E. Anderson, J. C. Crowe, and M. Vagins.
    1977. "Steam Generator Tube Integrity Program. Quarterly Report, January
    1-March 31, 1977." NUREG-0359. Pacific Northwest Laboratory, Richland,
    Washington.

Alzheimer, J. M., R. A. Clark, C. J. Morris and M. Vagins. 1979. "Steam
    Generator Tube Integrity Program Phase I Report." NUREG/CR-0718,
    PNL-2937, Pacific Northwest Laboratory, Richland, Washington.

Morris, C. J., G. H. Lyon, T. J. Davis and C. B. Perry. 1980. "Eddy-Current
    Inspection of INCONEL-600 Steam Generator Tubes at the Tube Sheet."
    NUREG/CR-1626, PNL-3472, Pacific Northwest Laboratory, Richland,
    Washington.

Clark, R. A. and V. PitzPatrick. 1981. "Steam Generator Transport: Surry,
    Virginia to Hanford, Washington," p. 826-827 in Trans. Am. Nucl. Soc.
    (United States), Vol. 39.

Wheeler, K. R. and R. A. Clark. 1982. "Initial Inspection of a Service
    Degraded Steam Generator Removed from Service," p. 297-298 in Trans. Am.
    Nuc. Soc. (United States), Vol. 41.

Clark, R. A. and M. Lewis. 1983. "Repair Research as Part of the Steam
    Generator Group Project," p. 493 in Trans. Am. Nucl. Soc. (United States),
    Vol. 44.

Clark, R. A. and M. Lewis. 1983. "Steam Generator Group Project Semi-Annual
    Progress Report, January - June 1983." PNL-4859, Pacific Northwest
    Laboratory, Richland, Washington.

Doctor, P. G., J. M. McIntyre, P. K. Alley, L. R. DesCamp, J. S. Littlefield,
    C. A. LoPresti and J. A. Buchanan. 1983. "The In-Service History of the
    Surry Unit 2A Steam Generator." PNL-4880, Pacific Northwest
    Laboratory, Richland, Washington.

Reece, W. D., G. R. Hoenes and M. A. Parkhurst. 1984. "Steam Generator Group
    Project Progress Report - Task 3 Health Physics." NUREG/CR-3578,
    PNL-4711, Pacific Northwest Laboratory, Richland, Washington.

Doctor, P. G., J. A. Buchanan, J. M. McIntyre, P. J. Hof and
    S. S. Ercanbrack. 1984. "Steam Generator Group Project Progress Report
    on Data Acquisition/Statistical Analysis." NUREG/CR-3579, PNL-3955,
    Pacific Northwest Laboratory, Richland, Washington.

Allen, R. P., R. L. Clark and W. D. Reece. 1984. "Steam Generator Group Project Task 6 - Channel Head Decontamination." NUREG/CR-3841, PNL-4712, Pacific Northwest Laboratory, Richland, Washington.

Clark, R. A. and M. Lewis. 1984. "Steam Generator Group Project Semi-Annual Progress Report July - December 1982." NUREG/CR-3580, PNL-4692, Pacific Northwest Laboratory, Richland, Washington.

Clark, R. A. and M. Lewis. 1984. "Steam Generator Group Project Annual Report - 1982." NUREG/CR-3581, PNL-4693, Pacific Northwest Laboratory, Richland, Washington.

Bickford, R. L., R. A. Clark, P. G. Doctor, H. E. Kjarma and C. A. LoPresti. 1984. "Eddy Current Round Robin Test on Laboratory Produced Intergranular Stress Corrosion Cracked Inconel Steam Generator Tubes." NUREG/CR-3561, PNL-4695, Pacific Northwest Laboratory, Richland, Washington.

Clark, R. A. and R. L. Bickford. 1984. "Steam Generator Tube Integrity Program Leak Rate Tests - Progress Report." NUREG/CR-3562, PNL-4629, Pacific Northwest Laboratory, Richland, Washington.

Wheeler, K. R., P. G. Doctor, L. K. Fetrow and M. Lewis. 1984. "Steam Generator Group Project Task 8 - Selective Tube Unplugging." NUREG/CR-3842, PNL-4876, Pacific Northwest Laboratory, Richland, Washington.

Schwenk, E. B. and K. R. Wheeler. 1984. "Steam Generator Group Project Task 10 - Secondary Side Examination." NUREG/CR-3843, PNL-5033, Pacific Northwest Laboratory, Richland, Washington.

Sinclair, R. B. 1984. "Secondary Side Photographic Techniques Used in Characterization of Surry Steam Generator." NUREG/CR-3094, PNL-5053, Pacific Northwest Laboratory, Richland, Washington.

Tanner, J. E., W. D. Reece and R. I. Scherpelz. 1984. "Steam Generator Group Project Progress Report - Task 3." PNL-5269, Pacific Northwest Laboratory, Richland, Washington.

Wheeler, K. R. 1984. "Initial Inspection of the Service Degraded Surry 2A Steam Generator, June 1982". PNL-5268, Pacific Northwest Laboratory, Richland, Washington.

Clark, R. A., M. Lewis and J. Muscara. 1984. "Steam Generator Group Project Semi-Annual Progress Report January Through June 1984." PNL-5267, Pacific Northwest Laboratory, Richland, Washington.

Birks, A. S., R. H. Ferris, P. G. Doctor and H. Harty. 1984. "Preliminary Report on Steam Generator Group Project - Task 9 NDE Round Robin." PNL-5499, Pacific Northwest Laboratory, Richland, Washington.

Clark, R. A. et al. 1984. "1983 Branch Annual Report - Steam Generator Integrity Program." NUREG-0975, Vol. 2, PNL-SA-11720, Pacific Northwest Laboratory, Richland, Washington.

Clark, R. A. 1984. "Status and Progress of Research on a Removed-from-Service Steam Generator." NUREG/CP-0048, Vol. 4, p. 98-116, in Proceedings of the Eleventh Water Reactor Safety Research Information Meeting, Pacific Northwest Laboratory, Richland, Washington.

Clark R. A. 1984. "Results of Research Utilizing a Retired from Service PWR Steam Generator." PNL-SA-12531, presented at Specialist Meeting on Steam Generator Problems, Stockholm, Sweden, October 1, 1984.

Clark, R. A. 1985. "Status and Progress of Research on a Removed-from-Service Steam Generator," p. 39-47, Nuclear Engineering and Design. Pacific Northwest Laboratory, Richland, Washington.

Clark, R. A. 1985. "Characterization of the Removed-from-Service Surry 2A Steam Generator." PNL-SA-12532, presented at 8th International Conference on Structural Mechanics in Reactor Technology, Brussels, Belgium, August 19, 1985.

Clark, R. A. 1985. "Metallurgical Analysis and Comparative Nondestructive Inspection Results on Specimens Removed from a Retired from Service PWR Steam Generator," International Symposium on Contribution of Materials Investigation to the Resolution of Problems Encountered in PWR Plants, Chinon, France, September 3, 1985.

Clark, R. A. and M. Lewis. 1985. "Observation of Denting and Other Deterioration in the Surry Steam Generator," PNL Report PNL-SA-13273, presented at American Society for Metals Meeting, San Diego, California, July 9, 1985.

Clark, R. A. and M. Lewis. 1985. "Observation of Denting and Other Deterioration in the Surry Steam Generator," p. 193-196 in Proceedings of the International Conference on Nuclear Power Plant Aging, Availability Factor and Reliability Analysis (American Society of Metals, Metals Park, Ohio).

Clark, R. A., E. R. Bradley, and R. J. Kurtz. 1985. "Investigation of Tube Sheet Samples Removed from the Retired Surry Steam Generator." PNL-SA-13467, presented at Workshop on Remedial Action for Intergranular Corrosion, Baltimore, Maryland, October 15, 1985.

Clark, R. A. and P. G. Doctor. 1985. "Surry Steam Generator Program and Baseline Eddy Current Examination," Vol. 4, p. 260-285, in Proceedings of the Twelfth Water Reactor Safety Research Information Meeting. NUREG/CP-0058, Vol. 4. Pacific Northwest Laboratory, Richland, Washington.

Clark, R. A. and M. Lewis. 1985. "Steam Generator Group Project Annual Report - 1983." NUREG/CR-4361, PNL-5017, Pacific Northwest Laboratory, Richland, Washington.

Clark, R. A. and M. Lewis. 1985. "Steam Generator Group Project Annual Report - 1984." NUREG/CR-4362, PNL-5417, Pacific Northwest Laboratory, Richland, Washington.

Clark, R. A. and M. Lewis. 1985. "Steam Generator Group Project Semi-Annual Progress Report, January through June 1985." PNL-5603, Pacific Northwest Laboratory, Richland, Washington.

Clark, R. A., R. L. Bickford, A. S. Birks, R. L. Clark, P. G. Doctor, R. H. Ferris, L. K. Fetrow, W. D. Reece, E. B. Schwenk, and G. E. Spanner. 1985. "1984 Branch Annual Report - Steam Generator Integrity Program." NUREG-0975, Vol. 3, PNL-SA-13015, Pacific Northwest Laboratory, Richland, Washington.

Clark, R. A., P. G. Doctor, and R. H. Ferris. 1986. "Surry Steam Generator - Examination and Evaluation," Vol. 2, p. 409-430 in Proceedings of the Thirteenth Water Reactor Safety Research Information Meeting, NUREG/CP-0072, Vol. 2. Pacific Northwest Laboratory, Richland, Washington.

Kurtz, R. J. and M. Lewis. 1986. "Steam Generator Group Project Semi-Annual Progress Report, January through June 1986." PNL-6012, Pacific Northwest Laboratory, Richland, Washington.

Kurtz, R. J. and R. A. Clark. 1986. "1985 Branch Annual Report - Steam Generator Integrity Program." NUREG-0975, Vol. 4, PNL-5772, Pacific Northwest Laboratory, Richland, Washington.

Clark, R. A., P. G. Doctor, and R. H. Ferris. 1987. "Surry Steam Generator - Examination and Evaluation," p. 123-134, Nuclear Engineering and Design.

Kurtz, R. J., M. Lewis and R. A. Clark. 1987. "Steam Generator Group Project Annual Report - 1985." NUREG/CR-4848, PNL-5771, Pacific Northwest Laboratory, Richland, Washington.

Kurtz, R. J. 1987. "Using a Retired Surry Unit to Assess ISI (In-Service Inspection) Reliability," Nuclear Engineering and Design, p. 37-39.

Schwenk, E. B. 1987. "Steam Generator Group Project Task 10 - Secondary Side Examination Final Report." NUREG/CR-4850, PNL-6045, Pacific Northwest Laboratory, Richland, Washington.

Kurtz, R. J. and M. Lewis. 1987. "Steam Generator Group Project Annual Report - 1986." PNL-6150, Pacific Northwest Laboratory, Richland, Washington.

Kurtz, R. J. 1987. "1986 Branch Annual Report - Steam Generator Integrity Program." NUREG-0975, Vol. 5, PNL-6110, Pacific Northwest Laboratory, Richland, Washington.

Bradley, E. R., P. G. Doctor, R. H. Ferris, and J. A. Buchanan. 1988. "Steam Generator Group Project - Task 13 Final Report - NDE Validation." NUREG/CR-5185, PNL-6399, Pacific Northwest Laboratory, Richland, Washington.

Doctor, P. G., H. Harty, R. H. Ferris and A. S. Birks. 1988. "Steam Generator Group Project - Task 9: Final Report - Nondestructive Evaluation Round Robin, Comments Vol. I: Description and Summary Data and Vol. II." NUREG/CR-4849 Vol. I and II, PNL-5868, Pacific Northwest Laboratory, Richland, Washington.

Doctor, P. G., A. S. Birks, R. H. Ferris, H. Harty and G. E. Spanner. 1988. "Steam Generator Group Project - Task 7: Final Report - Post-Service Baseline Eddy-Current Examination." NUREG/CR-5087, PNL-5940, Pacific Northwest Laboratory, Richland, Washington.

Kurtz, R. J., and R. A. Clark. 1988. "Compendium and Comparison of International Practice for Plugging, Repair, and Inspection of Steam Generator Tubing." NUREG/CR-5016, CSNI No. 140, PNL-6341, Pacific Northwest Laboratory, Richland, Washington.

Kurtz, R. J., J. M. Alzheimer, R. L. Bickford, R. A. Clark, C. J. Morris, E. A. Simonen and K. R. Wheeler. 1988. "Steam Generator Tube Integrity Program Phase II Final Report." NUREG/CR-2336, PNL-4008, Pacific Northwest Laboratory, Richland, Washington.

Kurtz, R. J. et al. 1988. "1987 Branch Annual Report - Steam Generator Integrity Program." NUREG-0975, Vol. 6, PNL-6401, Pacific Northwest Laboratory, Richland, Washington.

Kurtz, R. J., R. L. Bickford, W. M. Bowen, E. R. Bradley, P. G. Doctor, R. H. Ferris, L. K. Fetrow, and F. A. Simonen. 1988. "Surry Steam Generator Program - Final Results - Evaluation of NDE Performance and Technical Basis for Improved ISI and Plugging Criteria," Vol. 2, p. 429-457, in Proceedings of the Fifteenth Water Reactor Safety Research Information Meeting, USNRC Conference Proceeding NUREG/CP-0091, Vol. 2. Pacific Northwest Laboratory, Richland, Washington.

Bowen, W. M., P. G. Heasler, and R. B. White. 1989. "Evaluation of Sampling Plans for In-Service Inspection of Steam Generator Tubes: Part I." NUREG/CR-5161, PNL-6462, Pacific Northwest Laboratory, Richland, Washington.

Kurtz, R. J., R. A. Clark, E. R. Bradley, W. M. Bowen, P. G. Doctor, F. A. Simonen, and R. H. Ferris. 1990. "Steam Generator Tube Integrity Program/Steam Generator Group Project - Final Summary Report." NUREG/CR-5117, PNL-6446, Pacific Northwest Laboratory, Richland, Washington.

DISTRIBUTION

No. of
Copies

No. of
Copies

OFFSITE

2 J. Muscara
NRC/RES
Mail Stop NS 217C

L. R. Abramson
NRC/NRR
Mail Stop NLS372

C. Y. Cheng
NRC/NRR
Mail Stop 9 H15

H. F. Conrad
NRC/NRR
Mail Stop 9 H15

C. E. McCracken
NRC/NRR
Mail Stop 8 D1

E. L. Murphy
NRC/NRR
Mail Stop 9 H15

K. R. Wichman
NRC/NRR
Mail Stop 9 H15

M. Anderson
Northern States Power
414 Nicolett Mall
Minneapolis, MN 55401

T. Beeman
London Nuclear Services, Inc.
2 Buffalo Avenue
Niagra Falls, NY 14303

J. Benson, Assoc. Eng.
Northeast Utilities
PO Box 270
Hartford, CT 06101

3 R. A. Clark
Failure Analysis Associates
8411 154th Ave. NE
Redmond, WA 98052

D. Currier
Florida Power & Light
9250 W. Flagler
Miami, FL 33120

A. E. Curtis, III
Rochester Gas & Electric Corp.
89 East Avenue
Rochester, NY 14649

T. Fauble, Engineer
SMUD/Racho Seco
14440 Twin Cities Road
Herald, CA 95638

D. Halama
New York Power Authority
123 Main Street
White Plains, NY 10601

J. Haning, DMT-6C
Houston Lighting & Power Co.
PO Box 1700
Houston, TX 77001

E. Hayden
Westinghouse Electric Corp.
Steam Generator Services
PO Box 2728
Pittsburgh, PA 15230

No. of
Copies

C. W. Hendrix, Jr.
Duke Power Company
Nuclear Production Dept.
PO Box 33189
Charlotte, NC   28242

K. Hoffman
Baltimore Gas & Electric Co.
Calvert Cliffs Nuclear Power
 Plant
Lubsy, MD   20657

J. Kang
Pacific Gas & Electric Co.
Dept. of Eng. Research
3400 Crow Canyon Road
San Ramon, CA   94583

A. Matheny
Southern California Edison
PO Box 128
San Clemente, CA   92672

5   H. S. McKay
Virginia Electric Power Co.
PO Box 26666
Richmond, VA   23261

D. L. Sessler
Tennessee Valley Authority
1735 Chestnut St. Towers II
Chattanooga, TN   37401

G. Severance
Consumers Power Co.
1945 W. Parnall Road
Jackson, MI   49201

D. L. Smith
Virginia Electric & Power Co.
PO Box 26666
1 James river Plaza
Richmond, VA   23261

C. Spalaris
Quadrex Corporation
1700 Dell Avenue
Campbell, CA   95008

No. of
Copies

4   C. S. Welty
Electric Power Research
 Institute
3412 Hillview Avenue
PO Box 10412
Palo Alto, CA   94303

Foreign

C. Birac
DAS/STAS/SAM
Commissariat a l'Energie Atomique
CEN/FAR
B.P. No. 6
92265 Fontenay-aux-Roses
FRANCE

4   J. L. Campan
Department Manager
Water Reactor Service
C.E.A./Cadarche B.P. No 1
13115 Saint Paul Lez Durance
Cadarache, FRANCE

4   R. DeSantis
R&D Manager
Ansaldo DBGV
Viale Sarca 336
Milano, ITALY   20126

4   M. Oishi, Director
Steam Generator Project NUPEC
Shuwa Kamiya-Cho Bldg.
3-13, 4-Chome, Toranomon,
Minato-Ku, Tokyo 105
JAPAN

M. Russell
NDE Applications
CEGB
Bridgewater Road
Bedminster Down
Bristol, ENGLAND

No. of
Copies

J. Tomlinson
Central Electricity Generating
 Board
NDT Applications Centre
Manchester,
UNITED KINGDOM M23 9LL

ONSITE

50 Pacific Northwest Laboratory

R. J. Kurtz, K2-31 (43)
Publishing Coordination
Technical Report Files (5)

2. TITLE AND SUBTITLE

Steam Generator Tube Integrity Program/
Steam Generator Group Project

Final Project Summary Report

5. AUTHOR(S)

R. J. Kurtz, R. A. Clark, E. R. Bradley, W. M. Bowen
P. G. Doctor, R. H. Ferris, F. A. Simonen

8. PERFORMING ORGANIZATION – NAME AND ADDRESS *(If NRC, provide Division, Office or Region, U.S. Nuclear Regulatory Commission, and mailing address; if contractor, provide name and mailing address.)*

Pacific Northwest Laboratory
PO Box 999
Richland, WA   99352

10. SUPPLEMENTARY NOTES

11. ABSTRACT *(200 words or less)*

The Steam Generator Tube Integrity Program/Steam Generator Group Project was a three-phase program conducted for the U.S. Nuclear Regulatory Commission (NRC) by Pacific Northwest Laboratory. The main goal of the program was to provide the NRC with validated information on the reliability of nondestructive examination techniques to detect and size flaws in steam generator tubing and to determine the remaining integrity of service-degraded tubing. The program was performed in three phases. The first phase involved burst and collapse tests and single-frequency eddy-current (EC) examinations of typical steam generator tubing with precision machined flaws. The goal of Phase I was to develop empirical models of remaining tube integrity as a function of flaw type and size, and to determine the capability of EC inspection methods to detect and size tube degradation. In Phase II, a smaller number of specimens with the same flaw types were investigated, but tube specimens were degraded by chemical means rather than machining methods. This approach was used to better simulate the irregular geometry of service-induced degradation. In the final phase of the program, the retired-from-service Surry 2A Steam Generator was used as a test bed to investigate the reliability of inservice EC inspection equipment, personnel, and procedures, and as a source of service-degraded tubes for further validating the empirical equations of remaining tube integrity.

12. KEY WORDS/DESCRIPTORS *(List words or phrases that will assist researchers in locating the report.)*

steam generators, inservice inspection reliability, eddy
current testing, tube integrity, burst testing, collapse
testing, sampling plans, Surry
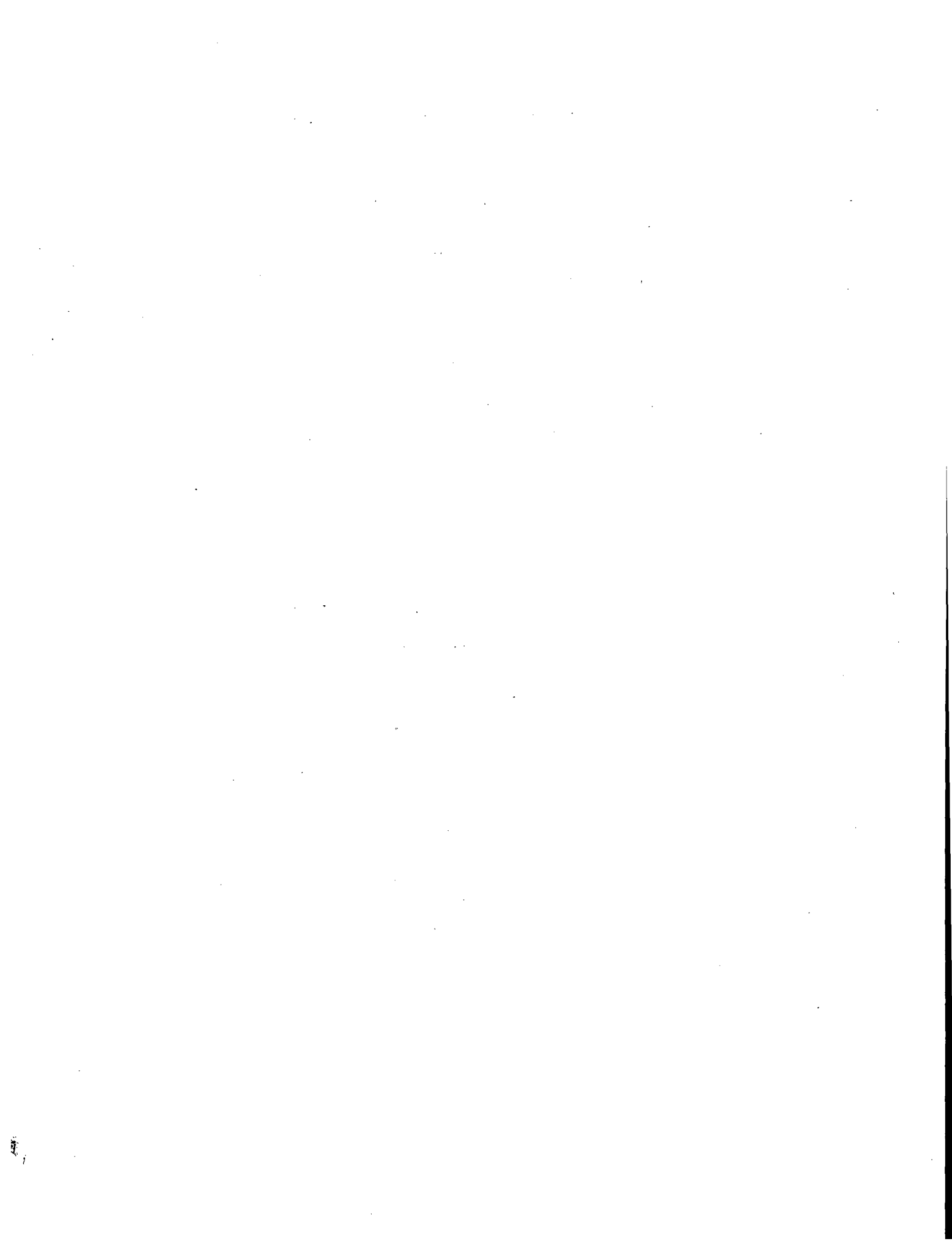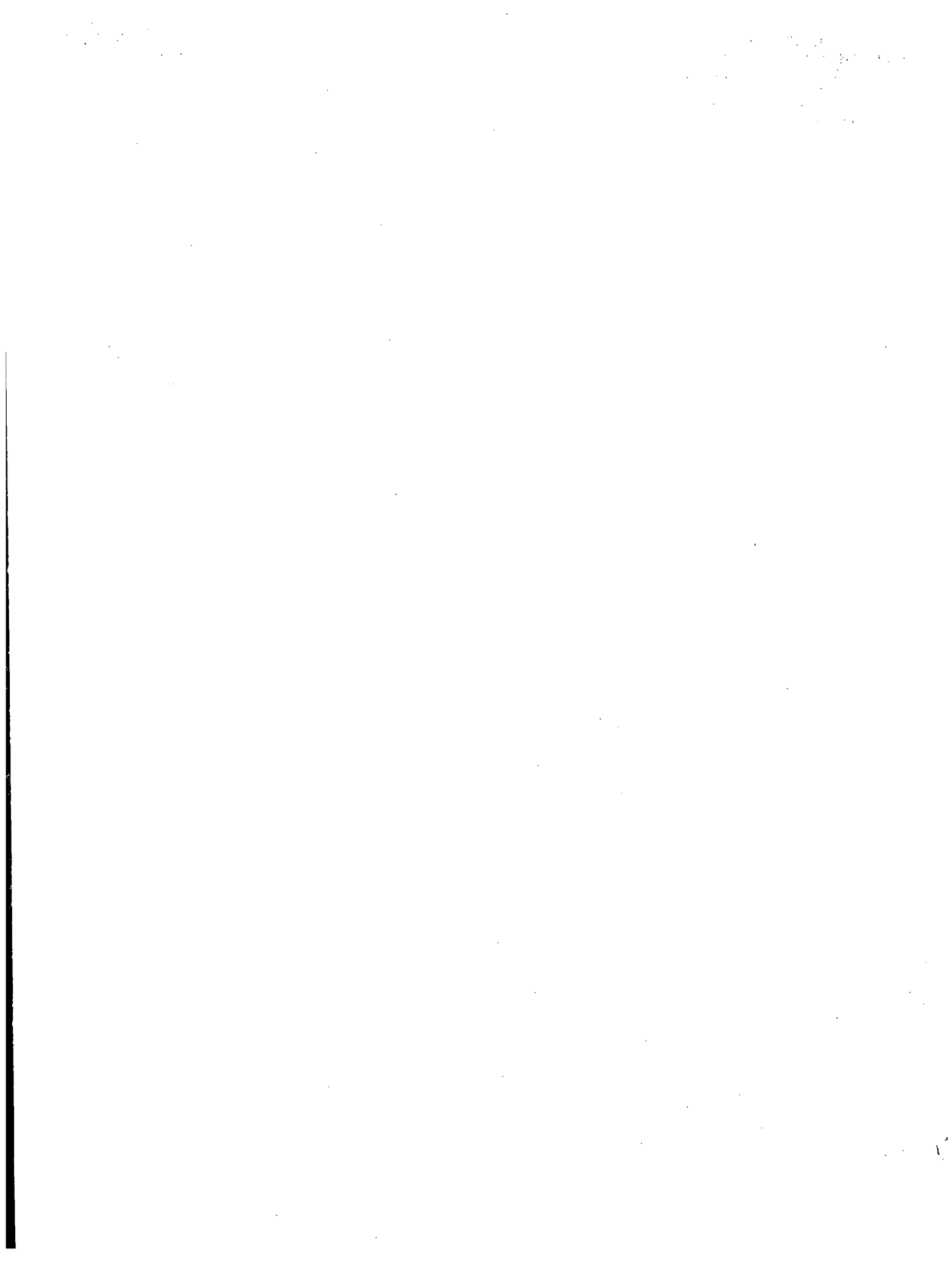
UNITED STATES
NUCLEAR REGULATORY COMMISSION
WASHINGTON, D.C. 20555

OFFICIAL BUSINESS
PENALTY FOR PRIVATE USE, $300

L. R. Abramson
NRC/NRR
Mail Stop NLS372